Universidad de Alcalá
COMISIÓN DE ESTUDIOS OFICIALES
DE POSGRADO Y DOCTORADO

ACTA DE EVALUACIÓN DE LA TESIS DOCTORAL

(FOR EVALUATION OF THE ACT DOCTORAL THESIS)

Año académico (*academic year):* 2017/18

DOCTORANDO *(candidate PHD)*: **JODRÁ APARICIO, JUAN ADRIÁN**
D.N.I. /PASAPORTE (*Id.Passport*): ******9348D**
PROGRAMA DE DOCTORADO *(Academic Committee of the Programme)*: **D446-QUÍMICA**
DPTO. COORDINADOR DEL PROGRAMA *(Department)*: **QUÍMICA ANALÍTICA, QUÍMICA FÍSICA E INGENIERÍA QUÍMICA**
TITULACIÓN DE DOCTOR EN *(Phd title)*: **DOCTOR/A POR LA UNIVERSIDAD DE ALCALÁ**

En el día de hoy 15/12/17, reunido el tribunal de evaluación, constituido por los miembros que suscriben el presente Acta, el aspirante defendió su Tesis Doctoral **con Mención Internacional** (*In today assessment met the court, consisting of the members who signed this Act, the candidate defended his doctoral thesis with mention as International Doctorate*), elaborada bajo la dirección de (*prepared under the direction of*) JESUS ALBERTO ESCARPA MIGUEL // MIGUEL ANGEL LOPEZ GIL.

Sobre el siguiente tema *(Title of the doctoral thesis)*: *MINIATURIZED IMMUNOSENSORS AND INNOVATIVE MOTOR-BASED (BIO-)SENSING STRATEGIES FOR ANALYTICAL APPLICATIONS*

Finalizada la defensa y discusión de la tesis, el tribunal acordó otorgar la CALIFICACIÓN GLOBAL[2] de (**no apto, aprobado, notable** y **sobresaliente**) *(After the defense and defense of the thesis, the court agreed to grant the GLOBAL RATING (fail, pass, good and excellent)*: SOBRESALIENTE /EXCELENT

Alcalá de Henares, a 15 de DICIEMBRE de 2017

Fdo. *(Signed)*: ARACELI GONZALEZ CORTÉS Fdo. *(Signed)*: DARIO COMPAÑ-MORE Fdo. *(Signed)*: MIGUEL GARCIA GARCIA

FIRMA DEL ALUMNO (candidate's signature),

Fdo. *(Signed)*: .....

Con fecha 20 de diciembre de 2017 la Comisión Delegada de la Comisión de Estudios Oficiales de Posgrado, a la vista de los votos emitidos de manera anónima por el tribunal que ha juzgado la tesis, resuelve:

☐ Conceder la Mención de "Cum Laude"
☒ No conceder la Mención de "Cum Laude"

La Secretaria de la Comisión Delegada

[2] La calificación podrá ser "no apto" "aprobado" "notable" y "sobresaliente". El tribunal podrá otorgar la mención de "cum laude" si la calificación global es de sobresaliente y se emite en tal sentido el voto secreto positivo por unanimidad. (*The grade may be "**fail**" "**pass**" "**good**" or "**excellent**". The panel may confer the distinction of "cum laude" if the overall grade is "Excellent" and has been awarded unanimously as such after secret voting.).*

Universidad de Alcalá

COMISIÓN DE ESTUDIOS OFICIALES
DE POSGRADO Y DOCTORADO

En aplicación del art. 14.7 del RD. 99/2011 y el art. 14 del Reglamento de Elaboración, Autorización y Defensa de la Tesis Doctoral, la Comisión Delegada de la Comisión de Estudios Oficiales de Posgrado y Doctorado, en sesión pública de fecha 20 de diciembre, procedió al escrutinio de los votos emitidos por los miembros del tribunal de la tesis defendida por *JODRÁ APARICIO, JUAN ADRIÁN*, el día 15 de diciembre de 2017, titulada *MINIATURIZED IMMUNOSENSORS AND INNOVATIVE MOTOR-BASED (BIO-)SENSING STRATEGIES FOR ANALYTICAL APPLICATIONS*, para determinar si a la misma se le concede la mención "cum laude", arrojando como resultado, 2 votos a favor y 1 en contra.

Por lo tanto, la Comisión de Estudios Oficiales de Posgrado **resuelve no otorgar la Mención de "cum laude"** a dicha Tesis.

Alcalá de Henares, 5 de enero de 2018
EL PRESIDENTE DE LA COMISIÓN DE ESTUDIOS
OFICIALES DE POSGRADO Y DOCTORADO

UNIVERSIDAD DE ALCALÁ · COMISIÓN DE ESTUDIOS OFICIALES DE POSGRADO Y DOCTORADO ·

Juan Ramón Velasco Pérez

Copia por e-mail a:
Doctorando: JODRÁ APARICIO, JUAN ADRIÁN
Secretario del Tribunal: MIGUEL GARCÍA GARCÍA. Investigador postdoral. Empresa Protheus Technologies.
Director/a de Tesis: JESÚS ALBERTO ESCARPA MIGUEL // MIGUEL ANGEL LÓPEZ GIL

Universidad de Alcalá

ESCUELA DE DOCTORADO
Servicio de Estudios Oficiales de Posgrado

DILIGENCIA DE DEPÓSITO DE TESIS.

Comprobado que el expediente académico de D./Dª JUAN ADRIÁN JODRA APARICIO reúne los requisitos exigidos para la presentación de la Tesis, de acuerdo a la normativa vigente, y habiendo presentado la misma en formato: ☐ soporte electrónico ☒ impreso en papel, para el depósito de la misma, en el Servicio de Estudios Oficiales de Posgrado, con el nº de páginas: 313 se procede, con fecha de hoy a registrar el depósito de la tesis.

Alcalá de Henares a 30 de OCTUBRE de 2017

Aurora Juárez Abril

Fdo. El Funcionario

Universidad de Alcalá

DEPARTAMENTO DE QUÍMICA ANALITICA, QUIMICA FISICA E INGENIERIA QUIMICA
Edificio Polivalente
Carretera Madrid-Barcelona, Km. 33,600
28871 Alcalá de Henares (Madrid)
Telf: 91 885 4 941
FAX: 91 885 5 088
E-mail: dpto.quimanafising@uah.es

Dr. **ALBERTO ESCARPA MIGUEL,** Coordinador del Programa de Doctorado en **Química** de la Universidad de Alcalá,

CERTIFICA:

Que el trabajo descrito en la presente memoria, titulado:

"Miniaturized immunosensors and innovative motor-based (bio-)sensing strategies for analytical applications"

ha sido realizado por **D. Juan Adrián Jodra Aparicio**, bajo la dirección de los **Dr. Alberto Escarpa Miguel** y **Dr. Miguel Ángel López Gil**, en el Área de Química Analítica del Departamento de Química Analítica, Química Física e Ingeniería Química de esta Universidad excepto un trabajo descrito en el Capítulo III que ha sido llevado a cabo en el Departamento de Nanoingeniería de la Universidad de California, San Diego (UCSD) (EEUU). Asimismo, reúne los requisitos científicos de originalidad y rigor metodológicos y autoriza su presentación para que sea defendido como Tesis Doctoral.

Y para que conste y surta los efectos oportunos, firma el presente en Alcalá de Henares a 27 de Octubre de 2017.

Fdo: Dr. Alberto Escarpa Miguel

Universidad de Alcalá

DEPARTAMENTO DE QUÍMICA ANALITICA, QUIMICA FISICA E INGENIERIA QUIMICA
Edificio Polivalente
Carretera Madrid-Barcelona, Km. 33,600
28871 Alcalá de Henares (Madrid)
Telf: 91 885 4 941
FAX: 91 885 5 088
E-mail: dpto.quimanafising@uah.es

Dr. **ALBERTO ESCARPA MIGUEL,** Profesor Titular de Química Analítica del Departamento de Química Analítica, Química Física e Ingeniería Química de la Universidad de Alcalá,

Dr. **MIGUEL ÁNGEL LÓPEZ GIL,** Profesor Titular de Química Analítica del Departamento de Química Analítica, Química Física e Ingeniería Química de la Universidad de Alcalá,

CERTIFICAN:

Que el trabajo descrito en la presente memoria, titulado:

"Miniaturized immunosensors and innovative motor-based (bio-)sensing strategies for analytical applications"

ha sido realizado por **D. Juan Adrián Jodra Aparicio**, bajo la dirección de los **Dr. Alberto Escarpa Miguel** y **Dr. Miguel Ángel López Gil**, en el Área de Química Analítica del Departamento de Química Analítica, Química Física e Ingeniería Química de esta Universidad excepto un trabajo descrito en el Capítulo III que ha sido llevado a cabo en el Departamento de Nanoingeniería de la Universidad de California, San Diego (UCSD) (EEUU). Asimismo, reúne los requisitos científicos de originalidad y rigor metodológicos y autoriza su presentación para que sea defendido como Tesis Doctoral.

Y para que conste y surta los efectos oportunos, firma el presente en Alcalá de Henares a 27 de Octubre de 2017.

Fdo: Dr. Alberto Escarpa Miguel **Fdo: Dr. Miguel Ángel López Gil**

Facultad de Biología, Ciencias Ambientales y Química
Departamento de Química Analítica, Química Física e Ingeniería Química

Programa de Doctorado en
QUÍMICA

Miniaturized immunosensors and innovative motor-based (bio-)sensing strategies for analytical applications

Tesis Doctoral

Juan Adrián Jodra Aparicio

Alcalá de Henares, Diciembre 2017

Universidad de Alcalá

DEPARTAMENTO DE QUÍMICA ANALITICA, QUIMICA FISICA E INGENIERIA QUIMICA
Edificio Polivalente
Carretera Madrid-Barcelona, Km. 33,600
28871 Alcalá de Henares (Madrid)
Telf: 91 885 4 941
FAX: 91 885 5 088
E-mail: dpto.quimanafising@uah.es

Dr. **ALBERTO ESCARPA MIGUEL,** Coordinador del Programa de Doctorado en **Química** de la Universidad de Alcalá,

CERTIFICA:

Que el trabajo descrito en la presente memoria, titulado:

"Miniaturized immunosensors and innovative motor-based (bio-)sensing strategies for analytical applications"

ha sido realizado por **D. Juan Adrián Jodra Aparicio**, bajo la dirección de los **Dr. Alberto Escarpa Miguel** y **Dr. Miguel Ángel López Gil**, en el Área de Química Analítica del Departamento de Química Analítica, Química Física e Ingeniería Química de esta Universidad excepto un trabajo descrito en el Capítulo III que ha sido llevado a cabo en el Departamento de Nanoingeniería de la Universidad de California, San Diego (UCSD) (EEUU). Asimismo, reúne los requisitos científicos de originalidad y rigor metodológicos y autoriza su presentación para que sea defendido como Tesis Doctoral.

Y para que conste y surta los efectos oportunos, firma el presente en Alcalá de Henares a 27 de Octubre de 2017.

Fdo: Dr. Alberto Escarpa Miguel

Universidad de Alcalá

DEPARTAMENTO DE QUÍMICA ANALITICA, QUIMICA FISICA E INGENIERIA QUIMICA
Edificio Polivalente
Carretera Madrid-Barcelona, Km. 33,600
28871 Alcalá de Henares (Madrid)
Telf: 91 885 4 941
FAX: 91 885 5 088
E-mail: dpto.quimanafising@uah.es

Dr. **ALBERTO ESCARPA MIGUEL,** Profesor Titular de Química Analítica del Departamento de Química Analítica, Química Física e Ingeniería Química de la Universidad de Alcalá,

Dr. **MIGUEL ÁNGEL LÓPEZ GIL,** Profesor Titular de Química Analítica del Departamento de Química Analítica, Química Física e Ingeniería Química de la Universidad de Alcalá,

CERTIFICAN:

Que el trabajo descrito en la presente memoria, titulado:

"Miniaturized immunosensors and innovative motor-based (bio-)sensing strategies for analytical applications"

ha sido realizado por **D. Juan Adrián Jodra Aparicio**, bajo la dirección de los **Dr. Alberto Escarpa Miguel** y **Dr. Miguel Ángel López Gil**, en el Área de Química Analítica del Departamento de Química Analítica, Química Física e Ingeniería Química de esta Universidad excepto un trabajo descrito en el Capítulo III que ha sido llevado a cabo en el Departamento de Nanoingeniería de la Universidad de California, San Diego (UCSD) (EEUU). Asimismo, reúne los requisitos científicos de originalidad y rigor metodológicos y autoriza su presentación para que sea defendido como Tesis Doctoral.

Y para que conste y surta los efectos oportunos, firma el presente en Alcalá de Henares a 27 de Octubre de 2017.

Fdo: Dr. Alberto Escarpa Miguel Fdo: Dr. Miguel Ángel López Gil

Dicen que es de bien nacidos ser agradecidos. Se lo oí por primera vez a mi abuela y considero que no hay mejor frase para comenzar. Antes de ponerme sentimental, quiero agradecer a las instituciones que han hecho posible mi camino en el doctorado como la Universidad de Alcalá (UAH) por los estudios y sus laboratorios, el Ministerio de Economía y Competitividad (MICIIN) por el proyecto que concedió al grupo y las becas que permitieron mi estancia en el extranjero, y a la University of California/San Diego por acogerme como estudiante, dejarme participar y disfrutar de su maravillosa universidad.

Y ahora toca recordar todas las vivencias en forma de gracias. Posiblemente alargaré esto más de lo deseado, pero necesito soltarlo.

Primero, a esa persona que hizo posible que empezara en el mundo díscolo de la investigación. Muchas gracias, Alberto Escarpa. Siempre recordaré ese examen en el que te acercaste, quizás otro momento hubiera sido más adecuado, pero lo guardaré con gran cariño. Gracias por las enseñanzas, por las palabras y por darme la oportunidad de haber formado parte del tu grupo. Espero que siga creciendo y haciendo "*cosas grandes de cosas pequeñas*". Miguel Ángel, tú también me enseñaste el camino a seguir, como hacer, trabajar y aprender. Me enseñaste a verle más el lado bueno y a saber reír en el laboratorio. Gracias por acompañarme, hacerme reír y mejorar, te debo mucho. Por último, Cristina González, que decirte a ti también. Muchas gracias por todos los consejos y ayudas. Voy a echar de menos las charlas y las visitas a solucionar los problemas informáticos. Has sido un gran apoyo y espero que sigas siendo como eres.

Mención especial al prof. Joseph Wang, ese gran científico que tanta pasión y esfuerzo demuestra por lo que hace. Muchas gracias por devolverme a ese niño que juega con la ciencia y la química, gracias por las enseñanzas, las palabras y el tiempo en tu laboratorio. Gracias por aceptarme y hacerme partícipe de la nanotecnología, y algo muy importante, por escuchar cada una de mis ideas. Espero que mantengas tu legado.

Special mention to prof. Joseph Wang, that great scientist who demonstrate such passion and effort for what he makes. I really appreciate to give me back that child

who plays with science and chemistry. Thanks for your teaching, words and time in your lab. Thank you for embracing me and involving me in the nanotechnology world, and something very important, for listening each and all my ideas. I wish you kept your legacy.

De empezar a pensar, la emoción comienza a salir, pero intentaré transmitir ese cariño que guardo en palabras que todos os merecéis.

A toda la gente con la que empecé, estaban y me acogieron en el labo como si llevara allí tanto como ellos… Muchísimas gracias. Gracias Cris por todas las palabras amables, consejos y risas; Vir, por los vaciles, las historias y hacerme sentir estúpido pero cómodo a la vez; Clari, por todos los buenos momentos; María, siempre tan guapa, por mostrar la personalidad que tienes y enseñarme tanto; Charlie, por los grandes recuerdos contigo, tus consejos y tu bondad; André, por tu experiencia, las risas y las enseñanzas; Paty, la polaca no rubia, por todos tus buenos consejos y las cervecitas; Elena, Estafanía, Romy, cuantos ratos hemos pasado, horas de laboratorio, pero que buenos momentos y cuantos recuerdos quedarán. También agradecer a todos los demás, María Ángeles, Matías, Miguelito, Jorge, os guardo a todos un gran cariño, que cada vez que mire esto, se me pondrá un nudo en la garganta por recordaros y agradeceros todo lo que hicisteis por mi, de verdad.

También agradecer a todos los nuevos que fueron llegando, que iban aportando cosas nuevas. Gracias Vale, por las noches de bailes, Raquel, por todas las risas y los buenos momentos, Felix, Jesús, Ignacio, Pablo, Sofía, Patricia, Mari Carmen, Samuel y Angelique. Gracias por seguir con el buen rollo que había.

Y cómo no, a mi gente del laboratorio… esos con los que compartí la mayor parte de mi tiempo, alegrías y frustaciones, los que me acogieron y lo que vinieron, todos ellos aportando cosas nuevas y generándome experiencia que me han ayudado a ser quien soy. Roberto, gracias por compartir tus cosas conmigo; Águeda, gracias por tu alegría y tu ilusión que hacen que se contagien todos; MariMore, gracias por tu experiencia, tus consejos y tu ayuda en todo; Laura, gracias por inocencia, por tu alegría, por tus ganas y por tu bondad, gracias por tu ayuda y por los buenos momentos; Diana,

gracias por todo lo que me enseñaste. También agradecer a todos los que pasaron por allí y me aguantaron, Jorge, Dani, Tania y Diego, gracias. Como no, ese pibe, buenísimo argentino pero con sus cosas, no gustarte el mate… Pero lo pasé muy contigo y con Cintia, muchas gracias Fede. Pero tengo que hacer mención especial a esa pequeña familia que se forjó en un laboratorio y me ha seguido acompañando durante esta aventura. Miri, siempre serás mi co-directora, me enseñaste todo lo que sabías y me aguantaste todas mis preguntas y mis tonterías, me diste un camino a seguir, confianza e ilusión para empezar. Y luego seguiste ahí, apoyándome y siendo mi amiga, miles de gracias. Migui, amigo, tú fuiste el primero en recibirme en el laboratorio cuando decidí empezar allí, sé que no te acuerdas, pero a mi no se me olvidará. Gracias por toda la ayuda, los consejos, las risas y encserñarme, tampoco lo olvidaré, mil gracias. A vosotros dos os debo todo mi comienzo. Pilar, ¡qué gran señora y elegancia! El saber estar hecho persona. Sabías como aconsejar, como afrontar las cosas, a pesar de los problemas que había, pero siempre sabías tener palabras y como comportarse. Muchísimas gracias. Y para terminar, Aída. Tú has compartido horas y horas, conversaciones, risas, problemas, hemos crecido juntos en ese laboratorio. Nuestras conversaciones filosóficas a última hora para solucionar cosas muy difíciles a veces, tanta ayuda y cariño que me has dado, que espero que sigamos siendo amigos y no dejemos nunca de compartir cosas. Millones de gracias. Y bueno, aunque no estaba en el laboratorio, pero llegó y enseguida hicimos buenas migas, la gente de Guada es lo que tiene. Me has ayudado, me has hecho reír, sigues preocupándote por mí, sigues estando ahí siempre y te agradezco todo lo que me has enseñado. Admiro como eres y me has ayudado a forjar un poco más como quiero ser. Mil gracias. Os debo gran parte de este camino que he seguido.

Además, agradecer a Lola y Ana todos los consejos, todas las buenas palabras y lo que me habéis hecho reír. Me alegro mucho de haberos conocido.

También tengo agradecer a toda esa gente que me acompañó en la maravillosa experiencia que viví en San Diego. Muchísimas gracias Berta por acogerme y enseñarme San Diego de esa manera. Muchas

gracias Julián por tu ayuda, acogerme también y por hacerme disfrutar de la ciudad. *Thank you to Virendra for sharing yor knowlegde about science and your culture.* Muchas gracias Mariana por ser mi compañera de escritorio, por las risas, compartir tu experiencia y conocimiento, saqué mucho de ti. Moito obrigado Jorge, gracias por las risas, los buenos momentos y compartir tu experiencia. *Thank you to all guys who share good and bad moments there.* Muchas gracias Cristian por los partidos y las risas echadas. *Thank you so much Kumi, thank you for showing me your city and your hidden places, and for taking me care. It was a real pleasure.* Muchas gracias Miguel, gracias por tu invitación a la boda, por hacerme sentir parte de todo aquello, por las charlas de labo mientras hacíamos y lavábamos motores. Fue un verdadero placer. Y para terminar, una persona fue clave para perder la cabeza y a la vez mantenerme cuerdo. Me ayudó cuando peor lo pasé porque vaya problemón de salud que surgió… Muchísimas gracias Fer. Muchas gracias por acogerme en tu casa, por molestarte tanto por mí, por enseñarme todo lo que sabes, abrir más mi mente y convertirte en mi amigo. Muchas gracias por cada controversia que generabas porque las risas podían ser muchas y a la vez aportabas mucho con tu manera de ver el mundo.

Como no agradecer a mis compañeros de clase, aquellos que compartieron horas y horas de clase, estudio, biblioteca, trabajos, laboratorio y de jugar a la escoba… ¡qué maravilla! ¡Cuántas alegrías y penas tuvimos! Pero al final conseguimos el objetivo que habíamos buscado. Gracias Antonio, Miguel y, en especial, Sergio, gracias por tanto.

Quisiera dedicar unas palabras a aquel profesor que me ayudo a decirme lo que quería ser y por enseñarme tanto. Muchas gracias Antonio.

Y ahora toca hablar de aquellos con los que crecí, todos los que me han acompañado y me siguen acompañando en todo este camino que hay que recorrer. Gracias a toda esa gente que siempre ha tenido un detalle o palabras buenas para mí. Gracias a mis amigos, a mi peña, a mis compañeros de clase, de fiesta, de alegrías, de penas, gracias por absolumente todo. Me habéis hecho ser más fuerte, ser mejor

persona, he aprendido mucho de vosotros y nunca dejaré de hacerlo. Mi compipiso, casi toda la vida juntos, muchas gracias Pablo. Rubén, muchas gracias por cada momento desde las peleas cuando éramos críos. Jesús, siempre con el humor fino y tus consejos, muchas gracias. Javi, siempre elegante y estirado, ayudando y preocupándote de todos, muchas gracias a ti también. Muchas gracias Daniel por tu bondad, siempre diré que eres más bueno que el pan, aunque últimamente como se te agria el carácter (con sentido del humor). Diego, muchas gracias por tu locura y a la vez por como has madurado, ver como has corregido esa cabeza que tienes enseña mucho a los demás. Álvaro, a ti también gracias por las risas y tus bombas de humo. No voy a olvidarme de vosotras, de todos esos bailes, conversaciones, risas, momentos divertidos y algunos tristes, pero siempre juntos y siempre ahí. Muchas gracias Isabel, Nuria, Elena, Clara, Marta, María y Begoña. También tú, Adela, por todo lo que me has apoyado y has compartido conmigo este tiempo.

Parte de mí, gran parte de lo que soy, toda la educación y conocimiento que me habéis dado. Millones de gracias familia. Muchas gracias a mis tíos, Jesús, Puri, Juani y María Ángeles, por la ayudar, por las vacaciones en vuestras casas y por todos los buenos momentos. Muchas gracias a mis tíos, Dani y María Ángeles, por toda la ayuda que dais y el estar siempre ahí. A pesar de la distancia que hay, muchas gracias tía Pili, por siempre acordarte de mí y estar pendiente, igual que cuando era pequeño y me cuidabas. Muchas gracias a todos mis primos, con los que he crecido, aprendido, madurado y disfrutado. Muchas gracias Pablo, Victor, Miguel, Elena, Moisés, Álvaro y Rocio. También a mi tía Isa, con la que he compartido canciones, ratos malos cuando no dormía de pequeño (perdón) y ratos muy buenos, sobre todo en el templo del madridismo. Muchísimas gracias por todo. También gracias a mi abuela Ana por cuidarme en vacaciones y los regalos que me diste.

Pero tengo que dejar en un epígrafe aparte a las personas que más tiempo han compartido conmigo dándome todo lo que tenían. Mis abuelos, Jesús y Pilar, tanto me han cuidado, ayudado, dado que no sé como agradecérselo. Tantas comidas largas, estar pendiente que no me escapara a la calle ni me cayese por las escaleras, tantos cuidados,

tantas partidas de cartas, y sobre todo, todo lo que me habéis enseñado. No tiene precio y esto también va por vosotros. Muchísimas gracias y, como diría mi abuelo, muchas veces y a menudo. Esas dos personas que aparecieron en mi vida dándome mucha alegría de pequeño y mucho orgullo de mayor. Muchísimas gracias a mis hermanos, Elima y Alejandro, me habéis dado muchas risas y penas pero siento orgullo y admiración en los que os habéis convertido. Siempre he pensado que erais mejores que yo y he tenido la suerte de poder comprobarlo. Seguid así. A mis padres, por no solo darme la vida, sino por darme la vida que tengo, sin ellos no habría sido posible. En parte quisiera incluso disculparme por todo lo malo que he hecho o fallaros, pero solo puedo estaros eternamente agradecido. Me habéis educado, formado, ayudado y dado tanto solo por verme sonreír. Ahora me gustaría devolveros todo eso porque gracias a vosotros soy lo que soy. Quisisteis ver mis sueños cumplidos y poco a poco los estoy logrando. Millones de gracias, Ina y Sagra. Os quiero de verdad.

Para lo último quiero dejar alguien que también ha cambiado mi vida. Siempre me gusta pensar en la serendipia, la casualidad, y que ver a esa chica en el instituto fue el comienzo de algo. Alguna vez me gustó saber que te podrías fijar en mí, pero esto es inimaginable. Millones y millones de gracias, amor. Cuando te dediqué las tesis, sé que te dio mucha vergüenza, que quién lo iba a ver, pero que esto me gustaría que lo viera todo el mundo. Porque quiero que realmente te vieran y te conocieran. Te he dicho tantas cosas que sé lo que repetitivo y pesado que soy, pero consigues que sea hasta bueno. No quiero exagerar pero voy a intentar hacerte justicia. Tu forma de ver la vida, como la afrontas, y tu forma de ser hacen que quiera seguirte más. Nunca te antepones a nadie y nada, pero no eres tonta. Nunca te das por vencida, siempre atenta a todo, viendo y conociendo todo lo que se pueda para saber como actuar e intentando hacerlo lo mejor posible. Admiro tu carácter fuerte. Siempre me has enseñado que se puede confiar en uno mismo sin caer en la arrogancia, siendo humilde y sin ser más que nadie. Siempre conservas tu esencia, tu personalidad, tu naturalidad, todo lo que te hace ser tú. Consigues que crea y confíe en mí como nunca. Me equilibras, contigo encuentro el balance entre

mis sueños y la realidad. Tu humor, tus risas, y como me vacilas me han engachado más y más a ti. Me comprendes y me apoyas en cada momento. Tú me haces ser yo. Tú me haces ser mejor, tú me complementas y me completas. Gracias por apostar tan fuerte por mí. Quiero devolvértelo, demostrándolo todos los días que te quiero. Te amo Jenni. Muchísimas gracias por todo de verdad.

Quiero devolveros todo lo que me habéis dado e invertido en mí. Gracias.

A mi familia

y a Jenni

“Vivir no es sólo existir…

sino existir y crear,

saber gozar y sufrir,

y no dormir sin soñar.

Descansar… es empezar a morir”

Gregorio Marañón

El desarrollo de nuevas tecnologías y metodologías para solucionar problemas analíticos reales es un aspecto clave y exigente en el campo de la química analítica. La tendencia actual en esta ciencia lleva a realizar análisis de forma sencilla, fiable y preferiblemente mediante dispositivos miniaturizados que puedan ser utilizados *in situ*. En este sentido, los biosensores conforman herramientas analíticas excelentes debido a la sensibilidad y la selectividad reconocidas, junto con su miniaturización inherente. Por otro lado, las metodologías analíticas basadas en nanotecnología, donde los nanomateriales y motores actúan de forma especial, constituyen instrumentos innovadores, prometedores e interesantes para llevar a cabo análisis en diferentes áreas. Estos motores, los cuáles se mueven autónomamente a través de energía obtenida de una reacción química, en una de las más conocidas variedades, permiten una estrategia de biosensado, la cual depende del movimiento continuo a través de muestras complejas asociado con distintas interacciones biomoleculares, llamadas "*en movimiento*". Tal movimiento a lo largo de la muestra ayuda a la interacción con el analito generando un nuevo paradigma en la química analítica.

Dentro del campo de la química analítica, el análisis de alimentos es uno de los aspectos más importantes. Teniendo en cuenta el riesgo en seguridad alimentaria debido a la presencia de sustancias tóxicas en los alimentos y productos derivados, existe una necesidad real de desarrollar métodos nuevos capaces de detectar estos productos perjudiciales, y así, asegurar la seguridad de los consumidores. De este modo, el análisis de micotoxinas, metabolitos

secundarios tóxicos producidos por hongos, es especialmente relevante debido a los efectos negativos provocados en la salud humana y animal.

En consecuencia, y siguiendo el objetivo de conservar la seguridad alimentaria, se han desarrollado nuevos procedimientos basados en biosensores y metodologías que hacen uso de motores sintéticos para mejorar los sistemas actuales de análisis y explorar otros modos de actuación, significando la principal inspiración para esta tesis doctoral. Las herramientas bioanalíticas rápidas, económicas, sensibles y fiables descritas aquí mismo son una alternativa prometedora a los métodos de referencia para el cribado y la detección de micotoxinas y otros analitos de relevancia.

Esta tesis se divide en dos bloques centrales. El primer capítulo (Capítulo II) describe el marco donde se enfoca la tesis, que a su vez se divide en tres partes (seguridad alimentaria –Sección II.1-, biosensores –Sencción II.2- y motores –Sección II.3-). El segundo bloque incluye los resultados más notables obtenidos de los experimentos y los artículos publicados (Capítulo III). Este capítulo se distribuye en tres epígrafes, llamadas inmunosensores electroquímicos (Sección III.1), micromotores catalíticos (Sección III.2) y micromotores no catalíticos (Sección III.3).

En relación con el **capítulo II**, la seguridad alimentaria y sus antecedentes se presentan en la **sección II.1**. Aquí, se incluye el Codex Alimentarius, donde se definen las regulaciones y estándares para cumplir la seguridad alimentaria, intereses económicos y de

salud, y las amenazas principales (alérgenos, patógenos y micotoxinas). La **sección II.2** revisa los biosensores, que son instrumentos analíticos prometedores y actuales para determinar sustancias peligrosas diferentes en el análisis de alimentos. También se revisan, resumidamente, los más importantes elementos de bioreconocimiento (centrados preferentemente en anticuerpos y aptámeros) y las técnicas de detección (electroquímicas y fluorescentes). Al final, la **sección II.3** consta del estado del arte y las características principales de los motores sintéticos, los cuáles están convirtiéndose en unas herramientas analíticas altamente notables.

El **capítulo III** expone y debate los resultados importantes logrados durante el trabajo de la tesis. El **epígrafe III.1** consta de dos trabajos científicos donde se han desarrollado magnetoinmunosensores electroquímicos con excelentes características analíticas para la determinación de micotoxinas como Fumonisinas y Ocratoxina A, y han sido evaluadas por medio de un material de referencia certificado y muestras reales. En ambos casos, la estrategia se basa en el uso de partículas magnéticas como soporte de inmovilización, las cuáles se confinan en la superficie del electrodo impreso de carbono después de la reacción inmunoquímica, y la detección electroquímica se da por la adicción del sustrato y mediador electroquímico adecuados. La **sección III.2** también incluye otros dos artículos científicos. El primero trata del desarrollo de un micromotor de grafeno de alta eficacia para la determinación de Fumonisina B1. El reconocimiento selectivo de la micotoxina es dado por un aptámero unido a un fluoróforo. Esta detección se acopla a la

amortiguación fluorescente "*en movimiento*" mediante el mecanismo de acoplamiento π sobre la capa exterior de grafeno. También basados en el uso de motores de grafeno, el segundo trabajo desarrollado en la estancia en Estados Unidos conlleva el retraso en la ignición y propulsión de microcohetes tubulares catalíticos basados en la eliminación de la aleación de la capa interna inducida por el combustible. El tiempo de retardo depende de la corrosión gradual, preferentemente del Cu de la aleación interna de Pt-Cu por el peróxido de hidrógeno. El tiempo de retardo en la activación del motor puede ser modulado tanto por el control de la composición de la capa de aleación de Cu-Pt como por el medio que lo rodea, incluyendo el combustible, la concentración de NaCl y el pH local. De hecho, este versátil control del encendido de estos motores químicos se demuestra en muestras reales como agua de mar o ácido gástrico.

El **epígrafe III.3** incluye el desarrollo de un motor tubular milimétrico no catalítico para el biosensado de H_2O_2 en importantes muestras clínicas y ambientales. Se basa en el movimiento autopropulsado por el efecto Marangoni, donde la liberación asimétrica del tensioactivo SDS induce la convección del fluido y una rápida dispersión de la enzima peroxidasa de rábano picante en la muestra. Este eficiente movimiento junto con la liberación continua de enzima fresca conlleva a acelerar de forma significativa la reacción enzimática sin necesidad de un agitador externo o una inmovilización química/física de la enzima como en los métodos de biosensado

clásico. En este caso, la detección puede realizarse de forma electroquímica, óptica o visual sin necesidad de instrumentación.

Debido a todo lo expuesto y comentado anteriormente, los resultados presentados en esta tesis doctoral revelan el diseño y desarrollo de nuevas estrategias y metodologías que permiten mejorar las herramientas analíticas actuales en el campo del análisis de alimentos y seguridad alimentaria, pudiendo abrir nuevos horizontes en el marco de la química analítica.

Development of new technologies and methodologies to solve real analytical problems is a key and challenging aspect in the Analytical Chemistry field. A current tendency of this discipline leads to perform the simple, easy-to-use, miniaturized, portable and *in-situ* analysis. In this sense, biosensors constitute excellent analytical tools due to their recognized selectivity and sensitivity together with their inherent miniaturization. On the other hand, nanotechnology-based analytical methodologies, where nanomaterials and motors play a unique role, constitute exciting and promising innovative tools for analysis in different areas. These motors, which autonomously move getting energy from a chemical reaction in one of the most known varieties, allow a (bio)sensing strategy that relies on their continuous movement through complex samples in connection with diverse *on-the-move* (bio)molecular interactions. Such movement along the sample promotes the interaction with the target analyte representing a new paradigm in Analytical Chemistry.

Among the Analytical Chemistry field, food analysis is one of the most significant issues. Considering the food safety risk due to the presence of hazards in food and derived products, a real need exists to develop new methods capable of detecting these compounds, and thus, ensure consumers safety. In this way, analysis of mycotoxins, toxic secondary metabolites produced by fungi, is especially relevant owing to their negative effects produced in animal and human health.

Consequently, following the goal to preserve the food safety, new approaches based on biosensors and motors methodologies to enhance the current performance and explore other ways have meant

the main inspiration of this Doctoral Thesis. Fast, cost-effective, sensitive and reliable bioanalytical tools described herein are a promising alternative to the reference methods for the screening and early determination of mycotoxins and other relevant analytes.

This Thesis is divided into two main blocks. First one (Chapter II) is related to describe the framework of this Thesis, which in turn is divided into three parts (food safety -Section II.1-, biosensors -Section II.2- and motors -Section II.3-). The second block includes the most relevant results obtained from the experiments and the published articles (Chapter III). This chapter is distributed in three sections, named electrochemical immunosensors (Section III.1), catalytic micromotors (Section III.2) and non-catalytic micromotors (Section III.3).

Regarding **chapter II**, food safety and its background are presented in **section II.1**. Thus, it includes Codex Alimentarius, where regulations and standards are defined to accomplish food safety, the economic and health concerns, and the main hazards (allergens, pathogens, and mycotoxins). **Section II.2** reviews the biosensors which are current promising analytical tools to determine different hazards in food analysis. The most important elements of biorecognition (mainly focused on antibodies and aptamers) and detection techniques (electrochemical and fluorescent) are briefly revised. Finally, **section II.3** addresses the state of the art and main characteristics of synthetic motors, which are becoming highly remarkable analytical tools.

Chapter III expounds and discusses the main results obtained during the Thesis work. **Section III.1** includes two scientific works where electrochemical magnetoimmunosensors with excellent analytical characteristics have been developed for the determination of Fumonisins and Ochratoxin A mycotoxins, and have been evaluated through the analysis of certified reference material and real samples. In both cases, the strategy is based on the use of magnetic beads (MBs) as immobilization support, which after the immunochemical reaction, are confined onto the surface of carbon screen-printed electrode (CSPE) and electrochemical detection is achieved by the addition of suitable substrate and mediator for the enzymatic tracer. **Section III.2** also includes two scientific works. The first one deals with the development of a high-performance graphene-based micromotor strategy for determination of Fumonisin B1. Selective recognition to the target mycotoxin is given from dye-labeled aptamers. This detection is coupled to fluorescence quenching "*on-the-move*" of the free aptamer by the outer graphene-microrocket layer via π-stacking mechanism. Also based on the use of graphene-motors technology, the second work, developed in the American stay, entails the delayed ignition and propulsion of catalytic tubular microrockets based on fuel-induced chemical dealloying of an inner alloy layer. Such timed delay motor activation process relies on the preferential gradual corrosion of Cu from the inner Pt–Cu alloy layer by the peroxide fuel. The motor activation time can thus be tailored by controlling the composition of the Cu–Pt alloy layer and the surrounding media, including the fuel, NaCl concentrations, and local pH. Indeed, the versatile "blastoff" control of these chemical

microrockets is demonstrated in an actual matrices such as sea water and gastric acid.

Section III.3 illustrates a millimeter-sized tubular motor for mobile biosensing of H_2O_2 in environmental and relevant clinical samples. The concept relies on the self-propelled motion by the Marangoni effect, where the asymmetric release of SDS surfactant induces fluid convection and rapid dispersion of Horseradish peroxidase (HRP) enzyme into the sample solution. This efficient movement together with the continuous release of the fresh enzyme leads to a substantially accelerated enzymatic reaction process without the need of external stirring or chemical/physical enzyme attachment as in classical biosensing approaches. Electrochemical, optical or naked-eye detection can be performed.

Owing to all the premises stated above, the results presented in this Doctoral Thesis show the development of strategies and approaches in the field of food analysis and safety, which can open new horizons in the framework of Analytical Chemistry.

Chapter I

Hypothesis, objetives and milestones

Research in Analytical Chemistry field has allowed the development of new techniques, methods, and even protocols to perform the analysis. In order to achieve a more accurate and precise analysis, it has been necessary the exploration of new technologies which satisfy these goals. In this way, the analyte is not only the important stuff, but the methods are also catching the attention being able to enhance assessments, even accomplishing some simultaneous analysis of the same analyte in diverse samples or different analytes in the same sample.

There are a broad variety of methods and techniques. From well-established and routinely techniques performed in central laboratories such as liquid and gas chromatography using spectroscopic detection to non-central techniques such as sensors, it is defined an amalgamation of research made of ensuring accurate and precise analysis. However, a current tendency of Analytical Chemistry leads to perform the simple, miniaturized and *in-situ* analysis. Miniaturized biosensors configure a very suitable alternative as an analytical tool in different fields following principles above.

Among all biosensors, there are different classes, depending on the biorecognition element. These elements can be such as enzymes, antibodies, aptamers, DNA, and RNA. Based on different biorecognition element, biosensors can be categorized in, i.e., biosensors (spreadly used for enzymes), immunosensor (antibodies are used), aptasensor (aptamers), or genosensor (DNA or RNA). Among them, these elements provide lesser or non-necessity of sample

treatment, reliability and allow fast detections. Furthermore, they possess other attributes such as selective, sensitive, simple, low-cost, disposable and portable devices. In addition, these methods are easily combined with electrochemical or fluorescent detection, playing a key role in this field, and configuring a kind of devices that offer high selectivity, sensitivity, low-cost, simplicity, speed, disposability, inherent miniaturization and high compatibility with other technologies and methodologies. Therefore, electrochemical and fluorescent techniques suit properly to create novel sensors and devices.

In the same way, nanomaterials and nanotechnologies have recently arisen, becoming a relevant protagonist. Within this framework, motors –milimotors, micromotors and nanomotors– constitute promising tools in innovative ideas for different life areas. The principle of these micromachines is to mimic natural motors, transforming different type of energy in motion. There is a class of micromachines, which move getting the energy from a chemical reaction. Thus, these micromotors can be used for several aims, even in Analytical Chemistry area. The motion-based (bio) sensing strategy relies on the continuous movement of the motors through complex samples within the framework of diverse (bio) molecular interactions together with the *on-the-move* approach. Such movement, along the sample, promotes the interaction between target analyte-receptor and represents a fundamentally new paradigm in Analytical Chemistry. This method to carry out (bio–)sensing can open new horizons for designing pioneering approaches such as point-of-care devices or novel analyte detection.

These micromotors make use of nanomaterials to get the motion or to give qualities. Besides, these materials can be tailored to improve also the performance, to provide alternative features, or to achieve original goals. Thus, these materials can be composed of a combination of various metals (alloy), new polymers (to protect the motor or to transport a cargo), or combination of both to give other attributes for new ways to perform the motion.

All methods are usually made to reach an aim, whether to detect an analyte or to improve the performance. Among the Analytical Chemistry field, food analysis is one of the most significant. In order to get better food production and to enhance its quality and quantity, farmers and specialists have developed better techniques, tools, and production ways during centuries. Nevertheless, dangerous substances or microorganisms can emerge to lessen the food quality, becoming meaningful the food control and analysis. For that reasons, exploring new technologies and methods, including electrochemical biosensors or motor-based assays, to meet all related aspects has become the key for Analytical Chemistry.

Consequently, following the goal to preserve the food safety, researching new approaches in different disciplines –immunosensors and motors– to enhance the current performance and explore other ways, and implementing ideas in actual work and samples has meant the main inspiration of this Doctoral Thesis.

According to this, this Doctoral Thesis has three well-defined objectives:

1. To develop miniaturized and portable electrochemical immunosensors for significant food analytes such as mycotoxins (Fumonisins B and Ochratoxin A) in different food matrices to assure the food safety.
2. To explore new analytical methodologies, employing catalytic motors as mobile sensors to perform *on-the-move* biosensing and other applications.
   - *2.1.* To develop a novel *on-the-move* biosensing approach for FB1 detection based on dye-labeled aptamer as biorecognition element and graphene microrocket to perform mobile detection with fluorescent dye quenching.
   - *2.2.* Design, characterization, and implementation of new alloy nanomaterials for designing smart micromotors and providing pioneering analytical features.
3. To develop an enzyme-integrated non-catalytic motor within an end-cut pipette tip, based on the Marangoni effect as a mobile sensor for rapid and simple detection, both optical and electrochemical, of hydrogen peroxide as a model in relevant samples.

In view of above, the principal milestones reached in this Doctoral Thesis have been:

1.1. Development and optimization of a miniaturized biosensing strategy for fast and reliable detection of Fumonisins B and Ochratoxin A, using antibodies as selective recognition element together with sensitive electrochemical detection.

1.2. Demonstration of simultaneous simplified calibration and analysis protocol for both mycotoxins as an enhanced procedure. Analytical evaluation through the determination of a certified reference material and the analysis of real samples for both mycotoxins.

2.1. Design and development of a novel biosensing strategy using dye-labeled aptamers as specific bioreceptor element and graphene microrocket as a mobile sensor for *on-the-move* determination of mycotoxins in real food samples. Optimization of the detection principle based on fluorescence quenching of free labeled-aptamer by its π-π interaction with graphene.

2.2. Design of bimetallic alloy micromotors, and characterization by microscopy techniques (scanning electron microscopy (SEM)) and spectroscopic techniques (energy dispersive X-ray spectroscopy (EDX)). Study of the alloy micromotor behavior under different conditions and real samples.

3. Design and development of a new mobile biosensing strategy based on a friendly motion propulsion. Optimization of its simultaneous detection by two different techniques (optical and electrochemical) using the same performance. Evaluation

of their analytical characteristics and their application in relevant samples.

Chapter II

Introduction

II.1. Food Safety

Contemporary society is demanding high quality in many aspects of their lives. In developed countries, people ask for the highest food quality and safest food. In contrast, in developing countries, food quality is deprived instead of better food safety.

The interest in this fact is greater due to all consumers are paying much attention and demanding more information about whole food production procedure, from how it is produced to how it is distributed and marketed. For that, more governments and organization are managing more responsibilities, regulations, and laws to ensure the best food safety and quality, and consumer protection[1].

The Food and Agriculture Organization of the United Nations (FAO) and the World Health Organization (WHO) set already up guidelines for the food control, called *Guidelines for Developing an Effective National Food Control System* in 1976. This publication laid the foundations for over 25 years by different regulations. However, new changes as emerging detection tools, incipient laws and regulations, globalization in production and trade or market, guidelines from the organization as World Trade Organization (WTO), and the importance of Codex Alimentarius, have made necessary newer guidelines to adapt the old guidelines to this situation.

Furthermore, foodborne diseases, pathogen outbreaks, and chemical hazards are more well-known in the extent of the research

progresses. Then, it is necessary to share the knowledge and coordinate requirements, rules, and practices to ensure food control. To aim this objective, the Joint FAO/WHO created novel guidelines named *Assuring Food Safety and Quality: Guidelines for Strengthening National Food Control Systems* in 2003. New standards and regulations are made to improve and strengthen food control over the authorities, challenging different issues as:

- Increasing burden of foodborne illness and, new and emerging foodborne hazards
- Rapidly changing technologies in food production, processing, and marketing
- Developing science-based food control systems with a focus on consumer protection
- International food trade and need for harmonization of food safety and quality standards
- Changes in lifestyles, including rapid urbanization
- Growing consumer awareness of food safety and quality issues and increasing demand for better information

The collaboration between different organizations, institutions, governments, industries and other groups is essential to support and ensure food control, safety, and quality.

First of all, it is necessary to point the different terms out. Owing to the heterogeneity of the population, it is significant to compile all those perspectives and knowledge in unique standards. Therefore, Food

safety is defined as "*all those hazards, whether chronic or acute, that may make food injurious to the health of the consumer*". Food quality refers to "*all other attributes that influence a product's value to the consumer. This includes negative attributes such as spoilage, contamination with filth, discoloration, off-odors and positive attributes such as the origin, color, flavor, texture, and processing method of the food*". In addition, it is important to tell the difference between other significant term, food control, which is "*a mandatory regulatory activity of enforcement by national or local authorities to provide consumer protection and ensure that all foods during production, handling, storage, processing, and distribution are safe, wholesome and fit for human consumption; conform to safety and quality requirements; and are honestly and accurately labelled as prescribed by law*".

In order to establish objectives, it is meaningful to distinguish between quality and safety because it affects to policy and the most suitable food control method due to its nature and content[1]. Additionally, it is essential to consider the purchaser perspective as an extra worth to food safety and quality, called *adding value*[2].

For that reasons, these regulations and laws are focused on consumers, becoming the foremost principle to protect them against hazardous, contaminated and fraudulent food trade.

During the whole food chain supply, also named *farm-to-table* continuum, all the processes must be controlled to avoid inherent hazards or to eliminate possible contamination sources. The hazards can

occur by contaminated raw materials, ingredients and water; poor hygiene in manufacture processes; inadequate agricultural practices; lack of controls in food operations; mistreatment with chemical reagents; or incorrect storage. Special attention must be paid due to the raised concerns to:

- Microbiological hazards
- Pesticide residues
- Misuse of food additives
- Chemical contaminants, including biological toxins and metabolites
- Adulteration

Among this threats, some of them were selected to further discussion in the next chapters. The selected ones were allergens, pathogens, and mycotoxins. The significance of these hazards resides in their characteristics, novelty and emergence, and the ever-growing concern of their occurrence in nourishment.

II.1.1. Codex Alimentarius

FAO was founded in 1945 and WHO was founded in 1948. During next years, various committees and organizations worked on the control of food additives and chemical compounds at the regional level, as occurred with the *Codex Alimentarius Europaeus* pursued by European councils. However, some organizations and councils decided with WHO support to create the *Codex Alimentarius* (international

version) in 1960, and the Joint FAO/WHO set up the Codex Alimentarius Commission in 1961. According to its very book, *Codex Alimentarius* is a collection of standards, codes of practice, guidelines and other recommendations. Among this statement, there are standards for different categories and goals, which are referred to government-regulated features or describe production, processing, manufacturing, transport and storage practices. Furthermore, Codex Alimentarius is based on scientific knowledge. Scientific activity continues taking a meaningful part in the elaboration of a new standard. Many different disciplines can contribute together with the aim of improving the Codex Alimentarius. Excellence, independence, transparency, and universality are the values which Codex Alimentarius, its Commission and the Joint FAO/WHO try to reach using that scientific knowledge from the beginning[3]. Figure 1 describes how the process of Codex Alimentarius Commission elaborates the guidelines and standards.

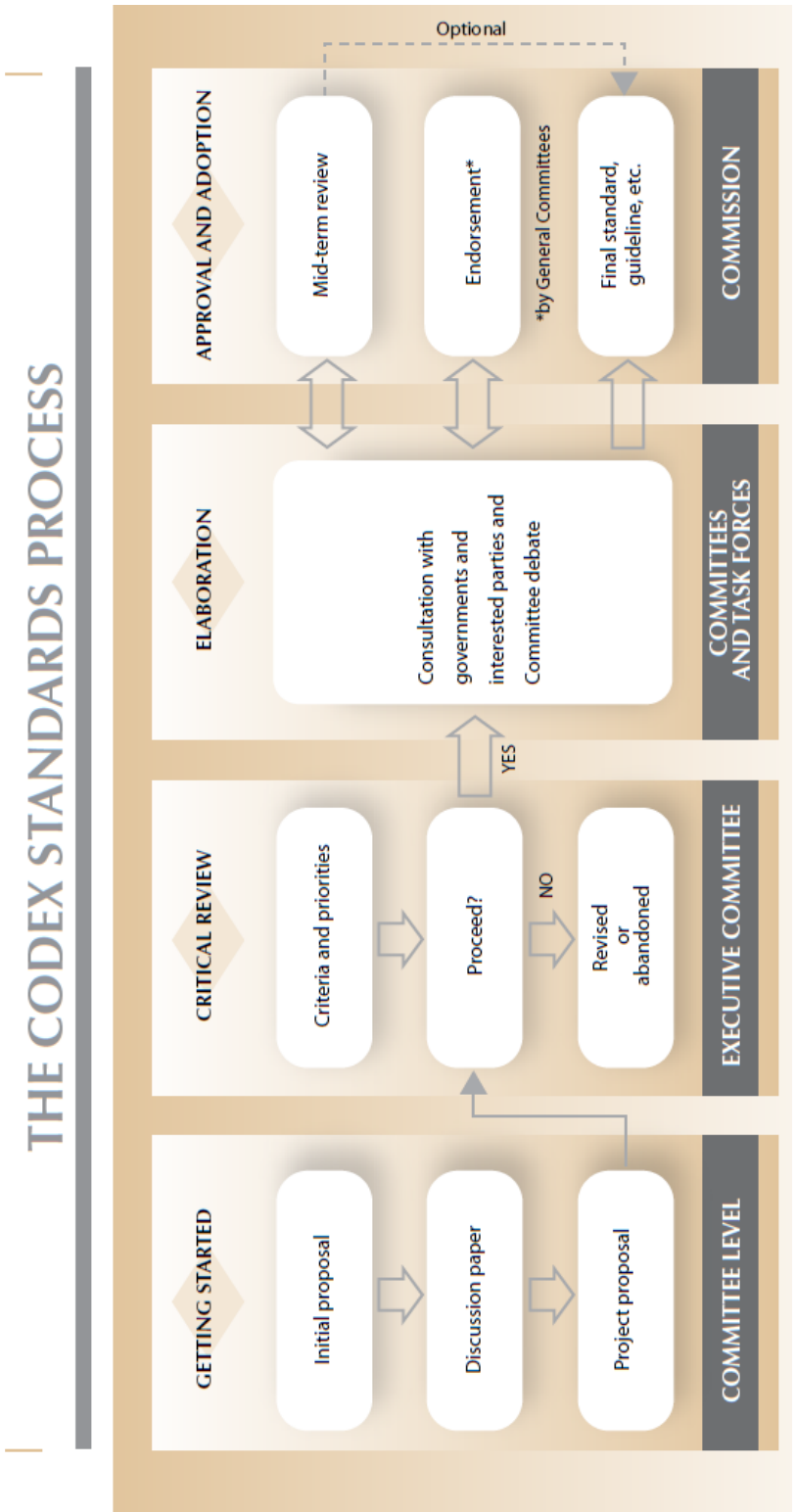

Fig. II.1. How Codex Alimentarius Commission works[3].

II.1.2. Economic and health concerns

A consumer is not aware of the compounds or microorganisms on the food. Due to the processes that food undergoes, different microorganisms can occur, or chemical residues can persist. There is an important risk to contract a foodborne disease or ingest chemically contaminated food, and the purchaser is not able to measure that risk. Economists define foodborne illness as a combination of two expressions, one called "*experience good*" and another named "*credence good*". "*Food is an experience good in that the consumer can determine whether it will cause illness only after it is consumed. Food is a credence good in that the consumer frequently cannot tell with certainty whether it actually caused an illness*", as both expressions are defined in the Food Safety Handbook. This refers to the gap between the ingestion of food and time in suffering the symptoms of a disease, being more challenging to discover the origin of that illness accurately. Therefore, avoiding this problem and the possibility of undergoing a disease, a domino effect can be produced along the *farm-to-table* chain[4].

From here, many hazards need to be controlled and determined to ensure the food safety. However, strengthening all laws, requirements, and levels to protect more the consumers raises the price of product due to the high inversion in control assays. Then, we must answer a question: *How much safety?* Suitable regulations can be produced appropriate food prices, non-expensive control assays, better

food quality and safety, leading to better consumer health and diminishing associated societal costs[4].

Thus, there are many examples in the literature where the burdens associated with foodborne diseases, foodborne outbreaks or chemically food contamination (such as biological toxins or mycotoxins) are very significant. For example, WHO estimated that 2.2 million of people (1.9 million children) pass away for foodborne and waterborne illness together[5]. As a consequence of salmonella infections, annual costs leveled on the health care system are estimated to be around 3 billion euros in the European Union[5].

Some studies say that 845,000 foodborne illnesses are caused by the pathogen annually and provoked $1.9 billion in economic burden. The economic burden of $903 million to $4.6 billion (90% credible interval) is produced by Campylobacter occurrence of 337,000 to 1.6 million cases (90% credible interval)[6].

In contrast with foodborne outbreaks, which are usually more acute than chronic as other threats (e.g., mycotoxins), chemical hazards can lead to other scenarios such as prolonged food infections or long-term diseases. For that reason, economic deficits are more focused on different matters, such as prevention, control, and detection[7]. In fact, rice is one of the most consumed nourishment and the most frequently described as mycotoxin occurrence. In 2013, the rice production was 746.4 million tonnes, being valued in $400-650 dollars for five different types and being obvious that mycotoxin contamination can produce the

economic losses and the global concerns (in society, industry and governmental administrations[7].

II.1.3. Hazards

Foodborne hazards have demonstrated to be an actual concern and issue for present population. Owing to the globalization of the food trade and its continuously variable situation, all foodborne hazards can be untraceable, missing the origin of that hazards and making tougher to resolve the problem. Likewise, the contamination can be spread from that source (animal feed, water, contaminated plants or cereals) to animals or, even, humans. As it has been told before, this, not just has health concerns, also has economic burdens as it was aforesaid[1].

In the introduction, different threats, perhaps the most meaningful, were named. They are well-known enough, but some of them do not have so much dissemination. According to their morphology, several threats can be found in nature. On the one hand, there are microbiological hazards which are composed by pathogens in the broadest idea of the meaning. On the other hand, there is diverse kind of chemical hazards which have a biological origin (mycotoxins and allergens are representative examples). Besides, there are chemical hazards whose origin is chemical or synthetic. Among these last ones, we can find pesticides, such as triazines (atrazine), carbamates (carbofuran), organochlorides (DDT) and organophosphate compounds (e.g., malathion, parathion, and chlorpyrifos)[8], heavy metals (Pb, Cr, Ar, Cd, and Hg), polychlorinated biphenyls (PCBs),

dioxins, phthalates and veterinary drugs (e.g., semicarbazide, clenbuterol, streptomycin, and tetracycline)[1,8].

For that reasons, selected hazards will be broadened in the next sections.

II.1.3.1. Allergen

The definition of allergen is an antigen which provokes an atypical and strong immune response. Although, there are other concepts which are lesser-known and introduce exciting ideas. The food allergy can be defined as "*an adverse health effect arising from a specific immune response that occurs reproducibly on exposure to a given food*", and food intolerance, "*as nonimmune reactions that include metabolic, toxic, pharmacologic, and undefined mechanisms*"[9]. Therefore, the intake of feed can produce different symptoms depending on the complaint of the individual, and in function of gravity of the complaint. Despite this, we are going to focus on food allergy and allergens.

Food allergy is a novel concern with great repercussion due to those antigens can provoke unpredictable and vastly random reactions, although consumption of the allergen is very low (even in traces) and it is influenced by the sensitivity of the individual[10]. Food allergies affect approximately 1-2% adults but less than 10% of the population, approximately 5% of young children, although the prevalence is growing according to recent studies[9,11,12]. In order to avoid adverse and uncontrolled reactions, new methodologies have to be developed to get

the determination more accurately and sensitively to improve the food safety and consumers' health[11]. In this sense, the reports informed that the most frequent allergies in infants are cow's milk (2.2%), peanut (1.8%), and tree nuts (1.7%), and the most frequent allergies in adults are shellfish (1.9%), fruits (1.6%), and vegetables (1.3%)[9].

Allergies are caused by an antigen and can be classified into 4 categories called immunoglobulin E (IgE)-mediated, non-IgE-mediated, mixed, or cell-mediated reactions, among the immune-mediated adverse food reactions by National Institute of Allergy and Infectious Diseases' Expert Panel[9]. Another classification is established based on the appearance of symptoms, where type I is the fastest appearance (immediate hypersensitivity) between minutes and 2 hours, and type IV is the slowest allergy (delayed hypersensitivity) where the development of disorders takes hours or days (usually given in cell-mediated reactions)[11]. **Table II.1** summarize foremost classes, allergens which trigger those signs, and symptoms[9].

Table II.1. Summary of allergy classes, allergens, and their symptoms.

Class	Allergen	Symptom
IgE antibody dependent (acute onset)	Egg, milk, wheat, soy, peanut, tree nuts, fish, shellfish, seafood, raw fruit and vegetables, beef, pork, lamb	Urticaria, angioedema, oral allergy syndrome, rhinitis, asthma, gastrointestinal hypersensitivity, anaphylaxis (and its varieties)
Mixed IgE antibody associated/cell-mediated (delayed-onset/chronic)	Atopic dermatitis, eosinophilic gastroenteropathies (dysphagia, ascites, weight loss, edema, obstruction)	Major allergens, particularly egg, milk
Non–IgE-mediated (delayed-onset/chronic)	Enterocolitis syndrome, allergic proctocolitis, Heiner syndrome, celiac disease (enteropathy and malabsorption)*	Cow's milk, soy, rice, oat, multiple other solids, and gluten (e.g., wheat, rye, barley)*
Cell mediated	Allergic contact dermatitis	Metals

*Autoimmune disorder

II.1.3.2. Pathogen

Microorganisms are very well-known since many decades ago. Notwithstanding that there are many methodologies against

microorganisms from early in the twentieth century (e.g., pasteurization), new microbiological hazards have become in a real threat to our health, and we need detection and prevention techniques as well as methods to kill pathogens. First discovered hazards were tuberculosis and salmonellosis in milk, and botulism in low acid foods, which were neutralized through heat the containers without losing their properties[1].

The pathogen illnesses are the second worldwide cause of morbidity according to WHO. Malnutrition, hygiene conditions and low water quality, among others, promote the contagion and propagation of pathogen in developing countries. Despite the bigger power of developed countries to get better methodologies and techniques, and enhanced medical cares (medicines and treatments) to combat and detect food-borne pathogens, they can occur from outbreaks or, even proliferate from food sources. Further these reasons, pathogens are significant, not only in food safety field, in other fields as well, such as drug discovery, clinical research, biological warfare, between others[13].

Global food trade makes easier the spread and capacity of infection in nourishments, plants, animals and people, managing more difficult the food control and incurring expenses in all involved matters (companies, administration, and health). Pathogens provoke about 40% of the ~50 million losses worldwide every year. In the United States, approximately 76 million illnesses were estimated by them, more than

300,000 hospitalizations and 5,000 demises each year[14]. In addition, two well-known pathogens, E. coli O157:H7 and Salmonella, produced approximately 1.4 million foodborne illness with $2.7 billion in associated medical costs, productivity deficits, and costs of premature losses in 2010[15].

These microbial hazards are composed bacteria, viruses, fungi and parasites[16]. The most common pathogens, which can be outlined, are Escherichia coli, Salmonella, Staphylococcus, Listeria monocytogenes and Aeromonas, and virus such as Norwalk virus, and Norovirus[14]. Principal features are outlined in **Table II.2**.

Escherichia coli (E. coli) is a principal specie inside the animal gut, and it is one of the most frequent pathogens in food. It is carried in the intestinal tract of cattle and other animals. It was first identified as a pathogen in hemorrhagic colitis outbreaks in 1982. Among this specie, E. coli O157:H7 is a strain of this and able to express Shiga toxins (even with small amount of cells, <10 cells) which provoked the diseases[14,17]. Other important specie is Salmonella. This bacteria leads to salmonellosis which can threaten life of the patient when it goes to blood circulation. In fact, salmonellosis outbreaks have been recognized to happen from enormously small infective amounts (<10–100 cells)[14,18,19].

Two other bacteria which deserve to be highlighted are Staphylococcus and Listeria monocytogenes. Staphylococcus is able to synthesize a coagulase enzyme. A strain of Staphylococcus, S. aureus

produces enterotoxins, e.g., staphylococcal enterotoxin A and B with superantigenic activities[14,20]. Listeria monocytogenes can cause a tremendously severe disease called listeriosis (mortality rate about 30%)[14,21]. Furthermore, there is a virus which is notorious for mentioning, Norovirus (NoV). It is a RNA virus in the family of Caliciviridae viruses or Calicivirus. With virus amounts smaller than 10^2 copies/mL, an infection is possible. The symptoms generated by NoV include vomiting, gastralgia, diarrhea, fever and, rarely, the death of the elderly or children due to dehydration[14,22].

Table II.2. Summary of most representative pathogens.

Pathogen	Genus	Species	Infection source	Symptoms
E. coli	Gram-negative	*E. coli* O157:H7	Unpasteurized milk, untreated water, and food related to animals (meats) or vegetables, fruits and byproducts	Gastroenteritis, urinary tract infections, hemorrhagic colitis and Crohn's disease.
Salmonella	Gram-negative	*S. enterica*, *S. typhimurium* and *S. pullorum*	Water, chickens' intestines and can also affect to ovaries (in hens)	Salmonellosis (fever, diarrhea, abdominal cramps and possible life risk)
Staphylococcus	Gram-positive	*S. aureus*	Medical-related procedures, applications or devices	Sialadenitis

Table II.2. Continued.

Pathogen	Genus	Species	Infection source	Symptoms
Listeria	Gram-positive	*L. monocytogenes*	Meats, milk, cheese, ice cream, raw vegetables, and muskmelon	Listeriosis (meningitis, septicemia, abortion, and febrile gastroenteritis)
Calcivirus	RNA virus	*Norovirus*	Via direct infection, person-to-person secondary infection, or spreading by food handlers	Gastroenteritis, nausea, vomiting, diarrhea, and abdominal pain with headache and low-grade fever.

II.1.3.3. Mycotoxin

The broad variety of chemical synthetic-origin hazards is significant because they are human-made, although we should regulate its synthesis and avoid them. Nevertheless, biological-origin hazards are more difficult to avoid. Microorganisms synthesize them as fungi. In reality, own plants and, its products and byproducts use as a substrate for growth of this kind of molds[1], making simpler the fungi spread through the crops and global market. In fact, the storage conditions, either suitable or unsuitable, favor the growth of fungi, increasing the risk of mycotoxin contamination. Actually, inappropriate storage conditions (i.e., high temperature and moisture) make more prone the proliferation of these fungal species[23]. This concern is manifest due to studies which reveal 25% of the worldwide crops are contaminated with fungal mycotoxins, entering the food chain and affecting to animal and human health[23–25].

A mycotoxin is a secondary metabolite produced naturally by filamentous fungi[26]. The most important species which produce the most toxic mycotoxins are *Aspergillus*, *Fusarium,* and *Penicillium*. Among these mycotoxins, we can find aflatoxins, ochratoxins, some trichothecenes (fumonisins, deoxynivalenol, T-2, HT-2, and zearalenone), patulin, citrinin, and ergot alkaloids[25]. The name for the disorder suffered by the ingestion of contaminated food with mycotoxins is "*mycotoxicoses*" and was considered as "neglected disease"[27]. Mycotoxins affect to animal and human lives, owing to strong

carcinogenic, teratogenic, and mutagenic effects that they possess[28]. In the tenth century, a chronicler related a disease called "St. Anthony's fire" which many people across Europe died as a result of the intake of moldy rye. They suffered epileptic attacks, vomits and signs of madness provoked by the sensation of internal burning. Currently, this disease is known as ergotism[23]. Aflatoxins, and among them, Aflatoxin B1 (AFB1) is the most studied and the most toxic mycotoxins. It was found out in the 1960s, establishing the beginning of mycotoxin recognition. From here, numerous regulations and guidelines were established to ensure the animal and human health, and avoid economic losses[27].

In this sense, the harmonization of regulations in countries, regions and worldwide level has improved and has been multiplied. This was demonstrated because, along the years, the number of nations with directives for mycotoxin increased 33 in 1981, 56 in 1987, 77 in 1995, and 100 in 2003[27]. Progressively, different communities, regions, and organizations started to work together with a goal in common. In this way, the European Union, MERCOSUR (Southern Common Market), Australia and New Zealand synchronized their regulations over national ones. Moreover, created organizations such as Joint FAO/WHO Expert Committee on Food Additives of the United Nations (JECFA) and the European Food Safety Authority (EFSA), and AOAC International and the European Standardization Committee (CEN) play an important role in strengthening regulations and official analytical methods to determine mycotoxin in foodstuff[27].

Aflatoxins were first identified due to the death of 100 000 turkeys for contaminated fodder (Turkey-X) in the United Kingdom in 1961[29]. They are produced by *Aspergillus flavus* and *Aspergillus parasiticus*, becoming the most toxic group of mycotoxins (e.g., Aflatoxin B1 (AFB1) is considered as group 1 carcinogen (potent human carcinogen) by de International Agency for Research on Cancer (IARC)). Due to that toxic power, AFB1 was used as biological warfare[30]. They are very persistent and can pass to the food chain, indeed, AFB1, after metabolizing in cows, is converted in Aflatoxin M1 (AFM1, its hydroxylated byproduct) and is excreted in milk[25]. Another significant aflatoxin is Aflatoxin G1 (AFG1), whose structure is collected in Figure 2, together with AFB1 and AFM1.

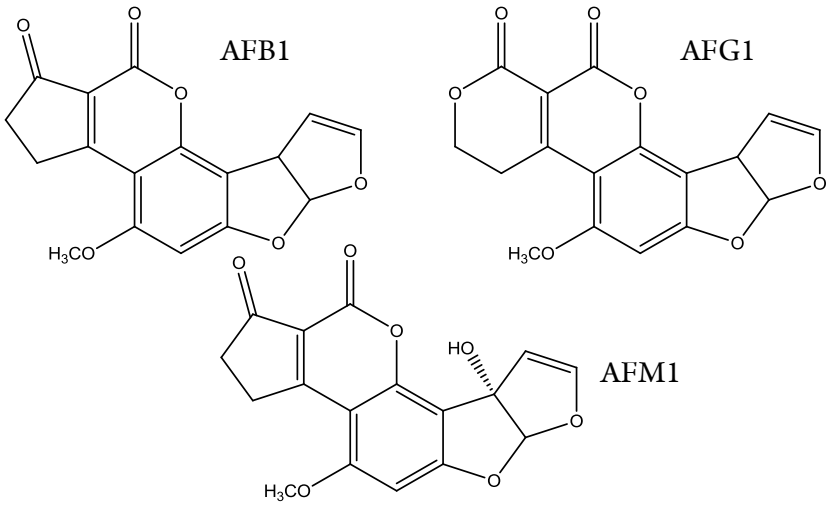

Fig. II.2. Scheme of structures of AFB1, AFG1, and AFM1.

Between the more important disorders, aflatoxins can attack to liver, kidney, nervous system, endocrine, and immune systems[25]. Aflatoxins can occur in many foodstuffs such as groundnuts, wheat,

maize, barley, milk, dried fruits and their products[30]. For these reasons, European Union Commission has specific regulations for aflatoxins, fixing the Maximum Residue Levels (MRLs), for example, in maize and rice at 5 μg Kg^{-1} [31] and 2 and 4 μg Kg^{-1} AFB1 and total aflatoxins in food, and 0.05 μg Kg^{-1} of AFM1 in milk[32].

Fusarium mycotoxin is another meaningful group of mycotoxin. They are produced by a type of fungi with the same name. Among these, we can find different toxins such as fumonisins (FBs, they will be further discussed), zearalenone (ZEA), moniliformin (MON) and trichothecenes[33]. These last ones are a kind of related cyclic sesquiterpenoids, divided into four groups (Type A-D), although the more significant are type A and B[33]. Between these two categories, T-2 and HT-2 represent of type A, and deoxynivalenol (DON) and nivalenol (NIV), of type B[34]. After T-2, DON is the most toxic in this group (**Fig. II.3** illustrates the structure). However the occurrence of DON is greater. It provokes feed refusal, vomiting, anemia, hemorrhage, and immunosuppression[34]. It can contaminant cereals such as corn, wheat, oats, barley or other processed products including bread, beer, and flour[35]. European Union Commission established MRLs ranges from 200 to 1750 μg Kg^{-1} depending on the class of cereal and cereal products[34,36]. ZEA is a nonsteroidal oestrogenic mycotoxin (**Fig. II.3**) produced by some species of *Fusarium* (*Fusarium graminearum (Gibberella zeae)*, *Fusarium culmorum* amongst others). It is stable, even at high temperatures, being able to remain in the feed and go to food chain[37,38]. It can occur in different cereals such as maize, barley,

oats, wheat, rice, and sorghum. Precocious puberty, hyperplasic and neoplastic endometrium, and human cervical cancer are the main disorders to be outlined, due to affect the estrogenic characteristics[39]. The MRLs for ZEA were regulated at 20, 75, and 100 g Kg^{-1} for baby food, cereal flour, and unprocessed cereals, respectively, by European Commission[37,40–42].

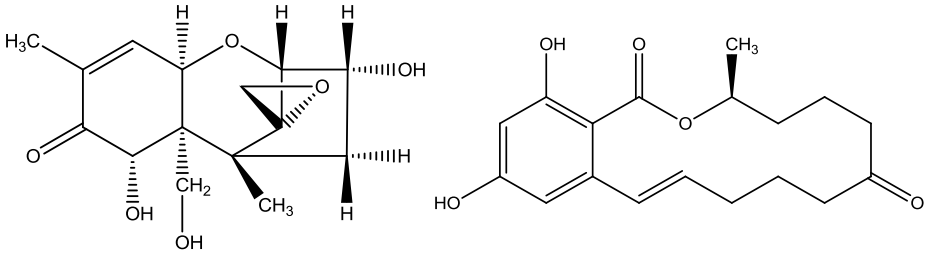

Fig. II.3. Illustration of structures of DON and ZEA.

Notwithstanding the importance and toxicity of these mentioned mycotoxins, there are more mycotoxins whose concern have enlarged in last years. Fumonisins are ones to be outlined, which are produced by different strains of *Fusarium* (*Fusarium moniliforme*, *Fusarium vertillioides* y *Fusarium proliferatum*). They are classified into three groups (A, B and C), though the most abundant and toxic mycotoxins are the group B between, at least, twenty-eight fumonisins described. Among these, Fumonisin B1 (FB1) is the most significant and hazardous (usually constitutes about 70% of the total FBs naturally found)[43], following of Fumonisin B2 (FB2) and Fumonisin B3 (FB3)[44]. These FBs have a very similar structure, just like it is shown in **Figure II.4**. FB1 was isolated for the first time in 1988[45]. It can provoke leukoencephalomalacia in horses[46], pulmonary edema in pigs[47], nephrotoxicity, and liver cancer in rats[48]. It can also produce liver, kidney

and esophageal cancer in humans[49–51]. For these reasons, IARC and U.S. Environmental Protection Agency categorized as a 2B carcinogen (possibly carcinogenic to humans)[52]. Fumonisins can usually appear in maize and maize-based feed naturally, but it can also contaminate such as barley, wheat, rice, peanut, pistachio, raisin, fig, fruits, and milk[53]. In fact, important derived foodstuff like beer was reported with FBs contamination[54,55]. U.S. Food and Drug Administration (FDA), as well as European Commission, decided to mark the MRLs for FBs (sum of FB1 and FB2), being ranged from 2 to 4 mg L^{-1} in animal studies[56] and from 200 μg Kg^{-1} for baby food to 4000 μg Kg^{-1} for raw maize, respectively[40–42].

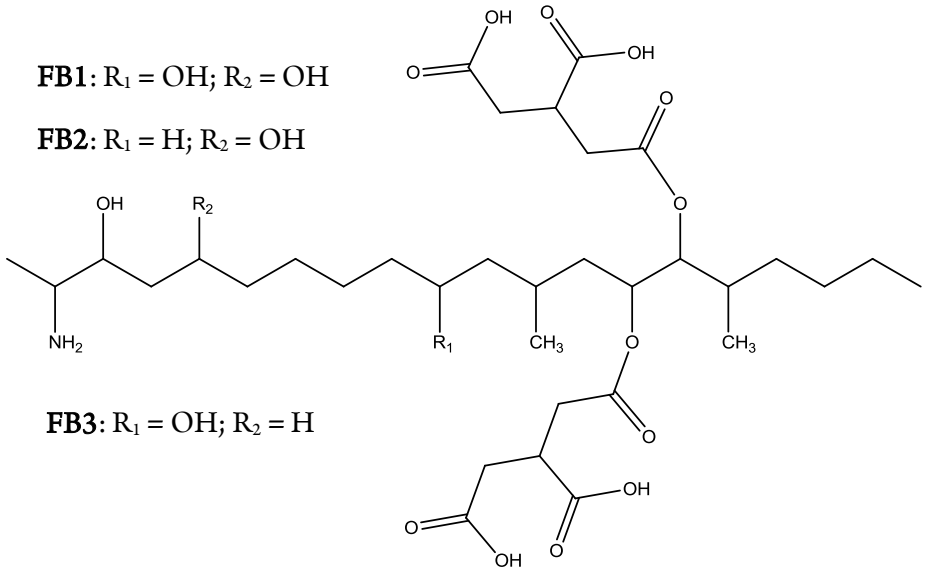

Fig. II.4. Scheme of the chemical structure of FB1, FB2, and FB3.

Ochratoxins are another important group of mycotoxins. There are proofs of its impact appearing on BBC news where the piece of news told about a contaminated wheat with ochratoxins to elaborate pasta and the health concern[23]. They were isolated in 1965, actually one of

them, Ochratoxin A (OTA, **Fig. II.5**)[25]. They are principally produced by *Aspergillus ochraceous*, *Aspergillus carbonarius* and *Penicillium verrucosum*[57,58]. There are other two ochratoxins (B and C), but their occurrence and toxicity are very low in comparison to OTA[59]. OTA is also considered a group 2B carcinogen by IARC due to nephrotoxic, hepatotoxic, teratogenic, and carcinogenic effects in animals and human[58,60]. This mycotoxin can appear in common nourishments such as cereals, beans, groundnuts, spices, dried fruits and pork meat, and furthermore, in very consumed derived products coffee, cocoa, milk, grape juice, beer, and wine[57,60]. Despite all decontamination and improving processes, OTA remains in feed due to its high stability. In fact, OTA can remain in the human blood and breast milk during several days (half-time life in serum ~35 days), after intake of contaminated foodstuff[57]. For that reasons, European Commission established strong requirements over OTA regulations. In that way, limits for OTA are 5 μg Kg^{-1} in raw cereals grains and 3 μg Kg^{-1} in processed cereals products for direct human consumption, 2 μg Kg^{-1} in wines and grape-containing beverages, 5 μg Kg^{-1} in roasted coffee beans and 10 μg Kg^{-1} in soluble coffee and 0.5 μg Kg^{-1} in baby foods[41,61].

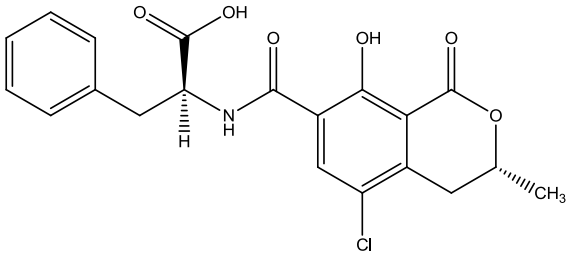

Fig. II.5. Structure of OTA.

II.2. Biosensors

To perform a true robust, reliable, sensitive, accurate, and precise analysis is necessary to develop a good methodology based on the right detection technique. In Analytical Chemistry, the measure or signal is one of the most important stuff with the aim of achieving an accurate value. This broad field is comprised of many methodologies and techniques, which can be suitable to make a reliable analysis.

On the one hand, we can find methodologies or techniques called routines, such as liquid chromatography (LC), coupled to mass spectrometry (MS), enzyme-linked immunosorbent assay (ELISA) or polymerase chain reaction (PCR). There are many combinations between them, developing a multitude of analysis methods in function of the goal we want to reach. These analytical methods are essentially focused on extraction, separation and detection or/and determination. Related to the food safety analysis, the found matrices are typically natural food (e.g., fruit), raw material (e.g., cereals), derived animal foodstuff (e.g., milk), and processed food (e.g., snacks). In this way, an important extraction step can be necessary to obtain the desired analyte. Once this is done, the next step is the identification of the analyte through a separation technique, followed by a detection technique.

In the literature, we can find a large number of examples about analysis methods of a huge variety of nourishment. Associated with the analysis of the different groups of analytes presented in the epigraph II.3, a plethora of techniques has been reported.

For instance, LC and LC-MS, ELISA, mainly using colorimetric detection, and DNA-based methods are the standard techniques and methodologies utilized to detect allergen in food[1,2].

Related to pathogen determination, DNA and antibody (Ab)-based methods are also broadly used. However, cell culture and colony counter are ones of the most conventional methods utilized since decades ago[3,4].

In mycotoxins, the food safety-related analytes studied in this Doctoral Thesis, thin layer chromatography (TLC), LC or high-performance liquid chromatography (HPLC), and gas chromatography (GC), also coupled to MS, are carried out. In addition, ELISA methodology is also performed for the same goal[5]. However, according to AOAC, HPLC was selected as an official method for mycotoxin detection and determination, existing approximately 45 official methods[6]. Moreover, on the way to get more sensitivity and selectivity, HPLC can combine to MS or MS tandem (LC-MS or LC-MS/MS)[5,7].

All in all, these methods are reliable, sensitive, accurate and robust. Notwithstanding all these features and those methods are increasingly improving, these methods are arduous and expensive, need of technical skills, and take much time to get results[8,9]. For these reasons and with new needs and issues appearing, novel analytical tools were developed due to vast growth of the technology. With this progress, technology produced sensors or biosensors as an actual alternative for different fields including food safety analysis.

According to Viswanathan et al., a biosensor "*is generally defined as a measurement system that consists of a probe with a biological recognition element, often called a bioreceptor, and a transducer*"[8]. In order to give an understandable information to the user, the transducer transforms the interaction between the biorecognition element and the analyte in some measurable stimuli (e.g., electrical signal), which matches with the number of recognized analyte. There are various kinds of biosensors, though electrochemical biosensors are the most widespread biosensors, owing to improvement of bioreceptors and transducers because of enhanced research in this field[8]. The first example found in the literature as a commercial device was the biosensor for glucose detection in blood, launched in 1975 by Yellow Spring Instruments[10,11].

From here, biosensors have evolved to reach more fields and analytes due to their attributes. These biosensors satisfy these new needs such as selectivity, sensitivity, low-cost, portability and rapid detection[8].

II.2.1. Elements of biorecognition

Biosensors are based on the aforementioned components and can adopt different ways to be performed, varying the biorecognition element. The function of these bioreceptors is to selectively recognize the analyte in complex matrices, avoiding potential interferences, which have awakened its great interest in the sensors field. The bioreceptor can be an enzyme, an antibody, a protein or a nucleic acid[12]. As biorecognition element, enzymes were the first one, and consequently,

biosensors took the name from them. In this case, enzymes transform a substrate into a product, which can be detected directly by the transducer. Moreover, some enzymes can need a cofactor to produce that reaction and detection, or even amplify the reaction. As it is aforesaid, the first example was the glucose biosensor with Glucose Oxidase (GOx)[11]. The starting point of biosensors (also known as enzyme sensor) was the entrapping into membranes or polymers[13]. However, the evolution of biosensors has made possible the vast number of combination of enzyme immobilization, from the physical union (physical entrapment or adsorption) to chemical binding (with linkers)[12,13]. Thus, the amalgamation of enzymes and materials on the electrode surface can be limitless.

For nucleic acids, DNA is the most known and plays a significant role in recognition of elements with a particular structure o sequence. The use of single DNA/RNA chain or synthetic oligonucleotides, called aptamers, is a highly interesting approach. They are a small chain (between 40–100 bases[8] or molecular mass 5–15 kDa[14]) and can detect many varied compounds, from ions and small molecules (toxins, low-molecular-weight ligands or peptides, drugs) to high weight molecules (such as proteins) and whole cells[8]. The binding mechanism is similar to antibodies through Van Der Waals forces, taking another three dimensional conformation[15]. Moreover, aptamers have more chemical and thermal stability, less variability and price compared to antibodies[15], and high reproducibility binding feature[14]. In this sense, the production of aptamers is made through Systematic Evolution of Ligands by

Exponential Enrichment (SELEX) process to improve the selectivity of the aptamer[16]. In order to realize that process, a library of random nucleic acids (approximately 10^{15}-10^{16}) is incubated with the target molecule to get the complex with the correct nucleic acid. Then, this complex is separated from the rest and the target molecule is released from the aptamer to elute the last one. Next, the selected chain is amplified to achieve the aptamer for the target molecule[16,17]. Thus, it is possible to obtain several different aptamers for numerous diverse epitopes and compounds.

However, the most used biorecognition element is the antibody (Ab). Abs are natural proteins which can bind specific molecules named antigen (Ag) or foreign body. These molecules provoke an immunologic reaction, which stimulates the Ab synthesis to bind specifically to them. This duality Ab-Ag is widely utilized in diagnosis and was implemented in biorecognition sensor called immunosensors[12,18,19]. This high specificity associated with the Ab-Ag interactions gives an elevated selectivity to immunosensors. Some sorts of Ab can be developed as polyclonal Ab (pAb), monoclonal Ab (mAb), recombinant Ab (rAb), and even, antigen-binding region (Fab) fragments or also known as nanobody (Nb)[20]. The specificity and purity vary in function of the type, being pAb, the lesser specific Ab[14,21]. In order to gain selectivity, mAb are purified and produced by particular methods, the same as rAb which is synthesized without the necessity of animals[14,21]. Antibodies fragments or nanobodies can be obtained by recombinant technologies to isolate the variable region (V_c)[14,21], or

obtained from the particular family of animals such as camelids (e.g., dromedaries, llamas, alpacas), or produced by bacteria and yeast[20,22]. Last ones become in good alternative to mAb, due to different characteristics such as less cost, renaturation, high solubility, stability, and resistance[20].

Most immunosensors are based on ELISA methodology, where one of the species is immobilized on a solid support, and makes use of an enzyme as a tracer of changes provoked in the Ag-Ab complex. One good advantage of employing an enzyme as the tracer is the possibility of amplifying the signal, due to specific Ag-Ab interactions, with the aim of increasing the sensitivity[8]. Among the most used enzymes, we can find glucose oxidase (GOx), alkaline phosphatase (ALP), and horseradish peroxidase (HRP)[23]. All these enzymes can utilize different co-substrates ELISA methodology was implanted in the development different strategies to detect analytes by immunosensor, being compatible with different detection techniques, as electrochemical techniques.

Different immobilization supports and strategies can be used. In electrochemical detection, immobilizing the antibody onto the working electrode surface can suppose laborious work with many steps, to be incompatible with large-scale fabrication, or to affect the working electrode surface (modifying its composition, reproducibility issues, passivation). The use of magnetic beads (MBs) avoids these troublesome features. These beads made of Fe_2O_3 and Fe_3O_4 are

covered by a functionalized polymer with linkers to modify the surface[24,25]. Among the advantages, MBs can enhance the immunosensor performance are higher sensitivity (more molecules can be immobilized), better immunological reaction (by lower reaction times and higher assay kinetics, due to high surface area), easy manipulation by a magnet, minimization of matrix effect, simplicity in washing steps, and compatible with mass production[26–29].

II.2.2. Electrochemical detection

Electrochemical techniques confer more qualities, such as the possibility of miniaturization, portability, low-cost, easy-to-use (non-specialized skills), sensitivity, mass production, analysis of small volumes, and compatible fabrication of custom-made electrodes (nanomaterials, metallic nanoparticles, or multiplexed analysis)[8,26]. Moreover, that inherent miniaturization property of the electrochemical techniques becomes a good partner for microfluidic methodologies such as microfluidic devices (i.e., microchip) and *lab-on-a-chip* (LOC) systems. Therefore, both together can become in an exceptional combination for food analysis[30].

All these features have become to electrochemical methods in a powerful tool for food analysis. For that, the area of electroanalysis has successfully achieved to satisfy the needs demanded by the previous and current food industry. Thus, electroanalysis has played a relevant role in food quality and food safety assessment in the last decades. Therefore, the combination of sensors and biosensors technology together with

suitable electrochemical techniques has allowed the implementation of affordable, disposable, rapid and reliable detection methods[13].

Electrochemical methods are classified according to the way to be performed. In this sense, they are organized into three principal groups: potentiometry, coulometry, and voltammetry[12]. Potentiometry measures the potential of a solution between two electrodes (reference electrode with a constant potential; and indicator electrode with changing potential depending on the composition of solution), evaluating its composition. Coulometry measures the concentration of the sample through the number of electrons that pass between the electrodes, or vice versa. The potential or current is applied to convert specie oxidation state totally. Voltammetry uses a three-electrode system (reference, counter, and working electrode). Applying a constant or variable potential, the current is measured on the working electrode surface. It gives the info of the reduction potential and its reactivity. In addition, there are other techniques which are based on other performances. For instance, electrochemical impedance spectroscopy (EIS) is an electrochemical technique based on alternating current (AC) voltage of small amplitude which is transformed in a current response. Thus, the changes in Faradaic processes describes the physicochemical processes of broadly different time constants, sampling electron transfer at high frequency and mass transfer at low frequency on the electrode surface[12,13].

Sensors or biosensor can be ordered in the same way by techniques. The most recurrent techniques are voltammetric techniques, concretely, differential pulse voltammetry (DPV), square wave voltammetry (SWV) and amperometry or chronoamperometry (AMP or cAMP)[26]. Each technique has its own characteristics, being able to use according to the analyte, methodology, and sample.

Furthermore, the working electrode gained attention with the development of new ways to fabricate and the appearance of new materials and nanomaterials. The evolution from conventional electrodes to novel electrodes (screen-printed electrodes, SPE) have transformed to the electrode in a powerful tool for the development of sensors. The election of a good electrode can suppose a better performance. For that reasons, SPE technology revolutionized the sensor world, because it combined better materials with portability, simplicity, mass production and low price. Furthermore, the planar and small design makes easier the modification of working electrode surface and reduces the consumption of sample volume. All in all, it is a perfect tool to develop a great sensor[26,31–33].

To sum up, **tables II.3**, **II.4**, and **II.5** outline different kind of sensor for the described analytes, summarizing the most relevant analytical features and in accordance with the electrochemical technique.

Table II.3. Summary table of allergen detection

Analyte	Assay format	Detection technique	LOD	DR	Precision (CVs)	Sample	Recovery (%)	Remarks	Ref.
Ara h 1	Sandwich ELISA	LSV	3.8 $\mu g\,L^{-1}$	12.6-2000 $\mu g\,L^{-1}$	< 8.7%	Cookies and chocolate	> 96.6	Total analysis time 3h 50min	34
	Stem-loop DNA	DPV	0.041 fM	10^{-16}-10^{-13} M	< 6.7% (in samples)	Peanut milk beverage	86.8-110.4	Outstanding LOD, reproducibility and stability	35
	Stem-loop DNA	EIS	0.35 fM	10^{-15}-10^{-10} M	---	Peanut milk beverage	---		36
Ara h 2	Sandwich ELISA	DPV	10 pM	$5x10^{-11}$-$5x10^{-8}$ M	7.22%	---	---		37
Ara h 2 Ab	Ara h 2-His-tagged peptide	AC voltammetry	1 pM	1-10 pM	---	---	---	Electrode reusability	38

Table II.3. Continued

Analyte	Assay format	Detection technique	LOD	DR	Precision (CVs)	Sample	Recovery (%)	Remarks	Ref.
Der p1	Sandwich ELISA	LSV	0.3 μg L^{-1}	---	5.3% (5 μg L^{-1}) and 1.5% (50 μg L^{-1})	Real house dust samples	---	Total analysis time 30min	39
Der p2	Anti-dust mIgG	EIS	1 pg mL^{-1}	10^{-6}-5 μg mL^{-1}	---	---	---	Corroboration by fluorescence	40
Der p2	Anti-dust mIgG	EIS	0.1 pg mL^{-1}	10^{-4}-10 ng mL^{-1}	---	---	---	Remarkable limit of detection	41
IgE (Anti-Der p2)	Sandwich ELISA	EIS	10 pg mL^{-1}	10^{-5}-1 μg mL^{-1}	---	Blood serum	---	Little sample consumption, short sample preparation and detection time	42

Table II.3. Continued

Analyte	Assay format	Detection technique	LOD	DR	Precision (CVs)	Sample	Recovery (%)	Remarks	Ref.
Ovalbumin (OVA)	Sandwich ELISA	LSV	5 nM	11-200 nM	---	---	---	Enables complex biological matrix and pre-concentration	43
Pen a 1 (tropomyosin)	Anti-shrimp tropomyosin with mast cell	EIS	0.15 μg mL^{-1}	0.25-0.5 μg mL^{-1}	< 5%	---	---	Excellent reproducibility	44
Pen a 1 (tropomyosin) and parvalbumin (PV)	Magnetoinfection of mast cells detection via-apoptosis onto magnetic GCE	EIS	0.03 μg mL^{-1} (Pen a 1) and 0.16 ng mL^{-1} (PV)	0.1-1.5 μg mL^{-1} (Pen a 1) and 0.5-4.5 ng mL^{-1} (PV)	2.32 (1000 cells mL^{-1}) and 7.71 (10000 cells mL^{-1})	Crucian carp and brown shrimp	99.55 (1000 cells mL^{-1}) and 97.77 (1000 cells mL^{-1})	Good sensitivity and specificity for different allergens, and exceptional reproducibility	45

Table II.3. Continued

Analyte	Assay format	Detection technique	LOD	DR	Precision (CVs)	Sample	Recovery (%)	Remarks	Ref.
β-lactoglobulin	Anti β-LB functionalization	DPV	0.85 pg mL^{-1}	0.001-100 ng mL^{-1}	---	Cheese snacks, cake, and sweet biscuits	---	Good correlation between ELISA and immunosensor for samples	46

CVs: Coefficients of variation; DPV: Differential pulse voltammetry; DR: Dynamic range; EIS: Electrochemical impedance spectroscopy; ELISA: Enzyme-linked immunosorbent assay; GCE: Glassy carbon electrode; LSV: Linear sweep voltammetry; LOD: Limit of detection; mIgG: Monoclonal immunoglobulin G; PV: Parvalbumin; β-LB: β-lactoglobulin

Table II.4. Summary table of pathogen detection

Analyte	Assay format	Detection technique	LOD	DR	Precision (CVs)	Sample	Recovery (%)	Remarks	Ref.
Aeromonas	Sandwich ELISA	DPV	10^2 CFU mL^{-1}	10^1-10^6 CFU mL^{-1}	---	Water samples	---	Significant limit of detection	47
Bacillus cereus	Sandwich ELISA	AMP	10 CFU mL^{-1}	$5.0x10^1$-$5.0x10^4$ CFU mL^{-1}	4.12%	Milk	90.12–106.33%	Fast detection, high sensitivity, high reproducibility and long-term stability	48
E. coli	DAMP	SPR	1 CFU mL^{-1}	2.5-$2.5x10^5$ CFU mL^{-1}	---	Spinach leaves	---	Electrode reusability and regeneration	49
E. coli O157:H7	Thi-SiO_2-Chi	CV	250 CFU mL^{-1}	$4.12x10^2$-$4.12x10^5$ CFU mL^{-1}	6.4%	Milk and water	---	Good agreement between sensor and, ELISA and counting method	50

Table II.4. Continued

Analyte	Assay format	Detection technique	LOD	DR	Precision (CVs)	Sample	Recovery (%)	Remarks	Ref.
E. coli O157:H7	Sandwich ELISA	DPV	$1.97x10^{-14}$ M	---	---	Fresh beef	---	High sensitivity and specificity	51
E. coli O157:H7	LF	EIS	10^1 (PBS) and $8.3x10^1$ CFU mL^{-1} (milk)	10^1-10^5 CFU mL^{-1}	---	Milk	---	No sample treatment for detection	52
E. coli O157:H7	Mangainin I-Fc-Lip	EIS	10^3 CFU mL^{-1}	10^3-10^7 CFU mL^{-1}	---	---	---	Better LOD than LF biosensor	53
E. coli O157:H7	E. coli Ab-CMs	EIS	4.7 CFU mL^{-1} (flower like) and $9.24x10^2$ CFU mL^{-1} (palm-leaf like)	10-$3x10^9$ CFU mL^{-1} (flower like) and 10^3-$3x10^9$ CFU mL^{-1} (palm-leaf like)	3.8% (flower like) and 5.2% (palm-leaf like)	---	---	Good specificity and different organic microstructures	54

Table II.4. Continued

Analyte	Assay format	Detection technique	LOD	DR	Precision (CVs)	Sample	Recovery (%)	Remarks	Ref.
E. coli O157:H7	Sandwich ELISA	MEIS	50 CFU mL^{-1}	50-500 CFU mL^{-1}	0.95%	---	---	Use of open-surface microfluidics platform and syringe pump	55
E. coli and S. aureus	Amplicon detection via LAMP amplification and pathogen lysis	SWV	30 CFU mL^{-1} (*E. coli*) and 200 CFU mL^{-1} (*S. aureus*)	30-3x10^7 CFU mL^{-1} (*E. coli*) and 200-2x10^5 CFU mL^{-1} (*S. aureus*)	1.7-3.8% (*E. coli*) and 1.7-4.8% (*S. aureus*)	Salmon	---	Real-time detection, multiplexed analysis and high sensitive POC	56
E. coli K-12 and S. aureus	E. coli antibody and S. aureus antibody	Current variations	10^2 CFU mL^{-1}	10^2-10^5 CFU mL^{-1}	---	---	---	Multiplexed analysis	57

Table II.4. Continued

Analyte	Assay format	Detection technique	LOD	DR	Precision (CVs)	Sample	Recovery (%)	Remarks	Ref.
E. coli O157:H7 and S. aureus	*E. coli*-Ab and *S. aureus*-Ab	EIS	10^2 CFU mL^{-1} (both pathogens)	10^2-10^5 CFU mL^{-1} (both pathogens)	9.6% (*E. coli O157:H7*) and 7.5% (*S. aureus*)	---	---	Good reproducibility and stability	58
E. coli O157:H7 and Salmonella typhimurium	Sandwich ELISA	EIS	$3.9x10^2$ CFU mL^{-1} (*E. coli O157:H7*) and $1.66x10^3$ CFU mL^{-1} (*S. typhimurium*)	10^2-10^6 CFU mL^{-1} (both pathogens)	0.95%	Ground beef (*E. coli O157:H7*) and chicken rinse water (*S. typhimurium*)	---	Easy to regenerate, stable, and easy handling	59

Table II.4. Continued

Analyte	Assay format	Detection technique	LOD	DR	Precision (CVs)	Sample	Recovery (%)	Remarks	Ref.
Listeria monocytogenes	Sandwich ELISA	CAMP	---	10^2-10^6 CFU mL^{-1}	---	Milk	---	Good correlation with plate count. Regeneration electrode	60
Norovirus	Direct ELISA	CV	35 copies mL^{-1}	10^2-10^6 copies mL^{-1}	4.38%	Lettuce	---	High sensitivity, selectivity, and reproducibility	61
Salmonella enterica	Sandwich ELISA	Chronocoulometry	$7.6x10^2$ CFU mL^{-1} (PBS) and $6.0x10^2$ CFU mL^{-1} (Water)	---	---	Agricultural water	---	Good specificity and reproducibility	62

Table II.4. Continued

Analyte	Assay format	Detection technique	LOD	DR	Precision (CVs)	Sample	Recovery (%)	Remarks	Ref.
Salmonella enteritidis	Sandwich ELISA	DPV	143 cells mL^{-1}	10^3-10^6 cells mL^{-1}	2.4%	Skimmed milk	83–94%	Good specificity, even in sample	63
Salmonella pullorum	*Salmonella* Ab-HRP	CV	$5.48x10^2$ CFU mL^{-1}	10^2-10^9 CFU mL^{-1}	---	Eggs and chicken meat	---	Good stability, reproducibility, and specificity	64
Salmonella pullorum and Salmonella gallinarum	Sandwich ELISA	CV	$3x10^3$ CFU mL^{-1}	10^4-10^9 CFU mL^{-1}	9.07%	Eggs and chicken meat	---	Good agreement with culture method	65
Salmonella pullorum	Sandwich ELISA	DPV	89 CFU mL^{-1}	10^2-10^6 CFU mL^{-1}	---	Chicken liver	---	Use of silica-coated magnetite particles (SiO_2/Fe_3O_4) and great agreement with culture method	66

Table II.4. Continued

Analyte	Assay format	Detection technique	LOD	DR	Precision (CVs)	Sample	Recovery (%)	Remarks	Ref.
Salmonella typhimurium	Sandwich ELISA	DPV	5 CFU mL^{-1}	10-10^5 CFU mL^{-1}	5.1%	Tap water and milk	---	Good agreement with counting method, good selectivity, and LOD	67
Salmonella typhimurium	Aptamer	EIS	3 CFU mL^{-1}	10^2-10^8 CFU mL^{-1}	5.2% (Standard) ; 11% (Samples)	Apple juice	---	LOQ of 100 CFU mL^{-1} s	68
Staphylococcus arlettae	Bacteriophage	EIS	2 CFU	2-2x10^6 CFU	2.5%	River water and apple juice	---	Fast time response (2 min) and great stability (3 months)	69

Table II.4. Continued

Analyte	Assay format	Detection technique	LOD	DR	Precision (CVs)	Sample	Recovery (%)	Remarks	Ref.
Staphylococcus aureus	Competitive ELISA	AMP	1 CFU mL^{-1}	10-10^7 CFU mL^{-1}	5.3%	Raw milk	106–112%	Good LOD and specificity	70
Staphylococcus aureus	Sandwich ELISA	DPV	1 CFU mL^{-1}	10-10^7 CFU mL^{-1}	---	Tap and river water	---	Good correlation between plate count and aptasensor.	71

Ab: Antibody; AMP: Amperometry; CAMP: Chronoamperometry; CFU: Colony-forming unit; Chi: Chitosan; CMs: Cystine microstructures; CVs: Coefficients of variation; CV: Cyclic voltammetry; DAMP: 1-Deoxy-1-aminomannopyranoside; DPV: Differential pulse voltammetry; DR: Dynamic range; EIS: Electrochemical impedance spectroscopy; DPV: Differential pulse voltammetry; ELISA: Enzyme-linked immunosorbent assay; Fc: Ferrocene; HRP: Horseradish peroxidase; LAMP: Loop-mediated isothermal amplification; LF: Label-free; Lip: Lipoic acid; LOD: Limit of detection; MEIS: Magnetoelectrochemical impedance spectroscopy; POC: *Point-of-care*; SPR: Surface plasmon resonance; SWV: Square wave voltammetry; Thi: Thionine

Table II.5. Summary table of mycotoxin detection

Analyte	Assay format	Detection technique	LOD	DR	Precision (CVs)	Sample	Recovery (%)	Remarks	Ref.
Aflatoxin B1	Ab-AFB1	DPV	0.16 ng mL^{-1}	1-8 ng mL^{-1}	4.92%	---	---	Promising material	72
Aflatoxin B1	Direct ELISA	DPV	3.5 pg mL^{-1}	0.01-100 ng mL^{-1}	3.69% (100 pg mL^{-1}) and 4.75% (100 ng mL^{-1})	Corn powder	---	High sensitivity, even in samples	73
Aflatoxin B1	Ab-AFB1	DPV	0.06 ng mL^{-1} (Buffer) and 0.19 ng mL^{-1} (Maize)	0.1-1 ng mL^{-1} and 1-30 ng mL^{-1} (Buffer) and 1.6-16 ng mL^{-1} (Maize)	0.98-12.76%	Maize	96.7-110.1%	Good LOD and fast detection	74
Aflatoxin B1	Ab-AFB1	EIS	5 ng mL^{-1}	5-20 ng mL^{-1}	---	---	---	USB portable sensor and electrode regeneration	75

Table II.5. Continued

Analyte	Assay format	Detection technique	LOD	DR	Precision (CVs)	Sample	Recovery (%)	Remarks	Ref.
Aflatoxin B1	Ab-AFB1	EIS	10 fg mL^{-1}	0.01-10 pg mL^{-1}	8.5%	Corn samples	80-112%	Excellent LOD	76
Aflatoxin B1	Aptamer	EIS	0.12 ng mL^{-1} (SeqA) and 0.25 ng mL^{-1} (SeqB)	0.125-16 ng mL^{-1}	---	Beer and wine	92-102%	Good sensitivity and specificity	77
Aflatoxin B1	Ab-AFB1	EQCM-CV	0.08 ng mL^{-1}	0.1-4.0 ng mL^{-1}	5.13%	Groundnut	---	Good LOD, selectivity and electrode regeneration	78
Aflatoxin B1	Ab-AFB1	EQCM-CV	8 pg mL^{-1}	0.008-0.3 ng mL^{-1} and 1-10 ng mL^{-1}	---	Corn-flakes samples	---	High sensitivity, two DR and electrode regeneration	79

Table II.5. Continued

Analyte	Assay format	Detection technique	LOD	DR	Precision (CVs)	Sample	Recovery (%)	Remarks	Ref.
Aflatoxin B1	Competitive ELISA	SWSV	0.2 pg mL^{-1}	0.001-100 ng mL^{-1}	3.8%	Milk and peanut oil	95.5–110% (Milk) and 90–102% (Peanut oil)	Disposable sensor and amplification with Cu-apatite	80
Aflatoxin M1	mAb-AFM1	EIS	1 pg mL^{-1}	6.25-100 pg mL^{-1}		Milk	---	Validation with CRM of milk	81
Aflatoxin M1	Aptamer	EIS	1.15 ng L^{-1}	2-150 ng L^{-1}	---	Milk	93.8-99.4%	Good correlation with commercial immunoassay	82
Deoxynivalenol	Competitive ELISA	AMP	6.25 ng L^{-1}	6.25-250 ng L^{-1}	---	Wheat	104.5-106.9%	Portable, fast and automated microfluidic system	83

Table II.5. Continued

Analyte	Assay format	Detection technique	LOD	DR	Precision (CVs)	Sample	Recovery (%)	Remarks	Ref.
Deoxynivalenol	Direct ELISA	DPV	5 pg L^{-1}	0.01-1000 ng L^{-1}	2.71-4.32%	Sorghum, infant food, and animal food	94.74-106.17%	Good LOD and specificity	84
Deoxynivalenol	Ab-DON	EIS	0.3 µg L^{-1}	6-30 ng L^{-1}	6.5-6.9%	Corn, roasted coffee and wheat	---	Good correlation with plate ELISA method	85
Deoxynivalenol and Fumonisin B1	Ab-DON and Ab-FB1	DPV	8.6 ppb (DON) and 4.2 ppb (FB1)	0.05-1 ppm (DON) and 0.2-4.5 ppm (FB1)	5.7% (DON) and 4.9% (FB1)	Corn samples	93.1–104.3%	Good specificity, even in sample	86

Table II.5. Continued

Analyte	Assay format	Detection technique	LOD	DR	Precision (CVs)	Sample	Recovery (%)	Remarks	Ref.
Fumonisin B1	Competitive ELISA	AMP	0.58 ng mL^{-1}	0.60-54 ng mL^{-1}	8.16% (15 ng mL^{-1})-7.8% (30 ng mL^{-1}) [Intradays] 12.9% (15 ng mL^{-1})-12.6% (30 ng mL^{-1}) [Interdays]	Maize samples	---	Good correlation with AOAC method	87
Fumonisin B1	Direct and Competitive ELISA	DPV	2 pg mL^{-1}	0.01-1000 ng mL^{-1}	3.13% (100 pg mL^{-1}) and 3.95% (100 ng mL^{-1})	Corn samples	96.34–115.95%	Good correlation with AOAC official method	88
Fumonisin B1	Sandwich ELISA	EIS	2 pM	0.1-1000 nM	4.8%	Maize samples	91–105%	Good accuracy and LOD	89

Table II.5. Continued

Analyte	Assay format	Detection technique	LOD	DR	Precision (CVs)	Sample	Recovery (%)	Remarks	Ref.
Fumonisins (B1, B2 and B3)	Competitive ELISA	AMP	0.33 μg L^{-1}	0.73-11.2 μg L^{-1}	5.6% and 2.9% (Intradays) 6.9% and 6.0% (Interdays)	Beers	85–96% (Maize CRM) and 87–105% (Beers)	Good LOD, accuracy and precision. Simplified calibration and analysis	90
Monilifor min	SAM of CA	CV	$8.3x10^{-10}$ mol L^{-1}	$4.75x10^{-7}$-$1.24x10^{-6}$ mol L^{-1}	3.1% and 3.6% (Intradays) ; 3.1% and 3.0% (Interdays)	Maize samples	---	Better LOD and good correlation with HPLC-UV-Vis	91
Ochratoxin A	Competitive ELISA	AMP	0.32 μg L^{-1} (PBS) and 0.26 μg L^{-1} (Coffee)	1.3–153.8 μg L^{-1} (PBS) and 1.3–153.8 μg L^{-1} (Coffee)	7% (Intradays) ; 10% (Interdays)	Instant coffee	73–90%	Simplified calibration and analysis	92

Table II.5. Continued

Analyte	Assay format	Detection technique	LOD	DR	Precision (CVs)	Sample	Recovery (%)	Remarks	Ref.
Ochratoxin A	Competitive ELISA	AMP	0.05 μg Kg^{-1}	---	2.88-6.42%	Apples	94-106.5%	Microfluidic device and good concordance with ELISA method	93
Ochratoxin A	HRP-CSPE	CAMP	---	23.85-203.28 nM	10%	Beer	98.70%	HRP-enzyme modified ink and direct detection	94
Ochratoxin A	Direct ELISA	CAMP	0.05 μg L^{-1} (PBS) and 0.05–0.06 μg L^{-1} (wine)	0.01-100 μg L^{-1} (PBS and wine)	---	Wine	---	LOQ of 100 CFU mL^{-1} s	95

Table II.5. Continued

Analyte	Assay format	Detection technique	LOD	DR	Precision (CVs)	Sample	Recovery (%)	Remarks	Ref.
Ochratoxin A	cDNA-Aptamer	DPV	0.8 pM	0.0001-1 nM	5.8%	Red wine	96.2–104.3%	High sensitivity with cDNA signal amplification	96
Ochratoxin A	Competitive ELISA	DPV	0.11 ng mL^{-1} (PBS) and 0.12 ng mL^{-1} (Wine)	0.26–8.87 ng mL^{-1} (PBS) and 0.24–8.33 ng mL^{-1} (Wine)	8.11% 8.46%	Red wine	105.23–109.31%	Good LOD, even in samples, and recovery rates	97
Ochratoxin A	Competitive ELISA	DPV	0.07 ng mL^{-1}	0.78-8.74 ng mL^{-1}	---	Wheat samples	102–104%	Good concordance with AOAC method and CRM	98
Ochratoxin A	Competitive ELISA	DPV	0.7 ng mL^{-1}	0.15-5 ng mL^{-1}	2.3-3.7%	Cocoa beans	82.1-85%	LOQ of 0.15 ng mL^{-1}	99

Table II.5. Continued

Analyte	Assay format	Detection technique	LOD	DR	Precision (CVs)	Sample	Recovery (%)	Remarks	Ref.
Ochratoxin A	Aptamer-ssDNA	DPV	4 nM (PBS); 10 nM (Wine); 2 nM (Pretreated wine) and 334 nM (Beer)	---	6.4%	Wine and beer	---	Signal "off" sensor	100
Ochratoxin A	Ab-OTA	EIS	0.25 ng mL^{-1}	0.3-20 ng mL^{-1}	5.18%	Red wine	94.56-102.91%	High sensitivity	101
Ochratoxin A	LF	EIS	0.15 ng mL^{-1}	0.15-2.5 ng mL^{-1}	4.3%	Cocoa beans	91-95%	Good agreement with HPLC method	102
Ochratoxin A	Ab-OTA	EIS	0.055 pg mL^{-1}	0.0001-30 ng mL^{-1}	6.3-8.4%	Red wine	96.8-106.5%	No H_2O_2 needed	103

Table II.5. Continued

Analyte	Assay format	Detection technique	LOD	DR	Precision (CVs)	Sample	Recovery (%)	Remarks	Ref.
Ochratoxin A	Aptamer	SPR	0.005 ng mL^{-1}	0.094-100 ng mL^{-1}	1.7%	Red wine and peanut oil	86.9-116.5%	Regenerable surface and microfluidic system	104
Ochratoxin A	Competitive ELISA	SWV	0.008 ppb	0.01-20 ppb	5.56%	Red wine	92-110%	Excellent LOD	105
Zearalenone	Competitive ELISA	AMP	0.4 µg L^{-1}	---	4-18%	Infant solid food	96-106% (Maize CRM) and 100-108% (Infant food)	Good accuracy and new methodology with integrated immunoassay	106

Table II.5. Continued

Analyte	Assay format	Detection technique	LOD	DR	Precision (CVs)	Sample	Recovery (%)	Remarks	Ref.
Zearalenone	Competitive ELISA	AMP	0.41 μg Kg^{-1}	---	2.74-6.41%	Feedstuff samples	96.4-107%	New performance with microfluidic device	107
Zearalenone	Competitive ELISA	DPV	2 pg mL^{-1}	0.004-9.5 ng mL^{-1}	---	Corn, wheat, and grain-based food	91.6-113.0%	Good LOD and accuracy	108

Ab: Antibody; AMP: Amperometry; CA: Cysteamine; CAMP: Chronoamperometry; cDNA: Complementary DNA sequence; CRM: Certified reference material; CSPE: Carbon screen-printed electrode; CVs: Coefficients of variation; CV: Cyclic voltammetry; DPV: Differential pulse voltammetry; DON: Deoxynivalenol; ELISA: Enzyme-linked immunosorbent assay; EQCM-CV: Electrochemical quartz crystal microbalance cyclic voltammetry; FB1: Fumonisin B1; HRP: Horseradish peroxidase; LF: Label-free; LOD: Limit of detection; PBS: Phosphate buffer saline; SAM: Self-assembled Monolayer; ssDNA: Single strain DNA; SPR: Surface plasmon resonance; SWSV: Square wave stripping voltammetry

II.2.3. Fluorescent detection

Fluorescence is another physical process used to performing sensors. The fluorescence spectroscopy has been performed as detection technique coupled to other conventional methodologies, such as HPLC, GC, etc[109–111].

This technique allows a fast and high sensitive real-time detection (down to single molecules) and is compatible with several methods, such as microfluidic chips[112]. Among this technique, there are various ways to carry out, depending on the dye or nearby substances. Thus, numerous of dyes can be found which can be excited to get fluorescence. These dyes are different in structure and, therefore, in excited and emission wavelength[113,114]. However, other approaches to executing that technique have been catching the attention. Thereby, fluorescence quenching has interesting features. One of them is the Fluorescence Resonance Energy Transfer (FRET), which is based on the transfer of nonradiative energy from donors to acceptors. They are especially close to each other (normally 1–10 nm) to let that transfer. The energy is given by donors, such as organic fluorescent dyes, semiconductor quantum dots, and upconversion fluorescence nanoparticles (UCNPs), and acceptors receive it and quench it. These acceptors can be organic quenchers, gold nanoparticles, and graphene[115].

Nanomaterials play an important role in the development of these methods, overall carbon nanomaterials. Their capacity of quenching fluorescence, becoming in perfect acceptors to achieve this kind of

methods. On the other hand, dyes are used as donors. Although they produce the measurable signal, they cannot be as free reagent. Actually, they are labeled with a biorecognition element, usually an aptamer.

Thus, the mechanism of quenching is produced due to the interaction between the dye-labeled aptamer with carbon nanomaterials. That interaction is carried out by π-stacking between the π-conjugated aromatic rings and nucleotides bases from aptamer. That π-π interaction is sufficiently strong to hold the aptamer on the carbon nanomaterial surface. Then, dye transfers the fluorescence energy to carbon nanomaterial. When the analyte is present in the solution, the analyte-aptamer interaction is stronger than π-π interaction, releasing the complex analyte-aptamer and, consequently, the dye is not quenched. Also, the fluorescence can be measured in another way, when the carbon nanomaterial is in the solution[116–118].

II.3. Motors

II.3.1. State of art

Nanotechnology is trending topic in the science world. Although nanotechnology is young, it is growing but, actually, in exponential way. Such technology was born by the Richard Feynman's quote, "There's plenty of room at the bottom" in the 1959[1,2] . Nanotechnology is a broad field which deals with stuff such as nanomaterials or nanomachines. In this sense, this topic of nanotechnology, micro- and nanomachines, is attempting to mimic natural machines such as ATP synthase, kinesin motor or flagellum. There are many examples of natural or biological machines, as aforementioned ones, which convert chemical energy into movement by the decomposition or hydrolysis of adenosine triphosphate (ATP) into mechanical work[3]. This mechanical work is vital for different tasks such as cargo transport, biomolecules synthesis or cell movement. Therefore, these biological motors are an inspiration for the goal to set smart engines up, able to replace natural ones or carry novel applications out (clinical, sensing, bioremediation)[4].

Notwithstanding, the laws which govern the microscale change the behavior of the motors or engines. Thus, when the dimension decreases, forces are transformed as it happens with inertia. Owing to the small dimension of the particle, low Reynolds number is produced, and hence resistance force leads over inertia force. Additionally, Brownian effect turns into equivalent and can even dominate over

directional motion at microscale[5]. For these reasons, the motion is only caused by direct forces applied on the microengine or produced by itself.

Considering this, one of the first examples found in the literature is the motor developed by Whitesides *et al.* A millimeter-size motor (a thin polydimethylsiloxane (PDMS) plate 1–2 mm thickness and 9 mm diameter) used platinum (Pt) as a catalyst of decomposition of H_2O_2 in water and oxygen gas[6]. Two other groups, from the Pennsylvania State University and the University of Toronto, developed each bimetallic nanorods powered in H_2O_2 solution, whose explanation was found out afterwards[1,7].

From this point forward, different groups have created several diverse micromotors, microrockets, microjets or microengines for novel *proof-of-concept*, tasks, and bioapplications. Then, numerous strategies and methods of fabrication appeared as well as many types of micromotors (as Janus particles) and ways of propulsion (external fields and stimuli, or autonomous motion). This last one has been chosen to classify them.

II.3.2. Propulsion methods

Firstly, it should mention that variety of micromotors was synthesized. For instance, the principal classes are nanorods or nanowires, microrockets, microjets and Janus particles, among others less important. These shapes provide of several inherent features which can use of propulsion strategy and for applications.

To induce chemically-driven motion or by external-field movement in the motor, it is usually necessary to supply some asymmetry to them. This asymmetry can be made to the extent the fabrication is performed or by the very production method. As result of that, different ways to fabricate have been purposed, and they will be further described in this section together with the propulsion methods.

That energy given to microengines depends on the source. If the energy comes from an interior way (chemical reaction), two main methods are found, self-electrophoresis and bubble propulsion. However, other less important methods but promising strategies can be found in the literature such as self-diffusiophoresis. On the contrary, if that energy is provided through external field or stimuli, we can find ultrasound, magnetic and electric field, light source, pH or temperature, which yield own propulsion methods. The first methods will be further discussed, while the last ones will be briefly considered.

II.3.2.1. Self-electrophoresis propulsion

As its very name includes, this thrust is based on electrophoresis phenomena which consist on the migration of charged particles under the application of an electric field. Nevertheless, an external electric field is not applied. Therefore, this electric field is locally generated by a chemical gradient along the micromotor surface. Thus, the motion of the motor is the contrary response to that electric field.

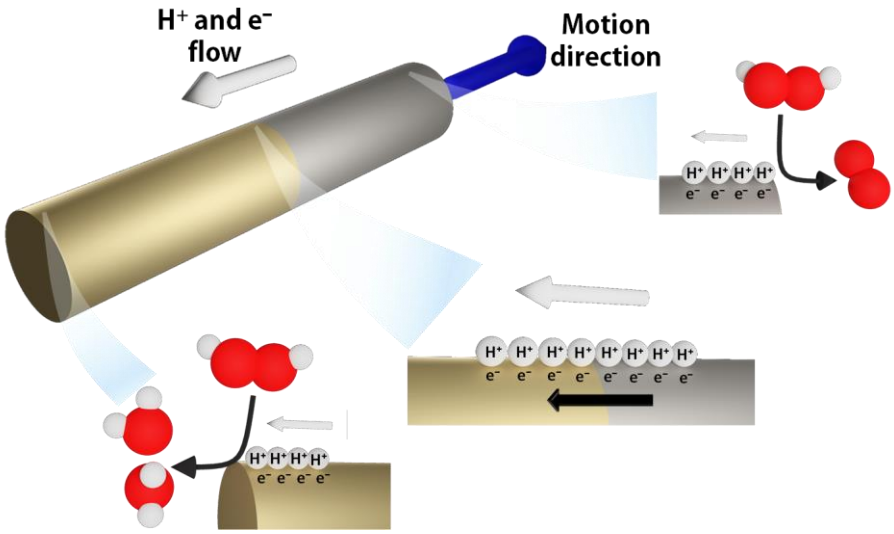

Fig. II.6. Scheme of generation of electric field on nanowire surface based on bimetallic structure. Two different catalytic metals (M1 and M2) and fuel solution (A, B and C, as reagents and products) are necessary to give the redox reactions, causing the electric field and corresponding motion.

Before describing the chemical explanation, it must be presented the fabrication to establish the foundations of nanowires. Nanowire fabrication is a well-known method, used in the synthesis of numerous metallic wires[8,9]. It is based on template-directed electrodeposition, making use of the pores of a membrane as a template to create tailor-made tubes of different materials (metals, conductive polymers, semiconductors and carbon materials). Such membranes are well-suited for this purpose, owing to their features such as a variety of monodisperse diameters, large pore density, and facility of mass production. These membranes are made of aluminum oxide. The

methodology for the nanowire fabrication consists firstly of the coating of those membranes with a sputtered gold or silver film on one side and then, together with the aid of an aluminum foil, both compose the working electrode. A Teflon plating cell plays as an electrochemical cell to perform the electrodeposition of different metals to make stripped rods. The membrane is the electrochemical template, and first of all, electrodepositing frequently a sacrificial layer of copper or silver. Next, other metals or materials are sequentially electrodeposited. The sputtered film and sacrificial layer are removed by mechanical polishing or chemical etching. In order to finish, alumina membrane is dissolved in NaOH solution and nanorods are released after rising and washing steps. All these steps are collected in **Fig. II.7**.

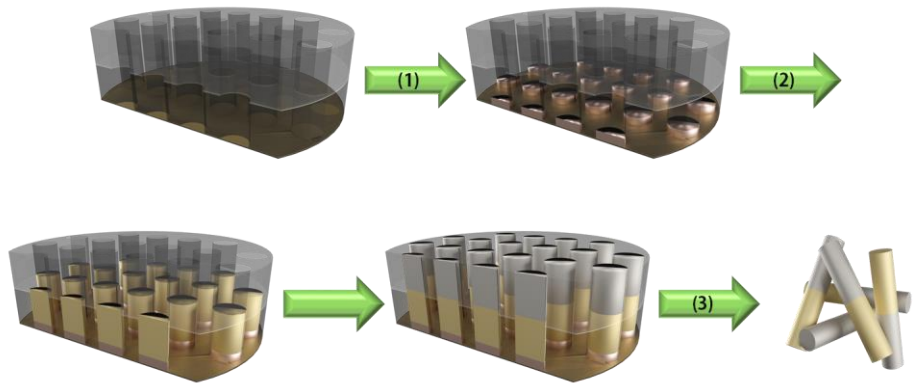

Fig. II.7. Schematic representation of nanowire electrosynthesis. (1) Electrodeposition of sacrificial layer in membrane template. (2) Consecutive electrodeposition of metals or materials. (3) Removal of sputtered film and sacrificial layer, and dissolution of membrane to release the nanowires.

The chemical explanation of the motion of this kind of motors was subsequently postulated. Before postulating the most accepted theory, the purposed mechanism was due to liquid-gas surface tension phenomena because of nanobubbles[1,7]. After that, another mechanism was purposed (being the most known mechanism) based on the self-electrophoresis phenomena. Thanks to that kind of bimetallic structure (nanorods or Janus particles), the particle has asymmetry. Furthermore, both metals play the role of anode (M_1) and cathode (M_2), where the oxidation and reduction of the substrate are produced respectively. When the oxidation is done at the end of the anode, the concentration of the protons grows on the surface. It leads to an asymmetric distribution of the charge, generating an electric field from the anode to the cathode as a consequence of the movement of electrons in the same direction. Due to that fluid of protons and electrons, a contrary effect is provoked, moving the micromotor. Different examples are found in the literature, using Au as M_1 and Pt as M_2[7,10,11], or Ni as M_2[1], and hydrogen peroxide as a substrate for the redox reaction (**Fig. II.6** illustrates the phenomena). Other solutions and catalysts are used to generate that electric field as hydrazine[12,13].

Following this strategy, several works are found in the literature summarized in **Table II.6**.

II.3.2.2. Bubble propulsion

Bubbles are generated by the oxidation of the fuel solution on the catalyst surface. For instance, Pt and Ir catalyze the oxidation of H_2O_2

and N_2H_4 in O_2 and N_2 bubbles. This type of transition metals is good catalyst for decomposition into gas bubbles such as silver, manganese, and nickel, among others. Using these metals, the more common reagent is hydrogen peroxide whose decomposition leads to water and oxygen gas, which formation provoked the motion. Nevertheless, hydrogen peroxide is very reactive and non-biocompatible or environmental compatible at actual working concentration. In this way, other strategies were born to avoid this fuel and to develop more environmental-free or biocompatible approaches. These strategies, which do not use H_2O_2 or other "toxic" fuel, and other catalysts, are the presented by Wang's group. They utilized an alloy of gallium/aluminum[14] or magnesium[15] to generate the breakdown of water, and the propulsion was based on H_2 bubbles. In addition, another catalyst for *in vivo* applications as zinc, which catalyzes the decomposition of hydrochloric acid in H_2 bubbles, in acid media[16] or inside the stomach[17].

Among this propulsion method, there are some ways to elaborate these micromotors, from modification of Janus particle or electrodeposition to rolled-up approach. In this context and due to the way of propulsion and shape, tubular micromotors are widely known as microrockets or microjets[18,19].

All these production strategies are based on two layers, outer and inner layer. In the case of Janus particle, the layers are disposed on both sides of the particle (to lend that asymmetry). **Figure II.8** sums up these

ways to fabricate them. The rolled-up technology was developed by Schmidt *et al.* founded on thin solid films deposited over etchant-sensitive material and substrate[20]. The deposition of photoresist sacrificial layer onto the substrate surface is patterned by photolithography. After, distinct layers of metals or materials are deposited by tilted physical vapor deposition (PVD) controlling the deposition rate and temperature, so that the bottom material has the higher lattice constant to produce the rolling process. This process is made after selective etching of the sacrificial layer, generating the rolling into a microtube (**Fig. II.8A**). Due to this random process, different opening shapes can be obtained[21]. Moreover, the microjet diameters range from 1 to 30 μm, varying the thickness and built-in strain of the substrate, and the length of them can measure some hundred microns[22].

The other technology is the modification of Janus particle. These particles have also been utilized to perform self-electrophoresis propulsion[13]. However, it is fascinating the developed ideas reached from that point and growing their applications. As it was aforesaid, Janus particles need of asymmetry, which is achieved by their modification. In that way, it can be started from inert (polystyrene, silica) or catalytic particle (Pt, Ag, Zn, etc.). On the one hand, if we begin from the inert particle, it is necessary to add another catalytic material (e.g., Pt) which is managed the fuel breakdown to thrust the particle[23–25]. On the other hand, if the base of the particle is the catalytic material, the asymmetry is given through sputtering another inert[26,27] or catalytic material[28]. **Fig. II.8B** illustrates the steps for these processes.

As it was before described, template electrodeposition is broadly carried out to fabricate nanowires. For that, it can be widespread for fabrication another kind of motors, as microrockets. Due to this hollow tubular shape, it is necessary to utilize other membranes, instead of alumina membranes, and with larger pore diameter. For this aim, cyclopore polycarbonate (PC) membranes are employed. These membranes have symmetrical double-cone pore structure, which is more marked to the extent the diameter is smaller[29,30]. The method is the same to the synthesis of nanowires. Firstly, a sputtered gold film is deposited onto one face of the membrane to provide conductivity and to make the working electrode. This sort of micromotor needs asymmetry as well. For that reason, different layers are deposited from outside to inside. Thus, the outer layer can be of several materials such as metals[31] or conductive polymers[32]. These last ones have got all the attention because of their versatility and easy use. On the basis of monomers such as aniline, 3,4-ethylenedioxythiophene, pyrrol, among others, a potential is applied to carry out the electropolymerization on the pore wall, making a hollow tube. Aforementioned monomers become in polymers, being the mostly used polyaniline (PANI), polypyrrole (PPy), poly-3,4-ethylenedioxythiophene (PEDOT). Subsequently, the catalytic material, typically Pt, is electrodeposited on the polymer inner face, creating the representative microrocket. Other materials have been utilized as copper[31], or carbon materials such as graphene[30] or other carbon materials[33]. Double conical shape with different lengths and diameters can be achieved, relying on the pore size

(1, 2, 5 μm) of membrane template (length of membrane change with the pore size)[34]. This microrocket has demonstrated ultrahigh speed and very low H_2O_2 concentration requirement.

This microengines have random trajectories as well as previous kind of motors. However, this can be avoided inducing one directionality via magnetic guidance. Additionally, another ferromagnetic metallic layer can be added to the assembly, providing a magnetic feature. In that way, the micromotor can be guided with the aid of external magnet or magnetic field, following the marked direction controlled by the magnetic field[22,35].

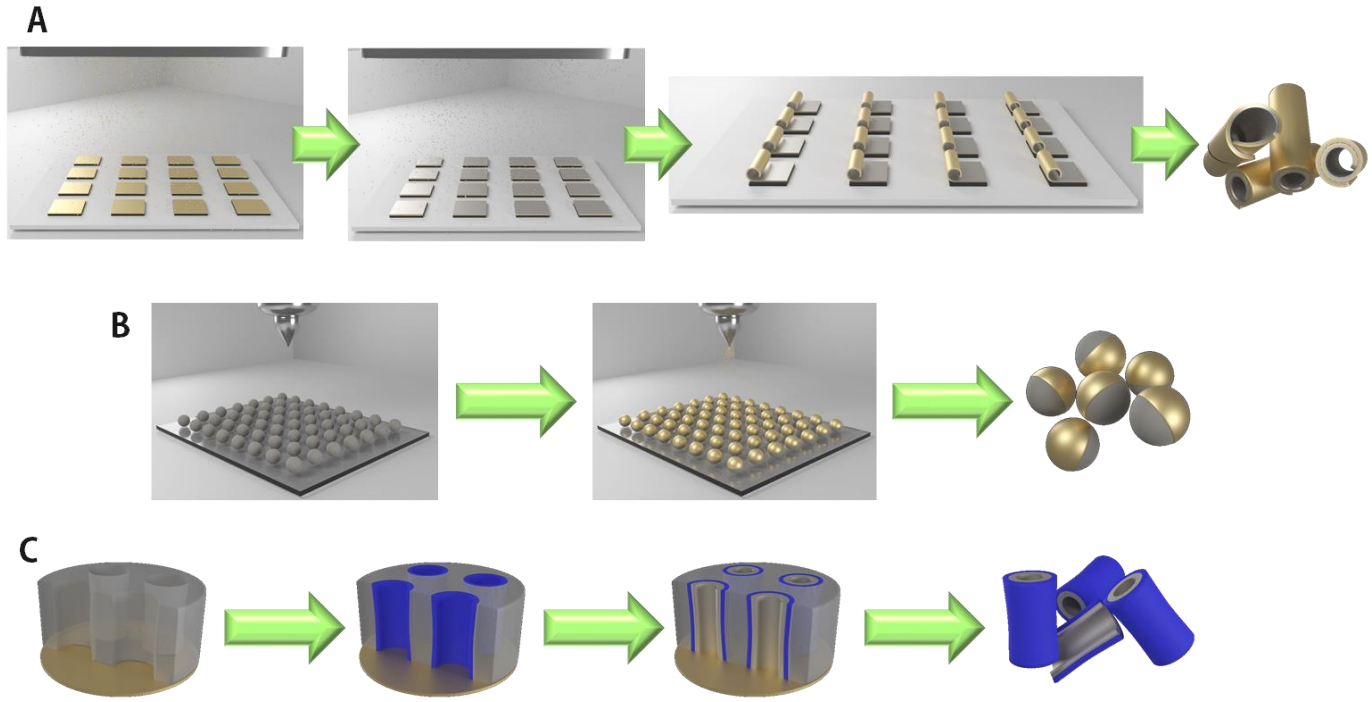

Fig. II.8. Illustration of main fabrication procedures. (A) Scheme of physical vapor deposition of material, selective etching of photoresist material and rolled-up technology. (B) Figurative fabrication of Janus particles from the monodisperse layer on a glass slide, sputtering another material layer to provoke asymmetry and release. (C) Electrodeposition of outer layer (conductive polymer, blue), next inner catalytic layer (e.g., Pt, silver) and last release.

In comparison to self-electrophoresis micromotors, hollow tubular micromotors have some advantages. First of all, the mechanism is based on the recoil force. This recoil force is caused by the bubble formation, migration, and exit (see **Figure II.9**)[19]. The fuel, principally H_2O_2, gets into the microrocket through one opening and after, the catalytic layer, usually Pt, makes the breakdown on the inner surface, generating O_2 gas. This oxygen nucleates and coalesces into bubbles that grow inside the microengine, expand and migrate along the cavity to another opening by the pressure gradient. Once the bubbles reach the exit extreme, they are ejected, provoking an opposite force which thrust the microrocket and its motion (recoil force)[36,37].

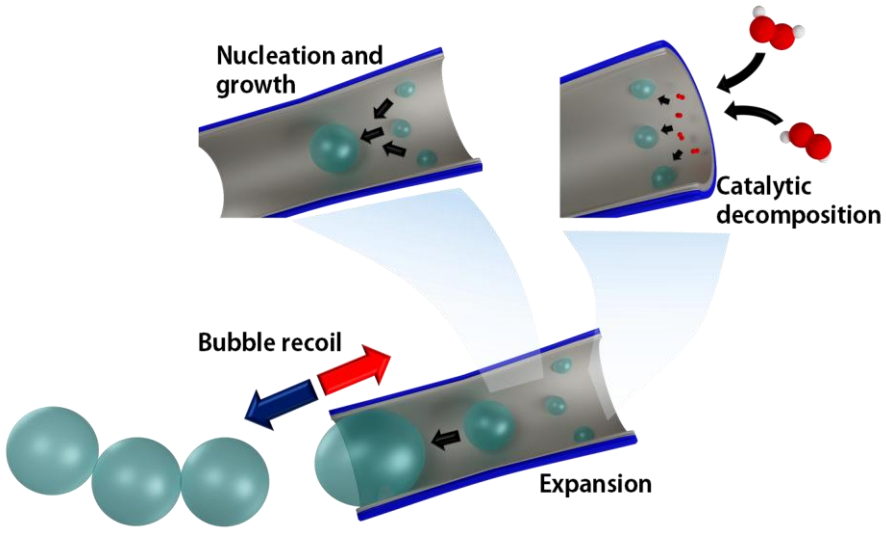

Fig. II.9. Mechanism of bubble propulsion based on recoil force.

This mechanism allows to accomplish more velocity or to work in strong media conditions (e.g., high ionic strength), or even in biological

media. Notwithstanding the impact of all procedures, the framework of this thesis is focused on hollow tubular micromotors and electrodeposition template production.

Many applications appeared last years, using them for example in cargo-delivery works, environmental approaches and *in vivo* applications. Despite the high interest in them, above all clinical applications, they can play an essential role as analytical tools, particularly as sensing field. Among these advantages, we can find lack of interferences, easy use, wireless control and very low used amount of sample. Although they present favorable features, poor reproducibility in fabrication. Thus, they have been utilized for detection of many different analytes (see **Table II.6**).

II.3.2.3. Self-diffusiophoresis propulsion

The same as it happens with self-electrophoresis propulsion, self-diffusiophoresis propulsion is based on a concentration gradient which causes a contrary effect, pushing the motor. In this sense, the flow is produced by diffusion phenomena due to that concentration gradient of surface active compounds leads to unbalanced interfacial strain stress and equivalent fluid flow. The phenomenon is called Marangoni effect[38]. This phenomenon is well illustrated by daily example when a soap drop is dropped on a pan filled with dirty or oily water. When this happens, the dirty on the water surface is pushed outwards. The variation of surface tension caused by the surfactant present in the soap, owing to

the low surface tension of surfactant. As water has high surface tension, a net force is generated, pulling the soap drop and enlarging it. This curious effect has been leveraged to create self-powered motors. This kind of motors has not reached the micrometer scale because the fabrication is more manual or necessary that scale for the experimental conditions[39,40]. The first examples of this kind of motors are the millimeter-sized plastic tube motor, developed by Velev *et al.*[39], and the millimeter-sized capsule motor, created by Pumera *et al.*[41]. On the one hand, the plastic tube is filled with ethanol infused hydrogel on one side and closed by a PDMS plug on the other. Then, ethanol is released provoking a surface tension gradient and pushing the tube along the Petri dish with water by Marangoni effect. On the other hand, the capsule motor made use of the gradient of surface tension between the interface liquid/liquid (water/oil). A mix of polysulfone polymer (PSf) in N,N′-dimethylformamide (DMF) was dropped on oil surface and, due to the higher density of capsule, went through oil to reach the interface water/oil. Then, PSf solidified instantaneously in contact with water, generating a capsule. DMF played as fuel, released from the capsule, and provoking the motion by Marangoni effect. However, this last one produces a continuous movement, the first generates a pulsated motion.

From this point, other works were developed due to the pros of motor characteristics. In this sense, the motion is caused by Marangoni effect. Namely, gradient originated by a compound or mixture with

lower surface tension which pushes the motor. This compound can be environmental-friendly or, even biocompatible. Furthermore, the production of that kind of motor does not need of expensive techniques, as metal sputtering or PVD, reducing the cost production. Nevertheless, the drawbacks are important because manufacture is still very manual and the reduction scale is a challenge.

The design of millimotors (millimeter scale) has been focused on a "boat" with one side opened and another closed. This boat can be made of a plastic tube[39] or a pipette tip[41]. As it is illustrated in Figure XX, a piece of pipette tip (normally the smaller part) is cut to get a small boat. The wide side is closed with wax, which is permeable and does not close totally, allowing the entry of water. The narrow side uses an exit of the fuel. The fuel is usually a mix of water and surfactant or alcohol. In the case of alcohol[39], it diminishes the surface tension, pulling the boat to zones with higher surface tension. On the other hand, the mix with a surfactant, typically sodium dodecyl sulfate (SDS), is ejected causing the same result[41].

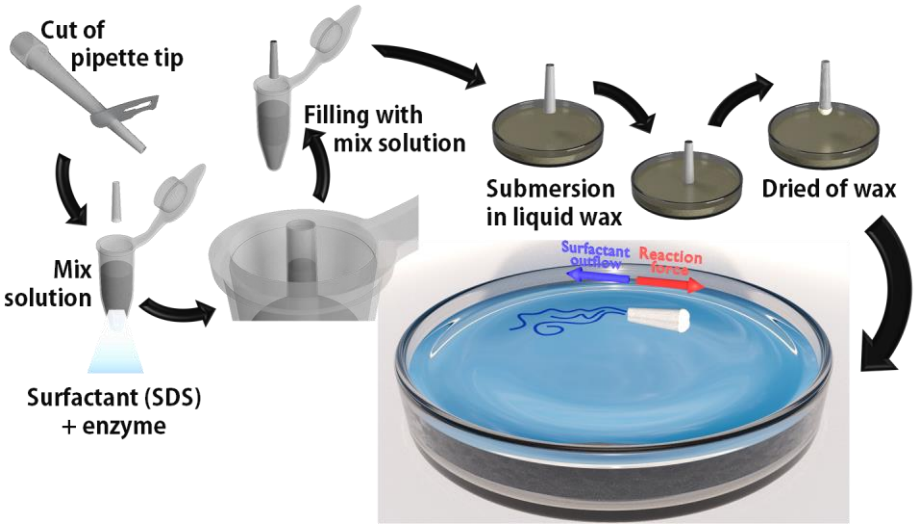

Fig. II.10. Illustration of manufacture of mobile sensor tip and filling with the mix of fuel (water and surfactant). Representation of Marangoni effect.

This strategy was followed in order to perform two main applications in different fields (see **Table II.6**).

II.3.2.4. Other propulsion methods

Previously described methods are produced by fuel-powered or self-powered thrust. Nonetheless, there are other techniques to induce that propulsion. These techniques are based on the employment of external field (ultrasounds, magnetic and electric fields) or stimuli (pH, temperature, and light). Among them, ultrasounds, magnetic field, and light are the most meaningful.

Ultrasounds are based on the acoustic energy applied, which presents good advantages against other methods. Such favorable

features as biocompatible, possible high miniaturization, and not very much harmful to biological tissues. The mechanism relies on that asymmetry on the micromotor. The fabrication process is accomplished by template-assisted electrodeposition. When nanowires grow inside de pores, they grow with a concrete shape. Once they are totally formed, the membrane and sacrificial layer are removed. The free nanowires have a concave shape at one extreme, and convex shape at another. On the concave extreme, high pressure is produced, while low pressure is produced on convex extreme. In this way, a pressure gradient is formed, pushing the wire from the high pressure to low pressure (acoustophoresis phenomena)[42]. This group has demonstrated the physical explanation about acoustic motor work, although other groups have worked in the same field[42,43]. Different particles have been used to perform ultrasound, however, depending on the material, size, shape, and compressibility of the particle, the behavior changes radically[42–45].

There are many diverse applications have been developed such as cargo-towing and release of drugs[46], bacteria killing[47], *proof-of-concept* inside the cells[48], magnetic red blood[49,50], developing of microcannons and micro-/nanobullets to tissue penetration[51,52], different shapes as nanoshells to explore new forms, even in vivo applications[53], and microRNA-21 detection inside cells in the sensing field[54].

Magnetic motors are also explored, and the motion of them is based on magnetic forces and torques. Helical-shape swimmers have been manufactured to prove the concept[55,56], even the aid of these

micromotors to thrust defective sperms[57]. Autonomous movement is searched to get self-propelled micromotor. In this sense, the automatic response to those stimuli opens new vias. In this context, light stimulus is also used to propel Janus particle[58]. Another formula is the employment of hydrogels which allow responding to different stimuli such as pH, generating a force to thrust particles[59].

II.3.3. Motor in biosensing field

Although motors belong to relatively young technology which dealt with the development of *proof-of-concept* in the beginning, its growth is still exponential increasing the number of applications. Due to motor features, the applications are commonly focused on the medical world because motors are very powerful tools. However, other applications in different fields are being explored, opening new horizons.

Special attention must be paid to Analytical Chemistry area. In this way, biosensing applications can be enormously significant. New approaches have been designed to detect many diverse analytes. They are summarized in the **Table II.6**. However, among these applications, there are some of them which are very promising. Those are the "*on-the-move*" detection. It consists of detection of the analyte while the micromotor is active, swimming in the solution with analytes. The biorecognition can be made by antibodies, aptamer or another element. They can be covalently joint or by physical attraction as π-stacking. Depending on the type of junction, different strategies can be proposed. Also, it can be performed adding an enzyme to get a mobile enzyme

sensor, which reacts with the analyte producing a kind of measurable signal (e.g., optical or electrochemical). Amount of strategies and approaches are carried out with the autonomy of options.

Table II.6. Summary of different applications according to propulsion mechanism.

Propulsion mechanism	Application	Target/Analyte	References
Self-electrophoresis	Proof-of-concept	---	1,7
	Cargo-towing and delivery	PS particles	60
		Drug-loaded particles	61
	Sensing	Ag^+	11
		DNA and bacterial ribosomal RNA	62
Self-diffusiophoresis	Proof-of-concept	---	39,41
	Bioremediation	Pollutants	40
	Sensing	H_2O_2	63

Ag^+: Silver ions; DNA: Deoxyribonucleic acid; PS: Polystyrene; RNA: Ribonucleic acid

Table II.6. Continued

Propulsion mechanism	Application	Target/Analyte	References
Bubble	Cargo-towing and delivery	Cells	64
		PS particles	35,65
	Environmental approaches	Heavy metals	66
		Organophosphate nerve agents	67
		Bacteria	68,69
	Clinical therapies	---	17,57,70,71

PS: Polystyrene

Table II.6. Continued

Propulsion mechanism	Application	Target/Analyte	References
Bubble	Sensing	Heavy metals	72,73
		Inorganic electrolytes in blood	74
		Dimethyl sulfoxide	75
		Uric acid	76
		Blood proteins (Bovine serum albumin, globulin, and glucose oxidase)	77
		Thiolated amino acids (cysteine, serine, and methionine) and peptides (glutathione)	75
		Proteins	78
		DNA	79
		Biological warfare weapons (ricin B)	80

DNA: Deoxyribonucleic acid

II.4. Bibliography

II.4.1. Food Safety

1. Joint FAO/WHO, Assuring food safety and quality: Guidelines for strengthening national food control systems, *FAO Food and Nutrition Paper*, **2003**, *73*, 1–73.
2. Grunert, K. G., Food quality and safety: consumer perception and demand, *Eur. Rev. Agric. Econ.*, **2005,** *32 (3)*, 369–391.
3. Joint FAO/WHO, *Understanding the Codex Alimentarius*, Joint FAO/WHO, 3rd Ed., Rome, Italy, **2006**.
4. Schmidt, R. H., Rodrick, G. E., *Food Safety Handbook*, Wiley, New Jersey, United States of America, **2003**.
5. Aung, M. M., Chang, Y. S., Traceability in a food supply chain: Safety and quality perspectives, *Food Control*, **2014**, *39*, 172–184.
6. Hoffmann, S., Maculloch, B., Batz, M., Economic Burden of Major Foodborne Illnesses Acquired in the United States, *Economic Research Service/USDA,* **2015**, *140*, 1–53.
7. Marroquín-Cardona, A. G., Johnson, N. M., Phillips, T. D., Hayes, A. W., Mycotoxins in a changing global environment – A review, *Food Chem. Toxicol.*, **2014**, *69*, 220–230.
8. Duffy, G. F., Moore, E. J., Electrochemical Immunosensors for Food Analysis: a Review of Recent Developments, *Anal. Lett.*, **2016**, 50, 1–32.
9. Sicherer, S. H, Sampson, H. A., Food allergy: Epidemiology, pathogenesis, diagnosis, and treatment, *J. Allergy Clin. Immunol.*, **2014**, *133*, 291–307.

10. Pilolli, R., Monaci, L., Visconti, A., Advances in biosensor development based on integrating nanotechnology and applied to food-allergen management, *TrAC, Trends Anal. Chem.*, **2013**, *47*, 12–26.
11. Alves, R. C., Barroso, M. F., González-García, M. B., Oliveira, M. B. P. P., Delerue-Matos, M. C., New Trends in Food Allergens Detection: Towards Biosensing Strategies, *Crit. Rev. Food Sci. Nutr.*, **2015**, *56 (14)*, 2304–2319.
12. Kagan, R. S., Food Allergy: An Overview, *Environ. Health Perspect.*, **2003**, *111*, 223–225.
13. Foudeh, A. M., Didar, T. F., Veres, T., Tabrizian, M., Microfluidic Designs and Techniques Using Lab-on-a-Chip Devices for Pathogen Detection for Point-of-Care Diagnostics, *Lab. Chip*, **2012**, *12*, 3249–3266.
14. Sharma, H., Mutharasan, R., Review of biosensors for foodborne pathogens and toxins, *Sens. Actuat. B-Chem.*, **2013**, *183*, 535–549.
15. Yoon, J.-Y., Kim, B., Lab-on-a-Chip Pathogen Sensors for Food Safety, *Sensors*, **2012**, *12*, 10713–10741.
16. Singh, R., Mukherjee, M. D., Sumana, G., Gupta, R. K., Sood, S., Malhotra, B. D., Biosensors for pathogen detection: A smart approach towards clinical diagnosis, *Sens. Actuat. B-Chem.*, **2014**, *197*, 385–404.
17. Abdalhai, M. H., Fernandes, A. M., Xia, X., Musa, A., Ji, J., Sun, X., Electrochemical Genosensor To Detect Pathogenic Bacteria (Escherichia coli O157:H7) As Applied in Real Food Samples (Fresh

Beef) To Improve Food Safety and Quality Control, *J. Agric. Food Chem.*, **2015**, *63*, 5017–5025.

18. Xiang, C., Li, R., Adhikari, B., She, Z., Li, Y., Kraatz, H.-B., Sensitive electrochemical detection of Salmonella with chitosan–gold nanoparticles composite film, *Talanta*, **2015**, *140*, 122–127.
19. Afonso, A. S., Pérez-López, B., Faria, R. C., Mattoso, L. H. C., Hernández-Herrero, M., Roig-Sagués, A. X., Maltez-da Costa, M., Merkoçi, A., Electrochemical detection of Salmonella using gold nanoparticles, *Biosens. Bioelectron.*, **2013**, *40*, 121–126.
20. Bhardwaj, N., Bhardwaj, S. K., Meht, J., Mohanta, G. C., Deep, A., Bacteriophage immobilized graphene electrodes for impedimetric sensing of bacteria (Staphylococcus arlettae), *Anal. Biochem.*, **2016**, *505*, 18–25.
21. Cheng, C., Peng, Y., Bai, J., Zhang, X., Liu, Y., Fan, X., Ning, B., Gao, Z., Rapid detection of Listeria monocytogenes in milk by self-assembled electrochemical immunosensor, *Sens. Actuat. B-Chem.*, **2014**, *190*, 900–906.
22. Hong, S. A., Kwon, J., Kim, D., Yang, S., A rapid, sensitive and selective electrochemical biosensor with concanavalin A for the preemptive detection of norovirus, *Biosens. Bioelectron.*, **2015**, *64*, 338–344.
23. Prieto-Simón, B., Campàs, M., Immunochemical tools for mycotoxin detection in food, *Monatsh. Chem.*, **2009**, *140*, 915–920.
24. Prieto-Simón, B., Noguer, T., Campàs, M., Emerging biotools for assessment of mycotoxins in the past decade, *TrAC, Trends Anal. Chem.*, **2007**, *26*, 689–702.

25. Vidal, J. C., Bonel, L., Ezquerra, A., Hernandez, S., Bertolin, J. R., Cubel, C., Castillo, J. R., Electrochemical affinity biosensors for detection of mycotoxins: A review, *Biosens. Bioelectron.*, **2013**, *49*, 146–158.
26. Fink-Gremmels, J., Mycotoxins: their implications for human and animal health, *Vet. Q.*, **1999**, *21*, 115–120.
27. van Egmond, H. P., Schothorst, R. C., Jonker, M. A., Regulations relating to mycotoxins in food, *Anal. Bioanal. Chem.*, **2007**, *389*, 147–157.
28. Li, P., Zhang, Z., Zhang, Q., Zhang, N., Zhang, W., Ding, X., Li, R., Current development of microfluidic immunosensing approaches for mycotoxin detection via capillary electromigration and lateral flow technology, *Electrophoresis*, **2012**, *33*, 2253–2265.
29. Ma, H., Sun, J., Zhang, Y., Bian, C., Xia, S., Zhen, T., Label-free immunosensor based on one-step electrodeposition of chitosan-gold nanoparticles biocompatible film on Au microelectrode for determination of aflatoxin B1 in maize, *Biosens. Bioelectron.*, **2016**, *80*, 222–229.
30. Goud, K. Y., Catanante, G., Hayat, A., Satyanarayana, M., Gobi, K. V., Marty, J. L., Disposable and portable electrochemical aptasensor for label free detection of aflatoxin B1 in alcoholic beverages, *Sens. Actuat. B-Chem.*, **2016**, *239*, 466–473.
31. European Commission, Commission Regulation (EC) No 1881/2006, **2006**.

32. Yao, H., Hruska, Z., Di Mavungu, J. D., Developments in detection and determination of aflatoxins, *World Mycotoxin J.*, **2015**, *8*, 161–191.
33. Krska, R., Welzig, E., Boudra, H., Analysis of *Fusarium* toxins in feed, *Anim. Feed Sci. Technol.*, **2007**, *137*, 241–264.
34. Romanazzo, D., Ricci, F., Volpe, G., Elliot, C. T., Vesco, S., Kroeger, K., Moscone, D., Stroka, J., van Egmond, H., Vehniainen, M., Palleschi, G., Development of a recombinant Fab-fragment based electrochemical immunosensor for deoxynivalenol detection in food samples, *Biosens. Bioelectron.*, **2010**, *25*, 2615–2621.
35. Qing, Y., Li, C-R., Yang, X-X., Zhou, X-P., Xue, J., Luo, M., Xu, X., Chen, S., Qiu, J-F., Electrochemical immunosensor using single-walled carbon nanotubes/chitosan for ultrasensitive detection of deoxynivalenol in food samples, *J. Appl. Electrochem.*, **2016**, *46*, 1049–1057.
36. Sunday, C. E., Masikini, M., Wilson, L., Rassie, C., Waryo, T., Baker, P. G. L., Iwouha, E. I., Application on Gold Nanoparticles-Dotted 4-Nitrophenylazo Graphene in a Label-Free Impedimetric Deoxynivalenol Immunosensor, *Sensors*, **2015**, *15*, 3854–3871.
37. Hervás, M., López, M. Á., Escarpa, E., Simplified calibration and analysis on screen-printed disposable platforms for electrochemical magnetic bead-based inmunosensing of zearalenone in baby food samples, *Biosens. Bioelectron.*, **2010**, *25*, 1755–1760.
38. Panini, N. V., Salinas, E., Messina, G. A., Raba, J., Modified paramagnetic beads in a microfluidic system for the determination of

zearalenone in feedstuffs samples, *Food Chemistry*, **2011**, 125, 791–796.

39. Hervás, M., López, M. Á., Escarpa, E., Electrochemical immunoassay using magnetic beads for the determination of zearalenone in baby food: An anticipated analytical tool for food safety, *Anal. Chim. Acta*, **2009**, *653*, 167–172.
40. European Commission, Commission Regulation (EC) No. 856/2005 of 6 June 2005, Amending Regulation (EC) No 466/2001 as regards Fusarium Toxins, *Off. J. Eur. Union.*, **2005**, *143*, pp. 3–8.
41. European Commission, Commission Regulation (EC) No. 1881/2006 of 19 December 2006, Setting Maximum Levels for Certain Contaminants in Foodstuffs, *Off. J. Eur. Union.*, **2006**, *L364*, pp. 5–24.
42. European Commission, Commission Regulation (EC) No. 1126/2007 of 28 September 2007, Amending Regulation (EC) No. 1881/2006 Setting Maximum Levels for Certain Contaminants in Foodstuffs as regards Fussarium Toxins in Maize and Maize Products, 2007, *Off. J. Eur. Union.*, **2007**, *L255*, pp. 14–17.
43. Yang, X., Zhou, X., Zhang, X., Qing, Y., Luo, M., Li, C., Li, Y., Xia, H., Qiu, J., A Highly Sensitive Electrochemical Immunosensor for Fumonisin B1 Detection in Corn Using Single-Walled Carbon Nanotubes/Chitosan, *Electronalysis*, **2015**, *27*, 2679–2687.
44. Mullet, W., Lai, E. P. C., Yeung, J. M., Immunoassay of Fumonisins by a Surface Plasmon Resonance Biosensor, *Anal. Biochem.*, **1998**, *258*, 161–197.

45. Bezuidenhout, S. C., Gelderblom, W. C. A., Gorstallman, C. P., Horak, R. M., Marasas, W. F. O., Spiteller, G., Vleggaar, R., Structure elucidation of the fumonisins, mycotoxins from Fusarium moniliforme, *J. Chem. Soc., Chem. Commun.*, **1988**, *11*, 743–745.
46. Marasas, W. F. O., Kellerman, T. S., Gelderblom, W. C. A., Coetzer, J. A. W., Thiel, P. G., Vanderlugt, J. J., Leukoencephalomalacia in a horse induced by fumonisin B_1 isolated from Fusarium moniliforme, *Onderstepoort J. Vet.*, **1988**, *55*, 197–203.
47. Harrison, L. R., Colvin, B. M., Greene, J. T., Newman, L. E., Cole, J. R., Jr., Pulmonary edema and hydrothorax in swine produced by fumonisin B1, a toxic metabolite of Fusarium moniliforme, *J. Vet. Diagn. Invest.*, **1990**, *2*, 217–221.
48. Gelderblom, W. C. A., Marasas, W. F. O., Controversies in fumonisin mycotoxicology and risk assessment, *Hum. Exp. Toxicol.*, **2012**, *31*, 215–235.
49. Dyoshizawa, T., Yamashita, A., Luo, Y., Fumonisin occurrence in corn from high- and low-risk areas for human esophageal cancer in China, *Appl. Environ. Microb.*, **1994**, *60*, 1626–1629.
50. Scott, P. M., Recent research on fumonisins: a review, *Food Addit. Contam. Part A*, **2012**, *29*, 242–248.
51. Sydenham, E. W., Thiel, P. G., Marasas, W. F. O., Shephard, G. S., Vanschalkwyk, D. J., Koch, K. R., Natural occurrence of some Fusarium mycotoxins in corn from low and high esophageal cancer prevalence areas of the Transkei, Southern Africa, *J. Agric. Food. Chem.*, **1990**, *38*, 1900–1903.

52. Ezquerra, A., Vidal, J. C., Bonel, L., Castillo, J. R., A validated multi-channel electrochemical immunoassay for rapid fumonisin B1 determination in cereal samples, *Anal. Methods*, **2015**, *7*, 3742–3749.
53. Waskiewicz, A., Beszterda, M., Golinski, P., Occurrence of fumonisins in food–an interdisciplinary approach to the problem, *Food Control*, **2012**, *26*, 491–499.
54. Rubert, J., Soler, C., Marín, R., James, K.J., Mañes, J., Mass spectrometry strategies for mycotoxins analysis in European beers, *Food Control*, **2013**, *30*, 122–128.
55. Torres, M. R., Sanchis, V., Ramos, A. J., Occurrence of fumonisins in Spanish beers analyzed by an enzyme-linked immunosorbent assay method, *Int. J. Food Microbiol.*, **1998**, *39*, 139–143.
56. Kadir, M. K., Tothill, I. E., Development of an electrochemical immunosensor for fumonisins detection in foods, *Toxins*, **2010**, *2*, 382–398.
57. Prieto-Simón, B., Campàs, M., Marty, J.-L., Noguer, T., Novel highly-performing immunosensor-based strategy for ochratoxin A detection in wine samples, *Biosens. Bioelectron.*, **2008**, *23*, 995–1002.
58. Vidal, J. C., Bonel, L., Ezquerra, A., Duato, P., Castillo, J. R., An electrochemical immunosensor for ochratoxin A determination in wines based on a monoclonal antibody and paramagnetic microbeads, *Anal. Bioanal. Chem.*, **2012**, *403*, 1585–1593.
59. Bonel, L., Vidal, J. C., Duato, P., Castillo, J. R., An electrochemical competitive biosensor for ochratoxin A based on a DNA biotinylated aptamer, *Biosens. Bioelectron.*, **2011**, *26*, 3254–3259.

60. Prieto-Simón, B., Samitier, J., "Signal Off" Aptasensor Based on Enzyme Inhibition Induced by Conformational Switch, *Anal. Chem.*, **2014**, *86*, 1437–1444.
61. European Commission, Commission Regulation (EC) No 123/2005 of 26 January 2005 amending Regulation (EC) No 466/2001 as regards ochratoxin A, *Off. J. Eur. Union.*, **2005**, *L25*, pp. 135.

II.4.2. Biosensors

1. Pilolli, R., Monaci, L., Visconti, A., Advances in biosensor development based on integrating nanotechnology and applied to food-allergen management, *TrAC, Trends Anal. Chem.*, **2013**, *47*, 12–26.
2. Alves, R. C., Barroso, M. F., González-García, M. B., Oliveira, M. B. P. P., Delerue-Matos, M. C., New Trends in Food Allergens Detection: Towards Biosensing Strategies, *Crit. Rev. Food Sci. Nutr.*, **2015**, *56 (14)*, 2304–2319.
3. Sharma, H., Mutharasan, R., Review of biosensors for foodborne pathogens and toxins, *Sens. Actuat. B-Chem.*, **2013**, *183*, 535–549.
4. Singh, R., Mukherjee, M. D., Sumana, G., Gupta, R. K., Sood, S., Malhotra, B. D., Biosensors for pathogen detection: A smart approach towards clinical diagnosis, *Sens. Actuat. B-Chem.*, **2014**, *197*, 385–404.
5. Turner, N. W., Subrahmanyam, S., Piletsky, S. A., Analytical methods for determination of mycotoxins: a review, *Anal. Chim. Acta*, **2009**, *632*, 168–180.

6. AOAC International, Official Methods of Analysis of AOAC International, *18th edn. AOAC International*, **2005**, Gaithersburg, USA.
7. van Egmond, H. P., Schothorst, R. C., Jonker, M. A., Regulations relating to mycotoxins in food, *Anal. Bioanal. Chem.*, **2007**, *389*, 147–157.
8. Viswanathan, S., Radecka, H., Radecki, J., Electrochemical biosensors for food analysis, *Monatsh. Chem.*, **2009**, *140*, 891–899.
9. Yoon, J.-Y., Kim, B., Lab-on-a-Chip Pathogen Sensors for Food Safety, *Sensors*, **2012**, *12*, 10713–10741.
10. Wang, J., Glucose Biosensors: 40 Years of Advances and Challenges, *Electroanalysis*, **2001**, *13*, 983–988.
11. Clark Jr., L., Membrane polarographic electrode system and method with electrochemical compensation, *US Patent 3539455*, **1970**.
12. Wang, J., *Analytical Electrochemistry*, Wiley-VCH, New Jersey, United States of America, **2006**.
13. Escarpa, A., González, M. C., López, M. Á., *Agricultural and Food Electroanalysis*, Wiley, West Sussex, United Kingdom, **2015**.
14. Bonel, L., Vidal, J. C., Duato, P., Castillo, J. R., An electrochemical competitive biosensor for ochratoxin A based on a DNA biotinylated aptamer, *Biosens. Bioelectron.*, **2011**, *26*, 3254–3259.
15. Vidal, J. C., Bonel, L., Ezquerra, A., Hernandez, S., Bertolin, J. R., Cubel, C., Castillo, J. R., Electrochemical affinity biosensors for detection of mycotoxins: A review, *Biosens. Bioelectron.*, **2013**, *49*, 146–158.

16. Stoltenburg, R., Reinemann, C., Strehlitz, B., FluMag-SELEX as an advantageous method for DNA aptamer selection, *Anal. Bioanal. Chem*, **2005**, *383*, 83–91.
17. Song, S., Wang, L., Li, J., Zhao, J., Fan, C., Aptamer-based biosensors, *TrAC, Trends Anal. Chem.*, **2008**, *27*, 108–117.
18. Aizawa, M., Kato, S., Suzuki, S., Membrane Potential Change Associated With An Immunochemical Reaction Between Membrane-Bound Antigen And Free Antibody, *J. Membr. Sci.*, **1977**, *2*, 125–132.
19. Aizawa, M., Morioka, A., Matsuoka, H., Suzuki, S., Nagamura, Y., Shinohara, R., Ishiguro, I., An Enzyme Immunosensor for IgG, *J. Solid-Phase Biochem.*, **1977**, *1*, 319–328.
20. Campuzano, S., Salema, V., Moreno-Guzmán, M., Gamella, M., Yáñez-Sedeño, P., Fernández, L. A., Pingarrón, J. M., Disposable amperometric magnetoimmunosensors using nanobodies as biorecognition element. Determination of fibrinogen in plasma, *Biosens. Bioelectron.*, **2014**, *52*, 255–260.
21. Li, P. W., Zhang, Q., Zhang, W., Immunoassays for aflatoxins, *TrAC, Trends Anal. Chem.*, **2009**, *28*, 1115–1126.
22. Hamers-Casterman, C., Atarhouch, T., Muyldermans, S., Robinson, G., Hamers, C., Songa, E. B., Bendahman, N., Hamers, R., Naturally occurring antibodies devoid of light chains, *Nature*, **1993**, *363*, 446–448.
23. Ricci, F., Volpe, G., Micheli, L., Palleschi, G., A review on novel developments and applications of immunosensors in food analysis, *Anal. Chim. Acta*, **2007**, *605*, 111–129.

24. Haukanes, B.-I., Kvam, C., Application of Magnetic Beads in Bioassays, *Nat. Biotechnol.*, **1993**, *11*, 60–63.
25. Yu, H., Use of an immunomagnetic separation–fluorescent immunoassay (IMS–FIA) for rapid and high throughput analysis of environmental water samples, *Anal. Chim. Acta*, **1998**, *376*, 77–81.
26. Ricci, F., Adornetto, G., Palleschi, G., A review of experimental aspects of electrochemical immunosensors, *Electrochim. Acta*, **2012**, *84*, 74–83.
27. Zacco, E., Adrian, J., Galve, R., Marco, M.-P-, Alegret, S., Pividori, M. I., Electrochemical magneto immunosensing of antibiotic residues in milk, *Biosens. Bioelectron.*, **2007**, *22*, 2184–2191.
28. Zhao, X., Shippy, S. A., Competitive Immunoassay for Microliter Protein Samples with Magnetic Beads and Near-Infrared Fluorescence Detection, *Anal. Chem.*, **2004**, *76*, 1871–1876.
29. Gessler, F., Hampe, K., Schmidt, M., Bohnel, H., Immunomagnetic beads assay for the detection of botulinum neurotoxin types C and D, Diagn. Microbiol. Infect. Dis., **2006**, *56*, 225–232.
30. Escarpa, A., Lights and shadows on Food microfluidics, *Lab. Chip*, **2014**, *14*, 3213–3224.
31. Skladal, P., Kalab, T., A multichannel immunochemical sensor for determination of 2,4-dichlorophenoxyacetic acid, *Anal. Chim. Acta*, **1995**, *316*, 73–78.
32. Wang, J., Pedrero, M., Sakslund, H., Hammerich, O., Pingarron, J., Electrochemical Activation of Screen-printed Carbon Strips, *Analyst*, **1996**, *121*, 345–350.

33. Hervás, M., López, M. Á., Escarpa, E., Electrochemical immunoassay using magnetic beads for the determination of zearalenone in baby food: An anticipated analytical tool for food safety, *Anal. Chim. Acta*, **2009**, *653*, 167–172.
34. Alves, R. C., Pimentel, F. B., Nouws, H. P. A., Marques, R. C. B., González-García, M. B., Oliveira, M. B. P. P., Delerua-Matos, C., Detection of Ara h 1 (a major peanut allergen) in food using an electrochemical gold nanoparticle-coated screen-printed immunosensor, *Biosens. Bioelectron.*, **2015**, *64*, 19–24.
35. Sun, X., Jia, M., Guan, L., Ji, J., Zhang, Y., Tang, L., Li, Z., Multilayer graphene-gold nanocomposite modified stem-loop DNA biosensor for peanut allergen-Ara h1 detection, *Food Chem.*, **2015**, *172*, 335–342.
36. Sun, X., Guan, L., Shan, X., Zhang, Y., Li, Z., Electrochemical Detection of Peanut Allergen Ara h 1 Using a Sensitive DNA Biosensor Based on Stem-Loop Probe, *J. Agric. Food Chem.*, **2012**, *60*, 10979–10984.
37. López, M. S.-P., Cabanillas, G. F., Castañón, M. J. L., López-Ruiz, B., Development of a genosensor for peanut allergen ARA h 2 detection and its optimization by Surface response methodology, *Biosens. Bioelectron.*, **2014**, *62*, 350–356.
38. Zaitouna, A. J., Lai, R. Y., An electrochemical peptide-based Ara h 2 antibody sensor fabricated on a nickel(II)-nitriloacetic acid self-assembled monolayer using a His-tagged peptide, *Anal. Chim. Acta*, **2014**, *828*, 85–91.

39. Kurita, R., Yanagisawa, H., Niwa, O., Indoor allergen assessment quantified by a thin-layer electrochemical cell and magnetic beads, *Biosens. Bioelectron.*, **2013**, *48*, 43–48.
40. Tsai, J.-J., Bau, I.-J., Chen, H.-T., Lin, Y.-T., Wang, G.-J., A novel nanostructured biosensor for the detection of the dust mite antigen Der p2, *Int. J. Nanomed.*, **2011**, *6*, 1201–1208.
41. Chen, Y.-S., Wu, C.-C., Tsai, J.-J., Wang, G.-J., Electrochemical impedimetric biosensor based on a nanostructured polycarbonate substrate, *Int. J. Nanomed.*, **2012**, *7*, 133–140.
42. Liu, Y.-F., Tsai, J.-J., Chin, Y.-T., Liao, E.-C., Wu, C.-C., Wang, G.-J., Detection of allergies using a silver nanoparticle modified nanostructured biosensor, *Sens. Actuat. B-Chem.*, **2012**, *171–172*, 1095–1100.
43. Cadková, M., Metelka, R., Holubová, D., Horák, D., Dvoráková, V., Bílková, Z., Korecká, L., Magnetic beads-based electrochemical immunosensor for monitoring allergenic food proteins, *Anal. Biochem.*, **2015**, *484*, 4–8.
44. Jiang, D., Ji, J., An, L., Sun, X., Zhang, Y., Zhang, G., Tang, L., Mast cell-based electrochemical biosensor for quantification of the major shrimp allergen Pen a 1 (tropomyosin), *Biosens. Bioelectron.*, **2013**, *50*, 150–156.
45. Jiang, D., Zhu, P., Jiang, H., Ji, J., Sun, X., Gu, W., Zhang, G., Fluorescent magnetic bead-based mast cell biosensor for electrochemical detection of allergens in foodstuffs, *Biosens. Bioelectron.*, **2015**, *70*, 482–490.

46. Eissa, S., Tlili, C., L'Hocine, L., Zourob, M., Electrochemical immunosensor for the milk allergen β-lactoglobulin based on electrografting of organic film on graphene modified screen-printed carbon electrodes, *Biosens. Bioelectron.*, **2012**, *38*, 308–313.
47. Fernandes, A. M., Abdalhai, M. H., Ji, J., Xi, B.-W., Xie, J., Sun, J., Noeline, R., Lee, B. H., Sun, X., Development of highly sensitive electrochemical genosensor base don multiwalled carbón nanotubes-chitosan-bismuth and lead sulfide nanoparticles for the detection of pathogenic *Aeromonas*, *Biosens. Bioelectron.*, **2015**, *63*, 399–406.
48. Kang, X., Pang, G., Chen, Q., Liang, X., Fabrication of *Bacillus cereus* electrochemical immunosensor based on double-layer gold nanoparticles and chitosan, *Sens. Actuat. B-Chem.*, **2013**, *177*, 1010–1016.
49. Yazgan, I., Noah, N. M., Toure, O., Zhang, S., Sadik, O. A., Biosensor for selective detection of *E. coli* in spinach using the strong affinity of derivated mannose with fimbrial lectin, *Biosens. Bioelectron.*, **2014**, *61*, 266–273.
50. Li, Y., Cheng, P., Gong, J., Fang, L., Deng, J., Liang, W., Zheng, J., Amperometric immunosensor for the detection of *Escherichia coli* O157:H7 in food specimens, *Anal. Biochem.*, **2012**, *421*, 227–233.
51. Abdalhai, M. H., Fernandes, A. M., Xi, X., Musa, A., Ji, J., Sun, X., Electrochemical Genosensor To Detect Pathogenic Bacteria (Escherichia coli O157:H7) As Applied in Real Food Samples (Fresh Beef) To Improve Food Safety and Quality Control, *J. Agric. Food Chem.*, **2015**, *63*, 5017–5025.

52. Joung, C.-K., Kim, H.-N., Lim, M.-C., Jeon, T.-J., Kim, H.-Y., Kim, Y.-R., A nanoporous membrane-based impedimetric immunosensor for label-free detection of pathogenic bacteria in whole milk, *Biosens. Bioelectron.*, **2013**, *44*, 210–215.
53. Li, Y., Afrasiabi, R., Fathi, F., Wang, N., Xiang, C., Love, R., She, Z., Kraatz, H.-B., Impedance based detection of pathogenic *E. coli* O157:H7 using a ferrocene-antimicrobial peptide modified biosensor, *Biosens. Bioelectron.*, **2014**, *58*, 193–199.
54. Pandey, C. M., Sumana, G., Tiwari, I., Nanostructuring of hierarchical 3D cysteine flowers for high-performance electrochemical immunosensor, *Biosens. Bioelectron.*, **2014**, *61*, 328–335.
55. Yang, Z., Liu, Y., Lei, C., Sun, X.-C., Zhou, Y., Ultrasensitive detection and quantification of *E. coli* O157:H7 using a giant magnetoimpedance sensor in an open-surface microfluidic cavity covered with an antibody-modified gold surface, *Microchim. Acta*, **2016**, *183*, 1831–1837.
56. Safavieh, M., Ahmed, M. U., Ng, A., Zourob, M., High-throughput real-time electrochemical monitoring of LAMP for pathogenic bacteria detection, *Biosens. Bioelectron.*, **2014**, *61*, 328–335.
57. Yamada, K., Choi, W., Lee, I., Cho, B.-K., Jun, S., Rapid detection of multiple foodborne pathogens using a nanoparticle-functionalized multi-junction biosensor, *Biosens. Bioelectron.*, **2016**, *77*, 137–143.
58. Tian, F., Lyu, J., Shi, J., Tan, F., Yang, M., A polymeric microfluidic device integrated with nanoporous alumina membranes for

simultaneous detection of multiple foodborne pathogens, *Sens. Actuat. B-Chem.*, **2016**, *225*, 312–318.

59. Xu, M., Wang, R., Li, Y., Rapid detection of *Escherichia coli* O157:H7 and *Salmonella Typhimurium* in foods using an electrochemical immunosensor based on screen-printed interdigitated microelectrode and immunomagnetic separation, *Talanta*, **2016**, *148*, 200–208.
60. Cheng, C., Peng, Y., Bai, J., Zhang, X., Liu, Y., Fan, X., Ning, B., Gao, Z., Rapid detection of *Listeria monocytegenes* in milk by self-assembled electrochemical immunosensor, *Sens. Actuat. B-Chem.*, **2014**, *190*, 900–906.
61. Hong, S. A., Kwon, J., Kim, D., Yang, S., A rapid sensitive and selective electrochemical biosensor with concanavalin A for the preemptive detection of norovirus, *Biosens. Bioelectron.*, **2015**, *64*, 338–344.
62. Wang, D., Wang, Z., Chen, J., Kinchla, A. J., Nugen, S. R., Rapid detection of *Salmonella* using a redox cycling-based electrochemical method, *Food Control*, **2016**, *62*, 81–88.
63. Afonso, A. S., Pérez-López, B., Faria, R. C., Mattoso, L. H. C., Hernández-Herrero, M., Roig-Saqués, A. X., Costa, M. M., Merkoçi, A., Electrochemical detection of *Salmonella* using gold nanoparticles, *Biosens. Bioelectron.*, **2013**, *40*, 121–126.
64. Wang, D., Dou, W., Zhao, G., Chen, Y., Immunosensor based on electrodeposition of gold-nanoparticles and ionic liquid composite for detection of *Salmonella pullorum*, *J. Microbiol. Methods*, **2014**, *106*, 110–118.

65. Fei, J., Dou, W., Zhao, G., A sandwich electrochemical immunosensor for Salmonella pullorum and Salmonella gallinarum based on a screen-printed carbon electrode modified with an ionic liquid and electrodeposited gold nanoparticles, *Microchim. Acta*, **2015**, *182*, 2267–2275.
66. Fei, J., Dou, W., Zhao, G., Amperometric immunoassay for the detection of *Salmonella pullorum* using a screen - printed carbon electrode modified with gold nanoparticle-coated reduced graphene oxide and immunomagnetic beads, *Microchim. Acta*, **2016**, *183*, 757–764.
67. Xiang, C., Li, R., Adhikari, B., She, Z., Li, Y., Kraatz, H.-B., Sensitive electrochemical detection of *Salmonella* with chitosan-gold nanoparticles composite film, *Talanta*, **2015**, *140*, 757–764.
68. Sheikhzadeh, E., Chamsaz, M., Turner, A. P. F., Jager, E. W. H., Beni, V., Label-free impedimetric biosensor for *Salmonella Typhimurium* detection based on poly[pyrrole-co-3-carboxyl-pyrrole] copolymer supported aptamer, *Biosens. Bioelectron.*, **2016**, *80*, 194–200.
69. Bhardwaj, N., Bhardwaj, S. K., Mehta, J., Mohanta, G. C., Deep, A., Bacteriophage immobilized graphene electrodes for impedimetric sensing of bacteria (*Staphylococcus arlettae*), *Anal. Biochem.*, **2016**, *505*, 18–25.
70. Esteban-Fernández de Ávila, B., Pedrero, M., Campuzano, S., Escamilla-Gómez, V., Pingarrón, J. M., Sensitive and rapid amperometric magnetoimmunosensor for the determination of *Staphylococcus aureus*, *Anal. Bioanal. Chem.*, **2012**, *403*, 917–925.

71. Abbaspour, A., Norouz-Sarvestani, F., Noori, A., Soltani, N., Aptamer-conjugated silver nanoparticles for electrochemical dual-aptamer-based sandwich detection of *staphylococcus aureus*, *Biosens. Bioelectron.*, **2015**, *68*, 149–155.
72. Srivastava, S., Kumar, V., Arora, K., Singh, C., Ali, M. A., Puri, N. K., Malhotra, B. D., Antibody Conjugated Metal Nanoparticles Decorated Graphene Sheets for Mycotoxin Sensor, *RSC Adv.*, **2016**, *6*, 56518–56526.
73. Zhang, X., Li, C.-R., Wang, W.-C., Xue, J., Huang, Y.-L., Yang, X.-X., Tan, B., Zhou, X.-P., Shao, C., Ding, S.-J., Qiu, J.-F., A novel electrochemical immunosensor for highly sensitive detection of aflatoxin B_1 in corn using single-walled carbon nanotubes/chitosan, *Food Chem.*, **2016**, *192*, 197–202.
74. Ma, H., Sun, J., Zhang, Y., Bian, C., Xia, S., Zhen, T., Label-free immunosensor based on one-step electrodeposition of chitosan-gold nanoparticles biocompatible film on Au microelectrode for determination of aflatoxin B_1 in maize, *Biosens. Bioelectron.*, **2015**, *68*, 149–155.
75. Li, Z., Ye, Z., Fu, Y., Xiong, Y., Li, Y., A portable electrochemical immunosensor for rapid detection of trace aflatoxin B_1 in rice, *Anal. Methods*, **2016**, *8*, 548–553.
76. Wang, D., Hu, W., Xiong, Y., Xu, Y., Li, C. M., Multifunctionalized reduced graphene oxide-doped polypyrrole/pyrrolepropylic acid nanocomposite impedimetric immunosensor to ultra-sensitively

detect small molecular aflatoxin B_1, *Biosens. Bioelectron.*, **2015**, *63*, 185–189.

77. Goud, K. Y., Catanante, G., Hayat, A., Satyanarayana, M., Gobi, K. V., Marty, J. L., Disposable and portable electrochemical aptasensor for label free detection of aflatoxin B1 in alcoholic beverages, *Sens. Actuat. B-Chem.*, **2016**, *235*, 466–473.
78. Chauhan, R., Solanki, P. R., Singh, J., Mukherjee, I., Basu, T., Malhotra, B. D., A novel electrochemical piezoelectric label free immunosensor for aflatoxin B1 detection in groundnut, *Food Control*, **2015**, *52*, 60–70.
79. Chauhan, R., Singh, J., Solanki, P. R., Manaka, T., Iwamoto, M., Basu, T., Malhotra, B. D., Label-free piezoelectric immunosensor decorated with gold nanoparticles: Kinetic analysis and biosensing application, *Sens. Actuat. B-Chem.*, **2016**, *222*, 804–814.
80. Wang, H., Zhang, Y., Chu, Y., Ma, H., Li, Y., Wu, D., Du, B., Wei, Q., Disposable competitive-type immunoassay for determination of aflatoxin B1 via detection of copper ions released from Cu-apatite, *Talanta*, **2016**, *147*, 556–560.
81. Bacher, G., Pal, S., Kanungo, L., Bhand, S., A label-free silver wire based impedimetric immunosensor for detection of aflatoxin M1 in milk, *Sens. Actuat. B-Chem.*, **2012**, *168*, 223–230.
82. Istamboulié, G., Panial, N., Zara, L., Granados, L. R., Barthelmebs, L., Noguer, T., Development of an impedimetric aptasensor for the determination of aflatoxin M1 in milk, *Talanta*, **2016**, *146*, 464–469.

83. Olcer, Z., Esen, E., Muhammad, T., Ersoy, A., Budak, S., Uludag, Y., Fast and sensitive detection of mycotoxins in wheat using microfluidics based Real-time Electrochemical Profiling, *Biosens. Bioelectron.*, **2014**, *62*, 163–169.
84. Qing, Y., Li, C.-R., Yang, X.-X., Zhou, X.-P., Xue, J., Luo, M., Xu, X., Chen, S., Qiu, J.-F., Electrochemical immunosensor using single-walled carbon nanotubes/chitosan for ultrasensitive detection of deoxynivalenol in food samples, *J. Appl. Electrochem.*, **2016**, *46*, 1049–1057.
85. Sunday, C. E., Masikini, M., Wilson, L., Rassie, C., Waryo, T., Baker, P. G. L., Iwuoha, E. I., Application on Gold Nanoparticles-Dotted 4-Nitrophenylazo Graphene in a Label-Free Impedimetric Deoxynivalenol Immunosensor, *Sensors*, **2015**, *15*, 3854–3871.
86. Lu, L., Seenivasan, R., Wang, Y.-C., Yu, J.-H., Gunasekaran, S., An Electrochemical Immunosensor for Rapid and Sensitive Detection of Mycotoxins B1 and Deoxynivalenol, *Electrochim. Acta*, **2016**, *213*, 89–97.
87. Ezquerra, A., Vidal, J. C., Bonel, L., Castillo, J. R., A validated multi-channel electrochemical immunoassay for rapid fumonisin B1 determination in cereal samples, *Anal. Methods*, **2015**, *7*, 3742–3749.
88. Yang, X., Zhou, X., Zhang, X., Qing, Y., Luo, M., Liu, X., Li, C., Li, Y., Xia, H., Qiu, J., A Highly Sensitive Electrochemical Immunosensor for Fumonisin B_1 Detection in Corn Using Single-Walled Carbon Nanotubes/Chitosan, *Electroanalysis*, **2015**, *27*, 2679–2687.

89. Chen, X., Huang, Y., Ma, X., Jia, F., Guo, X., Wang, Z., Impedimetric aptamer-based determination of the mold toxin fumonisin B1, *Microchim. Acta*, **2015**, *182*, 1709–1714.

90. Jodra, A., López, M. Á. Escarpa, A., Disposable and reliable electrochemical magnetoimmunosensor for Fumonisins simplified determination in maize-based foodstuffs, *Biosens. Bioelectron.*, **2015**, *64*, 633–638.

91. Toro, P. C. D., Arévalo, F. J., Fumero, M. V., Zon, M. A., Fernández, H., Very sensitive electrochemical sensor for moniliformin detection in maize samples, *Sens. Actuat. B-Chem.*, **2016**, *225*, 384–390.

92. Jodra, A., Hervás, M., López, M. Á., Escarpa, A., Disposable electrochemical magneto immunosensor for simultaneous simplified calibration and determination of Ochratoxin A in coffee samples, *Sens. Actuat. B-Chem.*, **2015**, *221*, 777–783.

93. Fernández-Baldo, M. A., Bertolino, F. A., Fernández, G., Messina, G. A., Sanz, M. I., Raba, J., Determination of Ochratoxin A in apples contaminated with *Aspergillus ochraceus* by using a microfluidic competitive immunosensor with magnetic nanoparticles, *Analyst*, **2011**, *136*, 2756–2762.

94. Alonso-Lomillo, M. A., Domínguez-Renedo, O., del Torno-de Román, L., Arcos-Martínez, M. J., Horseradish peroxidase-screen printed biosensors for determiantion of Ochratoxin A, *Anal. Chim. Acta*, **2011**, *688*, 49–53.

95. Heurich, M., Kadir, M. K. A., Tothill, I. E., An electrochemical sensor based on carboxymethylated dextran modified gold surface for ochratoxin A analysis, *Sens. Actuat. B-Chem.*, **2011**, *156*, 162–168.
96. Huang, K.-J., Shuai, H.-L., Chen, Y.-X., Layered molybdenum selenide stacking flower-like nanostructure coupled with guanine-rich DNA sequence for ultrasensitive ochratoxin A aptasensor application, *Sens. Actuat. B-Chem.*, **2016**, *225*, 391–397.
97. Vidal, J. C., Bonel, L., Ezquerra, A., Duato, P., Castillo, J. R., An electrochemical immunosensor for ochratoxin A determination in wines based on a monoclonal antibody and paramagnetic microbeads, *Anal. Bioanal. Chem.*, **2012**, *403*, 1585–1593.
98. Bonel, L., Vidal, J. C., Duato, P., Castillo, J. R., An electrochemical competitive biosensor for ochratoxin A based on a DNA biotinylated aptamer, *Biosens. Bioelectron.*, **2011**, *26*, 3254–3259.
99. Mishra, R. K., Hayat, A., Catanante, G., Istamboulie, G., Marty, J.-L., Sensitive quantitation of Ochratoxin A in cocoa beans using differential pulse voltammetry based aptasensor, *Food Chem.*, **2016**, *192*, 799–804.
100. Prieto-Simón, B., Samitier, J., "Signal Off" Aptasensor Based on Enzyme Inhibition Induced by Conformational Switch, *Anal. Chem.*, **2014**, *86*, 1437–1444.
101. Malvano, F., Albanese, D., Crescitelli, A., Pilloton, R., Esposito, E., Impedimetric Label-Free Immunosensor Disposable Modified Screen-Printed Lectrodes for Ochratoxin A, *Biosensors*, **2016**, *6*, 1–13.

102. Mishra, R. K., Hayat, A., Catanante, G., Ocaña, C., Marty, J.-L., A label free aptasensor for Ochratoxin A detection in cocoa beans: An application to chocolate industries, *Anal. Chim. Acta*, **2015**, *889*, 106–112.

103. Tang, J., Huan, Y., Zhang, C., Liu, H., Tang, D., Amplified impedimetric immunosensor based on instant catalyst for sensitive determination of ochratoxin A, *Biosens. Bioelectron.*, **2016**, *86*, 386–392.

104. Zhu, Z., Feng, M., Zuo, L., Zhu, Z., Wang, F., Chen, L., Li, J., Shan, G., Luo, S.-Z., An aptamer-based surface plasmons resonance biosensor for the detection of ochratoxin A in wine and peanut oil, *Biosens. Bioelectron.*, **2015**, *65*, 320–326.

105. Perrotta, P. R., Arévalo, F. J., Vettorazzi, N. R., Zón, M. A., Fernández, H., Development of a very sensitive electrochemical magneto immunosensor for the direct determination of ochratoxin A in red wine, *Sens. Actuat. B-Chem.*, **2012**, *162*, 327–333.

106. Hervás, M., López, M. A., Escarpa, E., Integrated electrokinetic magnetic bead-based electrochemical immunoassay on microfluidic chips for reliable control of permitted levels of zearalenone in infant foods, *Analyst*, **2011**, *136*, 2131–2138.

107. Panini, N. V., Salinas, E., Messina, G. A., Raba, J., Modified paramagnetic beads in a microfluidic system for the determination of zearalenone in feedstuff samples, *Food Chem.*, **2011**, *125*, 791–796.

108. Wang, Y.-K., Yan, Y.-X., Mao, Z.-W., Wang, H.-A., Zou, Q., Hao, Q.-W., Ji, W.-H., Sun, J.-H., Highly sensitive electrochemical

immunoassay for zearalenone in grain and grain-based food, *Microchim. Acta*, **2013**, *180*, 187–193.

109. Araki, A., Sako, Y., Determination of Free and Total Homocysteine in Human Plasma by High-Performance Liquid Chromatography with Fluorescence detection, *J. Chromatogr.*, **1987**, *422*, 43–52.
110. Bloom, N., Fitzgerald, W. F., Determination of Volatile Mercury Species at the Picogram Level by Low-Temperature Gas Chromatography with cold-Vapour Atomic Fluorescence, *Anal. Chim. Acta*, **1988**, *208*, 151–161.
111. Shephard, G. S., Sydenham, E. W., Thiel, P. G., Gelderblom, W. C. A., Quantitative Determination of Fumonisins B_1 and B_2 by High-Performance Liquid Chromatography with Fluorescence Detection, *J. Liq. Chromatogr.*, **1990**, *13*, 2077–2087.
112. Chabinyc, M. L., Chiu, D. T., McDonald, J. C., Stroock, A. D., Christian, J. F., Karger, A. M., Whitesides, G. M., An Integrated Fluorescence Detection System in Poly(dimethylsiloxane) for Microfluidic Applications, *Anal. Chem.*, **2001**, *73*, 4491–4498.
113. Smith, Ll. M., Sanders, J. Z., Kaiser, R. J., Hughes, P., Dodd, C., Connell, C. R., Heiner, C., Kent, S. B. H., Hood, L. E., Fluorescence detection in automated DNA sequence analysis, *Nature*, **1986**, *321*, 674–679.
114. Geng, X., Zhang, D., Wang, H., Zhao, Q., Screening interaction between ochratoxin A and aptamers by fluorescence anisotropy approach, *Anal. Bionanal. Chem.*, **2013**, *40*, 2443–2449.

115. Wu, S., Duan, N., Ma, X., Xia, Y., Wang, H., Wang, Z., Zhang, Q., Multiplexed Fluorescence Resonance Energy Transfer Aptasensor between Upconversion Nanoparticles and Graphene Oxide for the Simultaneous Determination of Mycotoxins, *Anal. Chem.*, **2012**, *84*, 6263–6270.
116. Zhu, Z., Yang, R., You, M., Zhang, X., Wu, Y., Tan, W., Single-walled carbon nanotube as an effective quencher, *Anal. Bionanal. Chem.*, **2010**, *396*, 73–83.
117. Guo, Z., Ren, J., Wang, J., Wang, E., Single-walled carbon nanotubes based quenching of free FAM-aptamer for selective determination of ochratoxin A, *Talanta*, **2011**, *85*, 2517–2521.
118. Lu, Z., Chen, X., Wang, Y., Zheng, X., Li, C. M., Aptamer-based fluorescence recovery assay for aflatoxin B1 using a quencher system composed of quantum dots and graphene oxide, *Microchim. Acta*, **2014**, *182*, 571–578.

II.4.3. Motors

1. Ozin, G. A., Manners, I., Fournier-Bidoz, S., Arsenault, A., Dream Nanomachines, *Adv. Mater.*, **2005**, *17*, 3011–3018.
2. Kim, K., Guo, J., Xu, X., Fan, L., Recent Progress on Man-Made Inorganic Nanomachines, *Small*, **2015**, *11 (33)*, 4037–4057.
3. Guix, M., Mayorga-Martínez, C. C., Merkoçi, A., Nano/Micromotors in (Bio)chemical Science Applications, *Chem. Rev.*, **2014**, *114*, 6285–6322.
4. Wang, J., Can Man-Made Nanomachines Compete with Nature Biomotors?, *ACS Nano*, **2009**, *3*, 4–9.

5. Mei, Y., Solovev, A. A., Sanchez, S., Schmidt, O. G., Rolled-up nanotech on polymers: from basic perception to self-propelled catalytic microengines, *Chem. Soc. Rev.*, **2011**, *40*, 2109–2119.
6. Ismagilov, R. F., Schwartz, A., Bowden, N., Whitesides, G. M., Autonomous Movement and Self-Assembly, *Angew. Chem. Int. Ed.*, **2002**, *41*, 652–654.
7. Paxton, W. F., Kistler, K. C., Olmeda, C. C., Sen, A., St. Angelo, S. K., Cao, Y., Mallouk, T. E., Lammert, P., E., Crespi, V. H., Catalytic Nanomotors: Autonomous Movement of Striped Nanorods, *J. Am. Chem. Soc.*, **2004**, *126*, 13424–13431.
8. Schönenberger, C., van der Zande, B. M. I., Fokkink, L. G. J., Henny, M., Schmid, C., Krüger, M., Bachtold, A., Huber, R., Birk, H., Staufer, U., Template Synthesis of Nanowires in Porous Polycarbonate Membranes: Electrochemistry and Morphology, *J. Phys. Chem. B*, **1997**, *101*, 5497–5505.
9. Kline, T. R., Tian, M., Wang, J., Sen, A., Chan, W. H. M., Mallouk T. E., Template-grown metal nanowires, *Inorg. Chem.*, **2006**, *45*, 7555–7565.
10. Laocharoensuk, R., Burdick, J., Wang, J., Carbon-Nanotube-Induced Acceleration of Catalytic Nanomotors, *ACS Nano*, **2008**, *2*, 1069–1075.
11. Kagan, D., Calvo-Marzal, P., Balasubramanian, S., Sattayasamitsathit, S., Manesh, K. M., Flechsig, G., Wang, J., Chemical sensing Based on Catalytic Nanomotors: Motion-Based Detection of Trace Silver, *J. Am. Chem. Soc.*, **2009**, *131*, 12082–12083.

12. Ibele, M. E., Wang, Y., Kline, T. R., Mallouk, T. E., Sen, A., Hydrazine fuels for bimetallic catalytic microfluidic pumping, *J. Am. Chem. Soc.*, **2007**, *129*, 7762–7763.
13. Gao, W., Pei, A., Dong, R., Wang, J., Catalytic Iridium-Based Janus Micromotors Powered by Ultralow Levels of Chemical Fuels, *J. Am. Chem. Soc.*, **2014**, *136*, 2276–2279.
14. Gao, W., Pei, A., Wang, J., Water-Driven Micromotors, *ACS Nano*, **2012**, *6*, 8432–8438.
15. Gao, W., Feng, X., Pei, A., Gu, Y., Li, J., Wang, J., Seawater-driven magnesium based Janus micromotors for environmental remediation, *Nanoscale*, **2013**, *5*, 4696–4700.
16. Gao, W., Uygun, A., Wang, J., Hydrogen-Bubble-Propelled Zinc-Based Microrockets in Strongly Acidic Media, *J. Am. Chem. Soc.*, **2012**, *154*, 897–900.
17. Gao, W., Dong, R., Thamphiwatana, S., Li, J., Gao, W., Zhang, L., Wang, J., Artificial Micromotors in the Mouse's Stomach: A Step towards *in Vivo* Use of Synthetic Motors, *ACS Nano*, **2015**, *9*, 117–123.
18. Mei, Y., Sololev, A. A., Sanchez, S., Schmidt, O. G., Rolled-up nanotech on polymers: from basic perception to self-propelled catalytic microengines, *Chem. Soc. Rev.*, **2011**, *40*, 2109–2119.
19. Li, J., Rozen, I., Wang, J., Rocket Science at the Nanoscale, *ACS Nano*, **2016**, *10*, 5619–5624.
20. Schmidt, O. G., Eberl, K., Thin solid films roll up into nanotubes, *Nature*, **2001**, *410*, 168.

21. Sololev, A. A., Xi, W., Gracias, D. H., Harazim, S. M., Deneke, C., Sanchez, S., Schmidt, O. G., Self-Propelled Nanotools, *ACS Nano*, **2012**, *6*, 1751–1756.
22. Sololev, A. A., Mei, Y., Ureña, E. B., Huang, G., Schmidt, O. G., Catalytic Microtubular Jet Engines Self-Propelled by Accumulated Gas Bubbles, *Small*, **2009**, *5*, 1688–1692.
23. Baraban, L., Tasinkevych, M., Popescu, M. N., Sanchez, S., Dietrich, S., Schmidt, O. G., Transport of cargo by catalytic Janus micro-motors, *Soft Matter.*, **2012**, *8*, 48–52.
24. Baraban, L., Streubel, R., Makarov, D., Han, L., Kamaushenko, D., Schmidt O. G., Cuniberti, G., Fuel-Free Locomotion of Janus Motors: Magnetically Induced Thermophoresis, *ACS Nano*, **2013**, *7*, 1360–1367.
25. Gao, W., Pei, A., Feng, X., Hennessy, C., Wang, J., Organized Self-Assembly of Janus Micromotors with Hydrophobic Hemispheres, *J. Am. Chem. Soc.*, **2013**, *135*, 998–1001.
26. Singh, V. V., Soto, F., Kaufmann, K., Wang, J., Micromotor-Based Energy Generation, *Angew. Chem. Int. Ed.*, **2015**, *54*, 1–5.
27. Chen, C., Karshalev, E., Li, J., Soto, F., Castillo, R., Campos, I., Mou, F., Guan, J., Wang, J., Transient Micromotors That Disappear When No Longer Needed, *ACS Nano*, **2016**, *10*, 10389–10396.
28. Singh, V. V., Jurado-Sánchez, B., Sattayasamitsathit, S., Orozco, J., Li, J., Galarnyk, M., Fedorak, Y., Wang, J., Multifunctional Silver-Exchanged Zeolite Micromotors for Catalytic Detoxification of

Chemical and Biological Threats, *Adv. Funct. Mater.*, **2015**, *25*, 2147–2155.

29. Sattayasamitsathit, S., Kou, H., Gao, W., Thavarajah, W., Kaufmann, K., Zhang, L., Wang, J., Fully Loaded Micromotors for combinatorial Delivery and Autonomous Release of Cargoes, *Small*, **2014**, *10*, 2830–2833.
30. Martín, A., Jurado-Sánchez, B., Escarpa, E., Wang, J., Template Electrosynthesis of High Performance Graphene Microengines, *Small*, **2015**, *11*, 3568–3574.
31. Zhao, G., Pumera, M., Concentric bimetallic microjets by electrodeposition, *RSC Adv.*, **2013**, *3*, 3963–3966.
32. Gao, W., Sattayasamitsathit, S., Orozco, J., Wang, J., Highly Efficient Catalytic Microengines: Template Electrosynthesis of Polyaniline/Platinum Microtubes, *J. Am Chem. Soc.*, **2011**, *133*, 11862–11864.
33. Maria-Hormigos, R., Jurado-Sánchez, B., Vázquez, L., Escarpa, E., Carbon Allotrope Nanomaterials Based Catalytic Micromotors, *Chem. Mater.*, **2016**, *28*, 8962–8970.
34. Gao, W., Sattayasamitsathit, S., Uygun, A., Pei, A., Ponedal, A., Wang, J., Polymer-based tubular microbots: role of composition and preparation, *Nanoscale*, **2012**, *4*, 2447–2453.
35. García, M., Orozco, J., Guix, M., Gao, W., Sattayasamitsathit, S., Escarpa, A., Merkoçi, A., Wang, J., Micromotor-Based Lab-on-Chip Immunoassays, *Nanoscale*, **2013**, *5*, 1325–1331.

36. Li, J., Huang, G., Ye, M., Li, M., Liu, R., Mei, Y., Dynamics of catalytic tubular microjet engines: Dependence on geometry and chemical environment, *Nanoscale*, **2011**, *3*, 5083–5089.
37. Li, L., Wang, J., Li, T., Songa, W., Zhanga, G., Hydrodynamics and propulsion mechanism of self-propelled catalytic micromotors: model and experiment, *Soft Matter.*, **2014**, *10*, 7511–7518.
38. Scriven, L. E., Sternling, C. V., The Marangoni Effects, *Nature*, **1960**, *187*, 186–188.
39. Sharma, R., Chang, S. T., Velev, O. D., Gel-Based Self-Propelling Particles Get Programmed To Dance, *Langmuir*, **2012**, *28*, 10128–10135.
40. Orozco, J., Vilela, D., Valdés-Ramírez, G., Fedorak, Y., Escarpa, A., Vazquez-Duhalt, R., Wang, J., Efficient Biocatalytic Degradation of Pollutants by Enzyme-Releasing Self-Propelled Motors, *Chem. Eur. J.*, **2014**, *20*, 1–7.
41. Zhao, G., Pumera, M., Liquid–Liquid Interface Motion of a Capsule Motor Powered by the Interlayer Marangoni Effect, *J. Phys. Chem. B*, **2012**, *116*, 10960–10963.
42. Wang, W., Castro, L. A., Hoyos, M., Mallouk, T. E., Autonomous Motion of Metallic Microrods Propelled by Ultrasound, *ACS Nano*, **2012**, *6*, 6122–6132.
43. Rao, K. J., Li, F., Meng, L., Zheng, H., Cai, F., Wang, W., A Force to Be Reckoned With: A Review Of Synthetic Microswimmers Powered By Ultrasound, *Small*, **2015**, *11*, 2836–2846.

44. Garcia-Gradilla, V., Orozco, J., Sattayasamitsathit, S., Soto, F., Kuralay, F., Pourazary, A., Katzenberg, A., Gao, W., Shen, Y., Wang, J., Functionalized ultrasound-propelled magnetically guided nanomotors: Toward practical biomedical applications, *ACS Nano*, **2013**, *7*, 9232–9240.
45. Xu, T., Soto, F., Gao, W., Dong, R., Garcia-Gradilla, V., Magan, E., Zhang, X., Wang, J., Reversible Swarming and Separation of Self-Propelled Chemically Powered Nanomotors under Acoustic Fields, *J. Am. Chem. Soc.*, **2015**, *137*, 2163–2166.
46. Garcia-Gradilla, V., Sattayasamitsathit, S., Soto, F., Kuralay, F., Yardimci, C., Wiitala, D., Galarnyk, M., Wang, J., Ultrasound-Propelled Nanoporous Gold Wire for Efficient Drug Loading and Release, *Small*, **2014**, *10*, 4154–4159.
47. Kiristi, M., Singh, V. V., Esteban-Fernández de Ávila, B., Uygun, M., Soto, F., Uygun, D. A., Wang, J., Lysozyme-Based Antibacterial Nanomotors, *ACS Nano*, **2015**, *9*, 9252–9259.
48. Wang, W., Li, S., Mair, L., Ahmed, S., Huang, T. J., Mallouk, T. E., Acoustic Propulsion of Nanorod Motors Inside Living Cells, *Angew. Chem. Int. Ed.*, **2014**, *53*, 3201–3204.
49. Wu, Z., Li, T., Li, J., Gao, W., Xu, T., Christianson, C., Gao, W., Galarnyk, M., He, Q., Zhang, L., Wang, J., Turning Erythrocytes into Functional Micromotors, *ACS Nano*, **2014**, *8*, 12041–12048.
50. Wu, Z., Esteban-Fernández de Ávila, B., Martín, A., Christianson, C., Gao, W., Thamphiwatana, S. K., Escarpa, A., He, Q., Zhang, L., Wang,

J., RBC micromotors carrying multiple cargoes towards potential theranostic applications, *Nanoscale*, **2015**, *7*, 13680–13686.

51. Kagan, D., Benchimol, M. J., Claussen, J. C., Chuluun-Erdene, E., Esener, S., Wang, J., Acoustic Droplet Vaporization and Propulsion of Perfluorocarbon-Loaded Microbullets for Targeted Tissue Penetration and Deformation, *Angew. Chem. Int. Ed.*, **2012**, *6*, 9415–9420.
52. Soto, F., Martín, A., Ibsen, S., Vaidyanathan, M., Garcia-Gradilla, V., Levin, Y., Escarpa, A., Esener, S. C., Wang, J., Acoustic Microcannons: Toward Advanced Microballistics, *ACS Nano*, **2016**, *10*, 1522–1528.
53. Soto, F., Wagner, G. L., Garcia-Gradilla, V., Gillespie, K. T., Lakshmipathy, D. R., Karshalev, E., Angeli, C., Chen, Y., Wang, J., Acoustically propelled nanoshells, *Nanoscale*, **2016**, *8*, 17788–17793.
54. Esteban-Fernández de Ávila, B., Martín, A., Soto, F., Lopez-Ramirez, M. A., Campuzano, S., Vásquez-Machado, G. M., Gao, W., Zhang, L., Wang, J., Single Cell Real-Time mi RNAs Sensing Based on Nanomotors, *ACS Nano*, **2015**, *9*, 6756–6764.
55. Li, J., Sattayasamitsathit, S., Dong, R., Gao, W., Tam, R., Feng, X., Ai, S., Wang, J., Template electrosynthesis of tailored-made helical nanoswimmers, *Nanoscale*, **2014**, *6*, 9415–9420.
56. Schamel, D., Pfeifer, M., Gibbs, J. G., Miksch, B., Mark, A. G., Fischer, P., Chiral Colloidal Molecules And Observation Of The Propeller Effect, *J. Am. Chem. Soc.*, **2013**, *135*, 12353–12359.
57. Medina-Sánchez, M., Schwarz, L., Meyer, A. K., Hebenstreit, F., Schmidt, O. G., Cellular Cargo Delivery: Toward Assisted

Fertilization by Sperm-Carrying Micromotors, *Nano Lett.*, **2016**, *16*, 555–561.

58. Dong, R., Zhang, Q., Gao, W., Pei, Allen, Ren, B., Highly Efficient Light-Driven TiO_2- Au Janus Micromotors, *ACS Nano*, **2016**, *10*, 839–844.
59. Breger, J. C., Yoon, C., Xiao, R., Kwag, H. R., Wang, M. O., Fisher, J. P., Nguyen, T. D., Gracias, D. H., Self-Folding Thermo-Magnetically Responsive Soft Microgrippers, *ACS Appl. Mater. Interfaces*, **2015**, *7*, 3398–3405.
60. Sundararajan, S. P., Lammert, E., Zudans, A. W., Crespi, V. H., Sen, A., Catalytic Motors for Transport of Colloidal Cargo, *Nano Lett.*, **2008**, *8*, 1271–1276.
61. Kagan, D., Laocharoensuk, R., Zimmerman, M., Clawson, C., Balasubramanian, S., Kang, D., Bishop, D., Sattayasamitsathit, S., Zhang, L., Wang, J., Rapid Delivery of Drug Carriers Propelled and Navigated by Catalytic Nanoshuttles, *Small*, **2010**, *6*, 2741–2747.
62. Wu, J., Balasubramanian, S., Kagan, D., Manesh, K. M., Campuzano, S., Wang, J., Motion-based DNA detection using catalytic nanomotors, *Nat. Commun.*, **2010**, *1*, 36.
63. Jodra, A., Soto, F., Lopez-Ramirez, M. A., Escarpa, A., Wang, J., Delayed ignition and propulsion of catalytic microrockets based on fuel-induced chemical dealloying of the inner alloy layer, *Chem. Commun.*, **2016**, *52*, 11838–11841.

64. Sanchez, S., Sololev, A. A., Schulze, S., Schmidt, O. G., Controlled manipulation of multiple cells using catalytic microbots, *Chem. Commun.*, **2011**, *47*, 698–700.

65. Sanchez, S., Sololev, A. A., Harazim, S. M., Schmidt, O. G., Microbots Swimming in the Flowing Streams of Microfluidic Channels, *J. Am. Chem. Soc.*, **2011**, *133*, 701–703.

66. Vilela, D., Parmar, J., Zeng, Y., Zhao, Y., Sanchez, S., Graphene-based microbots for toxic heavy metal removal and recovery from water, *Nano Lett.*, **2016**, *16*, 2860–2866.

67. Orozco, J., Cheng, G., Vilela, D., Sattayasamitsathit, S., Pak, O.S., Vazquez-Duhalt, R., Valdés-Ramírez, G., Escarpa, A., Kan, C., Wang, J., Micromotor-Based High-Yielding Fast Oxidative Detoxification of Chemical Threats, *Angew. Chem. Int. Ed.*, **2013**, *52*, 13276–13279.

68. Campuzano, S., Orozco, J., Kagan, D., Guix, M., Gao, W., Sattayasamitsathit, S., Claussen, J. C., Merkoçi, A., Wang, J., Bacterial Isolation by Lectin-Modified Microengines, *Nano Lett.*, **2012**, *12*, 396–401.

69. Delezuk, J. A. M., Ramírez-Herrera, D. E., Esteban-Fernández de Ávila, B., Wang, J., Chitosan-based water-propelled micromotors with strong antibacterial activity, *Nanoscale*, **2017**, *9*, 2195–2200.

70. Stanton, M. M., Simmchen, J., Ma, X., Miguel-López, A., Sanchez, S., Biohybrid Janus Motors Driven by Escherichia coli, *Adv. Mater. Interfaces*, **2016**, *3*, 1500505.

71. Li, J., Thamphiwatana, S., Liu, W., Esteban-Fernández de Ávila, B., Angsantikul, P., Sandraz, E., Wang, J., Xu, T., Soto, F., Ramez, V.,

Wang, X., Gao, W., Zhang, L., Wang, J., Enteric Micromotor Can Selectively Position and Spontaneously Propel in the Gastrointestinal Tract, *ACS Nano*, **2016**, *10*, 9536–9542.

72. Moo, J. G. S., Wang, H., Zhao, G., Pumera, M., Biomimetic Artificial Inorganic Enzyme-Free Self-Propelled Microfish Robot for Selective Detection of Pb^{2+} in Water., *Chem. Eur. J.*, **2014**, *20*, 4292–4296.
73. Orozco, J., Garcia-Gradilla, V., D'Agostino, M., Gao, W., Cortés, A., Wang, J., Artificial Enzyme-Powered Microfish for Water-Quality Testing, *ACS Nano*, **2013**, *7*, 818–824.
74. Wang, H., Zhao, G., Pumera, M., Blood electrolytes exhibit a strong influence on the mobility of artificial catalytic microengines, *Phys. Chem. Chem. Phys.*, **2013**, *15*, 17277–17280.
75. Zhao, G. J., Sanchez, S., Schmidt, O. G., Pumera, M., Poisoning of bubble propelled catalytic micromotors: the chemical environment matters, *Nanoscale*, **2013**, *5*, 2909–2914.
76. Wang, H., Zhao, G., Pumera, M., Blood metabolite strongly suppresses motion of electrochemically deposited catalytic self-propelled microjet engines, *Electrochem. Commun.*, **2014**, *38*, 128–130.
77. Wang, H: Zhao, G., Pumera, M., Blood Proteins Strongly Reduce the Mobility of Artificial Self- Propelled Micromotors, *Chem. Eur. J.*, **2013**, *19*, 16756–16759.
78. Morales-Narváez, E., Guix, M., Medina-Sánchez, M., Mayorga-Martinez, C. C., Merkoçi, A., Micromotor Enhanced Microarray Technology for Protein Detection, *Small*, **2014**, *10*, 2542–2548.

79. Kagan, D., Campuzano, S., Balasubramanian, S., Kuralay, F., Flechsig, G. U., Wang, J., Functionalized Micromachines for Selective and Rapid Isolation of Nucleic Acid Targets from Complex Samples, *Nano Lett.*, **2011**, *11*, 2083–2087.

80. Esteban-Fernández de Ávila, B., Lopez-Ramirez, M. A., Báez, D. F., Jodra, A., Singh, V. V., Kaufmann, K., Wang, J., Aptamer-Modified Graphene-Based Catalytic Micromotors: Off-On Fluorescent Detection of Ricin, *ACS Sens.*, **2016**, *1*, 217–221.

Chapter III

Results and Discussion

III.1. Immunosensor for mycotoxins

All features collected from the combination of ELISA methodology and electrochemical techniques in order to develop a suitable immunosensor for the chosen analyte were studied in this Thesis.

This thesis has followed the previous line of the research group, studying and developing immunosensor for mycotoxins with the purpose of preserving and assuring the food safety. As the properties of mycotoxins have been described before, it is critical their control, not only once the product has been manufactured, but in the beginning of the food chain as well. Thereby, immunosensors are a real great alternative to carry analysis out to all steps in the *farm-to-table* chain, thanks to that portability and easy-to-use.

Two further exposed mycotoxins, as FB1 and OTA, have been determined in real samples. It should be underscored that both mycotoxins are 2B carcinogens, therefore the magnitude of their prevention and detection, even in previous stages or in the moment of mold infection, is meaningful. For that, two of the most worldwide consumed beverages, such as beer and coffee, were analyzed with the aim of checking if samples were contaminated and our immunosensor were reliable in that kind of important samples.

These immunosensors are based on the magnetic beads, ELISA methodology, and amperometric detection. Firstly, the

magnetoimmunosensor was built with MBs as immunoassay support, FB1 monoclonal Ab, and OTA polyclonal Ab as biorecognition elements. Secondly, a CSPE was used to perform the electrochemical detection (amperometry) coupled to a magnetic holder. This magnetic holder allowed to confine the MBs on the working electrode surface and held them on the surface.

In order to evaluate the analytical parameters of the immunosensors, the CRM and samples were analyzed by a simplified calibration and analysis protocol. This protocol was performed simultaneously (calibration point and sample analysis), lessening times and labor.

Biosensors and Bioelectronics *DOI: 10.1016/j.bios.2014.09.054*

Disposable and reliable electrochemical magnetoimmunosensor for Fumonisins simplified determination in maize-based foodstuffs

Adrián Jodra, Miguel Ángel López and Alberto Escarpa∗

Department of Analytical Chemistry, Physical Chemistry and Chemical Engineering, University of Alcalá, Ctra. Madrid-Barcelona, Km. 33,600, E-28871 Alcalá de Henares (Madrid), Spain

∗ Corresponding author. Tel.: +34 91 885 49 95.

E-mail address: alberto.escarpa@uah.es (A. Escarpa).

Abstract

An electrochemical magnetoimmunosensor involving magnetic beads and disposable carbon screen-printed electrode (CSPE) for Fumonosins (FB1, FB2 and FB3) has been developed and evaluated through a certified reference material (CRM) and beer samples. Once the immunochemical reaction took places on the magnetic beads solution, they were confined on the surface of CSPE, where electrochemical detection is achieved through the addition of suitable substrate and mediator for enzymatic tracer (Horseradish peroxidase -HRP-). A remarkable detection limit of 0.33 μg L^{-1}, outstanding repeatability and reproducibility ($RSD_{intraday}$ of 5.6% and 2.9%; $RSD_{interday}$ of 6.9% and 6.0%; both for 0 and 5 μg L^{-1} FB1 respectively), and excellent accuracy with recovery rate of 85–96% showed the suggested system to be a very suitable screening tool for the analysis of Fumonisin B1 and B2 in food samples.

A simultaneous simplified calibration and analysis protocol allows a fast and reliable determination of Fumonisin in beer samples with recovery rate of 87–105%. This strategy enhanced the analytical merits of immunosensor approach towards truly disposable tools for food-safety monitoring.

Keywords: Mycotoxin, Fumonisin, magnetoimmunosensor, CSPE, electrochemical detection

Introduction

Nowadays, one of the most important areas in food analysis is the so called food safety. Usually defined as the area related to "*all those hazards, whether chronic or acute, that may make food injurious to the health of the consumer"* (Joint FAO/WHO, 2003) has produced a highly concern in contemporary society and research scene. Mycotoxins, secondary metabolites produced by different filamentous fungi, with a high impact related to health and economical aspects, are key analytes for monitoring in the food safety area. Included within this group, Fumonisins are a class of mycotoxins produced by certain species of *Fusaria* in foods under specific temperature and humidity conditions.

At least twenty eight different Fumonisins have been described and classified in three groups (A, B and C) based in structural similarities. Fumonisin B1 (FB1), Fumonisin B2 (FB2) and Fumonisin B3 (FB3) are the most common and dangerous analogues (**Fig. S1**). FB1 usually constitute about 70% of the total Fumonisins content found in naturally contaminated foods and feeds (Krska et al., 2007). Isolated in 1988 (Bezuidenhout et al., 1988), the Fumonisins have determined to cause leukoencephalomalacia in horses (Marasas et al., 1988), pulmonary edema in pigs (Harrison et al., 1990), nephrotoxicity and liver cancer in rats (Gelderblom et al., 1988). Also in humans, they can produce liver, kidney and esophageal cancer (Dyoshizawa et al., 1994; Scott, 2012; Sydenham et al., 1990) being considered as category 2B carcinogen by U.S. Environmental Protection Agency and International Agency for Research on Cancer (IARC).

Natural occurrence of Fumonisins has been mainly described in maize, maize-based food and feedstuffs. However, isolation of *Fusarium* species has been reported in other grains such as barley, wheat, rice, peanut, pistachio, as well as raisin, fig and other human foods like fruits and milk (Waskiewicz et al., 2012; Yang et al., 2012). Also beer, the oldest alcoholic beverage and the cereal-based product worldwide consumed, has been contaminated of Fumonisins (Rubert et al., 2013; Torres et al., 1998). Produced by brewing and fermentation of starches, mainly derived from cereals grains, such as barley, wheat, maize and rice; beer is a benefit beverage that can be part of a healthy diet. In spite of the fact that the main raw material for beer production is barley, brewing factories often replace a portion of barley by adjuncts, like maize grits, being a frequently way of Fumonisins contamination (Stewart, G.G., 1995). By other hand, beer is a complex matrix containing water, carbohydrates, protein substances, mineral salts and alcohol. The presence of alcohol as a fermentation sub-product can strongly influence the extraction of mycotoxins in this matrix.

Due to the adverse effects in animals and humans, the European Union has established maximum residue limits (MRLs) of Fumonisins (as the sum of FB1 + FB2) in maize-derived foodstuff, ranging from 200 μg Kg^{-1} for baby food to 4000 μg Kg^{-1} for raw maize (Commission Regulation No. 856/2005, 2005; Commission Regulation No. 1881/2006, 2006; Commission Regulation No. 1126/2007, 2007).

Analytical methods and research related to Fumonisins have been recently reviewed (Berthiller et al., 2014; Gelderblom and Marasas, 2012; Krska et al., 2007, 2008; Maragos and Busman, 2010; Prieto-Simón et al., 2007; Scott, 2012; Shephard et al., 2013; World Health Organization, 2006). Due to the absence of a good chromophore in the

Fumonisin structure, most widely used methods for Fumonisins detection are based on LC−MS (Devreese et al., 2012; Ediage et al., 2012b; Li et al., 2012; Pietri and Bertuzzi, 2012; Shephard et al., 2011; Song et al., 2013; Yang and Wu, 2012), derivatisation with fluorescence labels (LC−FLD) (Abrunhosa et al., 2011; Kong et al., 2012; Muscarella et al., 2011; Ndube et al., 2011; Solfrizzo et al., 2011) and those usually involve in the interaction with selective binding materials (antibodies, aptamers or synthetic materials) (Berthiller et al., 2014; Goryacheva et al., 2009; Prieto-Simón and Campàs, 2009; Vidal et al., 2013). Over the last years, and compared to LC−FLD a pronounced shift towards the use of LC−MS, particularly in the context of multitoxin methods has occurred. These methods require expensive equipment, complicated and time-consuming clean-up procedures and skilled operators that make them unsuitable methods for monitoring purposes. Since contamination by Fumonisins can occur at any stage of the food chain (e.g., on field, at harvest, during storage and transportation) frequent analyses are required to promptly detect any contamination, and reducing risks for the consumer. In this sense, immunoassays using a variety of formats (ELISAs, LFDs, biosensors) continue to be an active area of research. In recent years, even enzyme-linked immunosorbent assays for single Fumonisin analyte (Liu et al., 2013; Sheng et al., 2012; Wang et al., 2014) as well as multimycotoxin assays such as lateral flow devices (Lattanzio et al., 2012; Wang et al., 2013; Yan-Song et al., 2012) flow through immunoassay (Ediage et al., 2012a) membrane-based dot assay (He et al., 2012) chip-based microarray (Oswald et al., 2013; Wang et al., 2011) and enconding microespheras multiplexing assays (Czeh et al., 2012; Deng et al., 2013; Peters et al., 2013) have been widely used in agricultural and food-safety area. Biosensors and especially

electrochemical biosensors have received special focus in modern analysis because of their technical simplicity, sensitivity, low cost and possibility of decentralization in field analysis. Excellent reviews are available on general biosensors (Campas et al., 2009; Logrieco et al., 2005; Maragos and Busman, 2010; Prieto-Simón et al., 2007; van der Gaag et al., 2003) and electrochemical biosensors (Hervás et al., 2012; Palchetti and Mascini, 2008; Vidal et al., 2013; Viswanathan et al., 2009) for determining mycotoxin. In Fumonisins analysis, although some optical biosensors have been reported (Mirasoli et al., 2012; Mullett et al., 1998; Wu et al., 2012), to our knowledge only one electrochemical immunosensors have been described in the literature (Kadir and Tothill, 2010). Tabla S1 shows a comparison of the analytical characteristics of the developed electrochemical magneto-immunosensor with other reported immunoassays for Fumonisins determination.

This work explores for the first time, the use of disposable immunosensing surfaces on carbon screen-printed electrodes using magnetic beads coupled to ELISA method for determination of Fumonisins (FB1 + FB2) in different food matrices. The use of magnetic beads improves the performance of the immunological reaction due to an increase in the surface area, as well as the assay kinetics are achieved more rapidly since the beads are in suspension and the probability that antibody-coated magnetic beads meet the analyte is very high while keeping the solution under stirring. Furthermore, the magnetic beads can easily be manipulated through the use of permanent magnets, and the matrix effect is also minimized due to improved washing and separation steps which allows the analysis to be made without any pre-enrichment, purification, or pre-treatment steps. Besides, the use of magnetic beads as affinity reaction support implies that electrode surface is only used for

transduction step avoiding its shielding by deposition of the antibodies which can cause hindrance of the electron transfer and reducing electrochemical signal.

In order to obtain a simple and disposable analytical tool for fast, accurate and reliable determination of Fumonisins *in-field* analysis, a strategy based on simultaneous performing of simplified calibration and analysis protocol on the screen-printed immunosensing surfaces was accomplished in this work.

2. Materials and methods

2.1. Reagents and solutions

Fumonisin B1 (FB1), bovine serum albumin (BSA), hydrogen peroxide (30%), hydroquinone (HQN), benzoquinone (BQN) and Tween 20 were purchased from Sigma-Aldrich (Madrid, Spain). Monoclonal antibody anti-Fumonisin B1 and the enzyme tracer FB1 conjugated to horseradish peroxidase (HRP) were supplied by Soft Flow Hungary Ltd. (Pécs, Hungary). Fumonisin B2 and B3 (FB2 and FB3) were purchased from Romer Labs (Tulln, Austria). Standard Fumonisin B1, B2 and B3 solutions were prepared daily by dilution of stock solution (50 μg mL^{-1} in acetonitrile:water, 50:50). All other reagents were of the highest available grade.

All buffer solutions were prepared with MiliQ water. Phosphate buffer saline (PBS) was modified with Tween 20 and BSA. The composition of the PBS solution was phosphate buffer 10 mmol L^{-1}, pH 7.4, with 0.8% (w/v) NaCl. In other solutions, 0.05% (v/v) Tween 20 and 2.5% (w/v) BSA (blocking buffer) or 0.1% (w/v) BSA (dilution buffer) were also added.

2.2. Materials

Superparamagenetic polymer beads with protein-G covalently coupled to the surface (Dynabeads® Protein G) were supplied by Life Technologies (Oslo, Norway).

Screen-printed electrodes (DS110) based on carbon working, counter, and silver pseudo-reference electrodes were provided by Dropsens (Oviedo, Spain). The working electrode diameter was 4 mm. The magnetic holder (DRP−MAGNET) used for holding magnetic beads on the surface of the working electrode was supplied by Dropsens (Oviedo, Spain).

2.3. Samples

Fumonisins maize certified reference material ([FB1] = 2.0 ± 0.4 mg Kg^{-1}; [FB2] = 0.5 ± 0.2 mg Kg^{-1}; [FB3] = 0.2 ± 0.1 mg Kg^{-1}) was purchased from Pribolab® (Singapore). Beer samples were purchased from a local retail store (Madrid, Spain).

2.4. Equipment

Amperometric measurements were performed with a multipotenciost *μSTAT8000* and the software DropView 8400 from Dropsens (Oviedo, Spain), and magnetic stirrer *Microstirrer* from Velp Scientifica (Usmate, Italy).

The competitive curves were analysed with a four parameter logistic equation using the proper software GraphPad Prism 5.

2.5. Immunoassay procedure

The immunoanalytical methodology was developed on the basis of the competition scheme where mycotoxin FB1 and its enzyme-labelled derivative compete for binding sites of the specific monoclonal antibody.

Magnetic beads covered with covalently bounded protein G were used as an oriented immobilisation support for the capture of the anti−FB1 antibody. Once molecular recognition has been produced, the extent of the affinity reaction is evaluated by the addition of the enzymatic substrate and electrochemical mediator whose reduction on the electrode surface is directly related to the activity of the enzyme tracer (**Fig. 1**).

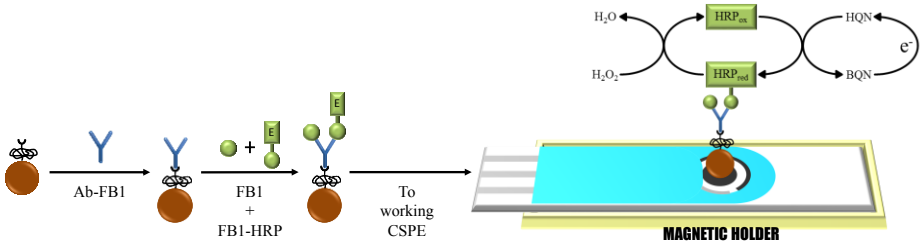

Fig. 1. Magnetoimmunosensor construction.

The competitive immunoassay was performed in ELISA microplate wells. Initially, Dynabeads® protein G magnetic beads were washed with PBS−T, pH 7.4, according to the manufacturer's protocol in order to eliminate the storage buffer and condition them for the IgG capture procedure. In this way, a volume of 1 µL of the commercial solution Dynabeads® was introduced into the well and washed three times with PBS−T. Thanks to the utilization of an external magnet, magnetic beads were captured at the bottom of the well for removing the supernatant. Afterwards, 50 µL of specific antibody (2.5 µg L^{-1}) prepared in PBS−T was added to the magnetic beads for coating to the immobilized protein G. The solution was gently stirred for 60 min at room temperature to obtain specific antibody-modified beads. For removing unbound antibody, the solution was washed five times with 100 µL of PBS−T by the aid of a magnet. In order to avoid non-specific adsorption, the modified magnetic beads were blocked with PBS−T−BSA 2.5% (w/v) during 60 min. Sequential competitive assay was performed by re-

suspending the anti-mycotoxin antibody-coated beads in 50 μL of PBS−T−BSA 0.1% containing Fumonisin standard solution or sample. After 30 min incubation time, the enzyme tracer (final dilution 1:64000) was added. The competitive immunological reaction was allowed to proceed with gentle stirring for 30 min at room temperature. The magnetic beads were washed five times with 100 μL of PBS−T to eliminate not bound species and re-suspended in 10 μL of citrate buffer.

2.6. Electrochemical measurements

The suspension of MBs modified with the immunoassay architecture was transferred and retained onto the surface of the working electrode of carbon screen-printed electrodes (CSPE) positioned on a magnet holding block. Amperometric measurements were performed after introduction of the assembled MBs−CSPE into an electrochemical cell containing 7 mL of citrate buffer, pH 5.0. The amperometric responses in stirred solutions (E_{app} = −0.25 V vs Ag pseudo-reference electrode) were recorded upon addition of 140 μL of hydrogen peroxide and hydroquinone (1 mM final concentration for both) until the steady-state current was reached. Figure S2 displays the representative amperometric signals obtained from a 0 and 100 μg L^{-1} FB1 standard solutions.
Amperometric signals, calculated as the difference between the steady-state and the background currents were fitted to the following four parameter logistic equation (sigmoidal) using the software Graph Pad Prism 5:

$$Y = i_1 + \frac{i_2 - i_1}{1 + 10^{[\log IC_{50} - x]p}}$$

where i_2 and i_1 are the maximum and minimum current values of the calibration graph obtained, IC_{50} is the analyte concentration producing

50% of the maximal amperometric signal, and p is the Hill slope at the inflection point of the sigmoid curve. The limit of detection (LOD) value was calculated as the analyte concentration for which the enzymatic tracer binding to the antibody was inhibited by 10%. The dynamic range (DR) was taken as the analyte concentration interval for which the inhibition of the binding of enzymatic tracer was between 20 and 80%.

2.7. Sample treatment

Both, solid and liquid samples were used to demonstrate the adequate performance of the developed magnetoimmunosensor. As solid sample and in order to evaluate accuracy of the immunosensor a maize certified reference material was analysed. According to the instructions recommended by the supplier, 1 g samples aliquots were extracted with 4 mL of acetonitrile:PBS (50:50, v/v) in cooling refrigeration conditions by a tip sonication (VCX130, Sonics, Newtown, USA) for 20 minutes (5 min/cycle) at 117 W. After centrifugation at 4000 rpm during 10 min, the supernatant was separated and diluted 400−fold with PBS−T−BSA (0.1%).

Beers, spiked with different concentration of FB1, FB2 and FB1+FB2, were previously degasified for 20 minutes in ultrasonic bath and, in case, diluted 10−fold with PBS−T−BSA (0.1%) to minimize the matrix effect.

3. Results and discussion

3.1. Optimization of the immunoassay

The direct magnetoimmunosensor performance can be divided in two main steps which occur at different places: (i) the affinity reaction, which takes place in solution (wells of microtiter plate) and (ii) the electrochemical transduction step which occurs on the surface of

disposable CSPE. Both steps are performed with the aids of MBs. Indeed, the affinity reaction process in solution entails the benefits of using MBs such as higher surface area, faster kinetic assay, easier access of mycotoxin and tracer to the immobilized antibodies, and facility of manipulation. Furthermore, the use of screen-printed electrodes as electrochemical platform where magnetic beads are entrapped for transduction event, improve sensitivity avoiding the shielding of the electrode surface by deposition of the specific antibodies, and then improving electron transfer. Additionally, this strategy diminishes the non-specific adsorption since affinity reaction is not performed on the electrode surface (Hervás et al., 2010).

In order to get the best analytical performance for the immunosensor, some experimental variables had to be optimized.

In this work, the coating of specific antibody to magnetic beads was achieved through the affinity of protein G for the Fc region of antibody molecules, getting its orientation and then, improving sensitivity. Since the amount of antibody available is directly related to the number of protein G modified beads, a titration was performed using different antibody concentrations for a limited volume of magnetic beads (1 μL). Using a fixed excess of the other immunoreagents and incubation times, higher signals were obtained for increasing antibody concentrations (0.15−5 μg mL^{-1}). Taking into account that typically low antibody concentrations render better LODs, an almost plateau concentration of 2.5 μg mL^{-1} was chosen for subsequent experiments, since a highly enough current was obtained (**Fig. S2**). Incubation time (range 1−60 min) for coating of specific antibody onto beads was also tested. A short period of incubation time of 10 min, as described by the manufacturer, produces an 85% of the maximum binding (data not shown).The time of

60 min were used to assure the total antibody immobilization. Also, two different buffers at different pH values (recommended by the supplier in different beads batches) were checked, since binding capacity may vary for different immunoglobulins. An increment of 21% of intensity current was encountered for PBS buffer (pH=7.4) instead of citrate buffer (pH=5), both for 2.5 μg mL^{-1} antibody concentration and 60 min incubation time.

Another key parameter to optimize is the amount of enzyme tracer dilution. Small variations in the number of antibody binding sites or concentration of FB1–HRP produce large variations of the immunosensor sensitivity. In this sense, the antibody modified MBs were titrated with different tracer dilutions, as much in an excess of FB1 (minimum assay signal) as well as without the mycotoxin (maximum assay signal). The results show the typical behaviour of a binding curve (**Fig. S3**). Using 1:64000 fold-dilution of the tracer stock solution produces the highest ratio for the amperometric currents obtained in absence and presence of an excess of the mycotoxin (1000 μg L^{-1} of FB1).

Other optimized experimental conditions were competition reaction time (1 to 120 min), temperature (room temperature or 37ºC), and competition scheme (simultaneous or sequential incubation of the standard/sample mycotoxin and tracer with immobilized antibody). Competition time of 30 min supposed an 85.4% of the maximum amperometric signal (those produced for 60 and 120 min with no significant differences); while a minimum and almost constant current was obtained in presence of an excess of the mycotoxin for incubation times assayed (**Fig. S4**). Increasing temperature from room temperature to 37ºC did not produce any significant signal difference, even for absence or presence of an

excess of the mycotoxin. Also, simultaneous and sequential incubation of the mycotoxin and the tracer with the immobilized antibody were tested. When sequential incubation of sample/standard and tracer (30 + 30 min) was performed, better IC_{50}, DR and LOD values in calibration curve were obtained related to simultaneous incubation of the standard and the tracer (**Table S1**).

3.2. Analytical characteristics of the developed magnetoimmunosensor

Fumonisin B1 was selected to evaluate the analytical performance of the developed immunosensor. The calibration graph obtained under the optimized experimental conditions summarized in **Table 1**, is shown in **Fig 2**. The LOD and IC_{50} calculated values were 0.33 and 2.86 μg L^{-1} respectively and the DR ranged between 0.73 and 11.2 μg L^{-1}. It is important to remark that this LOD is well below of the most restricted limits fixed by the European Union (200 μg Kg^{-1} for baby food) showing the suitability of the immunosensor as alarm tool for Fumonisin contaminations.

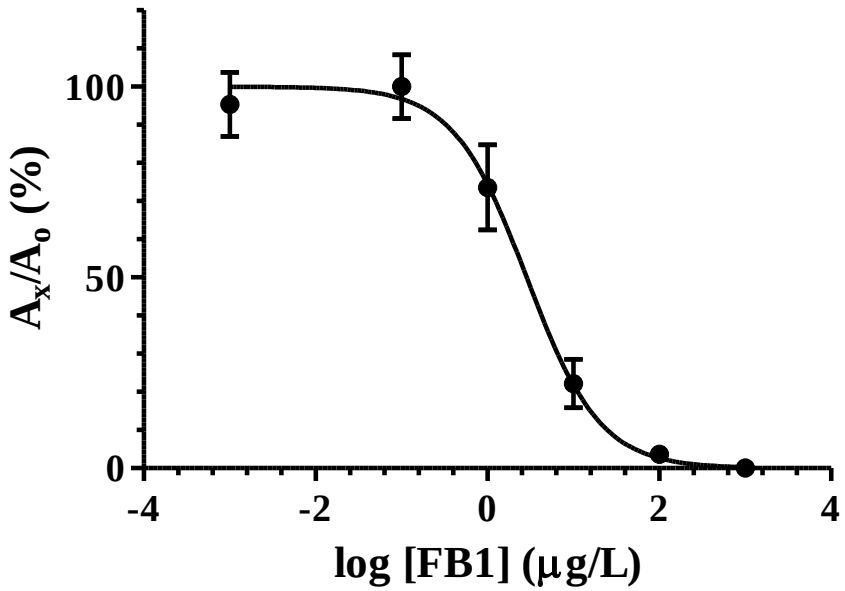

Fig. 2. Calibration curve for Fumonisin B1 determination using the competitive electrochemical immunosensor. Each point correspond to the A_x/A_o percentage ± SD, calculated for n = 4 repetitions.

Table 1

Optimized conditions to perform the calibration curve.

Experimental condition	Optimal value
Volume MBs	1 µL
[Ab-FB1]	2.5 µg mL^{-1}
Time of antibody incubation	60 min
Blocking step	PBS−T−BSA (2.5%)
Blocking time	60 min
Dil. FB1-HRP	1:64000
Time of tracer incubation	30 min
[HQN] and [H_2O_2]	1 mM
E_{app}	− 0.25 V

Intra-immunosensors repeatability and inter-immunosensors reproducibility for two levels of concentration (0 and 5 µg L^{-1} FB1) were studied. RSD values of 5.6% and 2.9% (n=5) were obtained within the same day; while RSD values of 6.9% and 6.0% (n=6) were obtained in different days, for both levels of concentration respectively.

The specificity of the developed immunosensor for the most abundant and dangerous Fumonisin analogues (FB1, FB2 and FB3) was investigated. Calibration curves were performed for each Fumonisin in the range of 0−1000 µg L^{-1} (**Fig. 3**). The cross-reactivity for FB1, FB2 and FB3 were of 100%, 133% and 52% respectively. Therefore, the reactivity of the monoclonal anti-Fumonisins antibody used in this magnetoimmunosensor allows determining the most important Fumonisins.

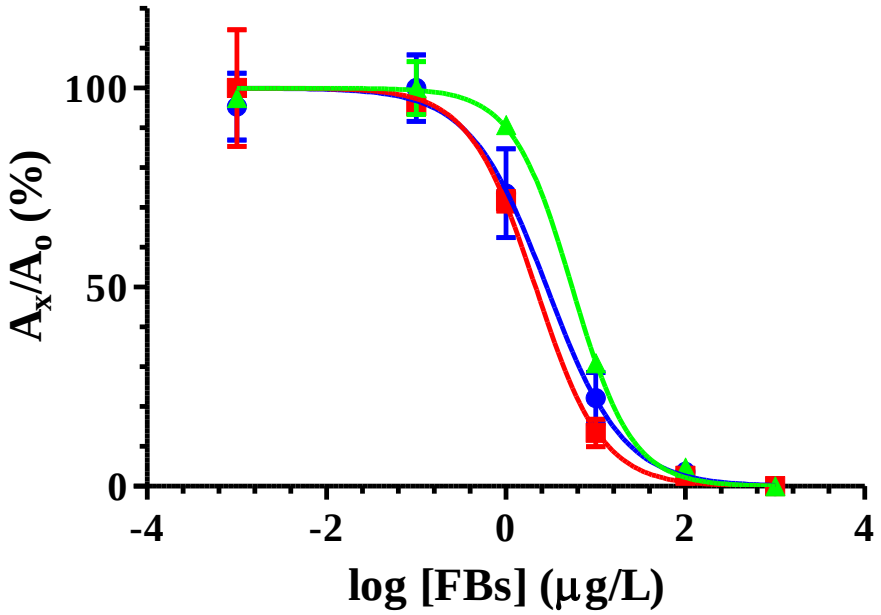

Fig. 3. Calibration curves for the most important Fumonisins B. Line blue (—) corresponding to FB1, line red (—) corresponding to FB2 and line green (—) corresponding to FB3.

The accuracy of the immunosensor was appraised by the analysis of maize certified reference material (CRM). The CRM extraction was realised by a combination of two different solvents, acetonitrile:PBS (50:50, v/v) and assisted with the use of a tip sonication. In the **Table 2**, it can be observed the found concentrations for three repeated assays of three different samples of the CRM. Taking into account that CRM material is contaminated with the three Fumonisins at different concentrations, and the cross-reactivitys of the antibody used to these analogues, the recovery values are in excellent agreement. The results were assessed by one-sample *t*-test, which indicates that no differences were found ($p>0.05$), and it demonstrated an outstanding accuracy of the method and reliability of the immunosensor.

Table 2

Analysis of certified reference material ([FB1] = 2.0 ± 0.4 mg Kg^{-1}; [FB2] = 0.5 ± 0.2 mg Kg^{-1}; [FB3] = 0.2 ± 0.1 mg Kg^{-1}).

Sample	$[FBs]^{CRM}_{Total}$ (mg Kg^{-1})	Found concentration (mg Kg^{-1})	Recovery (%)
1		2.6 ± 0.1	96 ± 1
2	2.7 ± 0.7	2.5 ± 0.1	93 ± 2
3		2.3 ± 0.1	85 ± 4
		2.5 ± 0.2	*91 ± 7*

3.3. Simplified calibration and analysis on board of disposable CSPE: Application to beer samples

To evaluate matrix effect, the magnetoimmunosensor was performed in diluted and undiluted beer samples. The use of undiluted beer samples implied a 32% decrease of the amperometric current compared with the signal produced in buffer for the absence of the mycotoxin. In this sense, different dilution values were tested, reaching that a 10−fold dilution of the beer sample in PBS buffer was needed to avoid the matrix effect. The calibration curve performed in these conditions showed similar analytical properties to those obtained without the presence of the matrix (**Fig. S6**). Therefore, beer analyses were performed in 10−fold dilution of the beer sample.

Non-linear calibration curves usually performed in immunoassays implies laborious and time consuming procedures for sample analysis. In a previous work (Hervás et al., 2010), simplified and integrated calibration analysis protocol on board of the same disposable SPE was proposed to overcome these disadvantages. In this work, this methodology implies the simultaneous determination of a selected concentration of the mycotoxin with calibration purpose and the analysis

of the analyte in the food sample. Comparison of both signals and after the adequate definition of the calibration factor, allows the determination of the mycotoxin in the sample. The calibration factor is calculated as $f_{calibration} = S_{FB1\ standard} \times [FB1]_{Standard}$. Since this calibration factor is a constant for each analysis, FB1 concentration in the sample can be calculated as $[FB1]_{Sample} = f_{Calibration}/S_{FB1\ sample}$. This methodology presents clear benefits such as: (1) it generates a simplification of the calibration procedure; (2) calibration and analysis are performed under equal conditions avoiding other sources or error; (3) the calibration step can be suitable designed using the same concentration for the control as the one expected in the sample, improving precision and accuracy of the analysis. The suitability of this simplified calibration strategy was demonstrated for the analysis of beer food samples.

To perform the simplified calibration and analysis protocol, beer samples were previously spiked at different level of concentration of Fumonisins (FB1, FB2 and the sum of FB1 + FB2). Then, samples were degasified and diluted 10−fold in PBS buffer and directly analysed without any extraction procedure. **Table 3** shows the results obtained for the different spiked beer samples. The calculated recoveries demonstrated the rightness of the proposed simplified analytical procedure, and the suitability of the developed immunosensor as a real alternative for reliable and disposable alarm screening of the most common fumonisins.

Table 3

Analysis of beer samples using the simultaneous simplified calibration and analysis protocol.

Fumonisin	Calibration ($\mu g\ L^{-1}$)[a]	Analysis ($\mu g\ L^{-1}$)[b]	Spiked concentration ($\mu g\ L^{-1}$)	Recovery (%)
FB1	20.0	21.0 ± 0.7	200	*105 ± 4*
	5.0	5.0 ± 0.4	50	*99 ± 7*
FB2	5.0	4.7 ± 0.4	50	*94 ± 8*
FB1 + FB2	10.0	8.7 ± 0.9	50 + 50	*87 ± 9*

Three samples were analysed for each concentration value.

[a]Standard concentration in the calibration.

[b]FBs concentration found in 10-fold diluted samples.

4. Conclusion

An electrochemical magnetoimmunosensor based on magnetic beads for Fumonisins (FB1, FB2 and FB3) detection has been successfully developed. This immunosensor presents a remarkable limit of detection, better than the previously reported in the literature for other electrochemical immunosensor, and most important, well below to the current, and probably in the near future more restricted legislation requirements. Their reliability and accuracy has been evaluated through the analysis of maize certified reference material and spiked beer as important world consumed beverage, getting exceptional results.

Furthermore, a simultaneous simplified calibration and analysis protocol has been performed, diminishing the analysis time, reducing the tedious and intense labour of calibration curves, and reaching exceptional accuracy. All these features, together with the portable, disposable and easy to use character of the developed immunosensor, grant to this methodology as an exceptional alarm tool for food safety diagnosis, which can be included in different steps of the agroalimentary chain.

Acknowledgement

The authors are very grateful to Soft Flow Biotechnology for kindly providing of the monoclonal antibody and the enzyme tracer. Financial support from the Spanish Ministry of Economy and Competitiveness CTQ2011−28153 (A.E.) and the AVANSENS program from the Community of Madrid (P2009/PPQ−1642) are acknowledged. D. Adrián Jodra acknowledges the FPI fellowship received from the Spanish Ministry of Economy and Competitiveness.

Supplementary data

Supplementary data associated with this article can be found.

References

Abrunhosa, L., Calado, T., Resende, T., Venâncio, A., 2011. J. Liq. Chromatogr. Related Technol. 34, 1594-1603.

Berthiller, F., Burdaspal, P.A., Crews, C., Iha, M.H., Krska, R., Lattanzio, V.M.T., MacDonald, S., Malone, R.J., Maragos, C., Solfrizzo, M., Stroka, J., Whitaker, T.B., 2014. World Mycotoxin J. 7, 3-33.

Bezuidenhout, S.C., Gelderblom, W.C.A., Gorstallman, C.P., Horak, R.M., Marasas, W.F.O., Spiteller, G., Vleggaar, R., 1988. J. Chem. Soc., Chem. Commun., 743-745.

Campas, M., Prieto-Simon, B., Marty, J.L., 2009. Seminars in cell & developmental biology 20, 3-9.

Czeh, A., Mandy, F., Feher-Toth, S., Torok, L., Mike, Z., Koszegi, B., Lustyik, G., 2012. J. Immunol. Methods 384, 71-80.

Deng, G., Xu, K., Sun, Y., Chen, Y., Zheng, T., Li, J., 2013. Anal. Chem. 85, 2833-2840.

Devreese, M., De Baere, S., De Backer, P., Croubels, S., 2012. J. Chromatogr. A 1257, 74-80.

Dyoshizawa, T., Yamashita, A., Luo, Y., 1994. Appl. Environ. Microb. 60, 1626-1629.

Ediage, E.N., Di Mavungu, J.D., Goryacheva, I.Y., Van Peteghem, C., De Saeger, S., 2012a. Anal. Bioanal. Chem. 403, 265-278.

Ediage, E.N., Di Mavungu, J.D., Song, S., Wu, A., Van Peteghem, C., De Saeger, S., 2012b. Anal. Chim. Acta 741, 58-69.

European Commission, Commission Regulation (EC) No. 856/2005 of 6 June 2005, Amending Regulation (EC) No 466/2001 as regards Fusarium Toxins. Off. J. Eur. Union. 143, pp. 3-8.

European Commission, Commission Regulation (EC) No. 1881/2006 of 19 December 2006, Setting Maximum Levels for Certain Contaminants in Foodstuffs. Off. J. Eur. Union. L364, pp. 5-24.

European Commission, Commission Regulation (EC) No. 1126/2007 of 28 September 2007, Amending Regulation (EC) No. 1881/2006 Setting Maximum Levels for Certain Contaminants in Foodstuffs as regards Fusarium Toxins in Maize and Maize Products, 2007. Off. J. Eur. Union. L255, pp. 14-17.

Gelderblom, W.C.A., Jaskiewicz, K., Marasas, W.F.O., Thiel, P.G., Horak, R.M., Vleggaar, R., Kriek, N.P.J., 1988. Appl. Environ. Microb. 54, 1806-1811.

Gelderblom, W.C.A., Marasas, W.F.O., 2012. Hum. Exp. Toxicol. 31, 215-235.

Goryacheva, I.Y., Rusanova, T.Y., Burmistrova, N.A., Saeger, S., 2009. J. Anal. Chem.+ 64, 768-785.

Harrison, L.R., Colvin, B.M., Greene, J.T., Newman, L.E., Cole, J.R., Jr., 1990. Journal of veterinary diagnostic investigation : official

publication of the American Association of Veterinary Laboratory Diagnosticians, Inc 2, 217-221.

He, Q.-H., Xu, Y., Wang, D., Kang, M., Huang, Z.-B., Li, Y.-P., 2012. Food Chem. 134, 507-512.

Hervás, M., Lopez, M.A., Escarpa, A., 2010. Biosens. Bioelectron. 25, 1755-1760. Hervás, M., López, M.A., Escarpa, A., 2012. TrAC, Trends Anal. Chem. 31, 109-128.

Joint FAO/WHO, 2003. FAO Food and Nutrition Paper, 73, 1-73.

Kadir, M.K., Tothill, I.E., 2010. Toxins 2, 382-398.

Kong, W., Xie, T., Li, J., Wei, J., Qiu, F., Qi, A., Zheng, Y., Yang, M., 2012. The Analyst 137, 3166-3174.

Krska, R., Welzig, E., Boudra, H., 2007. Anim. Feed Sci. Tech. 137, 241-264.

Krska, R., Schubert-Ullrich, P., Molinelli, A., Sulyok, M., MacDonald, S., Crews, C., 2008. Food Addit. Contam. Part A, Chemistry, Analysis Control, Exposure & Risk Assessment 25, 152-163.

Lattanzio, V.M., Nivarlet, N., Lippolis, V., Della Gatta, S., Huet, A.C., Delahaut, P., Granier, B., Visconti, A., 2012. Anal. Chim. Acta 718, 99-108.

Li, C., Wu, Y.-L., Yang, T., Huang-Fu, W.-G., 2012. J. Chromatogr. Sci. 50, 57-63.

Liu, X., Xu, Y., He, Q.-h., He, Z.-y., Xiong, Z.-p., 2013. J. Agric. Food. Chem. 61, 4765-4770.

Logrieco, A., Arrigan, D.W.M., Brengel-Pesce, K., Siciliano, P., Tothill, I., 2005. Food Addit. Contam. 22, 335-344.

Maragos, C.M., Busman, M., 2010. Food Addit. Contam. Part A, Chemistry, Analysis Control, Exposure & Risk Assessment 27, 688-700.

Marasas, W.F.O., Kellerman, T.S., Gelderblom, W.C.A., Coetzer, J.A.W., Thiel, P.G., Vanderlugt, J.J., 1988. Onderstepoort J. Vet. 55, 197-203.

Mirasoli, M., Buragina, A., Dolci, L.S., Simoni, P., Anfossi, L., Giraudi, G., Roda, A., 2012. Biosens. Bioelectron. 32, 283-287.

Mullett, W., Lai, E.P.C., Yeung, J.M., 1998. Anal. Biochem. 258, 161–167.

Muscarella, M., Magro, S.L., Nardiello, D., Palermo, C., Centonze, D., 2011. Methods Mol. Biol. (Clifton, N.J.) 739, 187-194.

Ndube, N., van der Westhuizen, L., Green, I.R., Shephard, G.S., 2011. J. Chromatogr. B, Analytical Technologies in the Biomedical and Life Sciences 879, 2239-2243.

Oswald, S., Karsunke, X.Y.Z., Dietrich, R., Maertlbauer, E., Niessner, R., Knopp, D., 2013. Anal. Bioanal. Chem. 405, 6405-6415.

Palchetti, I., Mascini, M., 2008. Anal. Bioanal. Chem. 391, 455-471.

Peters, J., Thomas, D., Boers, E., de Rijk, T., Berthiller, F., Haasnoot, W., Nielen, M.W., 2013. Anal. Bioanal. Chem. 405, 7783-7794.

Pietri, A., Bertuzzi, T., 2012. Food Anal. Method. 5, 1088-1096.

Prieto-Simón, B., Campàs, M., 2009. Monatshefte für Chemie - Chemical Monthly 140, 915-920.

Prieto-Simón, B., Noguer, T., Campàs, M., 2007. TrAC, Trends Anal. Chem. 26, 689-702.

Rubert, J., Soler, C., Marín, R., James, K.J., Mañes, J., 2013. Food Control 30, 122-128.

Scott, P.M., 2012. Food Addit. Contam. Part A, Chemistry Analysis Control Exposure & Risk Assessment 29, 242-248.

Sheng, Y., Jiang, W., De Saeger, S., Shen, J., Zhang, S., Wang, Z., 2012. Toxicon 60, 1245-1250.

Shephard, G.S., Berthiller, F., Burdaspal, P.A., Crews, C., Jonker, M.A., Krska, R., Lattanzio, V.M.T., MacDonald, S., Malone, R.J., Maragos, C., Sabino, M., Solfrizzo, M., van Egmond, H.P., Whitaker, T.B., 2013. World Mycotoxin J. 6, 3-30.

Shephard, G.S., van der Westhuizen, L., Sewram, V., van Zyl, J., Rheeder, J.P., 2011. Food Addit. Contam. Part A, Chemistry Analysis Control Exposure & Risk Assessment 28, 1712-1716.

Solfrizzo, M., De Girolamo, A., Gambacorta, L., Visconti, A., Stroka, J., van Egmond, H.P., 2011. J. AOAC Int. 94, 900-908.

Song, S., Ediage, E.N., Wu, A., De Saeger, S., 2013. J. Chromatogr. A 1292, 111-120.

Stewart, G.G., 1995. Adjuncts, in: W.A. Hardwick (Ed.), Hand-book of brewing, Marcel Dekker, New York, pp. 121-132.

Sydenham, E.W., Thiel, P.G., Marasas, W.F.O., Shephard, G.S., Vanschalkwyk, D.J., Koch, K.R., 1990. J. Agric. Food. Chem. 38, 1900-1903.

Torres, M.R., Sanchis, V., Ramos, A.J., 1998. Int. J. Food Microbiol. 39, 139-143.

van der Gaag, B., Spath, S., Dietrich, H., Stigter, E., Boonzaaijer, G., van Osenbruggen, T., Koopal, K., 2003. Food Control 14, 251-254.

Vidal, J.C., Bonel, L., Ezquerra, A., Hernandez, S., Bertolin, J.R., Cubel, C., Castillo, J.R., 2013. Biosens. Bioelectron. 49C, 146-158.

Viswanathan, S., Radecka, H., Radecki, J., 2009. Monatshefte für Chemie - Chemical Monthly 140, 891-899.

Wang, X., Zhang, H., Liu, H., He, C., Zhang, A., Ma, J., Ma, Y., Wu, W., Zheng, H., 2011. J. Food Safety 31, 408-416.

Wang, Y.-K., Shi, Y.-B., Zou, Q., Sun, J.-H., Chen, Z.-F., Wang, H.-a., Li, S.-Q., Yan, Y.-X., 2013. Food Control 31, 180-188.

Wang, Y.-K., Wang, Y.-C., Wang, H.-a., Ji, W.-H., Sun, J.-H., Yan, Y.-X., 2014. Food Control 40, 41-45.

Waskiewicz, A., Beszterda, M., Golinski, P., 2012. Food Control 26, 491-499.

World Health Organization, G., 2006. FAO food and nutrition paper 82, 1-778.

Wu, S., Duan, N., Ma, X., Xia, Y., Wang, H., Wang, Z., Zhang, Q., 2012. Anal. Chem. 84, 6263-6270.

Yan-Song, L., Yu, Z., Shi-Ying, L., De-Jun, G., Hong-Lin, R., Xian-Mei, M., Bai-Hui, Z., Chao, L., Zhe, W., Xiao-Bing, L., Zeng-Shan, L., 2012. Food Control 24, 72-77.

Yang, G., Jia, F., Zhang, L., Wang, J., 2012. In: Wu, J., Yang, J., Nakagoshi, N., Lu, X., Xu, H. (Eds.), Natural Resources and Sustainable Development Ii, Pts 1-4, pp. 2180-2187.

Yang, Q.F., Wu, Y.L., 2012. Chromatographia 75, 1075-1080.

Sensors and Actuators B: Chemical DOI: 10.1016/j.snb.2015.07.007

Disposable electrochemical magneto immunosensor for simultaneous simplified calibration and determination of Ochratoxin A in coffee samples

Adrián Jodra, Mirian Hervás, Miguel Ángel López and Alberto Escarpa∗

Department of Analytical Chemistry, Physical Chemistry and Chemical Engineering, University of Alcalá, Ctra. Madrid-Barcelona, Km. 33,600, E-28871 Alcalá de Henares (Madrid), Spain

∗ Corresponding author. Tel.: +34 91 885 49 95.

E-mail address: alberto.escarpa@uah.es (A. Escarpa).

Abstract

In food producing and developing countries having a reliable and inexpensive tool for the analysis of agricultural commodities is essential. This article describes a reliable disposable electrochemical magnetoimmunosensor for monitoring of coffee samples for Ochratoxin A contamination. The electrochemical detection performed on carbon screen-printed electrodes (CSPEs) used magnetic beads as antibody immobilization support and enzyme horseradish peroxidase as tracer. A remarkable limit of detection of 0.32 μg L^{-1}, well below of the legislative requirements, demonstrated the suitability of the proposed system as a screening tool for the analysis of Ochratoxin A in coffee samples.

A simultaneous simplified Ochratoxin A calibration and coffee sample analysis strategy allowed the accurate determination of the mycotoxin with recoveries of 90% reducing the long times used in conventional calibration. This strategy enhanced the analytical merits of immunosensor approach towards truly disposable tools for screening of Ochratoxin A in coffee samples and opens novel avenues for food-safety monitoring.

Keywords: Ochratoxin A, magnetoimmunosensor, CSPE, electrochemical detection, food safety, coffee samples

1. Introduction

In the last decades, determination of mycotoxins in food commodities is highly important since they are potent toxins causing negative effects on animals and humans health. Now they are considered the most important chronic dietary risk factor, even more than food additives or pesticide residues [1]. Mycotoxins are identified as inevitable natural secondary metabolites produced by about 200 hundred different filamentous fungi species under different environmental conditions around the world. Although several hundred different mycotoxins have been discovered, Ochratoxin A (OTA) has one of the greatest negative impacts on public health and trade. Produced mainly by *Aspergillus ochraceous, A. carbonarius* and *Penicillium verrucosum*, it has been identified as contaminant in various products as cereals, beans, groundnuts, spices, dried fruits, coffee, cocoa, milk, grape juice, beer, wine, and pork meat. OTA is a quite stable molecule, able to resist most food processing steps. It has been found in human blood and breast milk of individuals exposed to contaminated products, due to it long half-time life in serum (~35 days) [2]. Related to its health risk, OTA has been described by the International Agency for Research on Cancer as possibly carcinogenic in humans (group 2B). Furthermore, OTA has nephrotoxic, teratogenic and immunotoxic activity in several animal species. Due to these findings, regulatory limits for OTA have been established in many countries, especially in Europe where the European Commission has set maximum limits for OTA in cereals (5 μg Kg^{-1} in raw cereals grains and 3 μg Kg^{-1} in processed cereals products for direct human consumption), in wines

and grape-containing beverages (2 μg Kg^{-1}), in coffee (5 μg Kg^{-1} in roasted coffee beans and 10 μg Kg^{-1} in soluble coffee) and baby foods (0.5 μg Kg^{-1}) (EC. No. 123-2005, EC. No. 1881-2006).

Due to the highly concern about OTA contamination, different high-performance detection techniques have been developed for quality assessment. Currently, the methods commonly used for OTA determination comprise immunoaffinity clean-up (IAC) followed by HPLC separation with fluorescence detection (OTA presents native fluorescence) or MS, among others [3-6]. Although they are sensitive methods with proper limit of detection, they face several disadvantages such as high cost of equipment, use of high amount of harmful solvents, precise qualified staff together with increased analysis time and cost. On-going alternatives are based on the use of immunological methods, however, common enzyme linked immunosorbent assay (ELISA) also requires of highly training personnel, and have a long tedious time of analysis, thus, immunosensors, in general terms, and particularly electrochemical immunosensors are presented as an alternative. The latter has been proven to be sensitive, accurate, fast, and inexpensive, might achieve adequate limit of detection and is very suitable for decentralization in field analysis [7-10]. These advantageous features have been reflected in an increase of the number of articles based on OTA immunosensors determinations appeared in the last years. These electrochemical immunosensors for OTA determination, besides the different employed electrochemical techniques, vary in the support for specific antibody immobilization, since an adequate antigen-antibody interaction is improved by the right orientation of the antibody in the sensor surface. In this sense, different strategies have been reported such as immobilization onto the electrode surface, by simple adsorption [2,

11, 12] or through functionalized electrode surface [13-17], both included in polymer matrices [18-23] or by using micro and nano (magnetic) particles [24-28]. The latter use of magnetic beads improves the performance of the immunological reaction due to an increase in the surface area. Likewise, the assay kinetics is achieved more quickly because the beads are in suspension, and the probability that antibody-coated magnetic beads recognize the analyte improve while keeping the solution under stirring. Furthermore, the magnetic beads can be easily manipulated through the use of permanent magnets, and the matrix effect is also minimized due to improved washing and separation steps. Besides, the use of magnetic beads as affinity reaction support implies that electrode surface is only used for transduction step, avoiding its shielding by deposition of the antibodies which can cause hindrance of the electron transfer, thus the reduction of the electrochemical signal.

In this work, disposable immunosensing surfaces on carbon screen-printed electrodes using magnetic beads coupled with ELISA method has been developed for determination of OTA in a highly concern and shortly explored matrix such as soluble coffee (instant coffee). While wine is considered to be a major source of daily OTA intake in humans, and consequently, most of the reported immunosensors for OTA determination are focused on wine analysis [2, 11, 18, 24, 26-28], coffee is a widely consumed product with potential and significant exposure to the mycotoxin. Coffee, as raw foodstuff, is one of the most exported product around the world and it has a recognized high prevalence of OTA contamination, being found in variable amounts in all forms of commercialized coffee, even after recognized mitigation strategies such as roasting and high temperature extraction. [29] Since the coffee is a worldwide consumed beverage and has been found with different level

of contamination in many countries, a disposable analytical tool for fast, accurate and reliable determination of OTA is needed. In this work, this challenge is accomplished through a strategy based on simultaneous performing of simplified calibration and analysis protocol on screen-printed immunosensing surfaces, demonstrated as accurate and sensitive for the concentration levels required by the legislation in coffee samples.

2. Materials and methods

2.1. Reagents and solutions

Ochratoxin A (OTA), bovine serum albumin (BSA), hydrogen peroxide (30%), hydroquinone (HQN), benzoquinone (BQN) and Tween 20 were purchased from Sigma-Aldrich (Madrid, Spain). Polyclonal antibody anti-OTA and the enzyme tracer OTA conjugated to horseradish peroxidase (HRP) were supplied by ImmuneChem (Burnaby, Canada). Standard OTA solutions were prepared daily by dilution of stock solution (50 mg L^{-1} in PBS–T). All other reagents were of the highest available grade.

All buffer solutions were prepared with MilliQ water. Phosphate buffer saline (PBS) was modified with Tween 20 and BSA. The composition of the PBS solution was phosphate buffer 10 mmol L^{-1}, pH 7.4, with 0.8% (w/v) NaCl. In other solutions, 0.05% (v/v) Tween 20 and 2.5% (w/v) BSA (blocking buffer) or 1% (w/v) BSA (dilution buffer) were also added.

2.2. Materials

Superparamagnetic polymer beads (2.8 μm, uniform size) with protein-G covalently coupled to the surface (Dynabeads® Protein G) were supplied by Life Technologies (Oslo, Norway).
Screen-printed electrodes (DS110) based on carbon working, counter, and silver pseudo-reference electrodes were provided by Dropsens (Oviedo, Spain). The working electrode diameter was 4 mm. The magnetic holder (DRP–MAGNET) used for holding magnetic beads on the surface of the working electrode was supplied by Dropsens (Oviedo, Spain).

2.3. Samples

Coffee samples (instant coffee) were purchased from a local retail store (Madrid, Spain).

2.4. Equipment

Amperometric measurements were performed with a multipotenciostat *μSTAT8000* and the software DropView 8400 from Dropsens (Oviedo, Spain), and magnetic stirrer *Microstirrer* from Velp Scientifica (Usmate, Italy).
The competitive curves were analysed with a four parameter logistic equation using the proper software GraphPad Prism 5.

2.5. Immunoassay procedure

The immunoanalytical methodology was developed on the basis of the competition scheme where mycotoxin OTA and its enzyme-labelled derivative compete for binding sites of the specific polyclonal antibody. Magnetic beads covered by protein-G were used as an oriented immobilisation support for the capture of the anti-OTA antibody. Once

molecular recognition has been produced with OTA and/or OTA–HRP, the extent of the affinity reaction is evaluated by the addition of the enzymatic substrate and electrochemical mediator, which reduction on the electrode surface is directly related to the activity of the enzyme tracer.

The competitive immunoassay was performed in ELISA microplate wells. Dynabeads® protein-G magnetic beads were washed with PBS–T, pH 7.4, according to the manufacturer's protocol with the aim of eliminating the storage buffer and conditioning them for the IgG capture procedure. In this way, a volume of 0.5 μL of the commercial solution Dynabeads® was introduced into the well and washed three times with PBS–T. Through the assistance of an external magnet, magnetic beads were attracted to the bottom of the well to remove the supernatant. Afterwards, 50 μL of specific antibody (10 μg mL^{-1}) prepared in PBS–T was added to the magnetic beads for coating to the immobilized protein-G. The solution was gently stirred for 60 min at room temperature to obtain specific antibody-modified beads. Five times of washed step with 100 μL of PBS–T was subsequently performed. To avoid non-specific adsorption, the modified magnetic beads were blocked with PBS–T–BSA 2.5% (w/v) during 60 min. Sequential competitive assay was performed by re-suspending the anti-mycotoxin antibody-coated beads in 50 μL of PBS–T–BSA 1% solution which contains OTA standard or sample. After 30 min incubation time, the enzymatic tracer (final dilution 1:2000) was added. The competitive immunological reaction was allowed to proceed with gentle stirring for 15 min at room temperature. The magnetic beads were washed five times with 100 μL of PBS–T to remove not bound species and were re-suspended in 10 μL of citrate buffer.

2.6. Electrochemical measurements

The suspension of MBs modified with the immunoassay architecture was transferred and retained onto the surface of the working electrode of carbon screen-printed electrodes (CSPE) positioned on a magnet holding block. Amperometric measurements were performed after introduction of the assembled MBs–CSPE into an electrochemical cell containing 7 mL of citrate buffer, pH 5.0. The amperometric responses in stirred solutions (E_{app} = – 0.25 V vs Ag pseudo-reference electrode) were recorded upon addition of 140 µL of hydrogen peroxide and hydroquinone (1 mM final concentration for both) until the steady-state current was reached.

Amperometric signals, calculated as the difference between the steady-state and the background currents were fitted to the following four parameter logistic equation (sigmoidal) using the software Graph Pad Prism 5:

$$Y = i_1 + \frac{i_2 - i_1}{1 + 10^{[\log IC_{50} - x]p}}$$

where i_2 and i_1 are the maximum and minimum current values of the calibration graph obtained, IC_{50} is the analyte concentration producing 50% of the maximal amperometric signal, and p is the Hill slope at the inflection point of the sigmoid curve. The limit of detection (LOD) value was calculated as the analyte concentration for which the enzymatic tracer binding to the antibody was inhibited by 10%. The dynamic range (DR) was taken as the analyte concentration interval in which the inhibition of the binding of enzymatic tracer was between 20 and 80%.

2.7. Sample treatment

Solid samples of worldwide highly consumed food product, such as coffee, were analysed to demonstrate the adequate performance of the developed magnetoimmunosensor. Soluble instant coffee powder samples spiked with different concentration of OTA were analysed. 1 g samples were solubilized in 5 mL of PBS–T–BSA (1%), filtered with a nylon syringe filter of 0.45 μm of pore and 5-fold diluted with PBS–T–BSA (1%).

3. Results and discussion

3.1. Optimization of the immunoassay for OTA determination

The analysis was carried out in two key stages which occur at different places: (i) the affinity reaction, which takes place in solution (individual wells of microtiter plate), and (ii) the electrochemical transduction step, which occurs on the surface of disposable CSPE. Both steps are performed taking advantage of MBs' features involving their high surface area, fast kinetic assay, easy access of mycotoxin and tracer to the immobilized antibodies, and facility of manipulation. Moreover, the use of screen-printed electrodes as electrochemical platform, where magnetic beads are entrapped for transduction event, improves sensitivity avoiding the shielding of the electrode surface by deposition of the specific antibodies, and increases electron transference. Furthermore, since affinity reaction is performed in the microplate wells, this strategy diminishes the non-specific adsorption.

In order to get the best analytical performance for the immunosensor, some experimental variables were optimized. As previously detailed, MBs covered with protein-G were used as immobilization support for

specific antibody. The affinity of protein-G for the Fc region of antibody molecules involves their adequate orientation. In this sense, quantity of modified MBs was optimized to get a reasonable amperometric signal. Using a fixed excess of other reagents and parameters, different volumes of the stock MBs solution (0.25, 0.50 and 1.0 μL) were assayed. Measuring the signals produced in absence (maximum signal) and a high amount of the mycotoxin OTA (minimum or non-specific signal), 0.5 μL of the stock MBs commercial vial was found as those which produced the best signal to background ratio (data not shown).

Subsequently, using 0.5 μL as a limited volume of MBs, a titration curve was performed using different antibody concentrations from 0.6 to 20 μg mL^{-1} and keeping a fixed excess of the other immunoreagents and incubation times. As shown in **Fig. 1**, increased concentrations produced higher signals, reaching a plateau for 10 μg mL^{-1} as indicator of all protein G binding sites are occupied. Incubation time (range from 5–120 min) for coating of specific antibody onto beads was also tested. Although an incubation time of 30 min almost reach a plateau (83% maximum signal), 60 min were used to assure the total antibody immobilization onto available MBs protein-G binding sites.

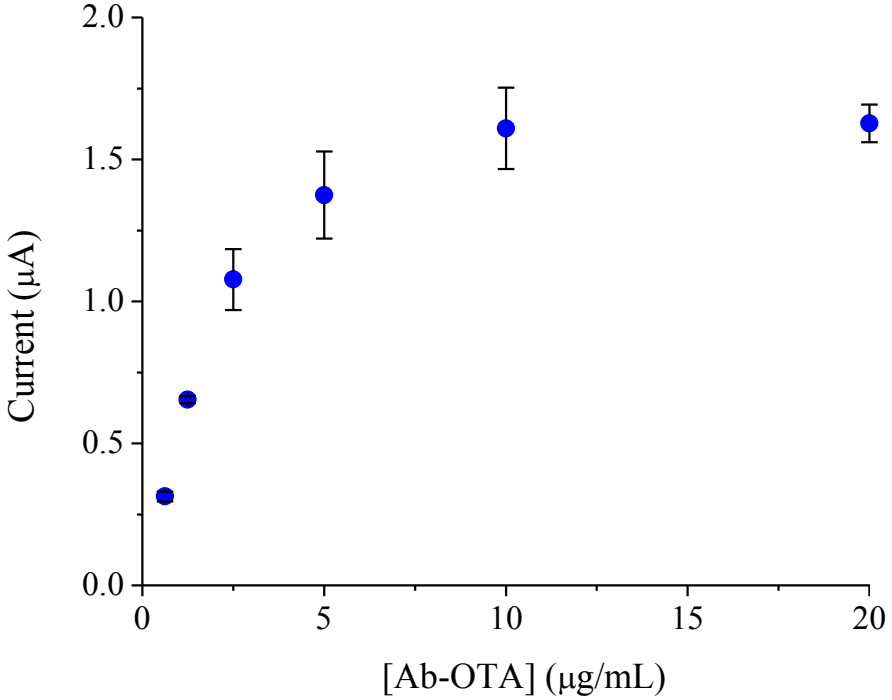

Fig. 1. Optimization of antibody concentration. Conditions: 0.5 μL magnetic beads, excess of the enzyme conjugate.

To avoid nonspecific adsorption, mainly of the enzymatic tracer onto MBs, even concentration and incubation time with BSA solution as blocking step were studied. The best ratio for maximum and minimum signals was obtained for 2.5% BSA and incubation time of 60 min.

Another key parameter to optimize is the amount of enzyme tracer related to the immobilized antibody. Antibody modified MBs were titrated with different tracer dilutions, in an excess of OTA and without the mycotoxin to achieve the best signal ratio. **Fig. 2** shows the binding curve for 10 μg mL^{-1} Ab concentration titrated with different OTA–HRP dilutions, where a tracer dilution 1:2000 showed an adequate competition with the OTA presented in the sample. Likewise, the optimization of incubation time with the tracer in absence and competition of excess of mycotoxin were tested. Signal increment was

obtained with time, where 15 min of incubation produced the best (specific/non-specific signals) ratio and represented an 82% of the maximum signal produced for the assayed times (5 to 120 min). In contrast, rising temperature from room temperature to 37ºC did not produce any significant signal difference in the affinity reaction, even in absence or presence of the mycotoxin.

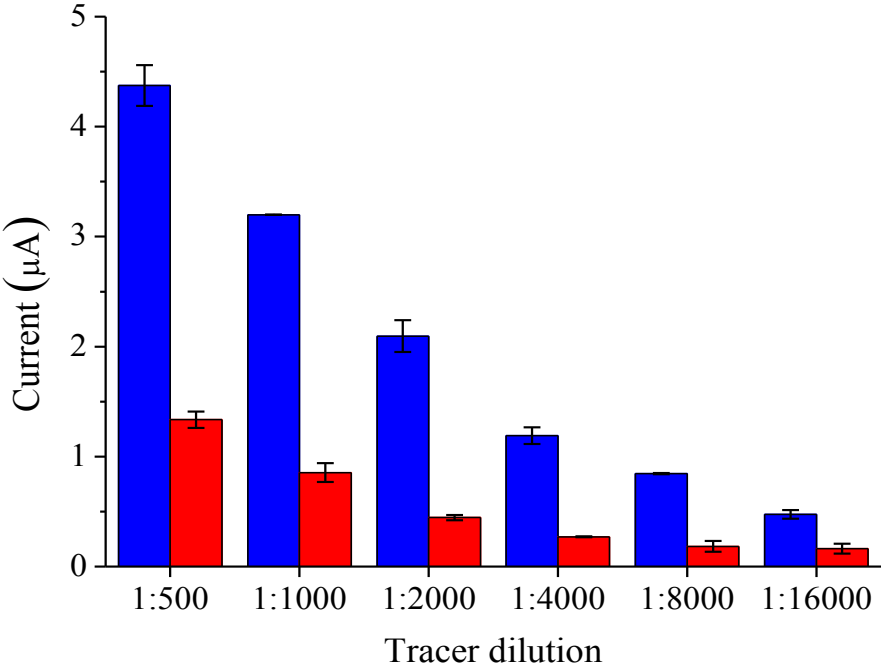

Fig. 2. Optimization of tracer dilution. Blue bars represent the maximum signal; red bars represent the minimum signal. Conditions: Volume of MBs 0.5 μL; Ab concentration: 10 μg mL^{-1}.

Amperometric detection of the HRP conjugated enzyme activity was carried out at – 0.25 V using H_2O_2 and HQN as the substrate and the electrochemical mediator, respectively. The optimum working electrode potential for the reduction of the enzymatically produced BQN in this sensor configuration was selected using amperometry. The highest signal to background current ratio in presence of H_2O_2 was obtained at – 0.25

V, chosen as working potential. Besides, optimal concentrations of H_2O_2 and HQN were assessed for maximal amperometric current intensity. When concentrations of both reagents were evaluated within the range of 0.05–1.5 mM, as shown in **Fig. 3**, the highest signal was achieved at 1.0 mM, ensuring that all enzymatic molecules were substrate bound and that V_{max} was reached.

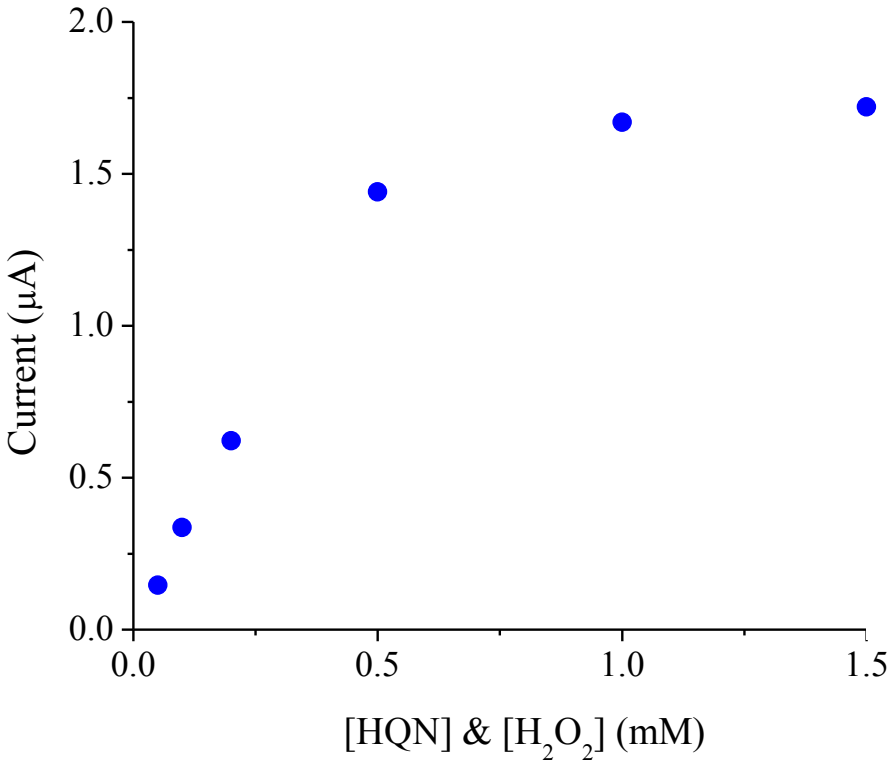

Fig. 3. Optimization of electrochemical mediator and enzymatic substrate (HQN and H_2O_2, respectively). The same concentration was used for both compounds. Conditions: Volume of MBs: 0.5 μL; Ab concentration: 10 μg mL^{-1}; OTA–HRP dilution: 1:2000; Incubation time of Ab-OTA: 60 min; Incubation time of OTA–HRP: 15 min.

3.2. Analytical features of the OTA magnetoimmunosensor

Fig. 4 shows the calibration curve obtained under the optimizedconditions described in **Table 1**. As it is listed in **Table 2**, the LOD (90%) and IC_{50} calculated values were 0.32 and 14.2 μg L^{-1} respectively and the DR ranged between 1.3 and 153.8 μg L^{-1}. This LOD was found well below the limit fixed by the European Union (10 μg Kg^{-1} for soluble coffee samples) showing the suitability of the immunosensor as an emergency tool for OTA contaminations in coffee samples.

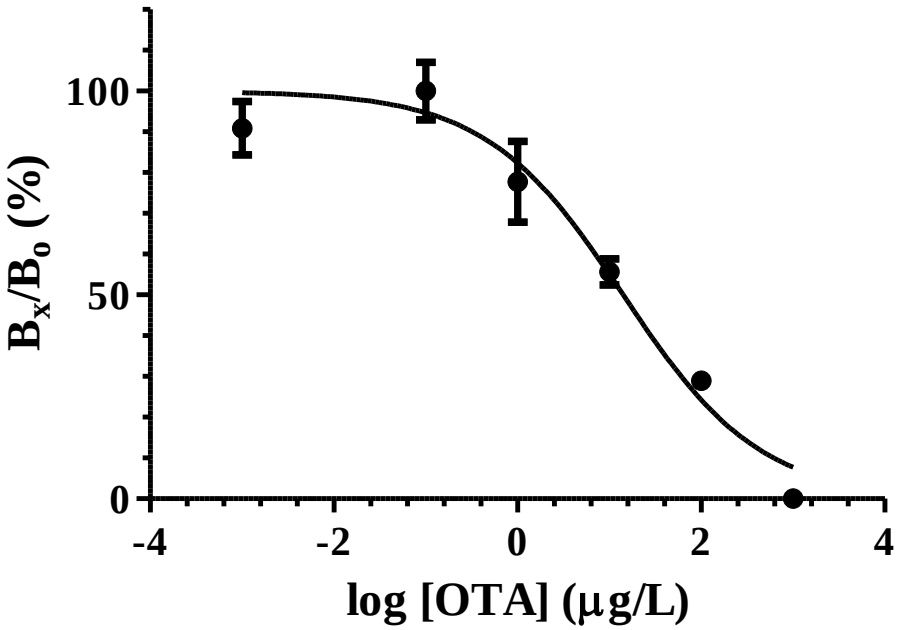

Fig. 4. Calibration curve for Ochratoxin A determination. Each point correspond to the $\mathbf{B_x/B_o}$ percentage ± SD, calculated for n = 3 repetitions. (B_o is the maximum signal obtained without competition and B_x is the signal obtained during the competition process).

Also, precision was carefully evaluated. Intra-immunosensor repeatability and inter-immunosensor reproducibility for the maximum signal were studied. RSD value of 7% (n=3) was obtained within the same day; while RSD value of 10% (n=6) was obtained in different days.

Table 1

Optimized conditions to perform the calibration curve.

Variable	Optimized value
Volume MBs	0.5 μL
[Ab-OTA]	10 μg mL^{-1}
Time of antibody incubation	60 min
Blocking solution	PBS−T−BSA (2.5%)
Blocking time	60 min
Dilution OTA−HRP	1:2000
Time of tracer incubation	15 min
[HQN] and [H_2O_2]	1 mM
E	− 0.25 V

In addition, since the coffee samples require a previous sol-ubilization step and due that the final matrix could significantlyinfluence on the LOD and sensitivity of the assay, calibration curvewas also performed under optimum sample analysis conditions inthis matrix. To this end, sample analysis was firstly performed justdissolving 1 g in 5 mL of PBS. However, the analysis carried outunder these conditions produced only an 11.8% of the amperomet-ric current for the maximum signal obtained in PBS buffer. To avoidthis matrix interference, solubilized coffee samples were suitablydiluted in PBS buffer being 1:5 (v/v) the optimum dilution value.Interestingly, the calibration curve, performed under these condi-tions, exhibited identical analytical properties to those obtained inPBS buffer as is also shown in **Table 2** confirming the absence ofmatrix interferences.

Table 2

Analytical parameters obtained for calibration curves performed in PBS buffer and diluted coffee matrix.

Calibration curve	LOD[a] (µg L^{-1})	IC_{50}[b] (µg L^{-1})	DR[c] (µg L^{-1})
Buffer	0.32	14.16	1.31-153.8
Diluted Coffee	0.26	10.2	1.0-104.0

[a]Limit of detection
[b]Inhibitory concentration 50%
[c]Dinamic range

3.3. Simultaneous simplified OTA calibration and determination on board of disposable CSPE: Application to soluble coffee samples

For routine sample analysis, the non-linear calibration curves usually performed in immunoassays implies laborious and time consuming procedures, limiting their operation for in field determinations. To avoid this disadvantaged protocol, our research group has demonstrated the suitability of using a simplified and integrated calibration analysis in these devices for other micotoxins determination. [30, 31] This methodology implies the simultaneous determination of a selected concentration of the mycotoxin with calibration purpose and the determination of the analyte in the food sample. Briefly, comparison of both signals and after the adequate definition of the calibration factor, allows the determination of the mycotoxin in the sample. The calibration factor is calculated as $f_{calibration} = S_{OTA\ standard} \times [OTA]_{Standard}$. Since this calibration factor is a constant for each analysis, the OTA concentration in the sample can simply be calculated as $[OTA]_{Sample} = f_{Calibration}/S_{OTA\ sample}$. Besides simplification, sources of error are minimized due to the fact that calibration and analysis are performed under equal conditions. Furthermore, the adequate selection of control concentration being similar to the one expected in the sample, improves accuracy of the analysis. In addition, as technical improvement, both analytical operations, mycotoxin calibration and sample analysis were

simultaneously performed using a multipotentiostat as it is illustrated in **Fig. 5,** reducing dramatically the analysis times and increasing the reliability of the analysis.

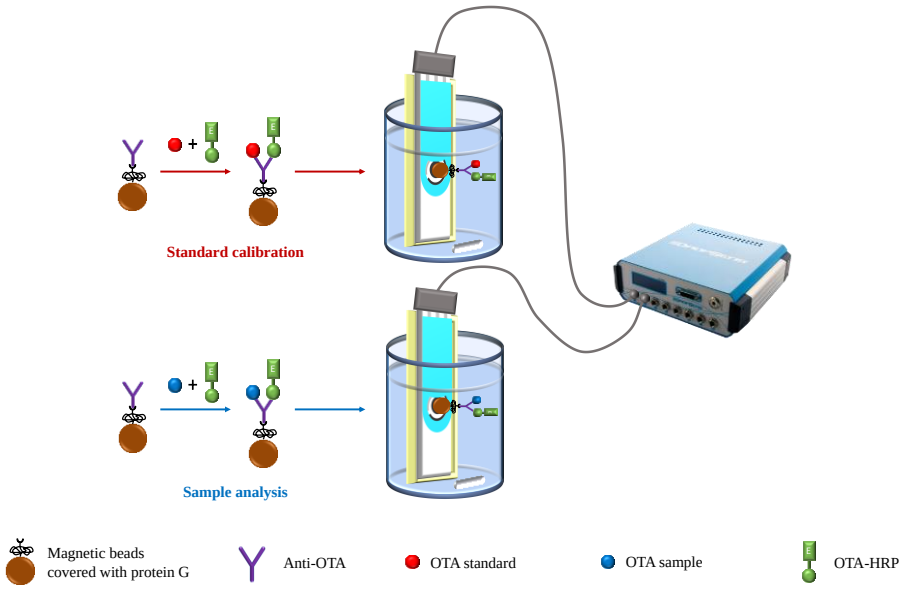

Fig 5. Scheme of the simultaneous simplified standard calibration and sample analysis. Color code: red for standard calibration, blue for sample analysis

Following this simplified calibration strategy, simultaneously performed with OTA determination into a parallel configuration, soluble coffee samples were spiked at the maximum level of concentration permitted by the legislation for those samples (10 μg Kg^{-1}) and analysed. Taking into account that previous solubilisation and dilution of the sample are needed, and to work in the dynamic range of the method, the solid samples were solubilized in a lower buffer volume (2 mL instead of the 5 mL used in the calibration curve performed in the matrix). In this case, the final OTA concentration was 1 μg L^{-1}. These samples were simultaneously analysed with the adequate control corresponding to the same concentration as the expected in the sample. Under these circumstances, the recoveries obtained were 90% (**Table 3**)

demonstrating the suitability of the proposed simplified analytical procedure and the convenience of the developed immunosensor as reliable and disposable alarm screening of OTA in coffee samples.

Table 3

Analysis of coffee samples using the simultaneous simplified calibration and analysis protocol[a].

Spiked concentration (µg Kg^{-1})	Solubilization volume (mL)[b]	Measured concentration (µg L^{-1})[c]	Found concentration (µg Kg^{-1})	Recovery (%)
10	2	1	9 ± 1	90 ± 10
10	5	0.4	7.3 ± 0.6	73 ± 6

[a]Number of repetitions (n = 3)
[b]Volume used for solubilisation of 1 g of instant coffee sample.
[c]Final volume after dilution of the solubilized sample 1:5 in PBS buffer.

When instant coffee samples, spiked at the same level of concentration (10 µg Kg–1), followed the sample preparation as done in the matrix calibration curve, the final OTA concentration to be measured was 0.4 µg L–1, which is very close to the LOD of the method. Following the suggested simplified calibration and analysis protocol, the obtained recoveries were 73% as it is also listed in **Table 3**. Although these recovery values are slightly lower, since we are measuring close to LOD, they confirm the detection capacity of the method, even for this extremely low concentration far away of the legislative requirements.

On the other hand, as it was previously stated, different electrochemical immunosensors have been developed for OTA determination. Among them, those using magnetical nanoparticles as antibody immobilization support constitute an important piece of developed work for the assessment of this mycotoxin as it is summarized in **Table 4**. As it is observed, most of the works have been devoted to analysis of wine

samples and reports excellent limit of detection and recoveries. Nevertheless, they still require a calibration curve and the associated drawbacks as laborious, time consuming and limiting their operation for real sample analysis into the field. Furthermore, previous immunosensors have not extensively explored the analysis of coffee samples, which is a highly concern matrix with a recognized high prevalence of OTA contamination. To the best of our knowledge only two non-magnetic beads-based impedimetric immunosensors have been used for OTA determination in this matrix [14,21]. Solanki et al. reported an impedimetric immunosensor for OTA detection with an excellent limit of detection but narrower working range. In this case, instant coffee samples were merely used to discern an increase in the impedance signal with concentration of the mycotoxin. Muchindu et al. also developed an impedimetric immunosensor for OTA determination in different matrix, but analysis of roasted coffee certified reference material presented recovery values below 33% of the vendor specifications.

Therefore, at the light of the previous reported literature, our work presents the first electrochemical immunosensor magnetic beads-based for OTA determination in coffee simples with an improved overall simplification without losing required performance accordingly to legal requirements.

In addition, it is worthy to point out that, the developed immunosensor can be easily adapted to obtain a real analytical tool for in field analysis. The assay time can be drastically reduced since the initials steps of the assay including immobilization of the anti- body on magnetic beads and block of non-specific adsorption could be performed in advance and considered as premade reagents. This also reduces the incubation and washing steps producing a more friendly methodology. Furthermore, the

use of a small, inexpensive and portable set-up together with a simple electrochemical detection technique enables the real sample in-field analysis.

Table 4. Electrochemical magnetic beads-based immunosensors for Ochratoxin A

Immobilization Support/ Assay format	Detection	Sample	IC_{50} ($\mu g\ L^{-1}$)	DR ($\mu g\ L^{-1}$)	LOD ($\mu g\ L^{-1}$)	Precision (CVs/%)	Recovery (%)	Remarks	Ref.
MBs-proteinG/ DCA	SWV	Wine	0.272	0.01-20	0.008	< 6	92-110	Direct sample measurement. Excellent LOD	[24]
MBs-streptavidin/DCA	DPV	Wine	0.108	0.24-8.33	0.11	< 9	105-109	Good agreement with official method (HPLC-FLD)	[26]
Gold-electrode-MBs/LFA	EIS	Wine	---	0.01-5	0.01	< 5	---	Label-free immunosensor	[27]
MBs-amino/LFA	SWV	Grapes	---	0.5-50	0.02	< 3	99.2-102	Direct oxidation of OTA on GCE. Excellent recoveries	[28]
MBs-protein G/ DCA	AMP	Instant coffee	14.2	1.3-153.8	0.32	<10	80-100	Simultaneous simplified calibration and determination. Wider DR	Present work

DPV: Differential Pulse Voltammetry; SWV: Square Wave Voltammetry; AMP: Amperometry; EIS: Electrochemical Impedance Spectroscopy; MBs: Magnetic Beads; DCA: Direct competitive assay; LFA: Label-free assay; IC_{50}: Inhibitory concentration 50%; DR: Dinamic Range; LOD: Limit of Detection.

4. Outlook and concluding remarks

An electrochemical immunosensor based on magnetic beads and disposable CSPE has been successfully developed for reliable assessment of OTA in highly worldwide consumed beverage as soluble coffee samples. This immunosensor presents a suitable LOD, well below of the maximum permitted concentration level, fulfilling the legislation requirements.

Additionally, a simultaneous simplified calibration and analysis protocol have been performed, reducing the analysis time, decreasing the tedious and intense labour of calibration curves, and reaching exceptional accuracy. These features, together with the portable, disposable possibilities of the developed immunosensor, provides to this methodology the fitness for purpose and offer an exceptional emergency tool for food safety and agro alimentary chain monitoring.

Acknowledgement

The authors are very grateful for the financial support from the Spanish Ministry of Economy and Competitiveness CTQ2011–28153 (A.E.) and from the NANOAVANSENS program from the Community of Madrid (S2013/MIT-3029). D. Adrián Jodra acknowledges the FPI fellowship received from the Spanish Ministry of Economy and Competitiveness.

References

[1] H.P. van Egmond, R.C. Schothorst, M.A. Jonker, Regulations relating to mycotoxins in food: perspectives in a global and European context, Anal. Bioanal. Chem., 389 (2007) 147-57.

[2] B. Prieto-Simon, M. Campas, J.L. Marty, T. Noguer, Novel highly-performing immunosensor-based strategy for ochratoxin A detection in wine samples, Biosens. Bioelectron., 23 (2008) 995-1002.

[3] N.W. Turner, S. Subrahmanyam, S.A. Piletsky, Analytical methods for determination of mycotoxins: a review, Anal. Chim. Acta, 632 (2009) 168-80.

[4] G.S. Shephard, F. Berthiller, P.A. Burdaspal, C. Crews, M.A. Jonker, R. Krska, et al., Developments in mycotoxin analysis: an update for 2011-2012, World Mycotoxin J., 6 (2013) 3-30.

[5] F. Berthiller, P.A. Burdaspal, C. Crews, M.H. Iha, R. Krska, V.M.T. Lattanzio, et al., Developments in mycotoxin analysis: an update for 2012-2013, World Mycotoxin J., 7 (2014) 3-33.

[6] R. Krska, P. Schubert-Ullrich, A. Molinelli, M. Sulyok, S. MacDonald, C. Crews, Mycotoxin analysis: an update, Food Addit. Contam. Part-A, 25 (2008) 152-63.

[7] I. Palchetti, M. Mascini, Electroanalytical biosensors and their potential for food pathogen and toxin detection, Anal. Bioanal. Chem., 391 (2008) 455-71.

[8] S. Viswanathan, H. Radecka, J. Radecki, Electrochemical biosensors for food analysis, Monatsh. Chem., 140 (2009) 891-9.

[9] F. Ricci, G. Adornetto, G. Palleschi, A review of experimental aspects of electrochemical immunosensors, Electrochim. Acta, 84(2012) 74-83.

[10] J.C. Vidal, L. Bonel, A. Ezquerra, S. Hernandez, J.R. Bertolin, C. Cubel, et al., Electrochemical affinity biosensors for detection of mycotoxins: A review, Biosens. Bioelectron., 49 (2013) 146-58.

[11] S.H. Alarcón, L. Micheli, G. Palleschi, D. Compagnone, Development of an Electrochemical Immunosensor for Ochratoxin A, Anal. Lett., 37(2004) 1545-58.

[12] S.H. Alarcon, G. Palleschi, D. Compagnone, M. Pascale, A. Visconti, I. Barna-Vetro, Monoclonal antibody based electrochemical immunosensor for the determination of ochratoxin A in wheat, Talanta, 69 (2006) 1031-7.

[13] X.P. Liu, Y.J. Deng, X.Y. Jin, L.G. Chen, J.H. Jiang, G.L. Shen, et al., Ultrasensitive electrochemical immunosensor for ochratoxin A using gold colloid-mediated hapten immobilization, Anal. Biochem., 389 (2009) 63-8.

[14] P.R. Solanki, A. Kaushik, T. Manaka, M.K. Pandey, M. Iwamoto, V.V. Agrawal, et al., Self-assembled monolayer based impedimetric platform for food borne mycotoxin detection, Nanoscale, 2 (2010) 2811-7.

[15] A.E. Radi, X. Munoz-Berbel, V. Lates, J.L. Marty, Label-free impedimetric immunosensor for sensitive detection of ochratoxin A, Biosens. Bioelectron., 24 (2009) 1888-92.

[16] A.-E. Radi, X. Muñoz-Berbel, M. Cortina-Puig, J.-L. Marty, An electrochemical immunosensor for ochratoxin A based on immobilization of antibodies on diazonium-functionalized gold electrode, Electrochim. Acta, 54 (2009) 2180-4.

[17] W.C. Tsai, C.K. Hsieh, QCM-Based Immunosensor for the Determination of Ochratoxin A, Anal. Lett., 40 (2007) 1979-91.

[18] M. Heurich, M.K.A. Kadir, I.E. Tothill, An electrochemical sensor based on carboxymethylated dextran modified gold surface for ochratoxin A analysis, Sens. Actuat. B-Chem., 156 (2011) 162-8.

[19] A. Kaushik, P.R. Solanki, A.A. Ansari, S. Ahmad, B.D. Malhotra, Chitosan–iron oxide nanobiocomposite based immunosensor for ochratoxin-A, Electrochem. Commun., 10 (2008) 1364-8.

[20] A. Kaushik, P.R. Solanki, M.K. Pandey, K. Kaneto, S. Ahmad, B.D. Malhotra, Carbon nanotubes — chitosan nanobiocomposite for immunosensor, Thin Solid Films, 519 (2010) 1160-6.

[21] M. Muchindu, E. Iwuoha, E. Pool, N. West, N. Jahed, P. Baker, et al., Electrochemical Ochratoxin A Immunosensor System Developed on Sulfonated Polyaniline, Electroanal., 23 (2011) 122-8.

[22] R. Khan, N.C. Dey, A.K. Hazarika, K.K. Saini, M. Dhayal, Mycotoxin detection on antibody-immobilized conducting polymer-supported electrochemically polymerized acacia gum, Anal. Biochem., 410 (2011) 185-90.

[23] R. Khan, M. Dhayal, Nanocrystalline bioactive TiO2–chitosan impedimetric immunosensor for ochratoxin-A, Electrochem. Commun., 10 (2008) 492-5.

[24] P.R. Perrotta, F.J. Arévalo, N.R. Vettorazzi, M.A. Zón, H. Fernández, Development of a very sensitive electrochemical magneto immunosensor for the direct determination of ochratoxin A in red wine, Sens. Actuat. B-Chem., 162 (2012) 327-33.

[25] L. Bonel, J.C. Vidal, P. Duato, J.R. Castillo, Ochratoxin A nanostructured electrochemical immunosensors based on polyclonal antibodies and gold nanoparticles coupled to the antigen, Anal. Method., 2 (2010) 335.

[26] J.C. Vidal, L. Bonel, A. Ezquerra, P. Duato, J.R. Castillo, An electrochemical immunosensor for ochratoxin A determination in wines based on a monoclonal antibody and paramagnetic microbeads, Anal. Bioanal. Chem., 403 (2012) 1585-93.

[27] L.-G. Zamfir, I. Geana, S. Bourigua, L. Rotariu, C. Bala, A. Errachid, et al., Highly sensitive label-free immunosensor for ochratoxin A based on functionalized magnetic nanoparticles and EIS/SPR detection, Sens. Actuat. B-Chem., 159 (2011) 178-84.

[28] M.A. Fernandez-Baldo, F.A. Bertolino, G.A. Messina, M.I. Sanz, J. Raba, Modified magnetic nanoparticles in an electrochemical method for the ochratoxin A determination in Vitis vinifera red grapes tissues, Talanta, 83 (2010) 651-7.

[29] S. Casal, T. Vieira, R. Cruz, S.C. Cunha, Ochratoxin A in commercial soluble coffee and coffee substitutes, Food Res. Int., 61 (2014) 56-60.

[30] M. Hervás, M.A. Lopez, A. Escarpa, Simplified calibration and analysis on screen-printed disposable platforms for electrochemical magnetic bead-based immunosensing of zearalenone in baby food samples, Biosens. Bioelectron., 25 (2010) 1755-60.

[31] A. Jodra, M.A. Lopez, A. Escarpa, Disposable and reliable electrochemical magnetoimmunosensor for Fumonisins simplified determination in maize-based foodstuffs, Biosens. Bioelectron., 64 (2015) 633-8.

III.2. Catalytic motors

Many applications have been explored during the development of different kind of motors. However, a wide variety of applications, overall in the Analytical Chemistry field in which this Thesis is focused on, have to be investigated yet. In this way, sensing applications are very significant and are still in the early stages.

First presented application is based on well-known graphene-platinum microrockets and dye-aptamers as bioreceptor element. The concept relies on the pioneering detection, "on-the-move" detection. The aptamer recognises the mycotoxin, generating an aptamer-mycotoxin complex. Thus, the free dye-aptamer is stuck on the microrocket surface, thanks to the π-π interaction between graphene and nucleotides. Consequently, the dye is quenched due to the proximity with the graphene layer.

Other one consisted of a new alloy material for *proof-of-concept* microrockets. This tailor-made alloy is manufactured with two metals, Cu and Pt in different ratios (Cu, in higher concentration than Pt), by electrochemical deposition. These micromotors are able to delay the initial blastoff, and that feature can measure the corrosion grade provoked by different chemicals, such as pH or salt, for example. Furthermore, they are introduced in real samples (seawater and gastric acid simulant), agreeing with initial assays.

Both are presented in the next section by respective articles.

Submitted

Determination of Fumonisin B1 based *on-the-move* fluorescence quenching of the specific labeled-aptamer by graphene-made micromotors

Department of Analytical Chemistry, University of Alcalá, Alcalá de Henares, Madrid E-28871, Spain.
Chemical Research Institute "Andrés M. del Río" (IQAR), University of Alcalá, Carretera Madrid-Barcelona, Km. 33,600, Alcalá de Henares, E-28871 Madrid, Spain.

Abstract

Due to negative effects of mycotoxins in animal and human health, reliable and fast mycotoxin determination continues being a challenge in food safety analysis. Besides, the ability of self-propelled micromotors to perform *on-the-move* interaction working with selected molecules in extremely low sample volumes have lead into a new paradigm in analytical chemistry. In this work, a biosensing approach based on the selective recognition from aptamers to Fumonisin B1 mycotoxin, and further fluorescence quenching through the *on-the-move* catch of free aptamer onto the outer layer of unmodified reduced graphene micromotors has been proposed. A fast (shorter than 20 minutes of total assay time), with high sensitivity (limit of detection of 0.7 ng mL^{-1}), good accuracy (E_r = 0.01%) and excellent quantitative recoveries (~104%) for the determination of real samples has been obtained. These excellent results confirm the developed approach as an innovative and reliable analytical tool for food safety monitoring.

Introduction

The motion of small self-propelled nano/micromachines in extremely low sample volumes is one of the most exciting areas with the aim to perform (bio)sensing in the contemporary Analytical Chemistry.[1–5] Regarding the motors chemically powered by bubble propulsion,[6,7] different aspects, such as its continuous movement along the sample and the associated mixing effect due to the generated microbubble tail, have allowed to greatly enhance the *on-the-move* target-receptor interaction, improving the binding efficiency and sensitivity of these assays. This ability of nano/microscale motors to capture and transport specific target analytes in complex biological matrices have laid the foundations for novel biosensing methods and applications[1,3,8,9]. Special mention is required to those self-propelled motors by hydrogen peroxide catalytic decomposition over last decade.[10,11]

Different efforts have been made in the construction of different shapes and sizes such as tubular microengines[6,7,12] by different approaches including top-down photolithography, e-beam evaporation, and stress-assisted rolling of functional nanomembranes on the polymer. However, template electrodeposition fabrication has demonstrated a simpler and more economical processes for the preparation of bimetallic catalytic nanowires[10,13] and microtubular motors.[14,15]

The inherent utilization of nanomaterials and nanotechnology has spread out an exciting field of future applications. Among nanomaterials, graphene has deserved a high attention in the scientific society thanks to their excellent properties such as high electrical and thermal conductivity, large surface area, remarkable elasticity and mechanical strength.[16–20] Its incorporation in tubular micromotors has improved the propulsion performance because of the enhanced catalytic activity and

efficient bubble evolution compared with smooth tubular micromotors.[21–23] Besides, the exceptional surface properties of graphene have also allowed the attachment of different receptors for toxins detection,[24,25] the capture and removal of nerve agents and heavy metals,[26] or excellent fluorescent quenching ability based on energy transfer mechanism.[27–30]

The use of aptamers as recognition elements has recently achieved a great interest because they present high selectivity and affinity to their targets analytes.[31,32] Aptamers, single-stranded oligonucleotides, adopt a defined three-dimensional structure when a specific target is binding to them, resulting in a promising alternative to antibodies.[33] Additionally, aptamers are easily synthesized for a wide range of targets and in an economical way, while they present outstanding specificity and stability.

On the other hand, mycotoxins are potent toxins that cause negative effects on animals and humans health, being now considered the most important chronic dietary risk factor, even more than food additives or pesticide residues.[34] Produced as secondary metabolites by different filamentous fungi species under different worldwide environmental conditions, their negative impact on public health has lead to the establishment of maximum permitted levels by the European Union (0.2 $\mu g\ mL^{-1}$ for FB1).[35] Thus, the development of selective and sensitive approaches is recommended.[36–38] Immunochemical methods and liquid chromatography coupled to tandem mass spectrometry (LC-MS/MS) have been included in a method update review as novel methodologies for mycotoxins determination.[39] Nevertheless, these methodologies are limited by their non-portability, need of trained personnel, and

complications in real-time monitoring, making difficult their actual implementation in several applications.

In the present work, a biosensing micromotor-based approach has been developed for mycotoxin determination as fast and reliable food-safety monitoring tool. Using non-functionalized graphene with platinum nanoparticles (GPH/PtNPs) microtubular engines, an *on-the-move* quenching strategy carries the catch of free fluorescent-labeled aptamer out after their specific interaction with the mycotoxin. This novel biosensor has been performed for FB1 determination in CRM and real samples. Excellent analytical performance in terms of selectivity, sensitivity, accuracy, and precision, in addition to the low sample volumes required for the developed sensor, will be demonstrated in the following sections.

Experimental

Reagents and samples

The fluorescein amidine (FAM) labeled at the 5' end aptamer, specific for the FB1 (FAM-5′-ATA CCA GCT TAT TCA ATT AAT CGC ATT ACC TTA TAC CAG CTT ATT CAA TTA CGT CTG CAC ATA CCA GCT TAT TCA ATT AGA TAG TAA GTG CAA TCT-3′), was synthesized by Microsynth (The Swiss DNA company, Switzerland). Graphene oxide (GO) was purchased from Sigma-Aldrich (2 mg mL^{-1} dispersion in H_2O, ref: 763705). FB1, hydrogen peroxide, sodium dodecyl sulfate (SDS), H_2SO_4, Na_2SO_4, H_2PtCl_6, boric acid, isopropanol, and ethanol were purchased from Sigma-Aldrich. Hydrogen peroxide solution (1 % v/v) was used as the chemical fuel, and SDS solution (1 % v/v) was used as a surfactant in all propulsion experiments. Aptamers were reconstituted in 10 mM Tris-HCl buffer (pH 7.5; 100 μM) and

stored at +4°C until use. Stock dilution of FB1 (50 μg mL^{-1}) was made in ethanol. 100 mM PBS solution (pH 7.5) prepared with Milli-Q water and 0.01% of Tween (PBS-T), and it was used for dilution of FAM-aptamer and FB1 as well. All chemicals used were of analytical-grade reagents, and deionized water was obtained from a Millipore Milli-Q purification system (18.2 MΩ cm at 25 °C).

Fumonisins maize certified reference material ([FB1] = 2.0 ± 0.4 mg Kg^{-1}; [FB2] = 0.5 ± 0.2 mg Kg^{-1}; [FB3] = 0.2 ± 0.1 mg Kg^{-1}) was purchased from Pribolabs (Singapore). According to the instructions recommended by the supplier, 1 g sample aliquots were extracted with 4 mL of acetonitrile: PBS (50:50, v/v) in cooling refrigeration conditions by a tip sonication (VCX130, Sonics, Newtown, USA) for 20 min (5 min/cycle) at 117 W. After centrifugation at 4000 rpm during 10 min, the supernatant was separated. Beer (Guinness® Draught, Dublin, Ireland) was firstly degasified for 20 min in ultrasonic bath and straightaway spiked with different FB1 concentration.

Apparatus

Template-assisted electrochemical deposition of micromotors was carried out using an electrochemical station μ-Autolab Type III (Eco Chemie, Utrecht, Holland). Scanning electron microscopy (SEM) images were obtained with a JEOL JSM 6335F instrument, using an acceleration voltage of 22 kV. Energy-dispersive X-ray mapping analysis was performed using an EDX detector attached to SEM instrument. Raman Dilor XY spectrometer, equipped with two types of detectors: one of type matrix and one photomultiplier, with measurement in the sample and by microscope. It is equipped with two alternative sources: Kr^+ Coherent Innova 70-K laser and Ar^+ Coherent Innova 90C

laser. An inverted optical microscope (Nikon Eclipse 80i upright microscope), coupled with different objectives (10X, 20X and 40X), a B2-A fluorescence filter (λ_{exc} 470 nm, λ_{ems} 520 nm) for FAM and a Hamamatsu digital camera C11440 and NIS Elements AR 3.2 software, were used for capturing images and movies at a rate of 30 frames per second. The speed of the micromotors was tracked using NIS Elements tracking module. The fluorescence signal produced by the hybridization process between the dye-aptamer and the target mycotoxin was estimated by analyzing the corresponding time-lapse images using the Gwyddion software.

Methods

Electrosynthesis of graphene micromotors

Briefly, the electrochemically reduced graphene (GPH) micromotors were prepared by electrochemical reduction of graphene oxide into 5 μm-diameter conical pores of a polycarbonate membrane (PC) (Catalog No. 7060–2513; Whatman, Maidstone, UK). The S4 branched side of the membrane was treated with a sputtered thin gold film to perform as a working electrode. The membrane was assembled in a Teflon plating cell with aluminum foil serving as an electrical contact to the working electrode for the subsequent electrodeposition. Graphene oxide (GO, 0.5 mg mL^{-1}) was first dispersed in a solution containing 0.1 M H_2SO_4 and 0.5 M Na_2SO_4 in an ultrasonic bath for 15 min. The electrochemical reduction of GO was carried out using cyclic voltammetry (CV, over +0.3 to −1.5 V vs. Ag/AgCl (3 M KCl), at 50 mV s^{-1}, for five cycles; n = 5), using a Pt wire as counter electrode. Afterwards, a platinum layer was plated inside the GPH tube. The inner PtNPs layer was deposited by amperometry at −0.4V for 750 s from an aqueous solution containing 4

mM of H_2PtCl_6 in 0.5 M acid boric. The sputtered gold layer was gently polished by hand with 1 μm alumina slurry. After that, the membrane was dissolved in methylene chloride for 30 min to release the microtubes completely. Successive washes with isopropanol and ethanol (both twice) and ultrapure water (18.2 Ω cm, three times) were performed respectively. All microtubes were stored in ultrapure water at room temperature when not in use. An illustration of template prepared micromotors is depicted in Figure 1.

Figure 1. Electrosynthesis of GPH/PtNPs micromotors. (1) Electrodeposition of outer sensing layer (GPH) and inner catalytic layer (PtNPs). (2) Micromotors release: polishing of sputtered gold layer and dissolving the polycarbonate membrane.

Mycotoxin micromotor-based assay

A solution containing a concentration 5 μM of the specific fluorophore-labeled aptamer and Fumonisin B1 mycotoxin were incubated at 25 ºC, under gently stirring, for their selective recognition during 15 minutes. Then, 5 μL of this mixture containing the aptamer-mycotoxin complex and/or free aptamers were transferred to a microcentrifuge tube containing around 4500 GPH/PtNPs micromotors, 1 μL of SDS (1% final concentration) and 5 μL of H_2O_2 (1% final concentration). Under these conditions, micromotors were allowed to autonomously swim into the solution to perform "*on-the-move*" catching of free aptamers by the outer layer of graphene micromotors (**Figure 2**). After 2 minutes, three

aliquots of 1 µL of the solution were transferred to an inverted optical microscope where the fluorescence signal was recorded. Fluorescence measurements were performed using a *B2-A filter* (λ_{exc}=470 nm, λ_{ems}=520 nm).

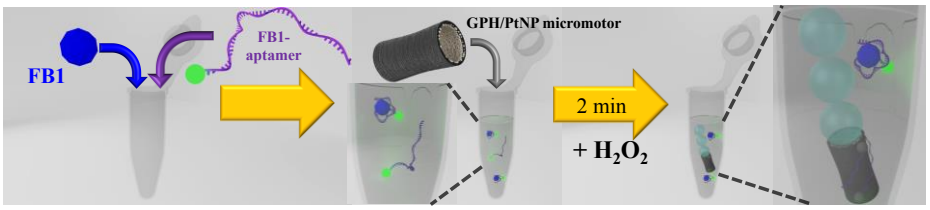

Figure 2. Biosensing strategy for mycotoxin detection using non-functionalized graphene-based micromotors.

Results and discussion

The assay principle is based on two different aspects: i) The selective recognition of the FB1 mycotoxin by aptamers, and ii) the adsorption of free dye-labeled aptamers onto the outer layer of graphene micromotors. That adsorption is realized by π-π interactions between ring structures from the nucleotide bases and the hexagonal cells of the graphene, which leads in the fluorescence quenching. In this context, the high-affinity binding of the specific aptamer to the mycotoxin causes the formation of the complex, which decreases the exposure of nucleotides to the graphene micromotor and hence, allowing their fluorescence emission. If there is more mycotoxin in the sample, there is higher fluorescence emission. This strategy allows the use of non-modified graphene-based micromotors, simplifying the synthesis and enhancing micromotor stability because of the absence of molecular recognition chemistry on the surface.

Characterization of graphene micromotors

Raman characterization of GPH/PtNPs micromotors was also performed. **Figure 3A** illustrates the Raman spectra of the GPH/PtNPs materials on micromotors. As expected, the Raman spectra displayed well-defined D bands at 1347 cm^{-1} and a G bands at 1601 cm^{-1}. The D band arises from the out-of-plane vibrational modes and is indicative of the number of sp^3 carbon atoms present, whereas the G band arises from the presence of in-plane sp^2 vibrations. Due to the large two-dimensional surface of graphene, single-stranded DNA can be bound via hydrophobic and π–stacking interactions between the ring structures from the nucleobases and the hexagonal cells of graphene.[29,30]

Further, **figure 3B** shows SEM images of the top and side views of a GPH/PtNPs micromotor. The micromotors are ~10 μm long and ~5 μm in diameter, reflecting the pore size of the PC membrane. An energy dispersive X-ray spectroscopy analysis (EDX), with the purpose of demonstrating the successful composition and modification of the GPH/PtNPs micromotor, was carried out as well. These EDX images (**Figure 3C**) clearly show the presence of carbon and platinum corresponding to the outer and inner layers, respectively.

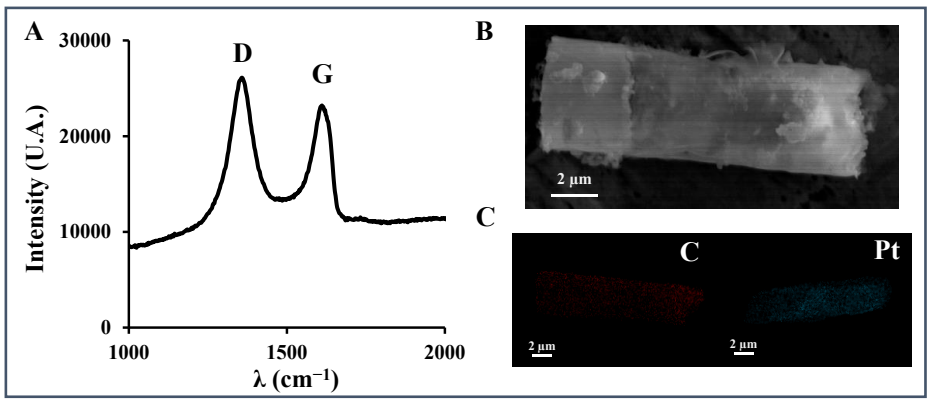

Figure 3. GPH/PtNPs based micromotors characterization. **(A)** Raman spectra of the graphene micromotors, **(B)** SEM images of the

GPH/PtNPs micromotors and **(C)** EDX analysis of carbon (red) and platinum (blue).

Optimization of the assay parameters

Different key parameters were carefully optimized to build up the graphene-based micromotor assay. In this sense, both, the suitable concentration of dye-labeled aptamers and the number of micromotors allowed to swim into the sample solution were first studied. Using a fixed aptamer concentration of 5 μM that produces enough fluorescence intensity, the influence of motors amount on the fluorescence quenching is presented in **Figure 4A**. In the absence of the mycotoxin, when the number of micromotors increases, fluorescence quenching also increases, becoming around 4500 the optimum number of motors to obtain the maximum quenching effect. Interestingly, when a 1 μg mL^{-1} concentration of FB1 is added to the solution, the maximum fluorescence emission is kept constant, demonstrating the negligible quenching effect of the aptamer/mycotoxin complex.

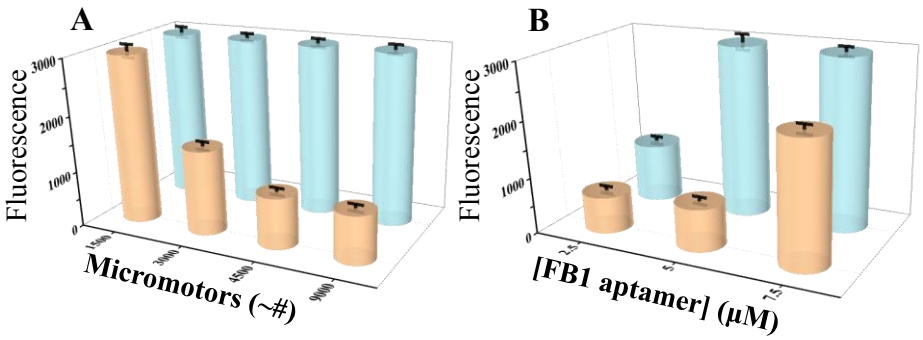

Figure 4. Variations of fluorescence signal under the influence of **A**. Volume of GPH/PtNPs. **B**. Aptamer concentration. Color blue and orange represents the presence and absence of 1 μg mL^{-1} mycotoxin, respectively.

Then, the influence of aptamer concentrations on the assay was also tested for the optimum micromotors number stated above. **Figure 4B** shows 5 μM as the most favorable concentration, since lower aptamers concentration produces a lower fluorescence signal, even in the presence of the mycotoxin, indicating the signal is limited by the total aptamer concentration and not by the quenching effect. On the other hand, the signal increased in the absence of the mycotoxin for higher aptamers concentrations, as a consequence of an excess of the dye-labeled aptamer over the micromotor amount and avoiding a total quenching effect.

It is remarkable that the motion of the micromotors along the low sample volume, the mixing effect due to the localized fluid convection and vortex streams associated with the rapid movement of the micromotors, together with the generated microbubbles tail, greatly improve the graphene motor/fluorescent aptamer interaction. In this sense, the required time for the micromotors to swim into the sample solution reaching the maximum quenching of free dye-labeled aptamers was as low as 2 minutes. This short time is clearly advantageous compared to a quiescent solution or external shaking procedure (as control), which required a minimum of 15 minutes to obtain a 50% and 70% of the fluorescence quenching, respectively. Upon mycotoxin-aptamer binding, the required time for the recognition event was also studied, being 15 minutes the optimum value needed to complete the mycotoxin-aptamer complexes.

Analytical performance and quantitative analysis

Quantitative analysis was deeply studied, since this aspect is rarely explored in the relevant literature, being a key feature in food analysis. The fluorescence signal variation produced by the non-quenched

aptamer-mycotoxin complex versus mycotoxin concentration is reported in **Figure 5**. An excellent linearity ($r \geq 0.990$) in the concentration ranges studied (0.005 to 1 µg mL^{-1}), together with a very good limit of detection (LOD = 0.7 ng mL^{-1}) and quantification (LOQ = 5 ng mL^{-1}) were obtained for the FB1 assay. These values, well below of the permitted levels determined by the legal requirements of the European Union (0.2 µg mL^{-1} for FB1), revealed the suitability of this novel strategy for FB1 assessment in foodstuffs.

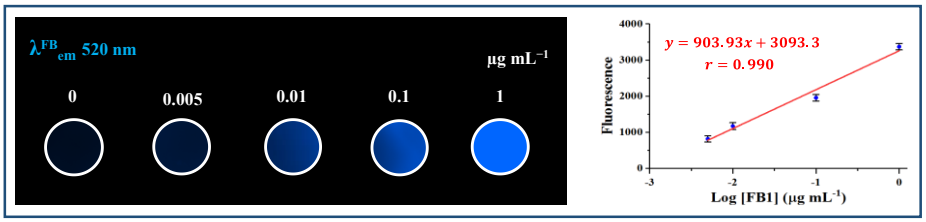

Figure 5. Calibration of **FB1** using GPH/PtNPs-based micromotors.

Precision was also evaluated at two mycotoxin concentrations (0.01 and 1 µg mL^{-1}), yielding excellent RSDs values of 7% and 5%, respectively (n=5, independent micromotor batches).

Selectivity experiments were also performed where the FB1 specific aptamer was incubated with a different mycotoxin such as Ochratoxin A (OTA) (**Figure 6**). As expected, the sole presence of the non-target mycotoxin did not avoid the quenching effect of the graphene micromotors.

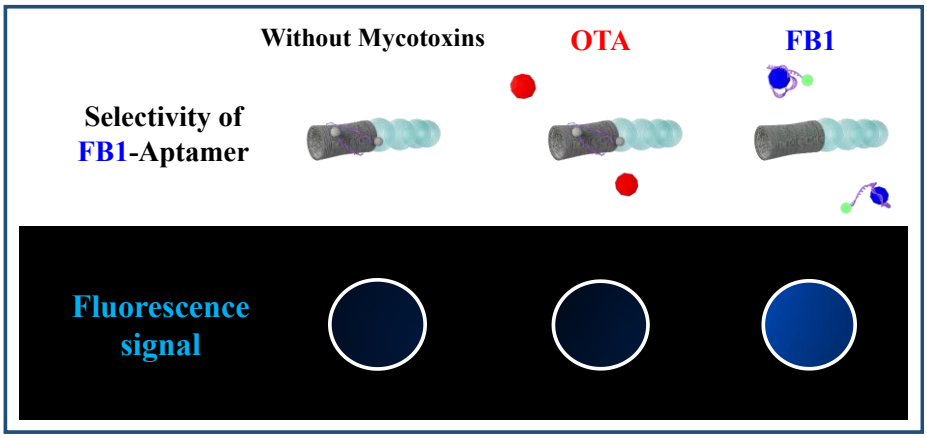

Figure 6. Aptamer selectivity of FB1: without mycotoxin, with 1 µg mL^{-1} **OTA**, with 1 µg mL^{-1} **FB1.**

Considering the excellent analytical characteristics attained, the applicability of the developed motor-based biosensor was evaluated through the analysis of a certified reference material and food samples.

As can be observed in **Figure 7** and video S1, the micromotor was able to swim in different real samples (A–C: PBS-T buffer, CRM, and beer) with speeds ranging between 100 and 120 µm s^{-1} when 1% H_2O_2 fuel was added (120 ± 30, 100 ± 20, 110 ± 30 µm s^{-1}, respectively). Furthermore, the fluorescence mycotoxin-aptamer complex in food samples and the quenching effect of the free aptamer by micromotors gave identical values in comparison with those obtained using standards. These results confirmed the efficient micromotors navigation in the food samples.

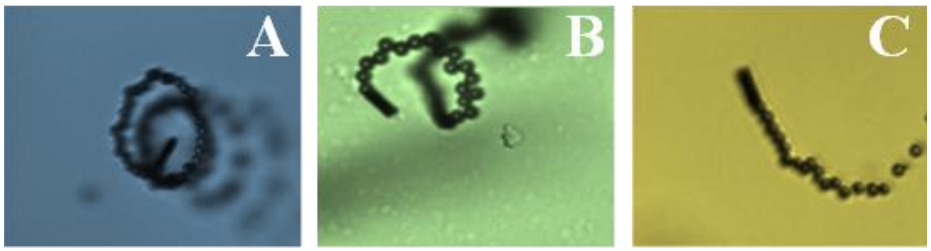

Figure 7. Micromotor swimming in different samples (from A to C: PBS-T buffer, CRM, and beer, respectively).

Finally, **Table 1** lists the results obtained in the analysis of food samples demonstrating an outstanding accuracy when the CRM was analyzed (Er < 0.01%) and a good reliability because of the quantitative recoveries (~104%) obtained during the analysis of food samples.

Table 1. Analysis of CRM and food samples.

Sample	Reference value ($\mu g\ mL^{-1}$)	Found value ($\mu g\ mL^{-1}$)	Er /Recovery (%)
CRM	0.23 ± 0.05	0.23 ± 0.02	0.01
Beer	0.20	0.21 ± 0.01	104 ± 4

Conclusions

In this paper, a high-performance graphene micromotor-based strategy for fast and reliable assessment of FB1 mycotoxin has successfully developed. This novel approach relies on the concept *on-the-move* fluorescence quenching, performed in a very short time (2 min), with excellent sensitivity (LODs well below of legal requirements), high selectivity and remarkable accuracy in a certified reference material as well as in complex food samples.

This novel approach adds valuable advantages over classic aptamer-based biosensors such as the lower sample required volume and washing steps are no longer required, simplifying the overall protocol, while the excellent accuracy, selectivity, sensitivity, and precision are preserved.

The excellent obtained results allow envisioning an exciting future for the novel applications of micromotors in unexplored fields such as food safety diagnosis.

Acknowledgments

This work has been financially supported by the NANOAVANSENS program from the Community of Madrid (S2013/MIT-3029), the Spanish Ministry of Economy and Competitiveness CTQ2011-28153, CTQ 2014-58643-R and SAF2014-53218-R from the Spanish Ministry of Science and Innovation (A. Escarpa). D. Adrián Jodra acknowledges the FPI fellowship received from the Spanish Ministry of Economy and Competitiveness. A. Molinero-Fernández acknowledges the FPI fellowship from the University of Alcala and M. Moreno-Guzmán acknowledges the NANOAVANSENS program from the Community of Madrid (S2013/MIT-3029) for her postdoctoral contract. We thank CAI and CNME of the Complutense University of Madrid for the Raman and SEM measurements.

References

[1] Guix, M., Mayorga-Martinez, C. C., Merkoçi, A., *Chem. Rev.*, **2014**, *114*, 6285–6322.

[2] Wang, J., *Biosens. Bioelectron.*, **2016**, *76*, 234–242.

[3] Wang, H., Pumera, M., *Chem. Rev.*, **2015**, *115*, 8704–8735.

[4] Katuri, J., Ma, X., Stanton, M. M., Sánchez, S., *Acc. Chem. Res.*, **2017**, *50*, 2–11.

[5] Li, J., Rozen, I., Wang, J., *ACS Nano*, **2016**, *10*, 5619–5634.

[6] Mei, Y. F., Huang, G. S., Solovev, A. A., Ureña, E. B., Mönch, I., Ding, F., Reindl, T., Fu, R. K. Y., Chu, P. K., Schmidt, O. G., *Adv. Mater.*, **2008**, *20*, 4085–4090.

[7] Solovev, A. A., Mei, Y. F., Ureña, E. B., Huang, G. S., Schmidt, O. G., *Small*, **2009**, *5*, 1688–1692.

[8] Wang, J., *Nanomachines: Fundamentals and Applications*, Wiley-VCH, Weinheim, Germany, **2013**.

[9] Sánchez, S., Soler, L., Katuri, J., *Angew. Chem. Int. Ed.*, **2015**, *54*, 1414–1444

[10] Laocharoensuk, R., Burdick, J., Wang, J., *ACS Nano*, **2008**, *2*, 1069–1075.

[11] Kherzi, B., Pumera, M., *Nanoscale*, **2016**, *8*, 17415–17421.

[12] Mei, Y., Solovev, A. A., Sanchez, S., Schmidt, O. G., *Chem. Soc. Rev.*, **2011**, *40*, 2109–2119.

[13] Paxton, W. F., Kistler, K. C., Olmeda, C. C., Sen, A., Angelo, S. K. St., Cao, Y., Mallouk, T. E., Lammert, P. E., Crespi, V. H., *J. Am. Chem. Soc.*, **2004**, *126*, 13424–13431.

[14] Gao, W., Sattayasamitsathit, S., Orozco, J., Wang, J., *J. Am. Chem. Soc.*, **2011**, *133*, 11862–11864.

[15] Zhao, G., Pumera, M., *RSC Adv.*, **2013**, *3*, 3963–3966.

[16] Martín, A., Escarpa, A., *TrAC, Trends Anal. Chem.*, **2014**, *56*, 13–26.

[17] Wang, J., *Faraday Discuss*. **2013**, *164*, 9–18.

[18] Gao, W., Sattayasamitsathit, S., Uygun, A., Pei, A.; Ponedal, A., Wang, J., *Nanoscale*, **2012**, *4*, 2447–2453.

[19] Stankovich, S., Dikin, D. A., Dommett, G. H. B., Kohlhaas, K. M., Zimney, E. J., Stach, E. A., Piner, R. D., Nguyen, S. T., Ruoff, R. S., *Nature*, **2006**, *442*, 282–286.

[20] Lee, C., Wei, X., Kysar, J. W., Hone, J., *Science*, **2008**, *321*, 385–388.

[21] Martin, A., Jurado-Sanchez, B., Escarpa, A., Wang, J., *Small*, **2015**, *11*, 3568–3574.

[22] Maria-Hormigos, R., Jurado-Sanchez, B., Vazquez, L., Escarpa, A., *Chem. Mater.* **2016**, *28*, 8962–8970.

[23] Vilela, D., Parmar, J., Zeng, Y., Zhao, Y., Sanchez, S., *Nano Lett.*, **2016**, *16*, 2860–2866.

[24] Cheng, H., Hu, C., Zhao, Y., Qu, L., *NPG Asia Mater.*, **2014**, *6*, 113.

[25] Esteban-Fernandez de Ávila, B., Lopez-Ramirez, M. A., Baez, D. F., Jodra, A., Singh, V. V., Kaufmann, K., Wang, J., *ACS Sens.*, **2016**, *1*, 217–221.

[26] Shao, Y., Wang, J., Engelhard, M., Wang, C., Lin, Y., *J. Mater. Chem.*, **2010**, *20*, 743–748.

[27] Morales-Narvaez, E., Merkoçi, A., *Adv. Mater.*, **2012**, *24*, 3298–3308.

[28] Green, N. S., Norton, M. L., *Anal. Chim. Acta*, **2015**, *853*, 127–142.

[29] Lu, C. H., Yang, H. H., Zhu, C. L., Chen, X., Chen, G. N., *Angew. Chem. Int. Ed.* **2009**, *48*, 4785–4787.

[30] Perez-Lopez, B., Merkoçi, A., *Microchim. Acta*, **2012**, *179*, 1–16.

[31] Loo, A. H., Bonanni, A., Pumera, M., *Nanoscale*, **2013**, *5*, 4758–4762.

[32] Song, S., Wang, L., Li, J., Zhao, J., Fan, C., *TrAC, Trends Anal. Chem.*, **2008**, *27*, 108–117.

[33] Famulok, M., Mayer, G., Blind, M., *Acc. Chem. Res.*, **2000**, *33*, 591–599.

[34] van Egmond, H. P., Schothorst, R. C., Jonker, M. A., *Anal. Bioanal. Chem*. **2007**, 389, 147–157.

[35] EC. No. 123-2005, EC. No.1881-2006, Commission Regulation No. 1126/ 2007, European Commission, 2007.

[36] Turnera, N. W., Subrahmanyamb, S., Piletskyb, S. A., *Anal. Chim. Acta.*, **2009**, *632*, 168–180.

[37] Jodra, A., López, M. A., Escarpa, A., *Biosens. Bioelectron.*, **2015**, *64*, 633–638

[38] Jodra, A., Hervás, M., López, M. A., Escarpa, A., *Sens. Actuat. B-Chem.*, **2015**, *221*, 777–783.

[39] Berthiller, F., Brera, C., Crews, C., Iha, M. H., Krska, R., Lattanzio, V. M. T., MacDonald, S., Malone, R. J., Maragos, C., Solfrizzo, M., Stroka, J., Whitaker, T. B., *World Mycotoxin J.*, **2016**, *9*, 5–29.

Chemical Communications *DOI: 10.1039/c6cc06632a*

Delayed ignition and propulsion of catalytic microrockets based on fuel-induced chemical dealloying of the inner alloy layer†

Adrián Jodra,[‡ab] Fernando Soto,[‡a] Miguel Angel Lopez-Ramirez,[a] Alberto Escarpa[b] and Joseph Wang*[a]

Department of Nanoengineering, University of California, San Diego, La Jolla, California 92093, United States.
Department of Analytical Chemistry, University of Alcalá, Alcalá de Henares, Madrid E-28871, Spain.
† Electronic Supplementary Information (ESI) available: Microrocket preparation, instrumentation, reagents, additional data, and videos.
‡ A.J. and F.S. contributed equally to this paper

The delayed ignition and propulsion of catalytic tubular microrockets based on fuel-induced chemical dealloying of an inner alloy layer are demonstrated. Such timed delay motor activation process relies on the preferential gradual corrosion of Cu from the inner Pt-Cu alloy layer by the peroxide fuel. The dealloying process exposes the catalytically active Pt surface to the chemical fuel, thus igniting the microrockets propulsion autonomously without external stimuli. The delayed motor activation relies solely on the intrinsic material properties of the micromotor and the surrounding solution. The motor activation time can thus be tailored by controlling the composition of the Cu-Pt alloy layer and the surrounding media, including the fuel and NaCl concentrations and local pH. Speed acceleration in a given fuel solution is also demonstrated and reflects the continuous exposure of the Pt surface. The versatile "blastoff" control of these chemical microrockets holds considerable promise for designing self-regulated chemically-powered nanomachines with a "built-in" activation mechanism for diverse tasks.

Chemically-powered nano/microscale motors have received considerable recent attention owing to their great promise for diverse practical biomedical and environmental applications.[1-12] Particularly

attractive for such applications are catalytic tubular microengines that display remarkably efficient propulsion driven by their bubble thrust.[13-17] The ability of these catalytic microengines to perform complex operations requires precise control of their motion and actuation.[18] Such control cannot be achieved by simply scaling down conventional designs used to regulate large-scale engines.[19,20] Unlike macroscale devices which rely on their internal fuel supply to power and ignite their engine on demand, chemically-powered microengines are submerged in their fuel solution and are thus always turned "on" from the start.[21-27] For this reason, different strategies have been proposed recently for activating the propulsion of chemically-powered micromotors, based on the use of different external stimuli.[28-35] However, complex operations and important applications of catalytic micromotors could greatly benefit from the ability to autonomously trigger the movement at preselected times without external perturbations.

Here we demonstrate a built-in delayed ignition of self-propelled catalytic microrockets based on autonomous chemical dealloying process in the fuel solution without external stimuli. The delayed activation strategy relies on the dealloying of a catalytically-inert Cu-Pt alloy inner layer of the microrocket by the hydrogen-peroxide fuel, exposing the catalytically active Pt surface to the fuel to initiate the propulsion at different predetermined times. The dealloying process involves chemically selective leaching of the less noble (copper) component of the alloy by the hydrogen peroxide.[36-38] This new built-in delayed ignition concept represents the first demonstration of utilizing the intrinsic material properties of a catalytic microengine to delay and activate their propulsion without using external stimuli. The mechanism and factors that allow these micromotors to operate in a programmed

timing and to activate the ignition of the motor in the fuel solution at different time delays are discussed. The motor activation time is controlled by tailoring the composition of the surrounding fluid, e.g., fuel concentration, pH and ionic environment. We also demonstrate the first example of changing motor speed at a given fuel concentration due to gradual increased exposure of the catalyst. Such built-in chemical approach for regulating autonomously the activation of catalytic microengines offers considerable promise for diverse future applications.

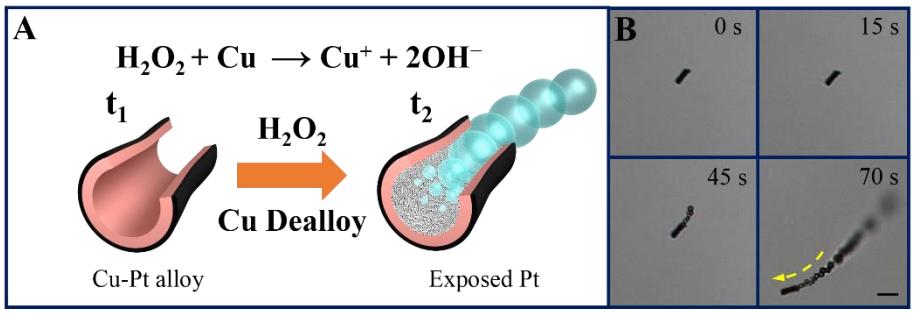

Figure 1. *Delayed ignition and propulsion of catalytic microrockets based on fuel-driven chemical dealloying of the inner layer.* ***A)*** *Schematic illustration of the time-dependent chemical activation of an erGO/Cu-Pt microrocket.* ***B)*** *Time-lapse images, taken from supporting information video 2, illustrating the delayed microrocket activation during the chemical dealloying, with bubbling and motion initiated after 44 seconds. Scale bar, 20 μm.*

The electrochemical-reduced graphene oxide/copper-platinum alloy (erGO/Cu-Pt) microrockets were fabricated by using a template electrodeposition protocol.[41,42] The alloy solution was composed by Cu and Pt mixture solution containing a large excess of copper, as detailed in the supporting information. A schematic illustration of the time-dependent delayed activation process of microrocket is given in Figure 1A and Video S1. The delayed propulsion strategy relies on the galvanic

and pitting corrosion of Cu from the inner Cu-Pt alloy surface. Based on the corrosive effect of hydrogen peroxide towards copper in the bimetallic alloy,[43,44] the peroxide fuel dissolves gradually the Cu constituent of the alloy, eventually exposing the catalytically active Pt surface to the fuel solution. This exposure initiates the decomposition of the fuel into oxygen, and leads to continuous ejection of oxygen microbubbles essential for generating the propulsion thrust.[45] The resulting microrockets display different types of motion trajectories, including straight line, circular, spiral and circular spiral (see video S3 and Figure SI3), characteristic of erGO/Cu-Pt microrockets.[42] The delayed ignition and propulsion of the microrockets are illustrated in the time-lapse images of Figure 1B (taken from video S2), where the movement is initiated autonomously 44 sec after immersing the motors in the fuel solution. Such delayed activation of the microrocket can be tailored by tuning its chemical environment (H_2O_2 concentration, pH and ionic strength conditions) and by controlling the alloy composition (via its electrodeposition conditions). The influence and role of these factors upon the delayed propulsion are discussed in the following sections.

Figure 2A displays SEM images of the morphology of an erGO/Cu-Pt alloy microrocket with a length of 15 μm and diameter of 5 μm. Furthermore, the energy dispersive X-ray spectroscopy (EDX) analysis (of Figure 2A) displays the microrocket composition, where Pt and Cu are distributed homogeneously, along with the presence of oxygen (that corresponds to the erGO outer layer). Figure 2 (B and C) display SEM images of the Cu-Pt alloy (grown onto an Au electrode) before and after dealloying with hydrogen peroxide, respectively. The untreated alloy exhibits a smooth and soft surface with some embedded cubes (Figure 2B); in contrast, after the chemical dealloying, the surface displays

higher surface area and roughness, with porous tentacle shaped-like structures (Fig. 2C). It should be noted that Cu remains in the interior of the alloy, owing to the significantly higher Cu^{2+} concentration during the alloy deposition.

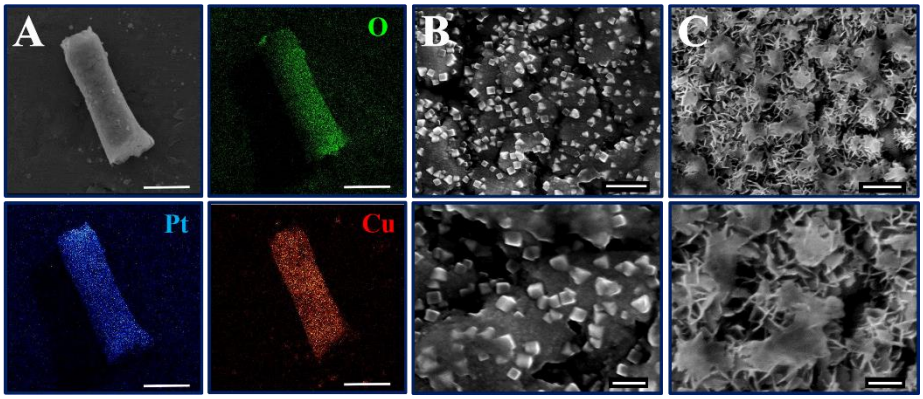

Figure 2. ***A)*** *SEM images of an erGO/Cu-Pt microrocket and corresponding EDX (O, Pt, Cu) images. Scale bar 5 µm.* ***B)*** *SEM images of a Cu-Pt alloy film on an Au bare electrode.* ***C)*** *SEM images of the surface of B after the complete reaction with 1% of H_2O_2. Scale bars (B, C), 500 nm (top), and 200 nm (bottom).*

To better understand the mechanism and factors responsible for the "built-in" programmed delayed catalytic ignition and propulsion of the microrockets, we investigated the effect of different chemicals upon the blastoff capacity. The ability to control the ignition of the microrockets was examined by measuring the delay in the motor launching time under different conditions. For example, Figure 3A illustrates clearly such control of the delayed motor actuation using a time-lapse images-matrix of the motion of microrockets at different times and fuel concentrations. These images illustrate different delay times, ranging from an immediate motor activation using a high fuel concentration (10% H_2O_2) to a ~25 minutes delayed activation using a low fuel concentration of 0.1% H_2O_2.

The latter reflects the slow dealloying process and hence the delayed Pt exposure.

Once activated, the microrockets display a gradual speed acceleration over time, as illustrated in Figure 3B. These data show an increasing motor speed with longer times and higher fuel concentration, with no apparent change after 30 min. For example, using 10% peroxide fuel, the speed ranges from 686 μm/s (at 0 min) to 987, 1195 and 1545 μm/s at 5, 15 and 30 minutes, respectively, after the initial contact with the H_2O_2 fuel. Such accelerated movement at a given fuel concentration has not been reported previously. This unique behavior reflects the continuous dealloying of Cu by the peroxide fuel, and the corresponding increasing exposure of the Pt catalyst. The remarkable speeds of over 1500 μm/s (~100 body lengths/sec) reflects the enhanced catalytic activity associated with the highly porous alloy surface (shown in Figure 2C).

The influence diverse chemical environments upon the delayed propulsion where also evaluated. The microrockets displayed delayed propulsion times of 0, 1, 7, 10, and 25 min after immersion in solutions containing different H_2O_2 concentrations of 10, 5, 2, 1, and 0.1%, respectively (Figure 4A). As expected, the higher the peroxide concentration, the faster is the Cu corrosion and the earlier the motors are activated. These changes in the delay time can be explained by the reaction between metallic Cu and H_2O_2 (eqs. 1, 2 and 3). Hydrogen peroxide promotes the preferential galvanic corrosion of Cu in the alloy, instead of the Pt as is nobler metal nature compared to that of Cu.[46] Once the galvanic corrosion occurs, and the Cu^+ reacts with OH^- product of the H_2O_2 reduction, a thin passivation layer of Cu_2O and to a lesser extend $Cu(OH)_2$, is formed on the alloy surface, slowing down the corrosion reaction (see extended discussion the supporting information).

$$Cu \rightarrow Cu^{+} + e^{-} \qquad E° = -0.521\ V \qquad (1)$$

$$H_2O_2 \leftrightarrows H^{+} + HO_2^{-} \qquad (2)$$

$$HO_2^{-} + H_2O + 2e^{-} \rightarrow 3OH^{-} \qquad E° = +0.87\ V \qquad (3)$$

Increasing the H_2O_2 concentration enhances the galvanic corrosion, facilitating partial dissolution of the oxide layer and Cu corrosion due to OH^{-} formation (analogous to the behavior observed at high pH; eqs. 5 and 6). This leads to further exposure of the catalytically active Pt surface to the peroxide fuel, and thus to the oxygen-bubble generation, tail and thrust responsible for the microrocket propulsion.[45] Additional support for the H_2O_2-based Cu dealloying process is obtained from cyclic voltammograms (CVs) for 1% of H_2O_2 using a GO/Cu-Pt alloy film (over an Au bare electrodes) and 0, 5, and 15 min of Cu dealloy times (Fig. 4E). These data illustrate increasing CV H_2O_2 current signals with longer times, reflecting the larger exposed Pt surface area associated with the continuous Cu dissolution (green and orange lines), compared to the initial response when the H_2O_2 is added (purple line). Such increased surface area is in agreement with the SEM images of Fig. 2C. No current is observed in a control experiment without H_2O_2 (black dotted line), illustrating no current signal. Overall, the CV data support the crucial role of hydrogen peroxide in the time-dependent galvanic and pitting corrosion of the alloy.

The pH effect was further examined to assess its role on the motor activation over the 2-12 pH range (using 1% of H_2O_2). Distinct pH effects are illustrated in Figure 4B. At basic conditions (pH=9.5 and pH=12), the microrocket ignition is nearly instantaneous, due to the enhanced Cu corrosion by an excess of OH^{-}. The resulting passivation layer (Cu_2O) is permeable and the $Cu(OH)_2$ layer is soluble in basic media, avoiding further precipitation of copper oxide. Furthermore,

galvanic and pitting corrosion occur simultaneously, accelerating the Cu corrosion (eqs. 4 and 5).[47]

$$2Cu + 2OH^- \rightarrow Cu_2O + H_2O + 2e^- \qquad E° = +0.36\ V \qquad (4)$$

$$Cu + 2OH^- \rightarrow Cu(OH)_2 + 2e^- \qquad E° = +0.222\ V \qquad (5)$$

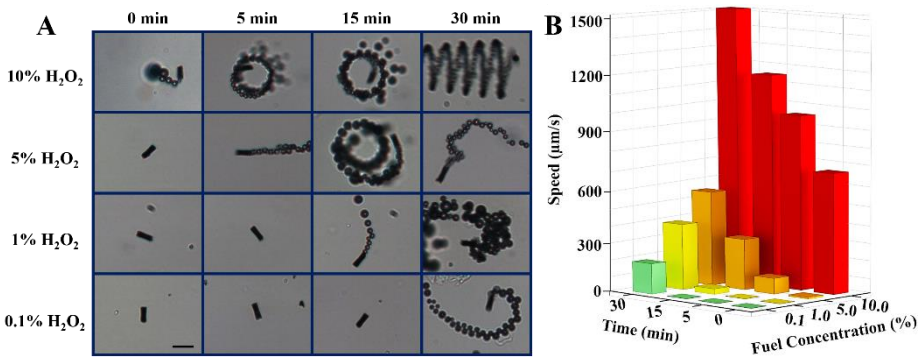

Figure 3. *Influence of the dealloying parameters upon the delayed ignition of the microrocket.* ***A)*** *Actual time-lapse images of erGO/Cu-Pt microrockets at different times (from 0 to 30 min) and varied H_2O_2 concentrations (from 0.1 to 10%), along with 1% of NaCh. Scale bar, 20 μm.* ***B)*** *Dependence of the microrocket speed upon dealloying parameters: fuel concentration and time.*

In contrast, under strong acidic conditions, e.g., pH=2, the microrocket displayed a longer delayed ignition, reflecting the slower Cu corrosion (due to non-oxidant nature of HCl). Furthermore, the acidic environment has an effect on the H_2O_2 fuel, due to a preferential reaction between H_2O_2 and HCl (eqs. 6 and 7).[48] Some H_2O_2 may react with Cu, resulting in a slower galvanic corrosion and a long delay time.

$$H_2O_2 + 2HCl \rightarrow Cl_2 + 2H_2O \qquad (6)$$

$$H_2O_2 + Cl_2 \rightarrow O_2 + 2HCl \qquad (7)$$

Using mildly acidic condition, e.g. pH=4.5, more H_2O_2 is available to react with Cu (instead interacting with the acid) accelerating the Cu

corrosion and decreasing the ignition delay time (to compare redox potential of eqs 3 and 8; see further discussion in supporting information).

$$H_2O_2 + 2H^+ + 2e^- \rightarrow 2H_2O \qquad E° = +1.776\ V \qquad (8)$$

The ionic strength, particularly the NaCl concentration, has a profound effect on the delayed microrocket movement. This was examined using different NaCl concentrations along with 1% H_2O_2 level (Figure 4C). High ionic strength concentration (10% NaCl) results in shorter ignition delayed times, e.g. ~1.5 min at 10% NaCl (w/v); even at low ionic strength of 0.1% NaCl, the ignition occurs at ~4.5 min. In contrast, a significantly longer delayed propulsion of ~10 min is observed without NaCl. This behavior reflects the Cl^- inhibition of the Cu^{n+}-OH^- reaction that diminishes the formation of a passivation layer over the nearest surface of the alloy. The Cl^- ion preferentially reacts with Cu^+, producing $CuCl_x^{n-}$ (most common complex is $CuCl_2^{2-}$; see supporting information) and Cu_2O can be produced as hydrolysis byproduct (eqs. 9 and 10). Moreover, Cl^- exhibits large penetration power, allowing the formation of $CuCl_x^{n-}$ instead of Cu_2O and lesser extent $Cu(OH)_2$, leading to pitting corrosion.[49]

$$Cu^+ + 2Cl^- \rightarrow CuCl_2^- \qquad (9)$$

$$CuCl_2^- + 2OH^- \rightarrow Cu_2O + H_2O + 2Cl^- \qquad (10)$$

The delayed activation time can also be tailored by using different electrochemical deposition currents. For example, Fig. 4D illustrates that while low deposition currents (below) −2 mA result in a 10 min delayed propulsion, a significantly larger (~28 min) delay is observed using −8 mA galvanostatic current. Apparently, higher deposition currents increase the copper level in the alloy, leading to delayed exposure of the

platinum surface. Further discussion is given in the Supporting Information. Note again the instantaneous propulsion observed in the control experiment without Cu (see Supporting Information). Similar effect and delays are expected upon increasing the Cu/Pt concentration ratio in the plating solution. The delayed activation of micromotor was tested in real-life environments, such as sea water and gastric acid, with delay times of 8 ± 1.9 min and 41.8 ± 9.3 min, respectively. Such times are in agreement with early studies of the ionic and pH effects, and further illustrate their applicability to practical environmental and biomedical applications.

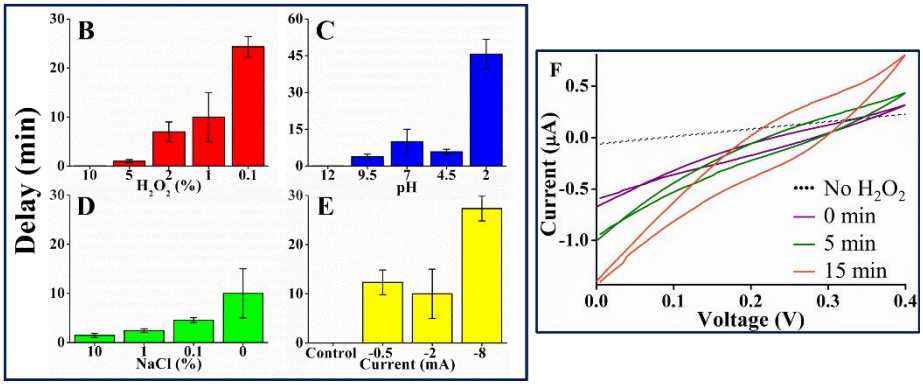

Figure 4. *Influence of the H_2O_2 fuel concentrations* ***(A)****, solution pH* ***(B)****, NaCl concentration* ***(C)****, and the alloy deposition galvanostatic current* ***(D)*** *on the delayed propulsion time. The latter includes Control without Cu (using current of −2 mA). H_2O_2 concentration (C-E), 1%. (n=3).* ***E)*** *Cyclic Voltammograms for 1% H_2O_2 recorded using Au electrode coated with a GO/Cu-Pt film at 0, 5, and 15 min Cu dealloy times; scan rate, 25 mV s^{-1}.*

Conclusions

In conclusion, we have developed a "smart" built-in delayed ignition of catalytic microrockets based on a chemical dealloying of their inner layer in the presence of fuel media. The delayed actuation of the micromotor propulsion depends solely on the intrinsic material properties of the microengine and its surrounding solution, and does not require any external stimuli. The specific motor activation time reflects the galvanic and pitting corrosion phenomena produced by the chemical environment in which the microrocket is submerged. Such delayed activation can be tailored by using different environmental chemical factors (fuel, pH and ionic strength) or by the material properties of the microengine itself (alloy composition). We also demonstrated for the first time the ability to change the motor speed at a given fuel concentration and attributed this unique phenomenon to changes in the catalyst (Pt) exposure. The delayed motion observed using real-life environments (sea water and gastric acid) and the ability to respond to changes in the surrounding environment suggest variety of potential practical applications. For example, the delayed activation could serve to measure directly water corrosion, or help position and activate the motors within the stomach or Gastrointestinal tract at tailored times towards enhanced cargo retention at specific sites. The concept of delayed movement can be expanded to other types of chemically-powered motors, based on other reactive metals (e.g., Ag, Zn). Future work will be aim at developing diverse built-in ignition switches that can be activated autonomously under selective conditions for such specific applications. Such autonomous delayed ignition of the micromotor propulsion represents a new approach of activating the motion of microengine without external perturbations through control of its material features. Creating a smart material microrocket, with "built-in"

blastoff capability and tailored-made speed regulation, would thus allow the development of new self-governing microengines, responding to changes in their surrounding environment. Such ability to tune the propulsion behavior of micromotor thus offers great promise for developing autonomous nano/microscale vehicles.

Acknowledgements

This project received support from the Defense Threat Reduction Agency-Joint Science and Technology Office for Chemical and Biological Defense (Grant No. HDTRA1-14-1-0064). A.J. and F.S. acknowledge fellowships from the Spanish Ministry of Economy and Competitiveness (EEBB-I-16-11442) and from UC MEXUS-CONACYT, respectively. This work was performed in part at the San Diego Nanotechnology Infrastructure (SDNI) supported by the National Science Foundation (Grant ECCS-1542148).

Notes and references

1. J. Wang, Nanomachines: Fundamentals and Applications, Wiley-VCH, Weinheim, Germany, 2013, ISBN 978-3-527-33120-8.

2. H. Wang and M. Pumera, *Chem. Rev*., 2015, **115**, 8704– 8735.

3. W. Wang, W. Duan, S. Ahmed, T. E. Mallouk and A. Sen, *Nano Today*, 2013, **8**, 531– 554.

4. K. Kim, J, Guo, X. Xu and D.L. Fan, *Small*, 2015, **11**, 4037– 4057.

5. X. Lin, Z. Wu, Y. Wu, M. Xuan and Q. He, *Adv. Mater.,* 2015, **28**, 1060–1072.

6. S. Sanchez, L. Soler and J. Katuri, *Angew. Chem. Int. Ed.,* 2015, **54**, 1414–1444.

7. M. Guix, C. C. Mayorga-Martinez and A. Merkoçi, *Chem. Rev.*, 2014, **114**, 6285–6322.

8. G. Ozin, A. I. Manners, S. Fournier-Bidoz, and A. Arsenault, *Adv. Mater.,* 2005, ***17*****,** 3011−3018.

9. M. Moreno-Guzman, A. Jodra, M. A. López and A. Escarpa, *Anal. Chem.,* 2015, **87**, 12380–12386.

10. D. Walker, B. T. Käsdorf, H. H. Jeong, O. Lieleg and P. Fischer, *Sci. Adv.,* 2015, ***1***, e1500501.

11. F. Soto, A. Martin, S. Ibsen, M. Vaidyanathan, V. Garcia-Gradilla, Y, Levin, A. Escarpa, S.C. Esener and J. Wang, *ACS Nano,* 2016, **10**, 1522–1528.

12. S. Fusco, H. W. Huang, K. E. Peyer, C. Peters, M. Häberli, A. Ulbers, A. Spyrogianni, E. Pellicer, J. Sort, S.E. Pratsinis and B. J. Nelson, *ACS App. Mater. Interfaces,* 2015, **7**, 6803–6811.

13. J. Li, I. Rozen and J. Wang, *ACS Nano,* 2016, **10**, 5619–5634.

14. A. A. Solovev, Y. F. Mei, E. B. Urena, G. S. Huang and O. G. Schmidt. *Small,* 2009, ***5***, 1688–1692.

15. B. Esteban-Fernández de Ávila, M. A. Lopez-Ramirez, D. F. Báez, A. Jodra, V. V. Singh, K. Kaufmann and J. Wang, *ACS Sens.,* 2016, **1**, 217–221.

16. J. Orozco, A. Cortes, G. Cheng, S. Sattayasamitsathit, W. Gao, X. Feng, Y. Shen and J. Wang, *J. Am. Chem. Soc.,* 2013, **135**, 5336–5339.

17. E. Morales-Narváez, M. Guix, M. Medina-Sánchez, C. C. Mayorga-Martinez and A. Merkoçi, *Small,* 2014, **10**, 2542–2548.

18. K. Manesh and J. Wang, *Small,* 2010, **6**, 338–345.

19. R. P. Feynman, *Eng. Sci.,* 1960*,* **23**, 22–36.

20. E. M. Purcell, *Am. J. Phys.,* 1977*,* **45**, 3–11.

21. W. Gao, A. Uygun and J. Wang, *J. Am. Chem. Soc*., 2012, **134**, 897–900.

22. T. C. Lee, M. Alarcón-Correa, C. Miksch, K. Hahn, J. G. Gibbs and P. Fischer. *Nano Lett*., 2014, **14***,* 2407–2412.

23. H. Zhang, W. Duan, L. Liu and A. Sen, *J. Am. Chem. Soc.,* 2013, **135**, 15734–15737.

24. L. K. E. A. Abdelmohsen, M. Nijemeisland, G. M. Pawar, G. A. Janssen, R. J. Nolte, J. C. M. Van Hest and D. A. Wilson, *ACS Nano*, 2016, **10**, 2652–2660.

25. H. Wang, G. Zhao and M. Pumera, *J. Am. Chem. Soc.,* 2014, **136**, 2719–2722.

26. M. Safdar, O. M. Wani and J. Jänis, *ACS Appl. Mater. Interfaces,* 2015, **7**, 25580–25585.

27. X. Ma, K. Hahn, and S. Sánchez, *J. Am. Chem. Soc.,* 2015, **137**, 4976–4979.

28. A. A. Solovev, E. J. Smith, C. C. Bof' Bufon, S. Sanchez and O. G. Schmidt, *Angew. Chem., Int. Ed.,* 2011, **50**, 10875– 10878.

29. S, Balasubramanian, D. Kagan, K. M. Manesh, P. Calvo-Marzal, G. Flechsig and J. Wang, *Small,* 2009, **5**, 1569–1574.

30. Z. Wu, X. Lin, Y. Wu, T. Si, H. Sun and Q. He, *ACS Nano,* 2014, **8**, 6097–6105.

31. S. Sánchez, A. N. Ananth, V. M. Fomin, M. Viehrig and O. G. Schmidt, *J. Am. Chem. Soc.,* 2011, **133**, 14860–14863.

32. D. Kagan, P. Calvo-Marzal, S. Balasubramanian, S. Sattayasamitsathit, K. M. Manesh, G. Flechsin and J. Wang, *J. Am. Chem. Soc.,* 2009, **131**,12082–12083.

33. T. Xu, F. Soto, W. Gao, V. Garcia-Gradilla, J. Li, X. Zhang and J. Wang, *J. Am. Chem. Soc.* 2014, **136**, 8552–8555.

34. R. Dong, Q. Zhang, W. Gao, A. Pei and B. Ren, *ACS Nano,* 2016, **10**, 839–844.

35. J. G. S. Moo, S. Presolski and M. Pumera, *ACS Nano,* 2016, **10**, 3543–3552.

36. L. Liu. E. Pippel, R. Scholz and U. Gösele, *Nano Lett.,* 2009, **9**, 4352–4358.

37. T. Feng, K. S. Siow, E. K. Teo, K. L. Tan and A. K. Hsieh, *Corrosion,* 1997, **53**, 389–398.

38. A. Sarkar and A. Manthiram, *J. Phys. Chem. C,* 2010**, 114***,* 4725.

39. R. Liu and A. Sen, *J. Am. Chem. Soc.,* 2011, **133**, 20064–20067.

40. G, Zhao and M. Pumera, *RSC Adv.,* 2013, **3**, 3963–3966.

41. W. Gao, S. Sattayasamitsathit, J. Orozco and J. Wang, *J. Am. Chem. Soc.,* 2011, **133**, 11862–11864.

42. A. Martin, B. Jurado-Sánchez, A. Escarpa and J. Wang, *Small,* 2015*,* **11**, 3568–3574.

43. G. Zhao, B. Khezri, S. Sánchez, O. G. Schmidt, R. D. Webster and M. Pumera, *Chem. Commun.,* 2013, **49**, 9125–9127.

44. J. G. S. Moo, H. Wang and M. Pumera, *Chem. Eur. J.,* 2016, ***22*****,** 355–360.

45. L, Li, J. Wang, T. Li, W. Song and G. A. Zhang, *J. Appl. Phys.,* 2015, **117**, 104308.

46. A. Kloke, C. Köhler, R. Gerwig, R. Zengerle and S. Kerzenmacher, *Adv. Mater.,* 2012, **24**, 2916–2921.

47. Y. Feng, K. S. Siow, W. K. Teo, K. L. Tan and A. K. Hsieh, *Corrosion*, 1997, ***53***, 389–398.

48. R. S. Livingston and W. C. J. Bray, *J. Am. Chem. Soc.,* 1925, **47**, 2069–2082.

49. G. Kear, B. D. Barker and F. C. Walsh, *Corrosion Science*, 2004, **46**, 109–135.

III.3. Non-catalytic motors

As it is commented before, different applications were explored in this Thesis. In this way, another application was developed to elaborate novel methods. The majority of applications are based on catalytic motors, which need a metal to produce fuel decomposition and to generate the motion.

Nevertheless, other thrust methods have been studied (e.g., magnetic or acoustic motors), providing new possibilities. In this way, a pipette tip is filled with a mixture solution of SDS and HRP following the strategy described in *section Self-diffusiophoresis propulsion*. SDS is utilized to cause the movement and HRP is the enzyme to react with the analyte (hydrogen peroxide) and subsequently, giving H_2O_2 detection. In this application, the pipette tip is introduced on the sample with H_2O_2, swimming along the sample and releasing the fresh enzyme. Free enzyme reacts with H_2O_2 and co-substrate (TMB), producing optical and electrochemical determination. The fluid convention owing to the release of mixture solution and move of the millimotor increases the reaction kinetics, enhancing the performance for both kinds of detections. It is assayed in real significant agricultural and clinical samples.

Next section presents the paper which describes this application.

Analytical Chemistry *DOI:10.1021/acs.analchem.5b03928*

Self-propelled enzyme-based motors for smart mobile electrochemical and optical biosensing

María Moreno-Guzman‡, Adrián Jodra‡, Miguel-Ángel López and Alberto Escarpa*

Department of Analytical Chemistry, University of Alcalá, Alcalá de Henares, Madrid E-28871, Spain.

ABSTRACT: A millimeter-sized tubular motor for mobile biosensing of H_2O_2 in environmental and relevant clinical samples is reported. The concept relies on the self-propelled motion by the Marangoni effect, where the asymmetric release of SDS surfactant induces fluid convection and rapid dispersion of Horse-radish-peroxidase (HRP) enzyme into the sample solution. This efficient movement together with the continuous release of fresh enzyme leads to a greatly accelerated enzymatic reaction processes without the need of external stirring or chemical and physical attachment of the enzyme as in common classical biosensing approaches. In this strategy, the use of a single millimeter-sized tubular motor during 120 s allows the reliable and accurate quantification of hydrogen peroxide in a set of different matrices such as tap and mineral waters, urine, plasma and tumor cells cultures treated with antineoplasic Cisplatin without any previous sample preparation. Furthermore, detection can be performed electrochemically, optically and visual detection, which makes this approach a clear candidate as a point-of-care analytical tool.

Introduction

Self-propelled motion of miniaturized objects through fluid environments constitutes nowadays an exciting field.[1-5] Such artificial nano-, micro- and millimeter scale motors utilize different propulsion mechanisms for its autonomous motion based on different energy

sources such as external energy fields, through consumption of "fuels" or via physicochemical processes. Included into the physicochemical processes, the so-called Marangoni effect, describes the movement of the object based on surface tension gradient. Objects move from lower surface tension to higher surface tension areas in an attempt by the system to attain the desirable lowest-free-energy state.[6] The surface tension gradient can be generated by asymmetric release of the chemical from the object or by modification of the surface the object moves on.[7] Marangoni flow is responsible for interfacial turbulence phenomena observed between two fluids, without equilibrium of heat rates, mass transfer and diffusion accompanied by a chemical reaction.[8,9]

Development of this kind of motors that move independently from external energy sources represents a very attractive alternative. Some relevant examples have been recently presented by Pumera's group such as an energy-independent millimeter-scale polymer capsule propelled by the self-release of an organic solvent that moves on a wide variety of liquid surfaces.[10] More recently, the same group reported surfactant-loaded polymer motors for the clean-up of oil droplets as potential application in environmental remediation.[11,12] Besides, Wang et al. have reported a self-propelled tubular motor involving simultaneous release of SDS surfactant and an enzyme remediation agent for efficient biocatalytic degradation of chemical pollutants.[13,14]

However, the exploration of these motors with biosensing purposes in real samples of high significance has not been explored yet. The present study shows both proof-of-concept and real applications with biosensing purposes of millimeter-sized tubular mobile motor, self-propelled by the surface induced Marangoni effect involving simultaneous release of SDS surfactant and HRP (Horse-radish-

peroxidase) enzyme. The enzyme catalytic activity allows H_2O_2 determination using electrochemical, optical and even visual detection in matrices of high significance in different analytical fields.

The movement generated by the propulsion of the motor offers effective fluid convection in the contaminated sample to disperse rapidly the enzyme without external stirring and to enhance the enzyme-substrate interactions. This efficient movement together with continuous releasing of the fresh enzyme, leads to a greatly accelerated enzymatic reaction process without the need to have a homogeneous sample or chemical and physical attachment of the enzyme as in common classical biosensing approaches. The motor biosensing capabilities have been tested in environmental (tap and mineral waters) and clinical samples of high significance such as urine and plasma as well as tumor cells cultures after antineoplasic (Cisplatin) treatment.

Indeed, detection of H_2O_2 presents a high concern in several fields such as food industrial processes, clinical practice, pharmaceutical and environmental analysis.[15,16] Different chemical reactions occur during water radiolysis, and various types of free radicals are produced which may then act as either oxidizing or reducing agents. The free hydroxyl radical (•OH) is one of the most important products of water radiolysis, whose combination produces hydrogen peroxide.[17] In different metabolic disorders or those processes where the organism has suffered cell death by free radicals, small amount of H_2O_2 can be found in urine and plasma samples. Recent studies have indicated that H_2O_2 produced by mammalian cells, plays a key mediating role in diverse physiological responses such as cell proliferation, differentiation and migration. Additionally, a determined H_2O_2 concentration in the body is considered as a parameter that represents the different states of cancer, Parkinson's

and Alzheimer's diseases.[18,19] Other significant matrices where H_2O_2 can be found are those corresponding to cancer lines[20] cultures treated with antineoplasic agents, which produce the cell death by free radicals.

There are several methods to measure H_2O_2, such as spectrophotometry,[21] fluorimetry[22] and electrochemistry.[23] The electrochemical detection is one of the promising approaches to achieve accurate, specific, economic and rapid H_2O_2 monitoring.[24] However, the direct reduction of hydrogen peroxide at a bare electrode is not suitable for analytical applications due to slow electrode kinetics and high potentials required for redox reactions.[25] To minimize or eliminate these limitations, various electrochemical sensors have been developed in order to overcome the problem.[26,27]

In the present work, the reported mobile biosensor for H_2O_2 determination, based on millimeter-sized motors to rapidly disperse the free enzyme in the sample, represents an attractive approach for qualitative/screening bio-detection and quantitative determination of hydrogen peroxide in environmental and clinical valuable samples.

Experimental

Reagents and solutions

Horseradish peroxidase (HRP) type VI-A, hydrogen peroxide (30% w/v solution) and 3,3´,5,5´-tetramethylbenzidine (TMB) were purchased from Sigma-Aldrich (Madrid, Spain). Sodium dodecyl sulfate (SDS) was acquired from Merck (Darmstadt, Germany). Dimethyl sulfoxide (DMSO) was purchased from Scharlau (Barcelona, Spain) and sulfuric acid was purchased from Panreac (Barcelona, Spain). All other reagents were of the highest available grade. Enzyme solution was prepared dissolving 1 mg of enzyme in 128 µL of water Milli-Q. SDS

solution was prepared in water Milli-Q. Hydrogen peroxide solution was prepared diluting with phosphate buffer saline (PBS 0.05 M, pH 7.4). TMB was suitable dissolved in DMSO. Enzymatic reaction was suitably stopped by using a 0.5 M sulfuric acid solution.

Samples

Tap water was obtained from the local water supply system of Alcalá de Henares and mineral water ("Lanjaron") was acquired from a local retail store (Madrid, Spain).

Urine samples were collected from volunteers and plasma samples were kindly provided by Dr. Goya Clinical Analysis Laboratory of Alcalá de Henares.

Cell cultures consisted on tumoral Kidney tubular cells in Dulbecco's Modified Eagle Medium: Nutrient Mixture F-12 (DMEM/F-12). These cells were treated with Cisplatin (25 μM) to produce their death. The samples were kindly provided by the research group of Professor Javier de Lucio at the Faculty of Medicine (University of Alcala).

Apparatus and electrodes

All electrochemical measurements were carried out using Autolab PGSTAT 12 potentiostat from Metrohm (Utrecht, The Netherlands). The electrochemical software was the general-purpose electrochemical system (GPES) (EcoChemie B.V.). Screen-printed carbon electrodes (4 mm diameter) were purchased from DropSens (Oviedo, Spain) and used as working electrodes. These electrodes include a silver pseudo-reference electrode and a carbon counter electrode. The optical measurements were performed with UV-Visible double beam

spectrophotometer Lambda 35 from Perkin Elmer (Madrid, Spain) with matched cells Eppendorf UVette® from Eppendorf (Madrid, Spain).

All experiments were performed at room temperature.

Preparation of SDS/HRP mobile biosensor

Pipette tips were suitably cut to the thinner end zone to obtain small pieces of length of 7 mm and a capacity of 2.25 μL. The tips were filled with a mixture of the HRP and SDS, and then the widest hole was carefully sealed with wax.

Petri dishes of 5.5 cm in diameter were employed for the assays as containers. They contained 5 mL of Milli-Q water and 0.08 M the TMB, and different levels concentration of hydrogen peroxide.

50 μL of the sample solution containing the oxidized TMB were quantified electrochemically by chronoamperometry at −0.2 V for 300 s, and 100 μL were optically measured by UV-Vis spectrophotometry at 450 nm wavelength.

Results and Discussion

Strategy and development of the self-propelled enzyme-based motor

Figure 1 illustrates the concept of self-propelled motor where both HRP enzyme and SDS surfactant are release in solution from inside the motor. The cone-shaped of pipette tips containing SDS and HRP, are propelled by the Marangoni effect, due to the release of SDS surfactant by the sharp end. This effect exerts a force and torque on the motors, which actions are responsible for their movement up to a balance in surface tension is reached. Besides, the simultaneous release of HRP into the sample produces the oxidation of TMB_{red}, which is proportional to the presence of hydrogen peroxide as analyte. TMB_{ox} can be measured

even by chronoamperometry through its reduction at –0.2 V in a carbon screen-printed electrode (CSPE) or spectrophotometrically by the produced blue color absorbance at 450 nm.

The self-propelled movement of the biosensor into the solution avoids external stirring and allows gradual release of fresh enzyme which ensures a sustained biocatalytic activity and enhancement of reaction efficiency compared with classical addition of enzyme in solution. Furthermore, this performance avoids chemical of physical attachment of the enzyme.

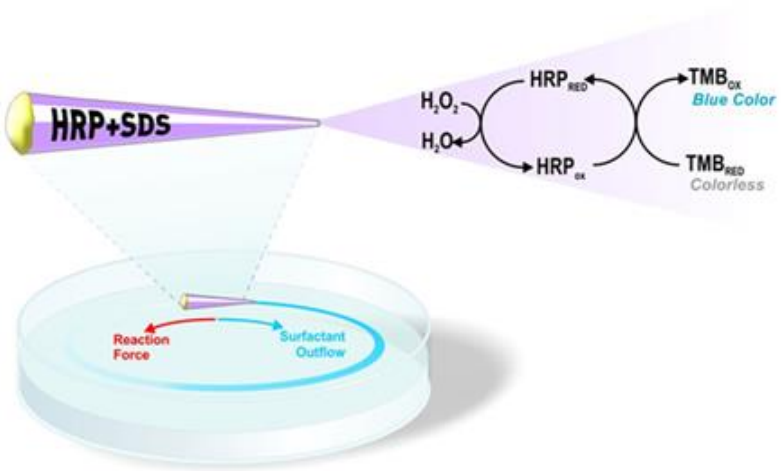

Figure 1. Scheme of self-propelled enzyme-based motor for hydrogen peroxide detection.

Different parameters such as amount of SDS into the motor and number of motors simultaneously used into the sample solution were firstly optimized.

The SDS/water ratio into the motor was carefully evaluated in order to obtain a homogeneous and efficient movement within the sample solution. A ratio SDS/water of 1:3 (v/v) produced the best

performance in terms of maximum velocity as well as the uniformity of the motor movement for more than 120 seconds (data not shown).

Considering the number of motors, up to two motors can simultaneously swim onto the solution without a loss of performance. However, when more than two motors are used, their movements are more irregular and slow, and they stop after 60 s due to the collisions occurred between them (see Video S-1).

Detection was accomplished by electrochemical and optical detection due to TMB redox activity and its blue color in the oxidized form. To optimize the concentration of TMB in the mixture, a series of experiments where performed with motors containing a fixed enzyme concentration (1.2 mg mL^{-1}), which were allowed to swim in a battery of increasing TMB concentrations, keeping a constant amount of 0.1 mM H_2O_2. Figure S-1A shows the largest current signal when a 0.08 M TMB concentration was added.

HRP concentration inside the motor was also titrated using a fixed concentration of both TMB (0.08 M) and H_2O_2 (0.1 mM). In Figure S-1B it can be observed how the highest current was obtained for motors containing 3.05 mg mL^{-1} of HRP enzyme.

The enzymatic reaction time was also assayed. As expected, the amount of enzymatically TMB_{ox} increased with time and 120 seconds was selected as an optimum reaction time (Figure S-2).

On the other hand, the capability of diminishing the total reaction time by increasing the number of motors that are simultaneously swimming, without affecting the detection capabilities of the sensor, was carefully studied. Figure 2 shows the electrochemical signals for each H_2O_2 concentration when 1, 2 or 3 motors are simultaneously swimming

during a period of time of 60 s (see detailed dashed lines in 2B) and when 1 or 2 motors are simultaneously used during a period of time of 120 s (see detailed dotted lines in 2B). It can be observed that even for 3 motors simultaneously swimming in the sample solution during 60 s, the released amount of HRP is not enough for detection of low amount of H_2O_2 (see dashed lines in 2B). This effect can be explained taking into account that a higher number of motors swimming simultaneously make their velocity slower due to a faster achievement of balance in the surface tension in/out the motor. These decrease speed reduce the total amount of enzyme released by each motor. However, when the enzyme-based motors swim for a period of 120 s, it was able to determine low concentrations of H_2O_2. Interestingly, no differences were observed by using one or two motors during 120 s, even for low H_2O_2 concentrations, indicating that the enzymatic reaction is complete under these conditions (see dotted lines in 2B). This fact constituted a valuable result since only one motor was able to perform the analysis, simplifying the overall analytical process (see video S-1). Furthermore, the analysis can be accomplished easily in parallel, performing different samples simultaneously into a multiplex format (see video S-2).

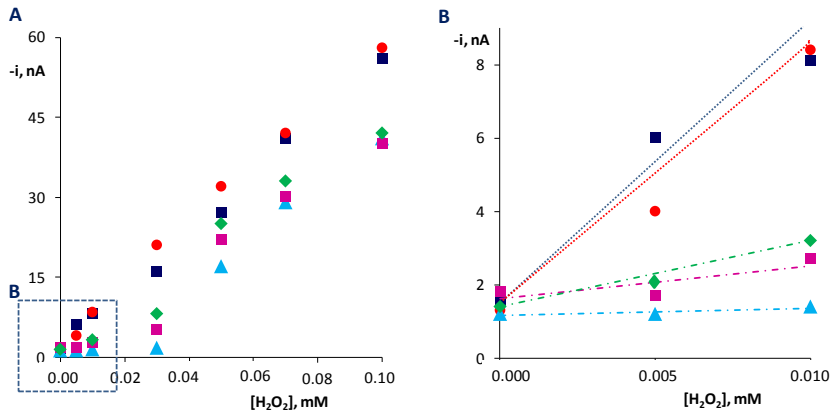

Figure 2. Capability of the self-propelled enzyme-based motors for hydrogen peroxide detection. For 60 s: 1 motor (▲), 2 motors (■) and 3 motors (◆). For 120 s: 1 motor (●) and 2 motors (■). B represents the inset of figure A.

Different control assays were also carefully performed to assure the biocatalytic activity of the motor. Firstly, negligible signals were obtained when hydrogen peroxide was not present in the sample. Secondly, when the same amount of enzyme contained into the motor was directly added to the solution, only a 26% of the signal provided by the motor was obtained.

Analytical characteristics of the enzyme-based motor

Under the optimized working conditions listed in Table 1, hydrogen peroxide external calibration protocol using chronoamperometry (E=−0.20V vs. Ag, t=300s) was performed (Figure 3). The mobile biosensor exhibited an excellent linearity (r=0.998) in the concentration range examined (0.005–0.1 mM), with a good analytical sensitivity (562.49 nA/mM) and very suitable limit of detection (LOD) (1.9 μM). LOD was calculated according to the 3sb/m criteria, where m is the slope in the calibration plot, and sb was estimated as the standard deviation of the amperometric signals measured at the lowest hydrogen peroxide concentration of the calibration graph (0.005 mM, n=10). Inter-motor reproducibility was also evaluated for two H_2O_2 concentration levels (0.005 and 0.1 mM) yielding values of RSDs < 7% (n=8 enzyme-based motor each). These results indicated an excellent reproducibility during the fabrication of the mobile sensor.

Table 1. Optimization of self-propelled enzyme-based motor.

Variable	Tested range	Selected value
Motors number	1 - 3	1
[HRP], mg/mL	0 - 4.27	3.02
[TMB], M	0.04 - 0.12	0.08
Reaction time, s	0 - 120	120

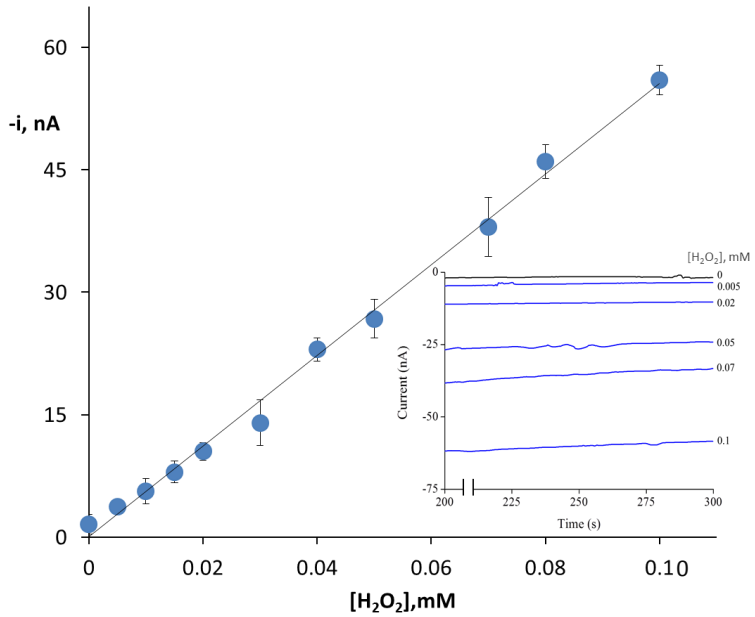

Figure 3. Calibration curve for hydrogen peroxide determination using chronoamperometry on CSPE (E=−0.20V vs. Ag, t=300s). Inset: Chronoamperograms obtained for selected hydrogen peroxide concentrations.

One important analytical feature of the proposed enzyme-based motor is that hydrogen peroxide detection can be also carried out using UV-Vis spectrophotometry. It constitutes an additional merit of this approach since the proposed mobile biosensor has the capability to operate with both electrochemical and optical detection. Figure 4A

shows the optical calibration curve for increased concentrations of H_2O_2. A very good linearity (r=0.9995) for the concentration range examined (0.005–0.1 mM), a good analytical sensitivity (1.9749 mM^{-1}) and an adequate LOD of 2.4 µM were also obtained in these calibration studies.

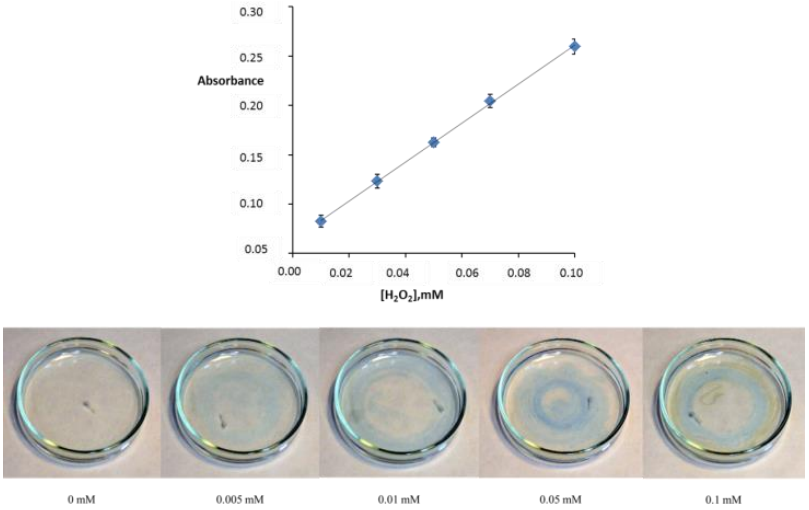

Figure 4. (A) Calibration curve for hydrogen peroxide determination using UV-Vis spectrophotometry (450 nm). (B) Photographs obtained for each hydrogen peroxide concentration.

Also, and thanks to the color change of TMB after the enzymatic reaction with H_2O_2 (colorless of the TMB_{red} / blue color of the TMB_{ox}), the presence of H_2O_2 in the sample can be simply detected by visual detection becoming an excellent screening tool. In Figure 4B, a blue trail can be observed after the movement of the enzyme-based motors with a direct dependence of the color intensity versus H_2O_2 concentration.

In addition, the enzyme reaction at the HRP mobile biosensor fitted well into Michaelis-Menten kinetics, demonstrating that the enzyme-based motor is operating as a real biosensor. The x parameter (0.99) was calculated from the corresponding Hill's plot ([log (i_{max}/i)−1)) vs the logarithm of hydrogen peroxide concentration and the Michaelis-Menten

kinetic constant (K_m), 0.89 mM, was calculated from the corresponding Lineweaver-Burk plot.

Determination of hydrogen peroxide in environmental and relevant clinical samples

The capabilities of the developed enzyme-based motor biosensor were further evaluated during the detection and determination of hydrogen peroxide in a set of matrices with high significance, involving environmental samples (mineral and tap waters), clinical (urine, plasma) and antineoplasic treated tumor cells cultures.

Figure 5 illustrates selected results obtained during the detection of H_2O_2 in the matrices assayed. Optical/visual (see photographs, Figure 5 left) and electrochemical detection (see chronoamperometry profiles, Figure 5 right) of H_2O_2 in mineral water (A), tap water (see Figure S-3), urine (B) and plasma (C) are shown for non-spiked and 0.1 mM H_2O_2 spiked samples.

Clear differences were noticed between both. Indeed a blue color (visual detection) as well as an increase in the amperometric reduction currents in the chronoamperograms were clearly noticed in spiked samples in comparison with those found in non-spiked ones (colorless and lower amperometric reduction currents). Plasma samples constitute an exception since they did not exhibit a color change, even though they present the corresponding higher reduction currents. Furthermore, it is worthy to underline that in the controls where no hydrogen peroxide was added (in both sample matrix and ultrapure water) produced negligible signals, indicating the absence of interferences.

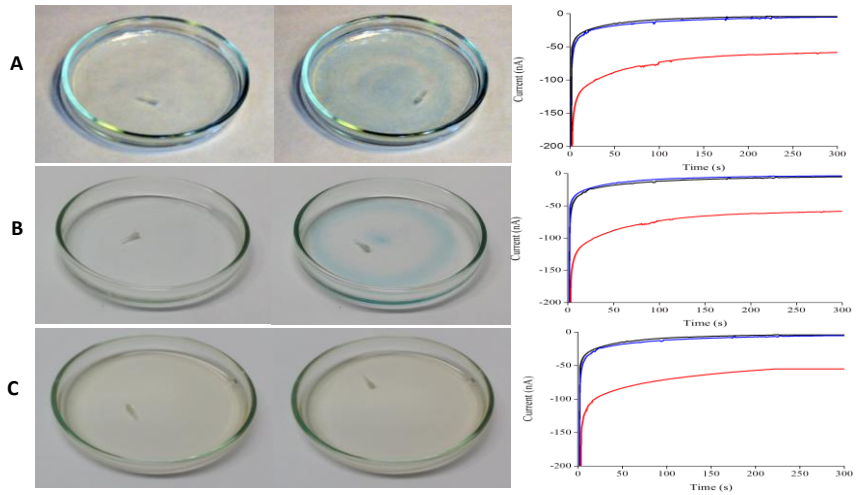

Figure 5. Visual (left) and chronoamperometry (right) detection of H_2O_2 in mineral water (A), urine (B) and plasma (C). Samples spiked with 0.1mM of H_2O_2 (—). Sample (—). Control: ultrapure water (—).

Quantitatively, Table 2 summarizes the sample dilution needed to obtain the efficient swimming of motor biosensors in each complex matrix and the mean recoveries for each sample using both electrochemical an optical detection approaches (see Tables S-1to S-3 for detailed recoveries).

Interestingly, for all the samples analyzed and under these dilution conditions, the use of just one single motor-based enzyme during 120 s allowed the selective and accurate determination of hydrogen peroxide (quantitative recoveries in all cases examined) using both electrochemical and optical approaches with independence of the chemical composition of the sample. In addition, a quick visual screening by change in color of the solution could be noticed in all samples except the plasma giving an additional value to the proposed approach as point-of-care (POC) application. This issue is very interesting for the analysis of non-invasive urine samples, where the measurements of total

hydrogen peroxide from diseases such as produced by *Vibrio Cholera* is extremely important[28] and it is under-exploited.

Another approach highly interesting relies on the determination of H_2O_2 produced in tumor cell cultures after their treatment with the antineoplasic Cisplatin. This treatment produces the cell death by free radicals, where H_2O_2 can subsequently be found. Figure 6 shows a signal change between the untreated cells in comparison with those treated with Cisplatin. Blue colors (visual detection) and an increment in the amperometric reduction currents in the chronoamperograms (electrochemical detection) were clearly noticed in cell cultures treated with Cisplatin. In both cases, untreated and treated cell cultures were spiked with 0.1 mM H_2O_2 generating the corresponding increase in both reduction currents and showing the suitability of the mobile biosensor. Table 3 lists the quantitative H_2O_2 levels found in the raw samples, and the quantitative recoveries obtained revealing a very good accuracy during the H_2O_2 determination in these samples. Overall, these achieved results were excellent since the mobile sensor was able to differentiate between untreated and treated cells, becoming an interesting tool for monitoring the activity of the antineoplasic.

Table 2. Determination of hydrogen peroxide in water and clinical samples using the self-propelled enzyme-based motor.

Analytical feature	Mineral Water	Tap Water	Urine	Plasma
Dilution (v/v)	1/1	1/1	1/10	1/5
Recovery[1] (%)	100 ± 3	101 ± 4	97 ± 4	99 ± 3
Recovery[2] (%)	102 ± 5	100 ± 3	99 ± 6	–
Visual detection	Yes	Yes	Yes	No

[1] Obtained using electrochemical detection. Values given as mean values ± standard deviation (n=3).

[2] Obtained using optical detection. Values given as mean values ± standard deviation (n=3).

Table 3. Determination of hydrogen peroxide in tumor cells cultures treated with Cisplatin using the self-propelled enzyme-based motor.

Sample	H_2O_2, mM[1]	H_2O_2, mM[2]	H_2O_2 Total mM	H_2O_2, mM[3]	Recovery, %
1		0	0.013	0.013±0.001	100
2	0.013	0.05	0.063	0.062±0.001	98±2
3		0.1	0.113	0.112±0.002	99±2

[1] Found in samples, [2] Added in samples, [3] Total found in samples.

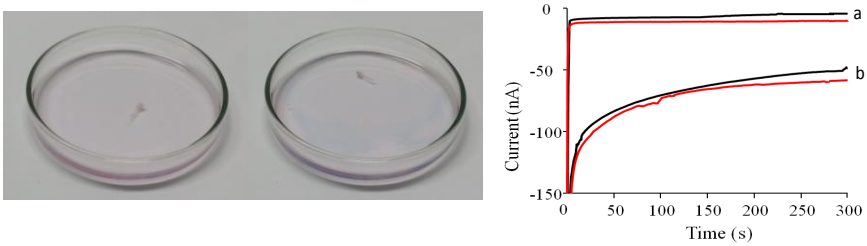

Figure 6. Visual (left) and chronoamperometry (right) detection of H_2O_2 in tumor cells cultures. Samples: non-treated cells with cisplatin (—), cells treated with cisplatin (—); a) non-spiked with H_2O_2, b) spiked with 0.1 mM of H_2O_2.

Conclusions

The self-propelled millimiter-sized enzyme-based motors have demonstrated their suitability for electrochemical and optical biosensing of hydrogen peroxide in different matrices with high significance in environmental and clinical fields.

The motion along the sample to find the analyte, the micromixing activity due to the fluid convection, the preservation of the biocatalytic activity due to its confinement inside the motor, together with the continuous release of fresh enzyme are some of the main advantages of this mobile biosensor strategy. Those features facilitate the adequate

enzyme-substrate interactions and accelerate the enzymatic reaction. Furthermore, the free form of enzyme inside the motor, avoids the physical or chemical attachment of the enzyme, which greatly simplifies the fabrication process of the biosensor. The mobile biosensor presents additional operational advantages such as simplicity, disposability, portability, low cost, together in connection with excellent analytical characteristics such as accuracy, sensitivity and reproducibility.

It is worth to emphasize that just a single enzyme-based motor operated during 120 s is able to determine H_2O_2 with excellent accuracy in all examined samples, being this performance independent of the bio-chemical sample environment. This approach becomes extremely interesting offering a clear reliable and simplified alternative to other well-established ones, opening novel avenues in environmental and clinical diagnosis as well as in POC applications.

The reported proof-of-concept and related relevant applications can be extended to the multiplexed analysis of highly concern related compounds, through the release of multiple enzymes (enzyme cocktail) from a single motor or from different motors. The single design and operational procedure make this approach a universal analytical tool for a plethora of target analytes in different fields.

ASSOCIATED CONTENT

Supporting Information

Optimization of experimental variables.
Determination of H_2O_2 in different samples.
Video S-1. Influence of the number of motors on the mobile biosensor swimming capability.
Video S-2. Motor swimming capabilities in multiplexed format for parallel samples analysis.

AUTHOR INFORMATION

Corresponding Author

∗ Corresponding author. Tel.: +34 91 885 49 95.
E-mail address: alberto.escarpa@uah.es (A. Escarpa)

Present Addresses

Department of Analytical Chemistry, Physical Chemistry and Chemical Engineering, University of Alcala, Ctra. Madrid-Barcelona, Km. 33,600, E-28871 Alcalá de Henares (Madrid), Spain

Author Contributions

‡ M. M. G. and A. J. contributed equally.

Notes

Any additional relevant notes should be placed here.

ACKNOWLEDGMENT

The authors are very grateful for the financial support from the Spanish Ministry of Economy and Competitiveness CTQ2014–58643-R (A.E.) and from the NANOAVANSENS program from the Community of Madrid (S2013/MIT-3029). M.M.G acknowledges the program NANOAVANSENS program from the Community of Madrid (S2013/MIT-3029) for her post-doctoral contract. A.J. acknowledges the FPI fellowship received from the Spanish Ministry of Economy and Competitiveness.

REFERENCES

(1) Wang, J., *Biosens. Biolectron*., **2015**, DOI:10.1016/j.bios.2015.04.095.
(2) Jurado-Sánchez, B.; Sattayasamitsathit, S.; Gao, W.; Santos,L.; Fedorak, Y.; Singh, VV.; Orozco, J.; Galarnyk, M.; Wang, J., *Small*, **2015**;*11*(4) 499-506
(3) Wang, W.; Duan, W.; Ahmed, S.; Mallouk,T. E., *A. Sen, Nano Today* **2013**, *8*, 531-554.
(4) Sanchez, S.; Soler, L.; Katuri, J., *Angew. Chem*. Int. Ed. **2015**, *54*, 1414 – 1444
(5) Zhao, G. and Pumera, M., Chem. Asian J., **2012**, *7*, 1994-2002, DOI: 10.1002/asia.201200206
(6) Zhao, G. and Pumera, M., *J. Phys. Chem. B* **2012**, *116* (35), 10960-10963.
(7) Sharma, R.; Chang, S. T.; Velev, O. D., *Langmuir* **2012**, *28* (26), 10128-10135.

(8) Kundan, A.; Plawsky, J. L.; Wayner, P. C.; Jr., *Langmui*r **2015**, *31* (19), 5377-86.
(9) Fath, A.; Horn, T.; Gambaryan-Roisman, T. P.; Stephan, D. B., *Int. J. Heat Mass Transfer* **2015**, *86*, 764-779.
(10) Zhao, G.; Seah, T.H.; Pumera, M., *Chem. Eur*. J **2011**, *17*, 12020–12026.
(11) Seah, T.H.; Zhao, G.; Pumera, M., *ChemPlusChem* **2013**, *78*, 395–397.
(12) Moo, J.G.S. and Pumera, M., *Chem. Eur. J* **2015**, *2*1, 58–72.
(13) Orozco, J.; Vilela, D.; Valdes-Ramirez, G.; Fedorak, Y.; Escarpa, A.; Vazquez-Duhalt, R.; Wang, J., *Chem. - Eur. J*. **2014**, 20 (10), 2866-71.
(14) Wang, J., *Nanomachines: Fundamentals and Applications;* Wiley: New York, 2014.
(15) Lin, Y.; Cui, X.; Li, L., *Electrochem. Commun*. **2005**, *7* (2), 166-172.
(16) Pournaghi-Azar, M. H.; Ahour, F.; Pournaghi-Azar, F., *Sens. Actuators, B* **2010**, *145* (1), 334-339.
(17) Tavakoli, H.; Baghbanan, A. A., *Bioelectrochemistry* **2015**, *104*, 79-84.
(18) Ohshima, H.; Tatemichi, M.; Sawa, T., *Arch. Biochem. Biophys*. **2003**, *417* (1), 3-11.
(19) Finkel, T.; Serrano, M.; Blasco, M. A., *Nature* **2007**, *448* (7155), 767-774.
(20) Rhee, S. G., *Science* **2006**, *312*, 1882.
(21) Zhou, M.; Yang, M.; Zhou, F., *Biosens. Bioelectron*. **2014**, *55*, 39-43.
(22) Hu, A. L.; Liu, Y. H.; Deng, H. H.; Hong, G. L.; Liu, A. L.; Lin, X. H.; Xia, X. H.; Chen, W., *Biosens. Bioelectron*. **2014**, *61*, 374-378.
(23) Lo, P. H.; Kumar, S. A.; Chen, S. M., *Colloids Surf*., B **2008**, *66* (2), 266-73.
(24) Zhang, L.; Fang, Z.; Ni, Y.; Zhao, G., *Int. J. Electrochem. Sci.* **2009**, *4,* 407-413.
(25) Li, Y.; Zhang, Y.; Zhong, Y.; Li, S., *Appl. Surf. Sci*. **2015**, *347*, 428-434.
(26) Bakker, E. and Qin, Y., *Anal. Chem*., **2006**, *78* (12), 3965–3984
(27) Pedrero, M.; Campuzano, S.; Pingarrón, J. M., *Sensors* **2009**, *9* 5503-5520
(28) Lam, H.; Oh, D.C.; Cava, F.; Takacs, C.N.; Clardy, J.; de Pedro, M.A.; Waldor, M.K., *Science* **2009**, *325* (5947), 1552-1555.

Chapter IV

Conclusions

A la vista de los resultados expuestos en esta tesis, tanto las estrategias analíticas desarrolladas como inmunosensores electroquímicos, así como aquellas metodologías innovadoras basadas en la utilización de motores sintéticos han demostrado sus beneficios como herramientas analíticas prometedoras y de gran significancia. Los inmunosensores son aproximaciones reales como dispositivos "*point-of-care*", mientras que los sensores basados en la utilización de motores han demostrado su capacidad para convertirse en verdaderos sistemas de detección. Del mismo modo, ambas estrategias pueden implementarse en distintos campos de aplicación tales como el agroalimentario o la seguridad alimentaria, e incluso convertirse en herramientas de gran interés en el análisis clínico.

1. La metodología inmunoanalítica junto con la detección electroquímica han permitido una determinación rápida, sensible y selectiva de importantes compuestos potencialmente tóxicos en el campo alimentario como las micotoxinas. La utilización de partículas magnéticas como soporte de inmovilización del anticuerpo específico, así como de una enzima marcadora y el mediador electroquímico adecuado para su detección amperométrica han permitido desarrollar una estrategia simple y fiable para la determinación *in situ* de Fumonisinas y Ocratoxina A. En ambos inmunosensores se han obtenido excelentes límites de detección, por debajo de los límites máximos permitidos, cumpliendo con los requisitos de la legislación. Además, la fiabilidad y exactitud evaluadas por medio del análisis de un

material de referencia certificado y de muestras reales correspondientes a bebidas mundialmente consumidas como son la cerveza y el café, han dado lugar a resultados excepcionales. Por otro lado, se ha diseñado un protocolo de calibración y análisis simultáneo que simplifica significativamente el análisis, disminuyendo la tediosa e intensa labor de las curvas de calibración y reduce los tiempos de análisis, sin que ello afecte a la excelente exactitud obtenida. Estas características, junto con su facilidad de uso *in situ* y el carácter desechable de los inmunosensores desarrollados, configuran a esta metodología como una alternativa excepcional en seguridad alimentaria y el cribado en la cadena agroalimentaria.

2.1. La importancia de las estrategias analíticas basadas en motores sintéticos ha crecido exponencialmente en los últimos años, llegando a ser una metodología que aporta una nueva forma de llevar a cabo los análisis. Respecto a los motores catalíticos, los microcohetes fabricados con grafeno han demostrado su potencial aplicación en el análisis de alimentos, mediante la determinación rápida, fiable y sencilla de fumonisinas. Basada en la rápida amortiguación "en movimiento" que presentan los micromotores de grafeno para aquellos aptámeros marcados fluorescentemente y que no hayan reaccionado con la micotoxina específica, se ha desarrollado una metodología de biosensado que ofrece ventajas únicas tales como un volumen de muestra extremadamente pequeño, alta sensibilidad (por debajo de los requerimientos de la legislación), elevada fiabilidad y un protocolo

simplificado. Los excelentes resultados obtenidos permiten concebir un futuro apasionante para las aplicaciones de micromotores en campos todavía sin explorar como el análisis alimentario, implicando diferentes maneras de realizar operaciones analíticas.

2.2. Por otro lado, el diseño de nuevas estrategias basadas en el uso de micromotores depende principalmente del desarrollo de nuevos materiales para su construcción. En este sentido, se ha desarrollado un microcohete catalítico "inteligente" que integra un encendido retardado, merced a la eliminación de la aleación de su capa interna, en presencia de combustible en el medio. La propulsión retardada del micromotor depende solamente de las propiedades intrínsecas del material del micromotor y la disolución que lo rodea, y no requiere ningún estímulo externo. Tal activación retardada puede ser confeccionada usando factores químicos ambientales diferentes (combustible, pH y fuerza iónica) o con las propias propiedades del material del micromotor (composición de la aleación). En este caso, se ha utilizado una aleación bimetálica compuesta por Cu-Pt como capa catalítica, donde el H_2O_2 (combustible) es capaz de atacarla por oxidación o corrosión del Cu, y reaccionar con los núcleos de Pt libres de Cu que generan burbujas y propulsan al micromotor. Diferentes condiciones y muestras reales han sido probadas para evaluar la corrosión y la ignición retardada, alcanzando un retraso del encendido de hasta 45 min. Tal habilidad de modificar el comportamiento de la

propulsión del microcohete resulta muy prometedor para el desarrollo de vehículos autónomos en la nano/microescala.

3. Finalmente, se ha desarrollado un sensor móvil basado en su propulsión por autodifusioforesis (efecto Marangoni por la disolución de tensioactivo en el interior de micropuntas de pipeta) para el biosensado, tanto electroquímico como óptico, de H_2O_2 en diferentes matrices. Esta estrategia pionera presenta algunas ventajas fundamentales, como son una capacidad de movimiento amigable con el medio ambiente para la búsqueda del analito a lo largo de la muestra, la autoagitación debida a la convección del fluido, la conservación de la actividad biocatalítica debido al confinamiento de la enzima dentro del motor, y la liberación continua de enzima "fresca" en la disolución. Estas características facilitan la adecuada interacción enzima-sustrato y aceleran la reacción enzimática. Esto conduce al hecho que un solo motor enzimático, operando durante 120 s sea capaz de determinar H_2O_2 con excelente exactitud en todas las muestras examinadas, siendo este hecho independiente de ambiente bioquímico de la muestra. Esta prueba de concepto se puede extender al análisis múltiple de compuestos de interés relacionados, a través de la liberación de diversas enzimas (cóctel de enzimas) desde un solo motor o desde motores distintos.

Debido a todo lo expuesto y comentado anteriormente, los resultados presentados en esta tesis doctoral revelan el diseño y desarrollo de nuevas estrategias y metodologías que permiten mejorar

las herramientas analíticas actuales y su desempeño. Asimismo, estos métodos se pueden implementar como dispositivos "*point-of-care*" para la detección en distintas disciplinas tales como la seguridad alimentaria y el campo médico, expandiendo las perspectivas de la química analítica actual.

In view of the results expounded in this very Thesis, innovative analytical approaches for electrochemical and fluorescent (bio-)sensing, and motor-based (bio-)sensing have demonstrated their benefits as noteworthy and promising analytical tools. Immunosensors are actual approaches as *point-of-care* devices, while motor-based sensors have proven their capability to become into real methods for analytical detection. Likewise, both strategies can be implemented in the framework of agro-alimentary and food safety fields, even for becoming in very suitable tools for clinical discipline.

1. Immunoanalytical methodology together with electrochemical detection has allowed fast, sensitive and selective determination of meaningful food hazards such as mycotoxins. Magnetic beads as antibody immobilization support together with the suitable enzymatic tracer and electrochemical mediator for amperometric detection have been successfully used to build a simple and reliable strategy to perform in-situ determination of Fumonisins and Ochratoxin A. Both developed magnetoimmunosensors have yielded excellent and suitable LODs, well below of the maximum permitted concentration levels, fulfilling the legislation requirements. Furthermore, reliability and accuracy have been assessed through the analysis of a certified reference material and highly worldwide consumed beverage as beer and coffee samples, getting exceptional results. Additionally, a simultaneous simplified calibration and analysis protocols have been performed, reducing the analysis time, decreasing the tedious and intense labor of calibration

curves, and reaching exceptional accuracy. These features, together with the portable, disposable possibilities of the developed immunosensors, provide to this methodology the fitness for purpose and offer an exceptional emergency tool for food safety and agro-alimentary chain monitoring.

2.1. Motor-based strategies have exponentially grown in importance in recent years, becoming a methodology which supplies a new performance in the analytical field. Related to the catalytic motors, graphene-based microrockets have demonstrated an agro-food safety diagnosis application for quantitative, fast, easily applied and reliable assessment of FBs. Based on a rapid "*on-the-move*" quenching of unreacted fluorescent-labeled aptamers with its specific mycotoxin, this methodology offers valuable advantages such as the extremely low sample volume required, high sensitivity (below legal requirements), high reliability, while it simplifies the overall protocol. The excellent results obtained allow envisioning an exciting future for the applications of micromotors in unexplored fields as food analysis, entailing a different way to perform analytical operations.

2.2. Besides, the design of novel strategies based on the use of microengines depends mainly on the development of new materials for their construction. In this sense, a "smart" built-in delayed ignition catalytic microrocket based on a chemical dealloying of its inner layer in the presence of fuel media has been developed. The delayed actuation of the micromotor propulsion depends solely on the intrinsic material

properties of the microengine and its surrounding solution and does not require any external stimuli. Such delayed activation can be tailored by using different environmental chemical factors (fuel, pH and ionic strength) or by the material properties of the microengine itself (alloy composition). A bimetallic alloy composed by Cu-Pt was built as the catalytic layer, where H_2O_2 (fuel) is able to attack this layer by oxidizing or corroding Cu, and reacting with Cu-free spots of Pt that generates bubbles to propel the micromotor. Different conditions and real samples were tried to assess the corrosion and the delayed ignition, reaching blastoff delaying times of 45 min. Such ability to tune the propulsion behavior of micromotor offers great promises for developing autonomous nano/microscale vehicles.

3. A mobile sensor based on pipette tip and self-diffusiophoresis propulsion (Marangoni effect by surfactant solution) has been developed for both electrochemical and optical biosensing of H_2O_2 in different matrices as a pioneering strategy. Some of the main advantages of this mobile sensor strategy are the environmental-friendly motion along the sample to find the analyte, the micromixing activity due to the fluid convection, the preservation of the biocatalytic activity due to its confinement inside the motor, and the continuous release of fresh enzymes. Those features facilitate the adequate enzyme-substrate interactions and accelerate the enzymatic reaction, which leads to the fact that just a single enzyme-based motor operating during 120 s is able to determine H_2O_2 with excellent accuracy in all examined samples,

being this performance independent of the biochemical sample environment. The reported proof-of-concept can be extended to the multiplexed analysis of highly concern related compounds, through the release of multiple enzymes (enzyme cocktail) from a single motor or different motors.

Owing to all aforementioned statements, the results presented in this Doctoral Thesis reveal that pioneering approaches and strategies can be carried out to improve the current analytical tools and their performance. Likewise, these methods can be implemented as *point-of-care* devices for detection in food safety and medical fields, expanding the perspectives in current Analytical Chemistry.

Chapter V

Appendices

Supplementary information

Disposable and reliable electrochemical magnetoimmunosensor for Fumonisins simplified determination in maize-based foodstuffs.

Adrián Jodra, Miguel Ángel López and Alberto Escarpa∗

Department of Analytical Chemistry, Physical Chemistry and Chemical Engineering, University of Alcalá, Ctra. Madrid-Barcelona, Km. 33,600, E-28871 Alcalá de Henares (Madrid), Spain

∗ Corresponding author. Tel.: +34 91 885 49 95.

E-mail address: alberto.escarpa@uah.es (A. Escarpa).

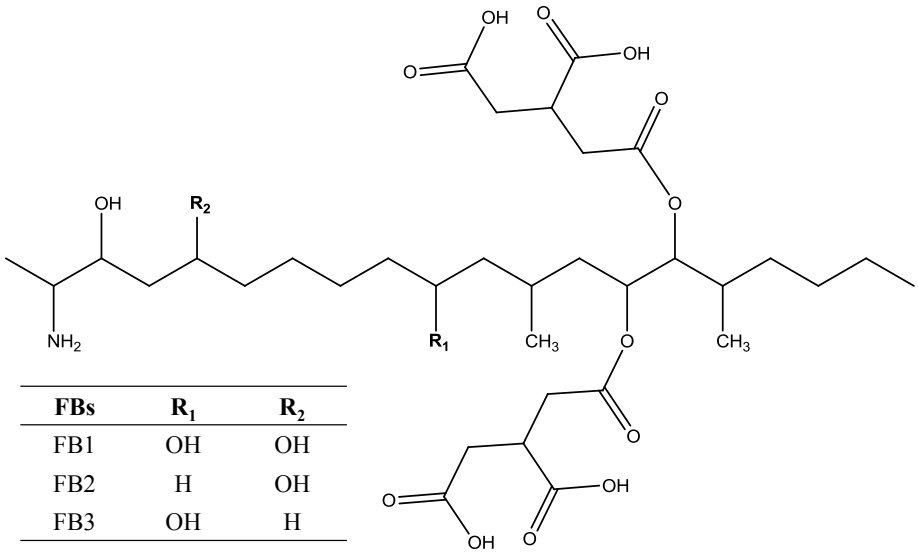

FBs	R_1	R_2
FB1	OH	OH
FB2	H	OH
FB3	OH	H

Fig. S1. Structures of Fumonisins B1, B2 and B3.

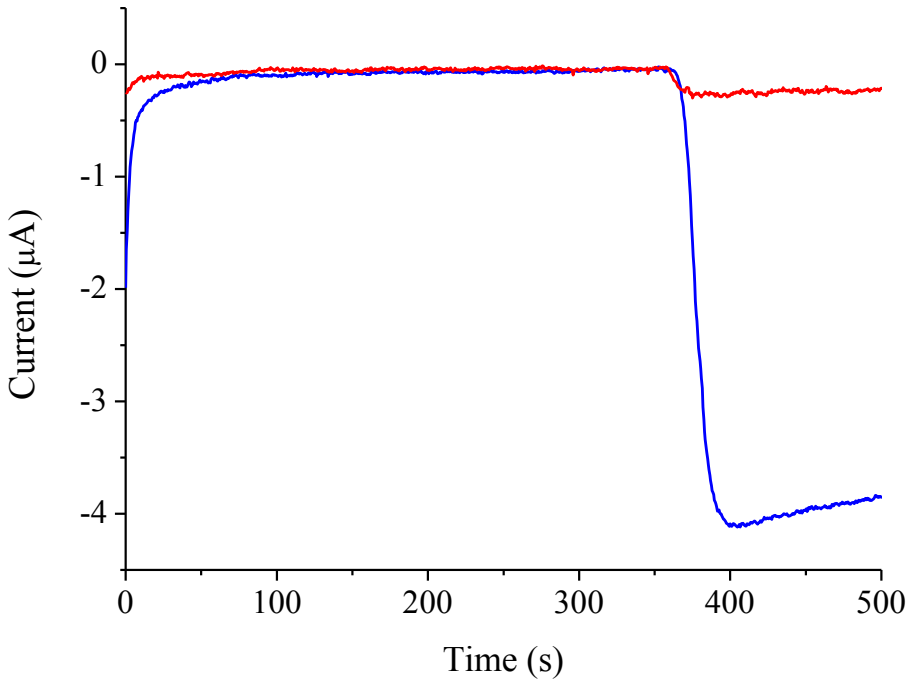

Fig. S2. Representation of the amperometric signal of the maximum signal (—) and the minimum signal (—). (Please, respect the colour of the lines)

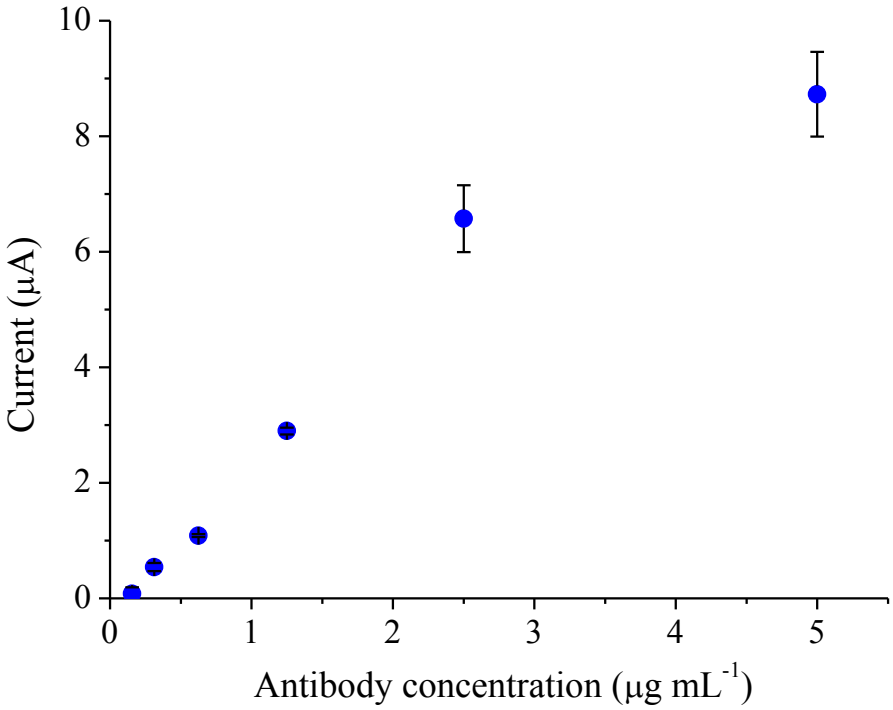

Fig. S3. Optimization of antibody concentration.

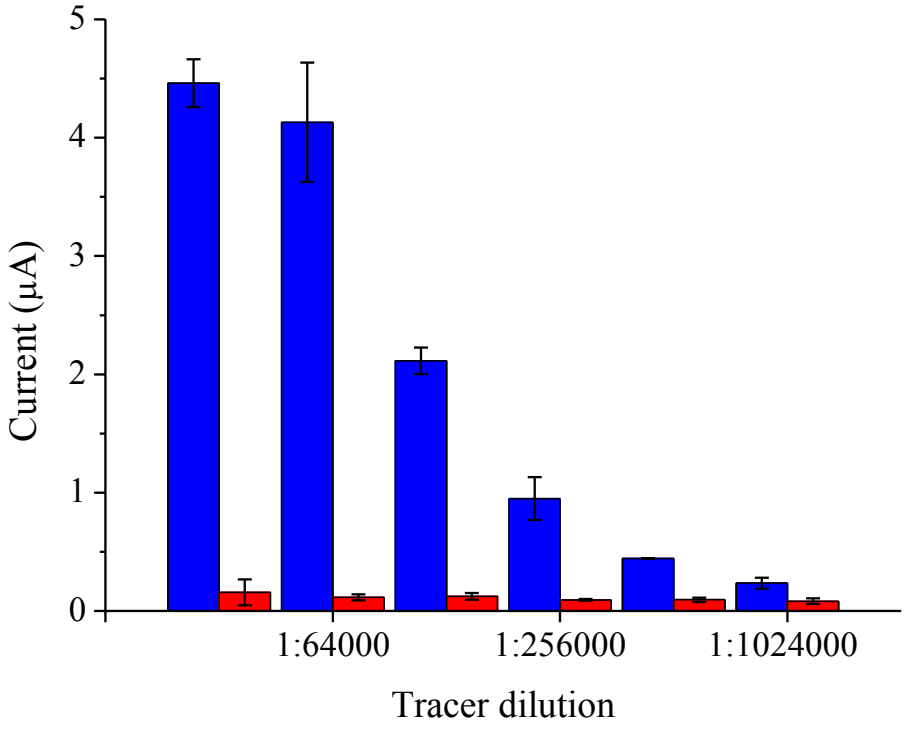

Fig. S4. Optimization of tracer dilution. Blue bars represent the maximum signal (not presence of FB1); red bars represent the minimum signal (in presence of excess of FB1).

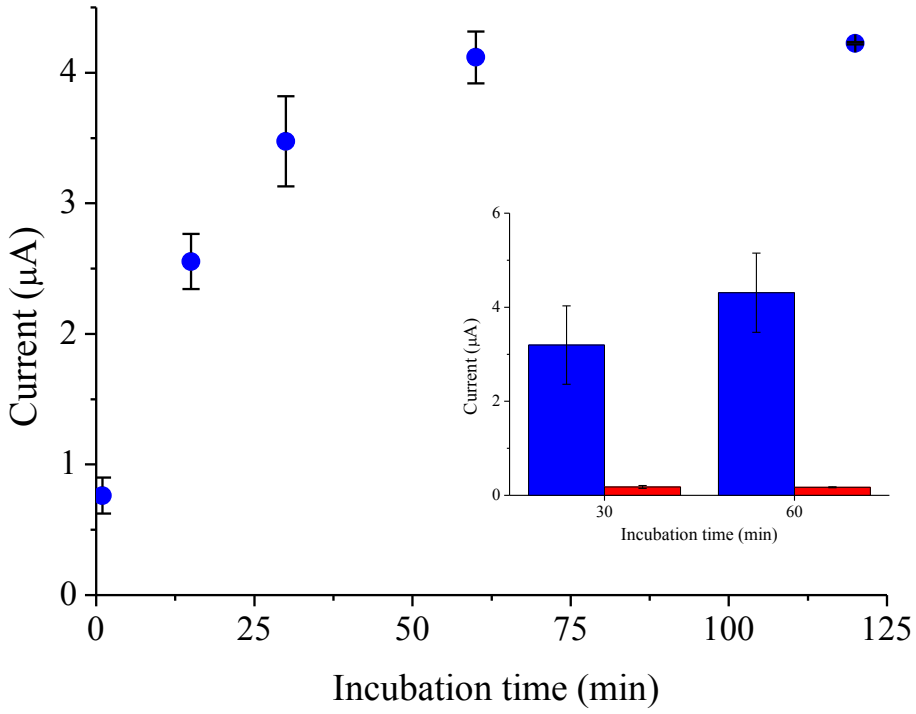

Fig. S5. Optimization of incubation time for enzymatic tracer. The inset shows relation between maximum and minimum signals (red bars denotes competition with 1000 μg mL^{-1} FB1).

Table S1

Comparison of analytical parameters for simultaneous and sequential incubation of standard/sample mycotoxin and tracer with the immobilized antibody.

Calibration curve	LOD (μg L^{-1})[a]	IC_{50} (μg L^{-1})[b]	DR (μg L^{-1})[c]
Simultaneous	0.40	3.32	0.87-12.6
Sequential	0.33	2.86	0.73-11.2

[a]Limit of detection

[b]Inhibitory concentration 50%

[c]Dinamic range

Table S2

Summary of analytical parameters of different and previous methods.

Immunoassay Format	Detection type	IC_{50}	DR	LOD	Precision (CVs/%)	Recovery (%)	Reference
Peptide ELISA	Optical	6.1 µg L^{-1}	1.8-20.7 µg L^{-1}	1.2 µg L^{-1}	< 15	90-105	Liu et al., 2013
ELISA	Optical	2.2 µg L^{-1}	---	5.4 µg Kg^{-1}	< 15	78-107	Sheng et al., 2012
ELISA	Optical	3.2 µg L^{-1}	0.54-26.3 µg L^{-1}	0.24 µg L^{-1}	< 9.5	80-115	Wang et al., 2014
Lateral Flow	Visual	1000 µg L^{-1}	---	---	---	---	Lattanzio et al., 2012
Lateral Flow	Visual	---	---	50 µg L^{-1}	---	---	Wang et al., 2013
Lateral Flow	Visual	---	2.5-40 µg L^{-1}	2.5 µg L^{-1}	---	---	Yang-Song et al., 2012
Flow through	Visual	---	---	1250 µg Kg^{-1}	---	---	Ediage et al., 2012a
Membrane-based dot immunoassay	Visual	8.3 µg L^{-1}	---	250 µg Kg^{-1}	---	---	He et al., 2012

Immunoassay Format	Detection type	IC_{50}	DR	LOD	Precision (CVs/%)	Recovery (%)	Reference
Microarray	Optical	645 μg Kg^{-1}	10.5-138.5 μg L^{-1} 168.1-2215.8 μg Kg^{-1*}	9.9 μg L^{-1} 159.0 μg Kg^{-1*}	< 18.5	55-80	Oswald et al., 2013
Microarray	Optical	---	---	109.1 μg L^{-1}	---	---	Wang et al., 2011
Microarray	Optical	---	0.001-10 μg L^{-1}	1 ng L^{-1}	< 11.5	79-124	Deng et al., 2013
Lateral Flow	Optical	20 μg L^{-1}	2.5-500 μg L^{-1} 25-5000 μg Kg^{-1*}	2.5 μg L^{-1} 25 μg Kg^{-1*}	< 18	90-115	Mirasoli et al., 2012
SPR	Optical	---	---	50 μg L^{-1}	---	---	Mullet et al., 1998
Immunosensor	Electrochemical	---	1-1000 μg L^{-1}	5 μg L^{-1}	---	76-112	Kadir and Tothill, 2010
Immunosensor	Electrochemical	2.86 μg L^{-1}	0.73-11.2 μg L^{-1}	0.33 μg L^{-1}	< 6.9	87-105	This work

* LOD value in the food matrix taking into account the extraction procedure
--- Not mentioned

Supporting Information

Determination of Fumonisin B1 based *on-the-move* fluorescence quenching of the specific labeled-aptamer by graphene-made micromotors

Department of Analytical Chemistry, University of Alcalá, Alcalá de Henares, Madrid E-28871, Spain.
Chemical Research Institute "Andrés M. del Río" (IQAR), University of Alcalá, Carretera Madrid-Barcelona, Km. 33,600, Alcalá de Henares, E-28871 Madrid, Spain.

CONTENTS

Supporting Information

Delayed Ignition and Propulsion of Catalytic Microrockets based on Fuel-Induced Chemical Dealloying of the Inner Alloy Layer

*Adrián Jodra, Fernando Soto, Miguel-Angel Lopez-Ramirez, Alberto Escarpa and Joseph Wang**

1. Experimental Section

Electrochemical Synthesis of Reduced Graphene Oxide (erGO)/Cu-Pt Micromotors

The electrochemically reduced graphene oxide (erGO)/Cu-Pt microrockets were prepared by a common template-directed electrodeposition methodology,[1] as illustrated in Figure S1. A thin gold film was sputtered first on one side of the porous polycarbonate (PC) membrane containing 5μm conical-shaped micropores (Catalog No. 7060-2513; Whatman, Maidstone, U.K.) to serve as the working electrode. The membrane was assembled in a Teflon plating cell with

aluminum foil serving as an electrical contact for the following electrodepositions. A Pt wire and an Ag/AgCl electrode (with 3M KCl) were used as counter and reference electrodes respectively. An electrochemical reduction of graphene oxide within the micropores was performed to prepare the outer layer of the microrocket.[1] The rapid formation of an erGO layer enhances the surface roughness and increases the surface area. This electrodeposited erGO film has higher conductivity compared to pure GO, enabling deposition of the inner metallic layer using galvanostatic methods. A Cu-Pt alloy was thus electrodeposited using a mixture composed of a commercial platinum plating solution (Platinum RTU, 1.5 g L^{-1}; Technic Inc, Anaheim, CA) and $CuSO_4 \bullet 5H_2O$ solution (250 g L^{-1}). The plating mixture solution was prepared by adding 3.75 g of the $CuSO_4 \bullet 5H_2O$ solution into 15 mL of water, followed by 5 mL of the commercial platinum solution. The alloy was electrodeposited at −2 mA by a galvanic method for a time of 500s. For the electrodeposition assays, galvanic methods at −0.5 and −8 mA for the alloy and −2 mA for the control (single Pt electrodeposition) were carried out, all for 500s.

The sputtered gold was gently removed by mechanical polishing with 3-4 µm alumina powder using cotton tip applicators. The membrane was then dissolved in methylene chloride for 5 min three times to release the microrockets. The resulting microrockets were separated and collected from the solution by centrifugation at 7000 rpm for 3 min followed by isopropanol, ethanol and ultrapure water (18.2 Ω cm at 25ºC), three times each. Finally, the microrockets from the whole piece of membrane were dispersed into 1 mL of ultrapure water at room temperature for storage when not in use (Fig. SI1). Also shown in Fig. SI1 is the dealloying of the Cu-Pt alloy surface upon it reaction with hydrogen peroxide (step 4).

Deposition of Graphene Oxide (GO)/Cu-Pt onto Gold Bare Electrodes

The graphene oxide (GO)/Cu-Pt deposition onto gold bare electrodes was performed using Pt wire and an Ag/AgCl (3M KCl) electrodes as counter and reference electrodes, respectively. The GO (0.1 g L^{-1}) was deposited by drop casting method, adding 3 µL until the drop dried completely. This step was repeated twice. Subsequently, a Cu-Pt alloy was electrodeposited onto the GO film using the metal mixture described earlier to prepare the microrockets. The alloy was electrodeposited at −2 mA by a galvanic method for a time of 500 s. The resulting modified Au electrodes were stored at room temperature for further characterization.

Equipment and Reagents

Template electrochemical deposition of microrockets was carried out using an electrochemical station µAutolab III (Eco Chemie, Utrecht, Holland). Scanning electron microscopy (SEM) images were obtained from a Phillips XL30 ESEM instrument, using an acceleration voltage of 15 kV. Energy-dispersive X-ray mapping analysis was performed using an Oxford EDX detector attached to SEM instrument and operated by INCA software. Aqueous hydrogen peroxide solutions (Sigma-Aldrich, cat. 95313), with concentrations ranging from 0.1–10% were used as the chemical fuel. Sodium cholate (Sigma-Aldrich, cat. 270911) was used as a surfactant in all experiments (at 1%), except for the experiment of pH 2, in which sodium dodecyl sulfate (Sigma-Aldrich, cat. 436143) was used as a surfactant (1%). Real-life samples involved a seawater sample (collected at Torrey Pines Beach in La Jolla, CA) and a simulated gastric fluid (from Fluka, 101499347). These samples were spiked with sodium cholate (1%) and hydrogen peroxide (1%). An inverted optical

microscope (Nikon Eclipse Instrument Ti-S), coupled with 10X and 20X objectives, and a Hamatsu digital camera C11440 and FrameLink Express software, were used for capturing the movies. A MetaMorph 7.6 software (Molecular Devices, Sunnyvale, CA) was used for capturing videos at a frame rate of 30 frames per sec. The speed of the micromotors was tracked using a MetaMorph tracking module. Each data point was considered for the individual microrockets after they started their autonomous motion.

Explanation of Cu-Pt co-electrodeposition

The co-electrodeposition of Cu and Pt is possible according to Figure SI2 that displays CVs for the corresponding Pt and Cu solutions. As the Cu concentration is larger, in comparison to Pt, the area of Cu reduction is extended from 0 V to −0.9 V. Therefore, when a current of −2 mA is applied, the generated potential corresponds to a voltage between −0.3 V and −0.2 V, leading to the reduction of both metals. Furthermore, the Cu electrodeposition is larger because of its higher concentration.

As shown in the CV of Fig. SI2, Pt is more readily electrodeposited than Cu; a higher potential is required to electrodeposit Cu compared to Pt (see Fig. SI2). This denotes differences according to the current used in the electrodeposition process: At −0.5 mA, the electrodeposition is produced in lesser extent and depends on the metal concentrations; hence, Cu is electrodeposited more favorably than Pt. At −2 mA, the potential is suitable for Pt, to increase the Pt content, while at −8 mA the Cu electrodeposition is more favorable.

Chemical Explanation of Diverse Dealloying Stimuli

Pt is a nobler metal compared to Cu, generating the galvanic corrosion of Cu. The galvanic corrosion of Cu is promoted by the hydrogen peroxide. As it is shown in the reactions S1-S3, Cu can be oxidized by the H_2O_2 fuel. Close to neutral pH, H_2O_2 behaves as a weak acid, as described in reaction S2. When the OH^- is generated, it can react with Cu^+ to form Cu_2O (reaction S4). It is possible that Cu^+ can be oxidized by H_2O_2 generating Cu^{2+}, further producing $Cu(OH)_2$ and, after a while, low amount of CuO after dehydration with time. A passivation layer can be formed by Cu_2O and, lesser extent, $Cu(OH)_2$ in its totality. To increase the Cu oxidation production, more OH^- is obtained from hydrogen peroxide and more galvanic corrosion is provoked. Also, the Cu_2O is permeable to OH^- and $Cu(OH)_2$ is soluble, even it is more soluble with more OH^-.

$$Cu \rightarrow Cu^+ + e^- \qquad E° = -0.521\ V \qquad (S1)$$

$$H_2O_2 \leftrightarrow H^+ + HO_2^- \qquad (S2)$$

$$HO_2^- + H_2O + 2e^- \rightarrow 3OH^- \qquad E° = +0.87\ V \qquad (S3)$$

$$2Cu(OH)_2 \leftrightarrow Cu_2O + H_2O \qquad (S4)$$

The Cu_2O formation is favored in S4. Reactions S5 and S6 explain how the Cu oxidation is thermodynamically favorable at basic pH, favoring a galvanic corrosion. Despite fast decomposition of H_2O_2 at basic pH, the galvanic corrosion is increased:

$$2Cu + 2OH^- \rightarrow Cu_2O + H_2O + 2e^- \qquad E° = +0.36\ V \qquad (S5)$$

$$Cu + 2OH^- \rightarrow Cu(OH)_2 + 2e^- \qquad E° = +0.222\ V \qquad (S6)$$

Cu_2O can be transformed into $Cu(OH)_2$ by reaction S7, although its precipitation as passivation layer is favored. Moreover, $Cu(OH)_2$ is soluble at basic pH because it can behave as a weak acid, leading to

$[Cu_n(OH)_{2n-2}]^{2+}$. This prevents the passivation layer that slows down the Cu - H_2O_2 reaction:

$$Cu_2O + 2OH^- + H_2O \rightarrow 2Cu(OH)_2 + 2e^- \quad E° = +0.08\ V \qquad (S7)$$

The hydrogen peroxide is more reactive in acidic media (S8) compared to a basic environment (S3).

$$HO_2^- + H_2O + 2e^- \rightarrow 3OH^- \qquad E° = +0.87\ V \qquad (S3)$$

$$H_2O_2 + 2H^+ + 2e^- \rightarrow 2H_2O \qquad E° = +1.776\ V \qquad (S8)$$

Nevertheless, as discussed in the main text, H_2O_2 reacts preferentially with HCl compared to Cu. In fact, the reaction mechanism and the compensating reactions that can explain the long delay time for the pH=2 have been reported:[2]

$$H_2O_2 + 2HCl \rightarrow Cl_2 + 2H_2O \qquad (S9)$$

$$H_2O_2 + Cl_2 \rightarrow O_2 + 2HCl \qquad (S10)$$

$$H_2O_2 + HCl \rightarrow HClO + H_2O \qquad (S11)$$

$$HClO + H_2O_2 \rightarrow HCl + H_2O + \tfrac{1}{2}O_2 \qquad (S12)$$

$$Cl_2 + H_2O_2 \leftrightarrow HClO + HCl \qquad (S13)$$

Cu does not react with diluted non-oxidant acids such as HCl. As a result, the galvanic and pitting corrosion are decelerated because it is more difficult to oxidize the Cu. Subsequently, the Cl^- can produce pitting corrosion (see extended explanation below).

Under mildly acidic conditions, e.g., pH=4.5 (i.e., less HCl) H_2O_2 remains in its form and is more reactive (reaction S8). In this case, the H_2O_2 produces more galvanic corrosion instead of reacting with HCl. Eqns S14 and S8 show the possible reactions since the both oxidations

are thermodynamically favorable due to the potential of the hydrogen peroxide. Also, Cl^- can generate pitting corrosion after the reaction.

$$Cu \rightarrow Cu^+ + e^- \qquad E° = -0.521\ V \qquad (S14)$$

$$H_2O_2 + 2H^+ + 2e^- \rightarrow 2H_2O \qquad E° = +1.776\ V \qquad (S8)$$

NaCl provokes more pitting corrosion in metals. This process reflects the penetration power of Cl^- and prevents the passivation layer. When the Cu is oxidized, the Cu^+ can react with Cl^- from the salt. The resulting CuCl can be slightly soluble in chloride solutions (by cuprous chloride complexes) and also can precipitate on the Cu-Pt alloy surface, thus avoiding the formation of the passivation layer over the nearest Cu-Pt alloy surface. CuCl is found in a balance between different anions:[3]

$$Cu^+ + Cl^- \leftrightarrow CuCl + Cl^- \leftrightarrow CuCl_2^- + Cl^- \leftrightarrow CuCl_3^- + Cl^- \leftrightarrow CuCl_4^- \qquad (S15)$$

$CuCl_x^{n-}$ reacts with OH^- and H_2O as reaction S17 and S18 present, giving the hydrolysis of these complexes. The hydrolysis can occur, depending on the cuprous chloride complex.

$$Cu^+ + 2Cl^- \rightarrow CuCl_2^- \qquad (S16)$$

$$CuCl_2^- + 2OH^- \rightarrow Cu_2O + H_2O + 2Cl^- \qquad (S17)$$

$$2CuCl + H_2O \rightarrow Cu_2O + 2HCl \qquad (S18)$$

The precipitation of Cu_2O results in the creation of a passive layer. Additionally, to the extent that H_2O_2 oxidizes Cu, more OH^- is created and consequently copper oxides (Cu_2O mostly, $Cu(OH)_2$ and some CuO). The chloride ion can penetrate through this layer, continuing with the pitting corrosion, and delaying the formation of that passivation layer.

2. Supporting Figures

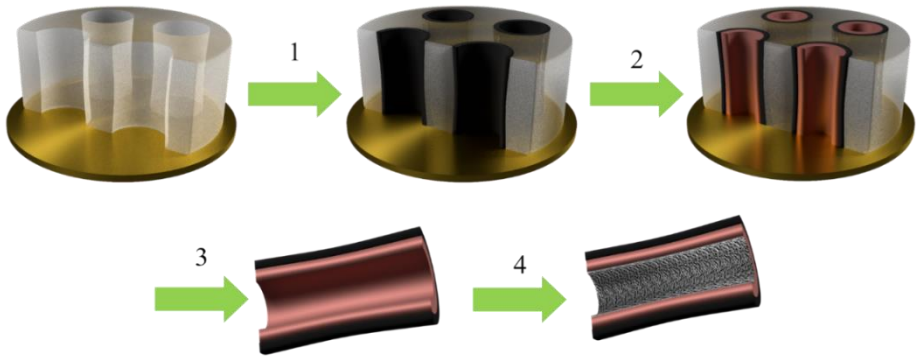

Figure SI1. *Schematic representation of the synthesis and release of erGO/Cu-Pt microrockets. 1) Graphene electrodeposition as an outer layer, 2) Cu-Pt alloy electrodeposition. 3) Microrockets release from the membrane. 4) Cu dealloying process and Pt exposure.*

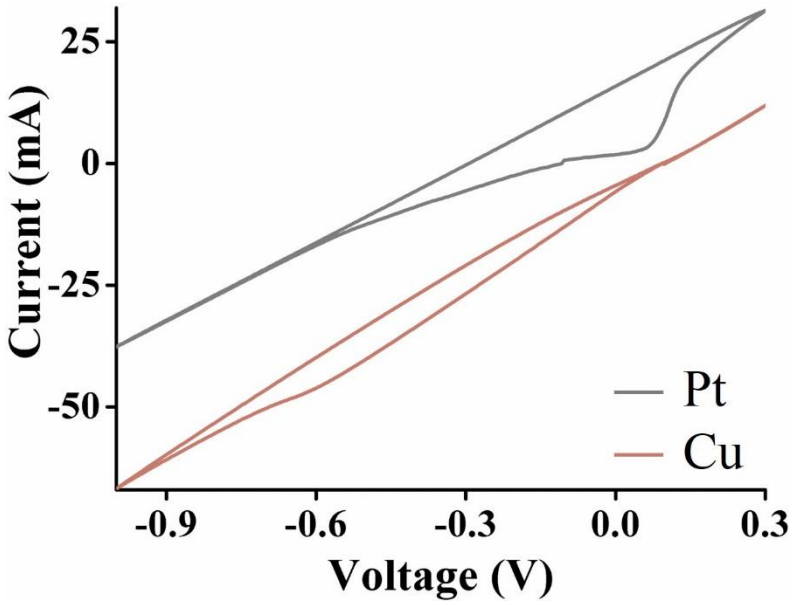

Figure SI2. *Cyclic voltammetry using the Pt (grey line) and Cu (copper-red line) solutions onto Au electrode (Scan rate=50 mV s^{-1}; number of scans=1; $CuSO_4 \cdot 5H_2O$ concentration=250 g L^{-1} (in water); Pt concentration=1.5 g L^{-1} (commercial solution)).*

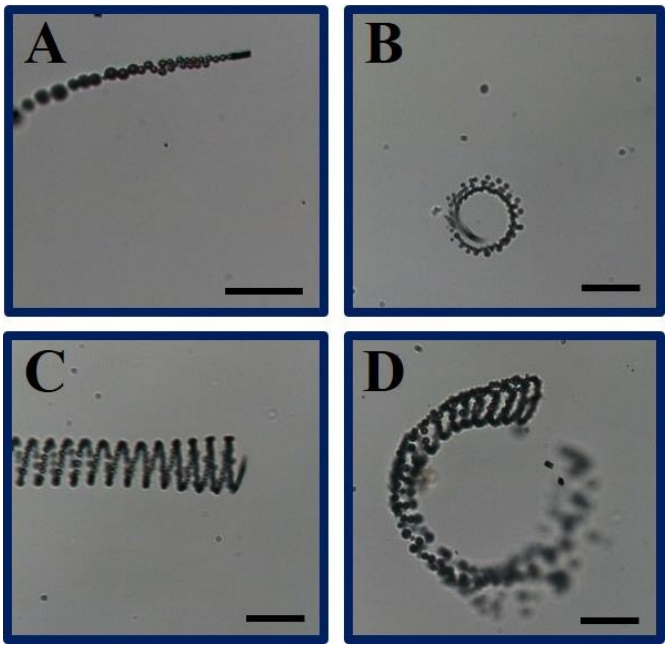

Figure SI3. *Directionality of erGO/Cu-Pt microrockets, a) linear motion is present for structures with a low defect. If defects are found in the structure, multiple directionalities arise, including b) circular motion, c) spiral and d) circular spiral. Scale Bar 50 um. Frames taken from video S3.*

3. Supporting Videos Description

Supporting Video S1. Schematic animation of chemical dealloying and blast-off of erGO/Cu-Pt microrocket.

Supporting Video S2. Delayed propulsion of an erGO/Cu-Pt microrocket.

Supporting Video S3. Directionality of different microrockets.

REFERENCES

1. A. Martin, B. Jurado-Sánchez, A. Escarpa and J Wang. *Small*, 2015, **11**, 3568–3574.

2. R. S. Livingston, and W. C. J. Bray, *Am. Chem. Soc.*, 1925, **47**, 2069–2082.

3. G. Kear, B. D. Barker and F. C. Walsh, *Corrosion Science*, 2004, **46**, 109–135.

Supporting Information

Self-propelled enzyme-based motors for smart mobile electrochemical and optical biosensing

María Moreno-Guzman‡, Adrián Jodra‡, Miguel-Ángel López and Alberto Escarpa*

CONTENTS

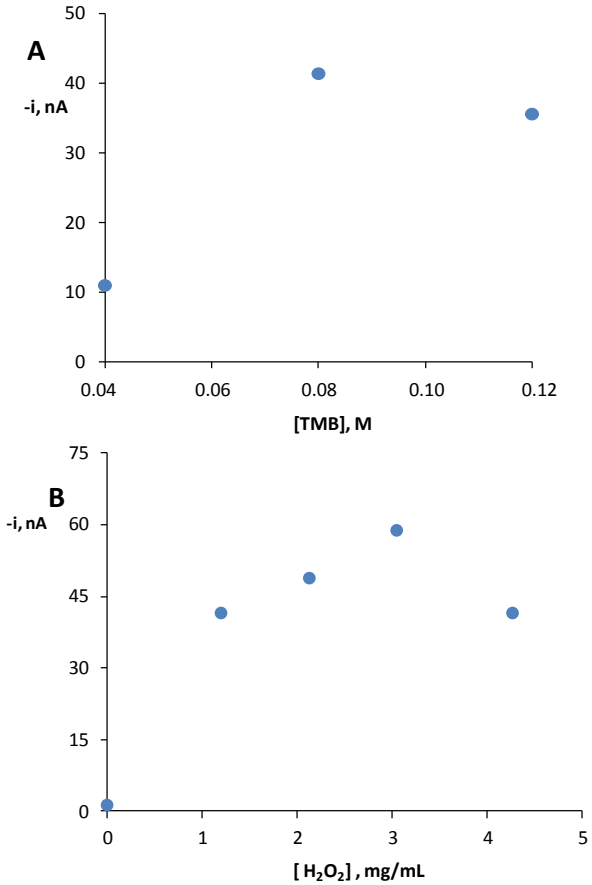

Figure S-1. (**A**) Optimization of TMB concentration. (**B**) Optimization of HRP concentration. Conditions: 0.1 mM H_2O_2; each point represents the signal obtained for one motor navigating during 120 seconds.

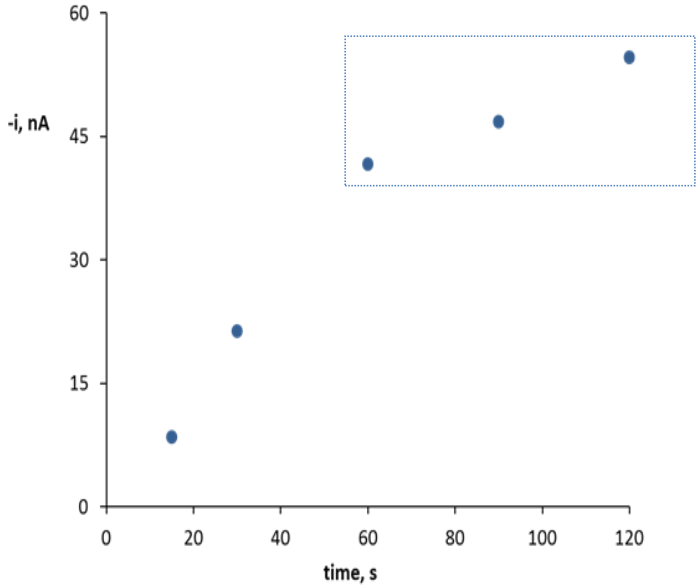

Figure S-2. Optimization of enzymatic reaction time. Conditions: 3.05 mg/mL HRP, 0.08 M TMB, 0.1 mM H_2O_2.

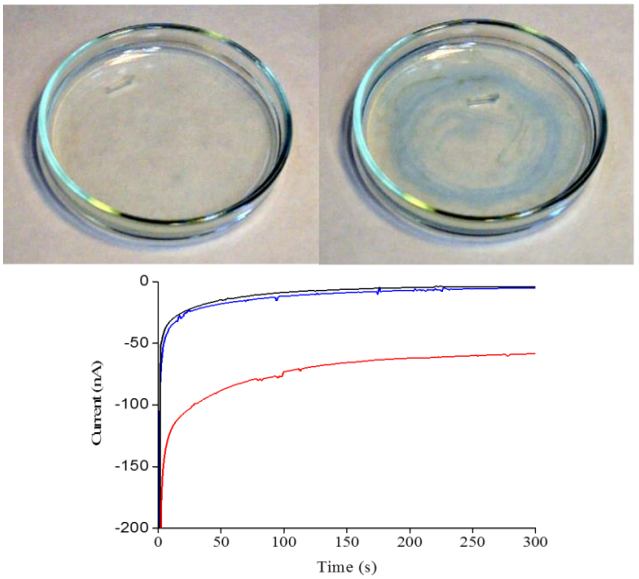

Figure S-3. Visual (left) and chronoamperometry (right) detection of H_2O_2 in tap water. Samples spiked with 0.1 mM of H_2O_2 (—). Sample (—). Control: ultrapure water (—).

Table S-1. Determination of H_2O_2 in water samples using the self-propelled enzyme-based motor.

H_2O_2 added, mM	H_2O_2 found, mM				Recovery, %			
	Amperometric		Optical		Amperometric		Optical	
	Mineral	Tap	Mineral	Tap	Mineral	Tap	Mineral	Tap
0.01	0.0100±0.0002	0.0102±0.0002	0.0103±0.0002	0.0100±0.0004	100±3	102±2	103±4	100±4
0.05	0.049±0.004	0.051±0.001	0.050±0.002	0.049±0.001	98±2	102±5	101±5	99±2
0.1	0.100±0.002	0.099±0.003	0.102±0.003	0.100±0.003	101±4	99±5	102±5	101±3

Table S-2. Determination of H_2O_2 in urine samples using the self-propelled enzyme-based motor.

H_2O_2 added, mM	H_2O_2 found, mM		Recovery, %	
	Amperometric	Optical	Amperometric	Optical
0.1	0.0097±0.0004	0.0099±0.0006	97±4	98±6
0.5	0.048±0.003	0.052±0.004	96±6	103±7
1	0.098±0.003	0.096±0.004	98±3	96±4

Table S-3. Determination of H_2O_2 in plasma samples using the self-propelled enzyme-based motor.

$H_2O_{2\ added}$, mM	$H_2O_{2\ found}$, mM	Recovery, %
0.05	0.0100±0.0003	100±3
0.1	0.049±0.001	99±4
0.5	0.097±0.002	97±3

V.1. List of tables

Chapter II

Chapter III

Disposable and reliable electrochemical magnetoimmunosensor for Fumonisins simplified determination in maize-based foodstuffs

Disposable electrochemical magneto immunosensor for simultaneous simplified calibration and determination of Ochratoxin A in coffee samples

Determination of Fumonisin B1 based *on-the-move* fluorescence quenching of the specific labeled-aptamer by graphene-made micromotors

Self-propelled enzyme-based motors for smart mobile electrochemical and optical biosensing

Appendices – Supporting Information

Disposable and reliable electrochemical magnetoimmunosensor for Fumonisins simplified determination in maize-based foodstuffs

Self-propelled enzyme-based motors for smart mobile electrochemical and optical biosensing

V.2. List of figures

Chapter II

Chapter III

Disposable and reliable electrochemical magnetoimmunosensor for Fumonisins simplified determination in maize-based foodstuffs

Disposable electrochemical magneto immunosensor for simultaneous simplified calibration and determination of Ochratoxin A in coffee samples

Determination of Fumonisin B1 based *on-the-move* fluorescence quenching of the specific labeled-aptamer by graphene-made micromotors

Delayed ignition and propulsion of catalytic microrockets based on fuel-induced chemical dealloying of the inner alloy layer

Self-propelled enzyme-based motors for smart mobile electrochemical and optical biosensing

Appendices – Supporting Information

Disposable and reliable electrochemical magnetoimmunosensor for Fumonisins simplified determination in maize-based foodstuffs

Delayed ignition and propulsion of catalytic microrockets based on fuel-induced chemical dealloying of the inner alloy layer

Self-propelled enzyme-based motors for smart mobile electrochemical and optical biosensing

V.3. Acronyms

Ab Antibody

AC Alternating current

AFB1 Aflatoxin B1

AFG1 Aflatoxin G1

AFM1 Aflatoxin M1

Ag Antigen

ALP Alkaline phosphatase

AMP Ampetrometry

AOAC Association of Official Agricultural Chemists

ATP Adenosine triphosphate

CA Cysteamine

cAMP Chronoampero-metry

cDNA Complementary DNA sequence

CEN European Standardization Committee

CFU Colony-forming unit

Chi Chitosan

CMs Cystine microstructures

CRM Certified reference material

CSPE Carbon screen-printed electrode

CV Cyclic voltammetry

CVs Coefficients of variation

DAMP 1-Deoxy-1-aminomannopyranoside

DDT Dichlorodiphenyl-trichloroethane

DMF N,N′-Dimethyl-formamide

DON Deoxynivalenol

DPV Differential pulse voltammetry

DR Dynamic range

EDX Energy dispersive X-ray spectroscopy

EFSA European Food Safety Authority

EIS Electrochemical impedance spectroscopy

ELISA Enzyme-linked immunosorbent assay

EQCM-CV Electrochemical quartz crystal microbalance cyclic voltammetry

erGO Electrochemically reduced graphene oxide

Fab Antigen-binding region fragments

FAM Fluorescein amidine

FAO Food and Agriculture Organization of the United Nations

FB1 Fumonisin B1

FB2 Fumonisin B2

FB3 Fumonisin B3

FBs Fumonisins

Fc Ferrocene

FDA U.S. Food and Drug Administration

FRET Fluorescence Resonance Energy Transfer

GC Gas chromatography

GCE Glassy carbon electrode

GO Graphene oxide

GOx Glucose Oxidase

HPLC High-performance liquid chromatography

HRP Horseradish peroxidase

IARC International Agency for Research on Cancer

IC_{50} Halfviv-maximal inhibitory concentration

IgE Immunoglobulin E

JECFA Joint FAO/WHO Expert Committee on Food Additives of the United Nations

LAMP Loop-mediated isothermal amplification

LC Liquid chromatography

LF Label-free

Lip Lipoic acid

LOC Lab-on-a-chip

LOD Limit of detection

LOQ Limit of quantification

LSV Linear sweep voltammetry

mAb Monoclonal Ab

MBs Magnetic beads

MEIS Magneto-electrochemical impedance spectroscopy

MERCOSUR Southern Common Market

mIgG Monoclonal immunoglobulin G

MON Moniliformin

MRLs Maximum Residue Levels

MS Mass spectrometry

Nb Nanobody

NoV Norovirus

OTA Ochratoxin A

pAb Polyclonal Ab

PANI Polyaniline

PBS Phosphate buffer saline

PC Polycarbonate

PCBs Polychlorinated biphenyls

PCR Polymerase chain reaction

PDMS Polydimethyl-siloxane

PEDOT Poly-3,4-ethylenedioxythiophene

POC Point-of-care

PPy Polypyrrole

PS Polystyrene

PSf Polysulfone polymer

PtNPs Platinum nanoparticles

PV Parvalbumin

PVD Physical vapor deposition

rAb Recombinant Ab

RSDs Relative standard deviations

SAM Self-assembled Monolayer

SDS Sodium dodecyl sulfate

SELEX Systematic Evolution of Ligands by Exponential Enrichment

SEM Scanning electron microscopy

SPE Screen-printed electrode

SPR Surface plasmon resonance

ssDNA Single strain DNA

SWSV Square wave stripping voltammetry

SWV Square wave voltammetry

Thi Thionine

TLC Thin layer chromatography

TMB 3,3′,5,5′-Tetramethylbenzidine

UCNPs Upconversion fluorescence nanoparticles

Vc Variable region

WHO World Health Organization

WTO World Trade Organization

ZEA Zearalenone

β-LB β-lactoglobulin